

Thiol–Disulfide Interchange: Design, Synthesis, and Evaluation of Reagents and
Organocatalysts for Chemical Biology

By

John C. Lukesh, III

A dissertation submitted in partial fulfillment of
the requirements for the degree of

Doctor of Philosophy

(Chemistry)

at the

UNIVERSITY OF WISCONSIN–MADISON

2014

Date of final oral examination: 08/20/2014

The dissertation is approved by the following members of the Final Oral Committee:
Ronald Raines, Henry Lardy Professor of Biochemistry, Biochemistry and Chemistry
Tehshik Yoon, Professor, Chemistry
Eric Strieter, Professor, Chemistry
Brian Fox, Professor, Biochemistry
Eric Shusta, Professor, Chemical and Biological Engineering

Table of Contents

| | |
|--|-------|
| Abstract | vii |
| Acknowledgements | x |
| List of Figures | xiii |
| List of Tables | xvii |
| List of Schemes | xviii |
| List of Abbreviations | xix |
| Chapter 1: Thiol–Disulfide Interchange: Design, Synthesis, and Evaluation of Reagents and Organocatalysts for Chemical Biology | 1 |
| 1.1 Abstract | 1 |
| 1.2 Introduction | 2 |
| 1.3. Development of disulfide-reducing agents for chemical biology..... | 3 |
| 1.4 Phosphorous Based Disulfide-Reducing Agents for Chemical Biology | 8 |
| 1.5 Immobilized Disulfide-Reducing Agents..... | 9 |
| 1.6 Catalysts for Thiol–Disulfide Interchange Chemistry | 10 |
| 1.7 Catalysts for Protein Folding..... | 11 |
| 1.8 Conclusions | 13 |
| Chapter 2*: A Potent, Versatile Disulfide-Reducing Agent from Aspartic Acid..... | 15 |
| 2.1 Abstract | 15 |

| | |
|---|----|
| 2.2 Author Contributions..... | 15 |
| 2.3 Introduction | 17 |
| 2.4 Results and Discussion..... | 18 |
| 2.5 Conclusions | 22 |
| 2.6 Acknowledgements | 22 |
| 2.7 Materials and Methods | 23 |
| 2.7.1 General | 23 |
| 2.7.2 Chemical Synthesis | 24 |
| 2.7.3 Purity of DTBA assessed by Ellman's assay for sulfhydryl groups | 31 |
| 2.7.3 Determination of thiol pK_a values | 32 |
| 2.7.5 Reduction potential of BMS..... | 36 |
| 2.7.6 Kinetic studies on the reduction potential of oxidized β ME | 36 |
| 2.7.7 Kinetic studies on the reduction of oxidized L-glutathione..... | 37 |
| 2.7.8 Kinetic studies on the reactivation of papain..... | 38 |
| 2.7.9 Kinetic studies on the reactivation of creatine kinase | 40 |
| 2.7.10 Separation of DTBA using ion-exchange resin..... | 41 |
| 2.7.11 Ultraviolet spectra of oxidized DTBA and oxidized DTT | 41 |
| 2.8 NMR Spectra..... | 43 |
| Chapter 3*: Thiols and Selenols as Electron-Relay Catalysts for Disulfide-Bond Reduction..... | 50 |
| 3.1 Abstract | 50 |

| | |
|--|----|
| 3.2 Author Contributions..... | 50 |
| 3.3 Introduction | 51 |
| 3.4 Results and Discussion..... | 52 |
| 3.5 Conclusions | 58 |
| 3.6 Acknowledgements | 58 |
| 3.7 Materials and Methods | 59 |
| 3.7.1 General | 59 |
| 3.7.2 Chemical Synthesis | 60 |
| 3.7.3 Coupling Yield determined by Ellman's assay for sulfhydryl groups..... | 65 |
| 3.7.4 Reduction potential of immobilized DTBA | 66 |
| 3.7.5 Reduction of small molecules with immobilized DTBA | 67 |
| 3.7.6 Reactivation of papain with immobilized DTBA..... | 71 |
| 3.7.7 Reactivation of papain using relay catalysts..... | 73 |
| 3.7.8 Reactivation of papain with DTBA and BMC | 74 |
| 3.8 NMR Spectra..... | 75 |
| Chapter 4*: Pyrazine-Derived Disulfide-Reducing Agent for Chemical Biology | 81 |
| 4.1 Abstract | 81 |
| 4.2 Author Contributions..... | 81 |
| 4.3 Introduction | 82 |
| 4.4 Results and Discussion..... | 84 |

| | |
|--|-----|
| 4.5 Conclusions | 89 |
| 4.6 Acknowledgements | 89 |
| 4.7 Materials and Methods | 89 |
| 4.7.1 General | 89 |
| 4.7.2 Computational procedures | 91 |
| 4.7.3 Chemical synthesis | 91 |
| 4.7.4 Determination of thiol pK_a values for BMMP | 94 |
| 4.7.5 Determination of thiol pK_a values for DMH | 96 |
| 4.7.6 Reduction potential of BMMP | 96 |
| 4.7.7 Reduction potential of DMH | 98 |
| 4.7.8 Equilibrium reaction with oxidized β ME | 99 |
| 4.7.9 Reduction kinetics on oxidized β ME | 100 |
| 4.7.10 Reactivation of papain | 101 |
| 4.7.11 Reactivation of creatine kinase | 102 |
| 4.7.12 Determination of BMMP solubility in buffered water | 103 |
| 4.8 NMR Spectra | 105 |
| 4.9 Cartesian Coordinates of Optimized Geometries and Partial Atomic Charges | 111 |
| Chapter 5*: Organocatalysts of Oxidative Protein Folding Inspired by Protein Disulfide Isomerase | 119 |
| 5.1 Abstract | 119 |
| 5.2 Author Contributions | 119 |

| | |
|---|-----|
| 5.3 Introduction | 120 |
| 5.4 Results and Discussion | 123 |
| 5.5 Conclusions | 128 |
| 5.6 Acknowledgements | 128 |
| 5.7 Materials and Methods | 128 |
| 5.7.1 General | 128 |
| 5.7.2 Chemical Synthesis | 130 |
| 5.7.3 Determination of thiol pK_a Values | 153 |
| 5.7.4 Determination of reduction potential..... | 155 |
| 5.7.5 Assay for isomerase activity..... | 155 |
| 5.8 NMR Spectra..... | 158 |
| Chapter 6: Future Directions | 187 |
| 6.1 New Disulfide-Reducing Agents for Chemical Biology..... | 187 |
| 6.2 Labeling of Proteins with Electron-Relay Catalysis System..... | 190 |
| 6.3 Hydrophobic Diselenide Oxidants as Catalysts for Protein Folding..... | 191 |
| Appendix 1*: Acetylated DTBA for the Treatment of Cystinosis | 193 |
| A1.1 Author Contributions..... | 193 |
| A1.2 Introduction | 193 |
| A1.3 Materials and Methods | 193 |
| A1.4 Chemical Synthesis..... | 194 |

| | |
|---|-----|
| A1.5 NMR Spectra | 196 |
| Appendix 2: Boronic Acid Inhibitors of HIV Protease | 197 |
| A2.1 Author Contributions | 197 |
| A2.2 Introduction | 197 |
| A2.3 Materials and Methods | 197 |
| A2.4 Chemical Synthesis..... | 198 |
| A2.5 NMR Spectra | 203 |
| Appendix 3: Selective Disulfide-Reducing Agents for Phosphatase and Tensin Homolog (PTEN) . | 207 |
| A3.1 Author Contributions | 207 |
| A3.2 Introduction | 207 |
| A2.3 Materials and Methods | 208 |
| A3.4 Chemical Synthesis..... | 209 |
| A3.5 NMR Spectra | 213 |
| References | 216 |

Abstract

Thiol–Disulfide Interchange: Design, Synthesis, and Evaluation of Reagents and

Organocatalysts for Chemical Biology

John C. Lukesh, III

Under the Supervision of Ronald T. Raines

At the University of Wisconsin–Madison

For proper function, many proteins contain thiols that need to be in a reduced state, or disulfide bonds that need to be in an oxidized state. Both *in vitro* and *in vivo*, small-molecule thiols and disulfides help regulate this process through thiol–disulfide interchange chemistry. Described herein is the design, synthesis, and evaluation of novel small molecules that can aid in important biochemical processes—disulfide-bond reduction and oxidative protein folding—by facilitating essential chemical reactivity.

Small-molecule thiols are preferred reagents for the reduction of disulfide bonds in proteins because of their ability to accomplish this task under mild conditions: in water, at neutral pH, and at room temperature. Dithiothreitol (DTT) has been the preferred reagent for this process during the past 50 years. DTT is a potent disulfide-reducing agent ($E^{\circ'} = -0.327$ V) resulting from the high effective concentration of its thiol groups and its forming a stable six-membered ring upon oxidation. Nonetheless, being that a thiolate initiates attack on the disulfide bond, the efficiency of the process is governed by thiol acidity. With thiol pK_a values of 9.2 and 10.1, greater than 99% of the thiol groups in a solution of DTT are protonated and thus unreactive at neutral pH. In Chapters 2 and 4, I report on the design, synthesis, and evaluation of

dithiobutylamine (DTBA) and 2,3-bis(mercaptomethyl)pyrazine (BMMP), two novel disulfide-reducing agents for chemical biology with enhanced physicochemical properties—namely, low thiol pK_a s and disulfide E° . Both DTBA and BMMP were found to be more efficacious than previously reported disulfide-reducing agents at reducing protein disulfide bonds under biological conditions, and both possess other distinct advantages over previously reported reagents.

A significant advantage of DTBA, for example, is its containing an amino group, which allows for its facile conjugation to a resin or surface. In general, small-molecule reducing agents typically need to be maintained at millimolar concentrations, and their removal diminishes process efficiency and economy. Hence, I reasoned that appending DTBA to an insoluble resin would enable its removal and reuse by filtration or centrifugation. In Chapter 3, I report on immobilized DTBA as an alternative to other costly biological reducing agents. Through the course of my studies, I found that that immobilized DTBA was quite efficient at reducing disulfide bonds in small-molecules. Still, I determined that its ability to reduce disulfide bonds in proteins can be greatly enhanced if used in conjunction with a soluble strained cyclic disulfide or mixed diselenide catalyst that can relay electrons from the resin to the protein. This biomimetic strategy confers several distinct advantages to using an excess of soluble reducing agent alone.

Thiol–disulfide interchange chemistry is also at the core of oxidative protein folding. The rate-determining step for the folding of many proteins is the formation of native disulfide bonds between cysteine residues. In cells, the enzyme protein disulfide isomerase (PDI) catalyzes this essential process. In Chapter 5, I discuss the development of small-molecule PDI mimics with low thiol pK_a and high disulfide E° values that also emulate the hydrophobic binding site of PDI.

These attributes result in efficient and selective catalysts for the proper folding of a misfolded protein.

Acknowledgements

These past five years at the University of Wisconsin–Madison have been some of the most enjoyable ones of my entire life. Throughout my studies, I have had the chance to work with numerous individuals who have had a profound impact on my development as a scientist. For that I am extremely grateful, and I wish to express my deepest appreciation.

First and foremost, I need to thank Professor Ron Raines for being an exceptional mentor and research advisor. From day one, he offered me the independence to pursue my own areas of scientific interest, but he also supplied the necessary support and guidance when needed. He provided an outstanding environment to conduct science and set me up for success by giving me access to outstanding instrumentation, facilities, and lab full of terrific colleagues. Over the past five years, he has been the epitome of professional, and he is someone who I really look up to. Professor Raines is a marvelous presenter and scientific writer, and he has taught me a lot in that regard during the course of my graduate career.

My colleagues within the Raines lab have also been of tremendous help in my development as a scientist. In particular, I would like to acknowledge my collaborators: Mike Palte, Brett VanVeller, Kristen Andersen, and Ian Windsor. Without their assistance and unconditional support, the contents within this thesis would not have been possible. I would also like to especially thank Kelly Wallin, an extremely talented undergraduate student who I had the pleasure to mentor over the past two and a half years. Her contributions were considerable, and she helped with the completion of several projects described herein. I also need to give a special thanks to Ho-Hsuan Chou, Amit Choudhary, and Nick McGrath for their guidance and mentorship during the early years of my studies, and for teaching me the fundamentals of

synthetic organic chemistry. Working alongside other talented graduate students and postdocs such as Matt Aronoff, Rasomoy Biswas, Christine Bradford, Ben Caes, Cindy Chao, Sayani Chattopadhyay, Wen Chyan, Kevin Desai, Chelcie Eller, Greg Ellis, Aubrey Ellison, Emily Garnett, Trish Hoang, Katrina Jensen, Sean Johnston, Mike Levine, Joelle Lomax, Langdon Martin, Kalie Mix, Robert Newberry, Rob Presler, Thom Smith, Nadia Sundlass, Caglar Tanrikulu, Val Tripp, Kaylee Underkofler, Jim Vasta, and Rex Watkins provided an ideal setting in which to talk about the results, ramifications, and future directions of my science.

The scientific staff at the University of Wisconsin–Madison has been nothing short of extraordinary and is owed a special thanks. I want to specifically thank Mark Anderson from the Nuclear Magnetic Resonance Facility, Martha Vestling from the Mass Spectrometry Facility, and Darrell McCaslin from the Biophysics Instrumentation Facility for their assistance and fruitful discussions regarding my research.

I am grateful for my prelim and thesis committee members: Professors W. W. Cleland, Hans Reich, Tehshik Yoon, Eric Strieter, Brian Fox, and Brian Shusta for their support and enabling advice. I want to thank Professor Reich, in particular, for his counsel on synthesizing sulfur and selenium containing compounds. Professor Cleland is owed a huge thanks for providing his expert advice on enzyme kinetics, and the various intricacies and nuances regarding the synthesis and characterization of disulfide-reducing agents. His pioneering work on dithiothreitol (DTT) is what inspired the majority of the work described in my thesis.

I am also especially thankful for the advice and mentoring I received from Professor Alan Schwabacher while working as an undergraduate research assistant in his lab at UW–Milwaukee. He is someone that I have looked up to ever since joining his research lab back in

2007 and is major reason why I attended graduate school in the first place. To this day, he has been an outstanding advocate for me and my career, and I can't thank him enough.

I also need to give a very special thanks to Mike Palte, Ben Caes, Greg Ellis, Ho-Hsuan Chou, and Amit Choudhary for welcoming me into the Raines lab and making my early years of graduate school so enjoyable. In my later years of grad school, Ian Windsor, Brett VanVeller, and Thom Smith became close confidants. The friends and memories that I have made during my time at Wisconsin are incalculable, and they will be cherished for the rest of my life.

Most importantly, I need to thank my family for their unwavering love and support. I will forever be indebted to my parents, John and Lois Lukesh. Their constant love and encouragement is something that can never be repaid. From a young age, they taught me the importance of education, having a strong work ethic, and to always pursue my dreams no matter how difficult or challenging they might be. Lastly, to my sisters—Julie Wondergem and Cheryl Donovan—thanks for your constant love and support and for being such terrific role models throughout my life.

List of Figures

| | |
|---|----|
| Figure 1.1 Schematic for thiol–disulfide interchange chemistry | 2 |
| Figure 1.2 Mechanism for the reduction of a disulfide bond with β ME (monothiol) | 4 |
| Figure 1.3 Mechanism for the reduction of a disulfide bond with DTT (dithiol)..... | 6 |
| Figure 1.4 Disulfide-reducing agents developed for chemical biology..... | 7 |
| Figure 1.5 Phosphorous-based disulfide-reducing agents | 8 |
| Figure 1.6 Putative mechanism of PDI-catalyzed disulfide bond isomerization..... | 12 |
| | |
| Figure 2.1 Time-course for the reduction of a mixed disulfide in small molecules by DTBA and DTT | 20 |
| Figure 2.2 Time-course for the reduction of a mixed disulfide in enzymatic active sites by DTBA and DTT | 21 |
| Figure 2.3 Effect of pH on absorbance at 238 nm of DTBA..... | 33 |
| Figure 2.4 Representative HPLC chromatogram of the redox equilibrium between DTBA and DTT ^{ox} | 35 |
| Figure 2.5 Representative HPLC chromatogram of the redox equilibrium between BMS and DTT ^{ox} | 36 |
| Figure 2.6 Ultraviolet spectrum of oxidized DTBA and oxidized DTT..... | 42 |
| | |
| Figure 3.1 Time-course for the reactivation of papain-Cys25–S–S–CH ₃ by immobilized DTBA (100 or 1000 equiv) | 53 |
| Figure 3.2 Time-course for the reactivation of papain-Cys25–S–S–CH ₃ by immobilized DTBA (100 equiv) and a solution-phase disulfide catalyst (30 mol%)..... | 55 |

| | |
|---|----|
| Figure 3.3 Time course for the reactivation of papain-Cys25-S-S-CH ₃ by immobilized DTBA (100 equiv) and a solution-phase diselenide catalysts..... | 57 |
| Figure 3.4 Representative ¹ H NMR spectrum of the redox equilibrium between immobilized DTBA and DTT ^{ox} (3.2). | 67 |
| Figure 3.5 Representative HPLC chromatogram of the redox equilibrium between DTBA and DTT ^{ox} | 67 |
| Figure 3.6 Representative ¹ H NMR spectrum of the reaction between cystamine (3.3) and 10-fold excess of immobilized DTBA. | 68 |
| Figure 3.7 Representative HPLC chromatogram of the reaction between βME ^{ox} (3.4) and 10 fold excess of immobilized DTBA | 69 |
| Figure 3.8 Representative ¹ H NMR spectrum of the reaction between DTBA ^{ox} (3.1) and a 10-fold excess of immobilized DTBA. | 70 |
| Figure 3.9 Representative ¹ H NMR spectrum of the reaction between DTT ^{ox} (3.2) and a 10-fold excess of immobilized DTBA. | 71 |
| Figure 3.10 Representative HPLC chromatogram of the reaction between DTT ^{ox} (3.2) and a 10-fold excess of immobilized DTBA | 71 |
| Figure 3.11 Time-course for the reactivation of papain-Cys25-S-S-CH ₃ by dithiols..... | 74 |
| Figure 4.1 Time-course for the reduction of βME ^{ox} (5 mM) by BMMP, DMH, DTBA, or DTT (5 mM) in buffered water..... | 87 |
| Figure 4.2 Time-course for the reduction of a mixed disulfide in proteins by BMMP, DTBA, or DTT | 88 |
| Figure 4.3 Effect of pH on absorbance by BMMP at 238 nm..... | 95 |
| Figure 4.4 Effect of pH on absorbance by DMH at 238 nm..... | 96 |

| | |
|---|-----|
| Figure 4.5 Representative HPLC chromatogram of the redox equilibrium between BMMP and DTT ^{ox} | 98 |
| Figure 4.6 Representative HPLC chromatogram of the redox equilibrium between DMH and DTT ^{ox} | 98 |
| Figure 4.7 Representative HPLC chromatogram of the redox equilibrium between BMMP and β ME. | 99 |
| | |
| Figure 5.1 Putative mechanism for catalysis of protein-disulfide isomerization by protein disulfide isomerase (PDI)..... | 120 |
| Figure 5.2 Small molecule PDI mimics assessed in this study..... | 124 |
| Figure 5.3 Scheme showing the connectivity of the four disulfide bonds in native RNase A | 125 |
| Figure 5.4 Catalysis of disulfide-bond isomerization by PDI and PDI mimics 5.1–5.7 | 126 |
| Figure 5.5 Effect of pH on absorbance by 5.2 at 238 nm..... | 154 |
| Figure 5.6 Effect of pH on absorbance by 5.5 at 238 nm..... | 154 |
| Figure 5.7 Effect of pH on absorbance by 5.7 at 238 nm..... | 155 |
| Figure 5.8 Yield of native RNase A achieved by PDI mimics 5.1-5.7 after 5 h | 157 |
| | |
| Figure 6.1 Proposed disulfide-reducing agents with enhanced reactivity that are pre-organized for disulfide bond formation. | 188 |
| Figure 6. 2 Proposed synthesis of 6.1 | 188 |
| Figure 6.3 Proposed synthesis of 6.2 | 189 |
| Figure 6. 4 Proposed synthesis of 6.3 | 190 |
| Figure 6.5 Hydrophobic cyclic diselenides for oxidative protein folding | 191 |

Figure A3.1 Electrostatic potential map of PTEN with red = anionic and blue = cationic, as generated by PyMOL 207

List of Tables

| | |
|--|-----|
| Table 2. 1 Physical properties of disulfide-reducing agents..... | 18 |
| Table 4.1 Physicochemical properties of dithiol reducing agents | 83 |
| Table 4.2 Values of k_{obs} ($\text{M}^{-1}\text{s}^{-1}$) for the reduction of disulfides by dithiols | 103 |
| Table 4.3 Cartesian coordinates of the optimized geometry of 4.4 (reduced BMMP)..... | 111 |
| Table 4.4 Partial atomic charges for the optimized geometry of 4.4 (reduced BMMP)..... | 112 |
| Table 4.5 Cartesian coordinates of the optimized geometry of 4.5 (oxidized BMMP);..... | 112 |
| Table 4.6 Partial atomic charges for the optimized geometry of 4.5 (oxidized BMMP)..... | 113 |
| Table 4. 7 Cartesian coordinates of the optimized geometry of reduced DTT | 113 |
| Table 4.8 Partial atomic charges for the optimized geometry of reduced DTT..... | 114 |
| Table 4.9 Cartesian coordinates of the optimized geometry of oxidized DTT..... | 114 |
| Table 4. 10 Partial atomic charges for the optimized geometry of oxidized DTT..... | 115 |
| Table 4.11 Cartesian coordinates of the optimized geometry of DMH..... | 115 |
| Table 4.12 Partial atomic charges for the optimized geometry of DMH..... | 116 |
| Table 4.13 Cartesian coordinates of the optimized geometry of oxidized DMH | 117 |
| Table 4.14 Partial atomic charges for the optimized geometry of oxidized DMH..... | 117 |
| Table 5.1 Properties of PDI and mimics..... | 127 |

List of Schemes

| | |
|--|----|
| Scheme 2.1 Synthetic route to DTBA..... | 19 |
| Scheme 3.1 Disulfides (3.1–3.6) and diselenides (3.7–3.9) used in this work | 51 |
| Scheme 3.2 Cycle for electron-relay catalysis of disulfide-bond reduction by soluble thiols (III , X = S) or selenols (III , X = Se)..... | 54 |
| Scheme 4.1 Synthetic route to BMMP (4.4)..... | 85 |

List of Abbreviations

| | |
|--------------------|---|
| β ME | 2-mercapoethanol |
| l | path length |
| ε | extinction coefficient |
| A | absorbance |
| Ac | acetyl |
| ACN | acetonitrile |
| BMC | (\pm)- <i>trans</i> -1,2-bis(2-mercaptoacetamido)cyclohexane |
| BMMP | 2,3-bis(mercaptomethyl)pyrazine |
| BMS | bis(2-mercaptoethyl)sulfone |
| c | concentration |
| Da | dalton |
| DCM | dichloromethane |
| ddH ₂ O | distilled, deionized water |
| DHLA | dihydrolipoic acid |
| DMF | dimethylformamide |
| DMH | <i>N,N'</i> -dimethyl- <i>N,N'</i> -bis(mercaptoacetyl)hydrazine |
| DMSO | dimethylsulfoxide |
| DTA | <i>meso</i> -2,5-dimercapto- <i>N,N,N',N'</i> -tetramethyladipamide |
| DTNB | 5,5'-dithiobis(2-nitrobenzoic acid) |
| DTBA | dithiobutylamine |
| DTT | dithiothreitol |
| EDTA | ethylenediaminetetraacetic acid |
| EtOAc | ethyl acetate |

| | |
|----------------|--|
| EtOH | ethanol |
| GSH | L-glutathione |
| GSSH | oxidized L-glutathione |
| h | hour |
| HCl | hydrogen chloride |
| HPLC | high performance liquid chromatography |
| HRMS | high resolution mass spectrometry |
| K_{eq} | equilibrium constant |
| k | rate constant |
| k_{obs} | observed rate constant |
| k_{cat} | first-order enzymatic rate constant |
| kDa | kilodalton |
| K_M | Michaelis constant |
| λ_{em} | emission wavelength |
| λ_{ex} | excitation wavelength |
| MeOH | methanol |
| min | minute |
| NaCl | sodium chloride |
| NaOH | sodium hydroxide |
| PDB | protein data bank |
| PDI | protein disulfide isomerase |
| PEG | polyethylene glycol |
| pK_a | log of the acid dissociation constant |
| RI | ribonuclease inhibitor |

| | |
|----------|---|
| RNA | ribonucleic acid |
| RNase A | bovine pancreatic ribonuclease |
| s | second |
| sRNase A | scrambled bovine pancreatic ribonuclease |
| t | time |
| TNB | 2-nitro-5-thiobenzoate |
| Tris | 2-amino-2-(hydroxymethyl)- 1,3 -propanediol |
| UV | ultraviolet |

Chapter 1: Thiol–Disulfide Interchange: Design, Synthesis, and Evaluation of Reagents and Organocatalysts for Chemical Biology

1.1 Abstract

Thiol-disulfide interchange chemistry is a fundamental process in biology that enables regulation of protein structure and redox homeostasis. For proper function, many biomolecules contain thiols that need to be maintained in a reduced state, or disulfide bonds that need to be maintained in an oxidized state. Both *in vivo* and *in vitro*, small molecule thiols and disulfides help regulate this process through thiol–disulfide exchange reactions. As a result, much work has gone into the development of new reagents that can efficiently mediate this essential chemistry. Here, an overview of thiol–disulfide interchange chemistry will be presented, including the development of new biological reagents that can be used for the reduction, isomerization, or formation of disulfide bonds in proteins and other biomolecules.

1.2 Introduction

Thiols and disulfides are functional groups that are ubiquitously found in the molecules of life, and play a critical role in both their structure and their function.¹⁻⁶ Disulfide bonds, for example, are essential for the proper structure of many extracellular proteins.⁷⁻¹² On the other hand, many cytosolic enzymes, cofactors, and peptides—such as glutathione—contain thiols that need to be maintained in a reduced state.^{13,14} In both cases, it is thiol–disulfide interchange chemistry that facilitates their required redox state.¹⁵

The mechanism for thiol–disulfide interchange has been studied in great detail.¹⁶⁻²² It involves the reaction between a thiol (RSH) and a disulfide (R'SSR') in which a new disulfide (RSSR') and thiol (R'SH) is formed (Figure 1.1). The reaction is quite unique in chemistry in that the cleavage and formation of a strong covalent S–S bond (bond energy of ~60 kcal/mol) occurs reversibly and under very mild conditions.^{4,5,21}

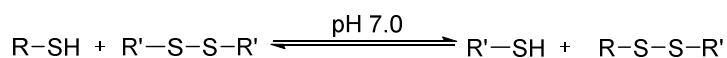


Figure 1.1 Schematic for thiol–disulfide interchange chemistry

In this chapter, I will discuss the design and use of small molecules that can facilitate these key exchange reactions in proteins and other biomolecules.

1.3. Development of disulfide-reducing agents for chemical biology

The reduction of unwanted disulfide bonds and the preservation of essential thiol groups is a common biochemical practice.^{5,23-32} Out of necessity, the reduction must take place under mild conditions. The use of small molecule thiols for this process is often preferred, as they can accomplish this task—through thiol–disulfide interchange chemistry—in neutral water, at room temperature, and in the presence of a multitude of other functional groups.^{4,5,15,24}

Several factors determine whether or not a small molecule thiol will be efficient at disulfide-reduction. There is some debate as to whether the mechanism for thiol–disulfide interchange chemistry goes by an S_N2 or addition–elimination pathway, but what is known is that it is the more nucleophilic thiolate that initiates this process.^{16,17,21,33-36} As a result, thiol acidity plays a vital role in developing new reagents. The reaction is second-order overall—first order in both thiolate and disulfide.³⁴ The observed rate of the exchange reaction between a thiol and a disulfide bond will therefore be dependent on both the p*K*_a of the thiol and the pH of the solution. Consequently, it has been predicted—and shown experimentally—that for a maximum observed rate, the thiol p*K*_a of the reducing thiol should match the pH of the solution under which the reaction will occur. These conditions provide the right balance between the amount of thiolate present (low p*K*_a is better) and its resulting nucleophilicity (high p*K*_a is better).^{34,37}

Disulfide reduction potential (*E*^{o'}), is another key property that needs to be assessed when determining the efficacy of a compound as a reducing agent. In particular, high thermodynamic stability of its oxidized form is a necessary attribute. In general, for efficient reduction, the resulting disulfide *E*^{o'} of the reducing thiol must be lower (more negative) than the *E*^{o'} of the disulfide that is to be reduced.^{5,24}

Because of their low cost, monothiols—such as β -mercaptoethanol (β ME) and cysteamine—are commonly used for the reductive unfolding of disulfide-containing proteins in reducing SDS–PAGE and other biochemical applications. L-glutathione (GSH), on the other hand, is a monothiol that is the most abundant non-protein thiol found in most cells.^{4,5,15} It along with its oxidized partner (L-glutathione^{ox} or GSSG) forms the chief redox buffer within the cell and is responsible for its protection against oxidative stress.¹⁵ Still, as is the case with all monothiols, these reagents are weakly reducing, with no real thermodynamic driving force—other than Le Chatelier's principle—capable of perturbing the equilibrium of their reaction with the disulfide of another molecule (Figure 1.2).²⁴ In general, the reduction of protein disulfides with these monothiols often leads to incomplete reduction and the formation of mixed disulfide intermediates (Figure 1.2). This detriment significantly deters their utility in buffered solutions and *in vitro* applications where a strong reducing presence is required.

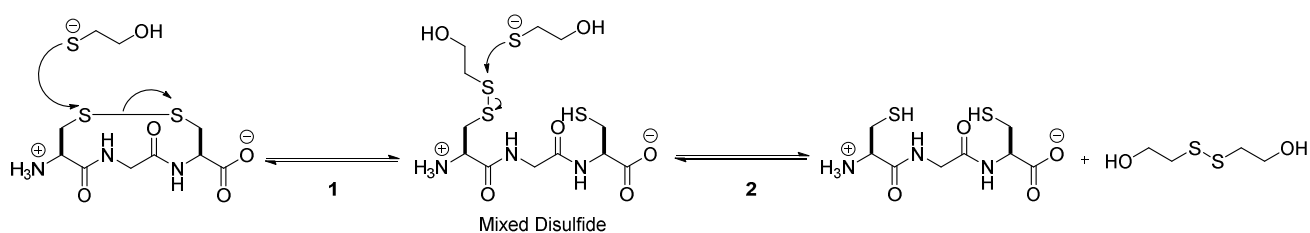


Figure 1.2 Mechanism for the reduction of a disulfide bond with β ME (monothiol)

In response to this dilemma, in 1964, Cleland put forth dithiothreitol (DTT; Figure 1.4), a dithiol capable of resolving mixed disulfides by forming a six-membered ring upon oxidation (Figure 1.3).²⁴ With a high effective concentration of reducing thiol (intramolecular ring-closing reaction), the formation of an enthalpically stable ring (six-membered), and generation of two

products from a single mixed disulfide intermediate (entropically favored), DTT is a potent disulfide-reducing agent with a disulfide E° of -0.327 V.³⁸

The enthalpic stability of its oxidized form is a crucial factor in determining the equilibrium for thiol–disulfide interchange reactions involving dithiols. The CSSC dihedral angle in cyclic disulfides is often displaced from its optimal angle of 90° .³⁹ In six-membered cyclic disulfides—such as DTT—this angle is 60° , whereas five-membered cyclic disulfides possess a CSSC dihedral angle of 30° . Even though 1,3-dithiols have a higher effective concentration of reducing thiol than do 1,4-dithiols, the more severe CSSC dihedral angle strain render them less strongly reducing.^{29,39,40} Larger rings, on the other hand, tend to possess CSSC dihedral angles that are closer to what is ideal. These larger ring systems, however, suffer from van der Waals strain and/or transannular strain.³⁹ In general, dithiols that form six-membered rings are the most strongly reducing (lowest disulfide E°), providing the proper balance between the high enthalpic stability of the incipient ring and the low entropic cost for its formation.

DTT is, however, not without a serious limitation. In addition to its high cost, DTT possess thiol pK_a s of 9.2 and 10.1 (Figure 1.4).³⁴ Therefore, at physiological pH, greater than 99% of the thiol groups of DTT are protonated and thus unreactive. As a result, several attempts have been made to develop biologically compatible disulfide-reducing agents that sport lower thiol pK_a values in attempts to increase kinetic efficiency near neutral pH.

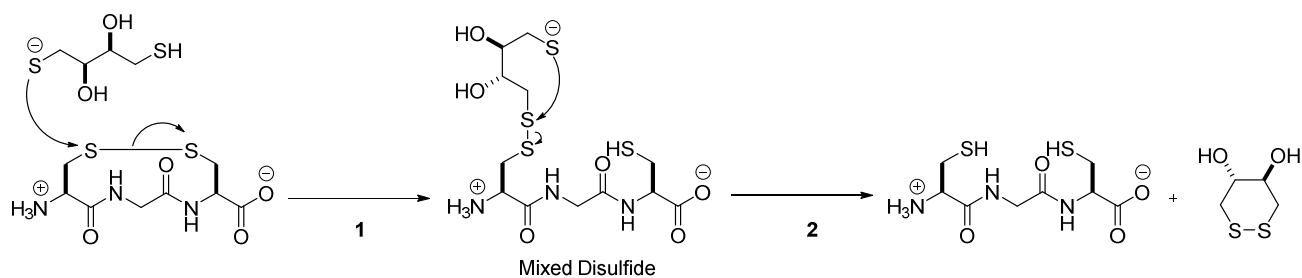


Figure 1.3 Mechanism for the reduction of a disulfide bond with DTT (dithiol)

Whitesides and co-workers first reported on *N,N'*-dimethyl-*N,N'*-bis(mercaptoacetyl)hydrazine (DMH; Figure 1.4) in 1991 as an alternative to DTT.²⁸ DMH has thiol pK_a s that have been estimated to be 8.0 and 9.1 and, as a result, was shown to reduce most disulfide-bonds ~ 5 – 7 times faster than DTT at pH 7.0.^{28,41} Yet, unlike DTT, DMH forms an eight-membered ring upon oxidation, which significantly reduces its thermodynamic potency, resulting in a disulfide E°' of -0.262 V.⁴¹

In attempts to improve upon their initial work, Whitesides and co-workers next reported on *meso*-2,5-dimercapto-*N,N,N',N'*-tetramethyladipamide (*meso*-DTA; Figure 1.4) and bis(2-mercaptoethyl) sulfone (BMS; Figure 1.4).^{27,29} Once again, depressed thiol pK_a s provided enhanced kinetics for *meso*-DTA and BMS relative to DTT. In the case of *meso*-DTA, however, it was found to only reduce disulfide bonds in proteins 2–5 fold faster than DTT, presumably due to the fact that *meso*-DTA is a secondary thiol. Moreover, these steric constraints also diminished its thermodynamic potency. Even though *meso*-DTA, like DTT, is capable of forming a six-membered ring upon oxidation, unfavorable 1,3-diaxial interactions present in its oxidized form severely hindered its reducing power (Figure 1.4).²⁷

BMS proved to be the most advantageous reagent developed by Whitesides, as it was found to reduce disulfide bonds in proteins ~5–7 times faster than DTT and possessed a thermodynamic potency that was superior to both DMH and *meso*-DTA.²⁹

| | pK_a | Disulfide E° |
|----------------------|------------|-----------------------|
| DTT | 9.2 (10.1) | -0.327 V |
| DMH | 8.0 (9.1) | -0.262 V |
| <i>meso</i> -DTA | 7.8 (8.9) | -0.269 V |
| BMS | 7.9 (9.0) | -0.291 V |
| DTBA | 8.2 (9.3) | -0.317 V |
| BMMP | 7.6 (9.0) | -0.301 V |

Figure 1.4 Disulfide-reducing agents developed for chemical biology

Still, none of these reagents came even close to matching DTT in terms of thermodynamic strength. In Chapters 2 and 4, I describe two novel reagents—DTBA and

BMMP—that I developed that were shown to be extremely efficacious at reducing disulfide-bonds in both proteins and peptides.^{41,42} Both DTBA and BMMP were shown not only to be kinetically superior to DTT, but also to form cyclic disulfides with a similar stability, endowing them with attributes that could allow either to supplant DTT as the preferred reagent for reducing disulfide bonds in biomolecules.

1.4 Phosphorous Based Disulfide-Reducing Agents for Chemical Biology

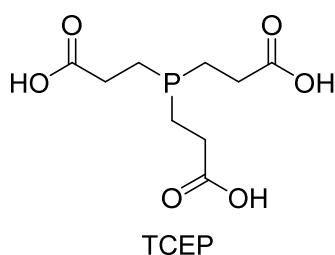


Figure 1.5 Phosphorous-based disulfide-reducing agents

The use of phosphorous-based disulfide-reducing agents has been fruitful in many biochemical applications.^{26,43-47} It has been known since the 1930's that trialkylphosphines can reduce disulfides to thiols.⁴⁸ Nonetheless, high cost, odor, and lack of water solubility hindered their use in the laboratory. This landscape changed in the 1990's with Whitesides' simple synthesis of tris(2-carboxyethyl)phosphine (TCEP; Figure 1.5).²⁶ TCEP has several advantages over sulfur-based disulfide-reducing agents. Below pH 8.0, TCEP displays improved kinetics and thermodynamic potency, quickly reducing disulfide bonds and doing so in an irreversible fashion. Although TCEP is able to reduce disulfide bonds in many proteins, it does so at an extremely slow rate. Due to the severe steric hindrance of the trivalent phosphine, it has been

reported that DTT can reduce the redox-active disulfide in *Escherichia coli* thioredoxin 117-fold faster than TCEP!⁴⁵

1.5 Immobilized Disulfide-Reducing Agents

Small-molecule reducing agents typically need to be maintained at mM concentrations and their removal diminishes process efficiency and economy significantly. Hence, several groups have attempted to develop supported disulfide-reducing agents that can be easily isolated, recycled, and reused. Immobilized disulfide-reducing agents have typically relied on either tris(2-carboxyethyl)phosphine (TCEP; Figure 1.5), which cannot be regenerated after use, or dihydrolipoic acid (DHLA), where the hydrophobic nature of DHLA can result in the non-specific binding of certain proteins.^{43,49-53} In addition, few immobilized reagents have been shown to be effective at reducing disulfide bonds in large biomolecules as their size precludes them from accessing the reducing sites on the resin.^{43,49,50,54} I envisioned that the amino group on DTBA would allow for its facile conjugation to any insoluble resin or surface. Moreover, I predicted that the hydrophilic nature of DTBA and its ability to be regenerated and reused would result in its immobilized form being a cost-effective and green alternative to current practices. In Chapter 3 of this thesis, I discuss the synthesis of immobilized DTBA as well as its application as a disulfide-reducing agent in chemical biology.⁵⁵

1.6 Catalysts for Thiol–Disulfide Interchange Chemistry

Several compounds have been tested for their ability to act as catalysts of thiol–disulfide interchange chemistry.⁵⁶ To date, only selenols have been shown unequivocally to provide significant enhancements in the overall rate.⁵⁵⁻⁶⁶

Selenols serve as effective catalysts only for exchange reactions involving strongly reducing dithiols. For example, the observed rate for the reduction of $\beta\text{ME}^{\text{ox}}$ with DTT in neutral water is enhanced by a factor of 15 in the presence of 5 mol% selenocystamine.⁵⁷ Diselenides typically have $E^{\circ'}$ values that are 0.15 V lower than those of analogous disulfides.^{57,66,67} Consequently, thiol–disulfide interchange reactions involving weakly reducing monothiols are not catalyzed by selenols, because these disulfides only facilitate the oxidation of selenols to diselenides.⁵⁷

Selenium has physicochemical properties that are similar to sulfur. Yet, selenols manifest several desirable attributes as catalysts for these exchange reactions.^{11,68-80} Selenols have $\text{p}K_{\text{a}}$ values that are typically three units lower than their corresponding thiol congener. This, along with the weak solvation and high polarizability of the resulting selenolate anion, significantly enhances their nucleophilicity near neutral pH and their ability to operate as a leaving group.⁵⁷ In addition, reactions with selenium as the electrophile can be 10^4 times faster than those with sulfur as the electrophile.⁶⁶ All of these factors enable selenols and diselenides to serve as efficient catalysts of thiol–disulfide interchange reactions.

In addition to diselenides, strained cyclic disulfides have also been shown to serve as catalysts for thiol–disulfide exchange reactions.^{40,55} It has been known that cyclic five-membered disulfides undergo ring-opening reactions with rate constants that are 10^3 -fold larger

than those for the opening of six- or seven-membered rings, providing a rationalization for the evolutionary selection of lipoamide (cyclic five-membered disulfide) as a cofactor in 2-oxo acid dehydrogenase complexes.^{18,40,81} In Chapter 3, I show that medium-sized 10-membered cyclic disulfides are also reduced at a much faster rate than are strain-free cyclic and acyclic disulfides. Their role as a catalyst in the presence of immobilized DTBA allowed for the biomimetic reduction of otherwise inaccessible disulfide bonds in proteins.⁵⁵

1.7 Catalysts for Protein Folding

Disulfide bonds are essential for the function and stability of many extracellular proteins.^{7-12,82,83} The formation of native disulfide bonds limits their folding, as non-native disulfides must be isomerized in order to achieve proper cysteine pairings. Therefore, it is not surprising that this crucial step is an enzyme-mediated process *in vivo*. Proteins with multiple cysteine residues tend to initially form disulfide bonds in a random and nonspecific fashion. It is the job of protein disulfide isomerase (PDI)—a 57 kDa enzyme located in the endoplasmic reticulum (ER) of eukaryotic cells—to reshuffle non-native disulfides until native linkages are formed.^{9,84-100}

PDI contains two CGHC active site motifs that are responsible for disulfide isomerization.^{87,101-103} The mechanism involves thiol–disulfide interchange chemistry that is initiated by the nucleophilic attack of a PDI active-site thiolate on a non-native protein-disulfide bond (Figure 1.6). This attack generates a mixed disulfide between PDI and its substrate protein while also generating a new substrate thiolate that is free to induce further isomerization until its proper fold is achieved.

PDI contains optimal physicochemical properties for facilitating disulfide bond isomerization *in cellulo*. With a low thiol pK_a (6.7) and a high disulfide E° (-0.18 V), it can be calculated that roughly 33% of PDI active sites will contain a reactive thiolate species in the ER.^{6,104,105} Moreover, the relatively high (less negative) reduction potential ensures that disulfide bond isomerization—rather than disulfide bond reduction—will take place as the second active-site cysteine is merely there to rescue itself from any prolonged mixed disulfide intermediates (Figure 1.6).

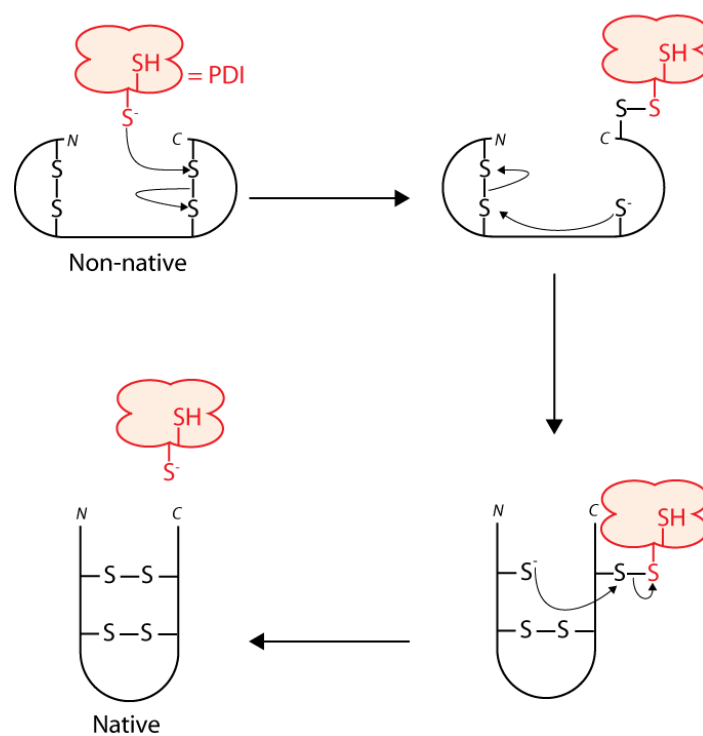


Figure 1.6 Putative mechanism of PDI-catalyzed disulfide bond isomerization

The production of proteins by recombinant DNA technology is a core practice in biotechnology. The *in vivo* overexpression of proteins typically results in the formation of

protein aggregates called inclusion bodies, which must be denatured and resolubilized before being folded properly.^{106,107} With nearly all protein-based pharmaceuticals containing disulfide bonds, the use of catalysts that can facilitate their folding is of great interest.^{108,109} The consistent use of PDI for *in vitro* protein folding, however, is not practical due to its high cost, instability, and difficulty in separation from substrate proteins of interest. As a result, much work has gone into the development of small molecule catalysts that can mimic the properties and effects of this essential protein.

In general, most small-molecule PDI mimics have focused on mimicking the physicochemical properties of the two CGHC active sites. Therefore, aromatic thiols and selenium-based catalysts have found widespread use due to their potent nucleophilicity at physiological pH.^{54,61,63,64,85,110-116} CXXC and CXC peptides that mimic the high disulfide E° of PDI, while still containing a second thiol in order to reduce the build-up of mixed disulfide intermediates, have also been employed with modest success.¹¹⁷⁻¹¹⁹ In Chapter 5, I describe the development of a series of novel PDI mimics that include various hydrophobic moieties in order to emulate the substrate-binding capabilities of PDI. I demonstrate that increased hydrophobicity appears to enhance both the observed rate of folding as well as the overall yield of properly folded protein with native disulfide bonds.

1.8 Conclusions

Thiol–disulfide interchange chemistry is a reversible process that readily takes place under biological conditions: in water, at physiological pH, and at room temperature. The process is extremely important in regulating both the structure and function of numerous biomolecules. As a result, small-

molecules that mediate this important process have found widespread use for common biochemical practices such as the reduction, isomerization, or formation of disulfide bonds, as well as maintaining intracellular redox homeostasis.

Chapter 2*: A Potent, Versatile Disulfide-Reducing Agent from Aspartic Acid

2.1 Abstract

Dithiothreitol (DTT) is the standard reagent for reducing disulfide bonds between and within biological molecules. At neutral pH, however, >99% of DTT thiol groups are protonated and thus unreactive. Herein, we report on (2S)-2-amino-1,4-dimercaptobutane (dithiobutylamine or DTBA), a dithiol that can be synthesized from L-aspartic acid in a few high-yielding steps that are amenable to a large-scale process. DTBA has thiol pK_a values that are ~1 unit lower than those of DTT and forms a disulfide with a similar E°' value. DTBA reduces disulfide bonds in both small molecules and proteins faster than does DTT. The amino group of DTBA enables its isolation by cation-exchange and facilitates its conjugation. These attributes indicate that DTBA is a superior reagent for reducing disulfide bonds in aqueous solution.

2.2 Author Contributions

R.T.R. proposed the use of DTBA as a disulfide-reducing agent. J.C.L. synthesized and characterized DTBA. M.J.P. established protocols for enzyme assays and taught J.C.L. how to perform and analyze enzyme kinetics. M.J.P. assisted with separation of DTBA using an ion-exchange resin. J.C.L. performed all other experiments and drafted the original manuscript and figures. J.C.L., M.J.P., and R.T.R. planned experiments, analyzed data, and edited the manuscript and figures.

*This chapter has been published, in part, under the same title. Reference: Lukesh, J. C., III; Palte, M. J.; Raines, R. T. *J. Am. Chem. Soc.* **2012**, *134*, 4057–4059 (Highlighted in Chemical & Engineering News. 90(10). March 5, 2012).

2.3 Introduction

Approximately 20% of human proteins are predicted to contain disulfide bonds between cysteine residues.¹²⁰ Small-molecule thiols can reduce these (and other) disulfide bonds, thereby modulating biomolecular function.^{5,14,24-27,29-32,45,121} The reaction mechanism involves thiol–disulfide interchange initiated by a thiolate.^{17,21,34-36,122-124} The ensuing mixed disulfide can become trapped if the reagent is a monothiol, such as β -mercaptoethanol (β ME). To overcome this problem, Cleland developed racemic (2S,3S)-1,4-dimercaptobutane-2,3-dithiol (dithiothreitol or DTT; Table 2.1), a dithiol that resolves a mixed disulfide by forming a six-membered ring.^{24,125} DTT is a potent reducing agent ($E^{\circ'} = -0.327$ V), and has been the preferred reagent for the quantitative reduction of disulfide bonds for decades, despite its high cost.

At physiological pH, DTT is a sluggish reducing agent. The reactivity of a dithiol is governed by the lower of its two thiol pK_a values.³⁴ With its lower thiol pK_a value being 9.2 (Table 2.1), <1% of DTT resides in a reactive thiolate form at pH 7.0.

We sought to develop a nonracemic dithiol with low thiol pK_a and disulfide $E^{\circ'}$. Moreover, we sought a reagent that could be accessed in high yield from an inexpensive source. We envisioned that (2S)-2-amino-1,4-dimercaptobutane (dithiobutylamine or DTBA; Table 2.1) could fulfill our physicochemical criteria, and be synthesized from L-aspartic acid, which is an abundant amino acid.^{126,127}

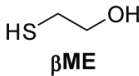
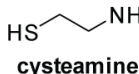
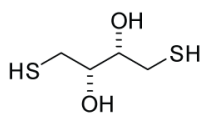
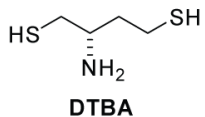
| | Thiol pK_a | Disulfide Reduction Potential ($E^{0'}$) |
|---|--|--|
|  βME | 9.61 ^a | -0.196 V ^b |
|  cysteamine | 8.37 ^c | -0.203 V ^b |
|  DTT (racemate) | 9.2 (10.1) ^d | -0.327 V ^e |
|  DTBA | 8.2 ± 0.2 (9.3 ± 0.1) ^f | (-0.317 ± 0.002) V ^f |

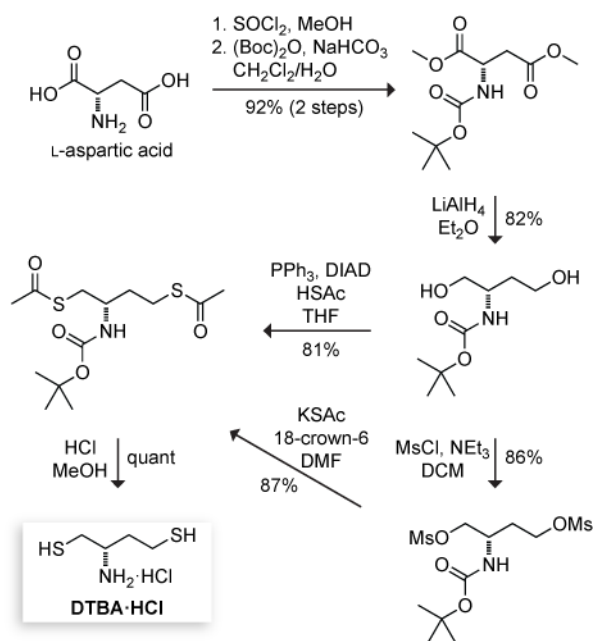
Table 2.1 Physical properties of disulfide-reducing agents. ^aValue is from ref 5. ^bValues are from ref 27. ^cValue is from 42. ^dValues are from ref 34. ^eValue is from ref 38. ^fValues are the mean \pm SE from this work.

2.4 Results and Discussion

We accessed DTBA via the two routes depicted in Scheme 2.1. A five-step route commenced with the esterification of the amino acid and protection of its amino group. Reduction with lithium aluminum hydride yielded a diol, which was subjected to Mitsunobu conditions to install the requisite sulfur functionality.¹²⁸ Deprotection gave DTBA as its HCl salt in 99% purity and an overall yield of 60%. A six-step route that avoids generation of triphenylphosphine oxide, a recalcitrant byproduct of the Mitsunobu reaction,¹²⁸ provided DTBA-HCl in an overall yield of 56%. In both routes, the product of every step is a white solid.

DTBA has desirable physicochemical properties. Its HCl salt is a nearly odorless white solid with high solubility in water. Using a pH-titration monitored by ultraviolet spectroscopy,^{116,129} we determined the thiol pK_a values of DTBA to be 8.2 ± 0.2 and 9.3 ± 0.1

(Figure 2.3; Table 2.1). These values are ~ 1 unit lower than those of DTT. This difference is comparable to that between cysteamine and β ME, and likely results from the strong Coulombic and inductive effects of the protonated amino group. By equilibrating reduced DTBA with oxidized DTT and using HPLC to quantify reduced and oxidized species, we found the reduction potential of oxidized DTBA to be $E^{\circ'} = (-0.317 \pm 0.002)$ V (Figure 2.4; Table 2.1). This $E^{\circ'}$ value is slightly more than that of DTT, consistent with more acidic thiols forming less stable disulfide bonds¹⁰¹ and with the preorganization of DTT for disulfide-bond formation by its hydroxyl groups, which can form an intramolecular hydrogen bond and manifest a *gauche* effect.



Scheme 2.1 Synthetic route to DTBA

DTBA is an efficacious reducing agent for disulfide bonds in small molecules. We found that DTBA reduces the disulfide bond in oxidized β ME 3.5-fold faster than does DTT at pH 7.0,

and 4.4-fold faster at pH 5.5 (Figure 2.1A). These rate accelerations are commensurate with the lower thiol pK_a of DTBA. At pH 7.0, DTBA reduces oxidized L-glutathione 5.2-fold more rapidly than does DTT (Figure 2.1B). As oxidized L-glutathione has a net charge of -2 near neutral pH, a favorable Coulombic interaction could contribute to this higher rate acceleration.

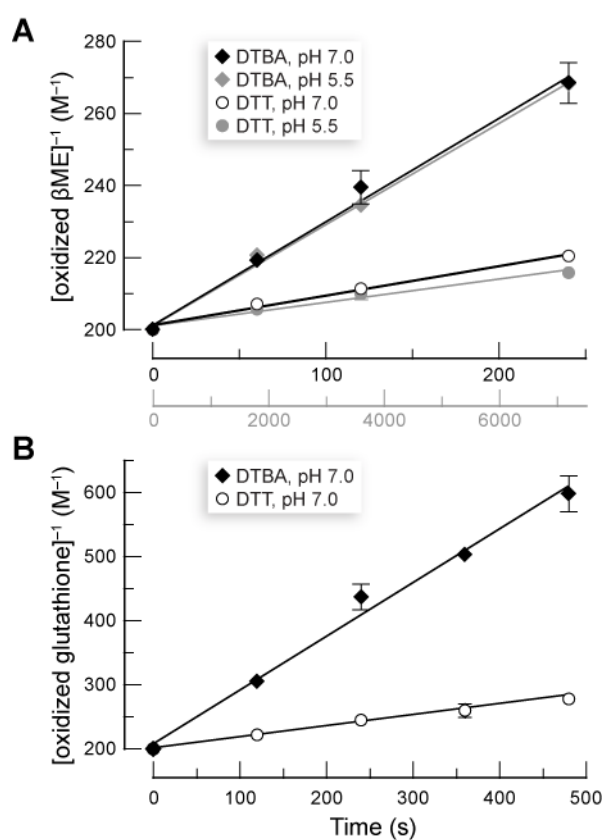


Figure 2.1 Time-course for the reduction of a mixed disulfide in small molecules by DTBA and DTT in 50 mM potassium phosphate buffer. (A) Reduction of oxidized β ME; $k_{obs}^{DTBA}/k_{obs}^{DTT} = 3.5$ at pH 7.0; $k_{obs}^{DTBA}/k_{obs}^{DTT} = 4.4$ at pH 5.5. (B) Reduction of oxidized L-glutathione; $k_{obs}^{DTBA}/k_{obs}^{DTT} = 5.2$ at pH 7.0.

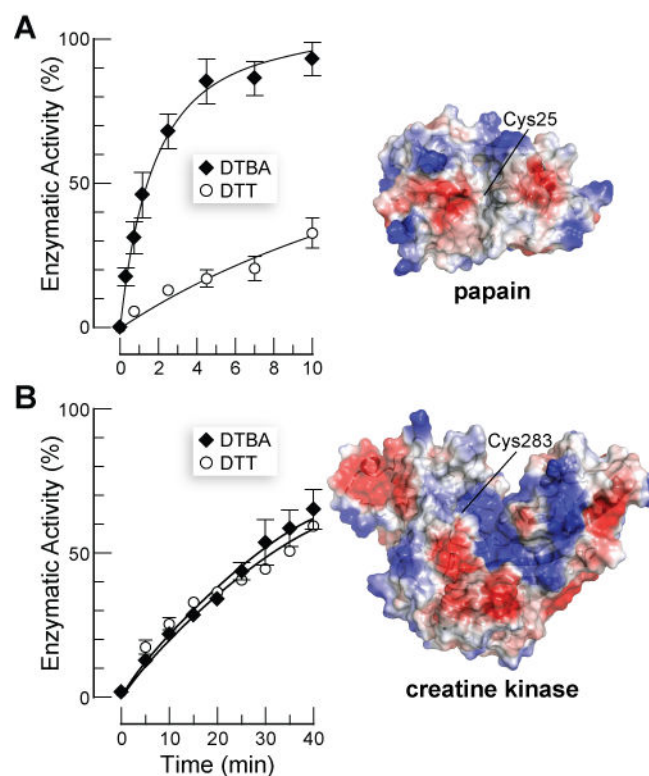


Figure 2.2 Time-course for the reduction of a mixed disulfide in enzymatic active sites by DTBA and DTT in 0.1 M imidazole-HCl buffer, pH 7.0, containing EDTA (2 mM). (A) Reduction of papain-Cys35-S-S-CH₃; $k_{obs}^{DTBA}/k_{obs}^{DTT} = 14$. (B) Reduction of creatine kinase-Cys283-S-S-L-glutathione; $k_{obs}^{DTBA}/k_{obs}^{DTT} = 1.1$. Insets: Electrostatic potential maps with red = anionic and blue = cationic, as generated by the program PyMOL (Schrodinger, Portland, OR) using PDB entries 1ppn¹³³ and 2crk¹³⁴.

DTBA is also an efficacious reducing agent for disulfide bonds in proteins. A cysteine residue resides within the active site of papain (Cys25) and near that of creatine kinase (Cys283). Forming a mixed disulfide with those cysteine residues is known to eliminate their enzymatic activities.^{14,130,131} These two enzymes differ, however, in the electrostatic environment of their active sites. The active site of papain is hydrophobic like its substrates, though there is an anionic region nearby (Figure 2.2A).^{132,133} In contrast, the active site of creatine kinase is cationic, complementary to its anionic substrates (Figure 2.2B).¹³⁴⁻¹³⁷ We found that DTBA reduces a

disulfide bond in the hydrophobic/anionic active site of papain 14-fold faster than does DTT (Figure 2.2A). In contrast, the two reagents reduce a disulfide bond near the cationic active site of creatine kinase at a similar rate.

2.5 Conclusions

The amino group of DTBA confers additional benefits. For example, a disulfide-reducing agent that can be readily isolated, regenerated, and reused incurs less cost and generates less waste.^{49,52,54} Moreover, extraneous disulfide bonds absorb light at 280 nm, which can confound standard measurements of protein concentration.¹³⁸ We reasoned that DTBA could be isolated by its absorption to a cation-exchange resin. Indeed, >99% of DTBA (but <1% of DTT) was removed from a sodium phosphate buffer, pH 8.0, upon addition of Dowex 50 resin. We also note that the amino group of DTBA enables its covalent attachment to a soluble molecule, resin, or surface by simple reactions, such as reductive amination (which preserves the cationic charge) or *N*-acylation. We conclude that the attributes of DTBA could enable it to supplant DTT as the preferred reagent for reducing disulfide bonds in biomolecules.

2.6 Acknowledgements

We are grateful to Professor W. W. Cleland and S. B. Johnston for enabling advice, and to N. McElfresh for preliminary work on this project. M.J.P. was supported by Molecular and Cellular Pharmacology Training Grant T32 GM008688 (NIH) and predoctoral fellowship 09PRE2260125 (American Heart Association). This work was supported by Grant R01 GM044783 (NIH).

2.7 Materials and Methods

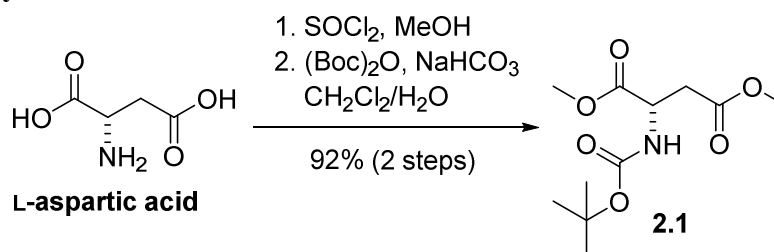
2.7.1 General

Commercial reagents were used without further purification. Dithiothreitol (DTT) was from Research Products International (Mt. Prospect, IL). Bis(2-mercaptoethyl)sulfone (BMS) was from Santa Biotechnology (Santa Cruz, CA). Papain (lyophilized powder from papaya latex), creatine kinase Cruz (lyophilized powder from rabbit muscle), hexokinase (lyophilized powder from *Saccharomyces cerevisiae*), glucose-6-phosphate dehydrogenase (ammonium sulfate suspension from baker's yeast), *N*_α-benzoyl-L-arginine-4-nitroanilide hydrochloride, (*S*)-methyl methanethiosulfonate (Kenyon's reagent), *trans*-4,5-dihydroxy-1,2-dithiane (oxidized DTT), oxidized L-glutathione, oxidized 2-mercaptoethanol, and DOWEX 50WX4-400 ion-exchange resin were from Sigma Chemical (St. Louis, MO). Bis(2-mercaptoethyl) sulfone disulfide (oxidized BMS) was synthesized as reported previously.²⁹

All glassware was oven or flame-dried, and reactions were performed under N₂(g) unless stated otherwise. Dichloromethane, diethyl ether, and tetrahydrofuran were dried over a column of alumina. Dimethylformamide and triethylamine were dried over a column of alumina and purified further by passage through an isocyanate scrubbing column. Flash chromatography was performed with columns of 40–63 Å silica, 230–400 mesh (Silicycle, Québec City, Canada). Thin-layer chromatography (TLC) was performed on plates of EMD 250-μm silica 60-F₂₅₄. The term “concentrated under reduced pressure” refers to the removal of solvents and other volatile materials using a rotary evaporator at water aspirator pressure (<20 torr) while maintaining the water-bath temperature below 40 °C. Residual solvent was removed from samples at high

vacuum (<0.1 torr). The term “high vacuum” refers to vacuum achieved by a mechanical belt-drive oil pump. ^1H NMR spectra were acquired at ambient temperature with a Bruker DMX-400 Avance spectrometer at the National Magnetic Resonance Facility at Madison (NMRFAM) and referenced to TMS or residual protic solvent. ^{13}C NMR spectra were acquired with a Varian MercuryPlus 300 and referenced to residual protic solvent. Electrospray ionization (ESI) mass spectrometry was performed with a Micromass LCT at the Mass Spectrometry Facility in the Department of Chemistry at the University of Wisconsin–Madison. Ellman’s assay for sulfhydryl groups was performed with a Varian Cary 50 Bio UV–Vis spectrophotometer. UV absorbance spectra of oxidized DTBA and oxidized DTT were acquired with a Varian Cary 300 Bio UV–Vis spectrophotometer. Thiol $\text{p}K_{\text{a}}$ values were determined by using a Varian Cary 50 Bio UV–Vis spectrophotometer. Equilibrium, reduction potential, and kinetic studies on peptides and small molecules were performed on an analytical HPLC (Waters system equipped with a Waters 996 photodiode array detector, Empower 2 software and a Varian C18 reverse phase column). Kinetic studies on proteins were carried out using a Varian Cary 300 Bio UV–Vis spectrometer with a Cary temperature controller.

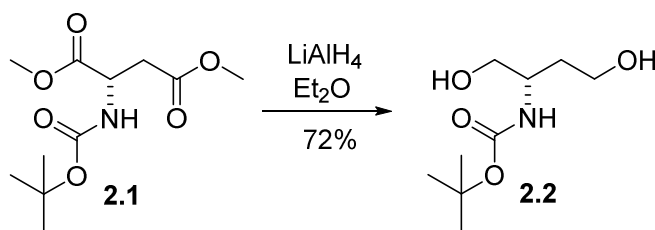
2.7.2 Chemical Synthesis



L-Aspartic acid (5.002 g, 37.58 mmol) was added to an oven-dried round-bottom flask and placed under an atmosphere of dry $\text{N}_2(\text{g})$. The starting material was then dissolved partially

with 60 mL of anhydrous methanol, and the mixture was cooled to 0 °C. Once the desired temperature was reached, thionyl chloride (8.2 mL, 110 mmol) was added drop-wise. After the addition was complete, the reaction mixture became homogenous, and was warmed slowly to room temperature and left to stir for 14 h. The reaction mixture was then concentrated under reduced pressure, and the resulting diester was dissolved in 150 mL of DCM and 100 mL of water. To this biphasic solution was added sodium bicarbonate (4.212 g, 50.14 mmol) and di-*t*-butyl dicarbonate (9.841 g, 45.09 mmol), and the reaction mixture was heated at reflux for 4 h. After the reaction was confirmed to be complete by TLC, the reaction mixture was allowed to cool to room temperature. The organic layer was separated, and the aqueous layer was extracted three times with 150 mL of DCM. The organic extracts were combined, washed with 250 mL of saturated NaCl(aq), dried over MgSO₄(s), and concentrated under reduced pressure. Flash chromatography (35% v/v ethyl acetate in hexanes) was used to isolate **2.1** as a white solid (9.080 g, 92%, 2 steps).

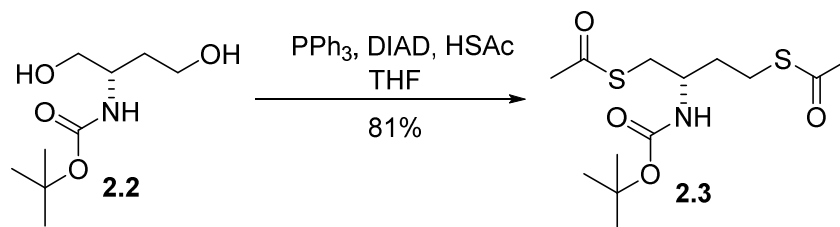
¹H NMR (400 MHz, CDCl₃) δ = 5.49 (d, J = 8.3 Hz, 1H), 4.60–4.57 (m, 1H), 3.76 (s, 3H), 3.70 (s, 3H), 3.01 (dd, J = 17, 4.4 Hz, 1H), 2.83 (dd, J = 17.0, 4.7), 1.45 (s, 9H); **¹³C NMR (75 MHz, CDCl₃)** δ = 171.6, 171.5, 155.5, 80.3, 52.8, 52.1, 50.0, 36.8, 28.4; **HRMS (ESI)** calculated for [C₁₁H₁₉NO₆Na]⁺ (M+Na⁺) requires m/z = 284.1105, found 284.1113.



An oven-dried round-bottom flask was charged with lithium aluminum hydride (0.870 g, 22.9 mmol) and placed under an atmosphere of dry N₂(g). The flask was cooled to 0 °C in an ice bath, and 100 mL of anhydrous diethyl ether was added. In a separate dry round-bottom flask, compound **2.1** (2.021 g, 7.735 mmol) was dissolved in 50 mL of anhydrous diethyl ether. Sonication was required to make the solution completely homogenous. The ester was then added drop-wise to the reaction mixture. Once the addition was complete, the reaction mixture was stirred at 0 °C for an additional 30 min, warmed to room temperature, and allowed to react for an additional 2 h. Subsequently, the reaction mixture was quenched at 0 °C by the slow, sequential addition of 0.87 mL of water, 0.87 mL of 15% w/w NaOH, and 2.6 mL of water. The mixture was left to stir at room temperature for 1 h. The aluminum salts were collected by vacuum filtration, and subjected to continuous solid–liquid extractions with dichloromethane using a Soxhlet apparatus. The organic extracts and the original organic filtrate were combined and concentrated under reduced pressure. Flash chromatography (ethyl acetate) was used to isolate **2.2** as a white solid (1.310 g, 82%). Compound **3** had been prepared from L-aspartic acid by a different route.¹²⁷

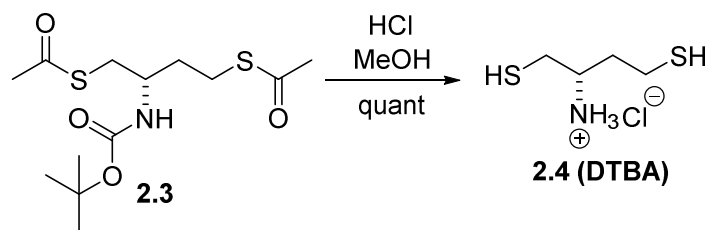
¹H NMR (400 MHz, DMSO-*d*₆) δ = 6.46 (d, *J* = 8.8 Hz, 1H), 4.56 (t, *J* = 5.7 Hz, 1H), 4.34 (t, *J* = 5.1 Hz, 1H), 3.46–3.37 (m, 3H), 3.32 (dt, *J* = 10.6, 5.4 Hz, 1H), 3.23 (dt, *J* = 10.6, 5.9 Hz, 1H), 1.69–1.61 (m, 1H), 1.45–1.37 (m, 1H), 1.37 (s, 9H); **¹³C NMR (75 MHz, CDCl₃)** δ =

157.2, 80.1, 65.4, 58.9, 49.5, 35.0, 28.5; **HRMS** (ESI) calculated for $[\text{C}_9\text{H}_{19}\text{NO}_4\text{Na}]^+$ ($\text{M}+\text{Na}^+$) requires $m/z = 228.1207$, found 228.1201.



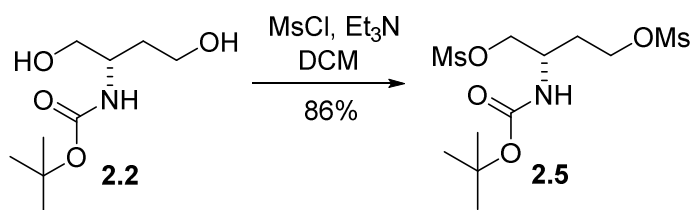
A dry round-bottom flask was charged with triphenylphosphine (1.711 g, 6.523 mmol) and placed under an atmosphere of dry $\text{N}_2(\text{g})$. Anhydrous THF (27 mL) was then added, and the solution was placed in an ice bath and cooled to 0 °C. Diisopropyl azodicarboxylate (1.3 mL, 6.6 mmol) was added drop-wise to the flask. Once the addition was complete, the reaction mixture was allowed to stir for an additional 20 min. Compound **2.2** (0.559 g, 2.72 mmol) in 10 mL of dry THF and thioacetic acid (0.47 mL, 6.6 mmol) was then added with stirring. The reaction mixture was stirred at 0 °C for 1 h, and then at room temperature for 16 h. (Longer reaction times resulted in lower yields.) The mixture was concentrated under reduced pressure. Flash chromatography (30% v/v ethyl acetate in hexanes) was used to isolate **2.3** as a white solid (0.711 g, 81%). Compound **2.3** had been prepared from L-aspartic acid by a different route.¹²⁷

^1H NMR (400 MHz, CDCl_3) $\delta = 4.59$ (d, $J = 7.9$ Hz, 1H), 3.85–3.76 (m, 1H), 3.12–2.95 (m, 3H), 2.82 (ddd, $J = 13.7, 8.5, 7.1$ Hz, 1H), 2.36 (s, 3H), 2.33 (s, 3H), 1.84–1.75 (m, 1H), 1.74–1.64 (m, 1H), 1.44 (s, 9H); **^{13}C NMR (75 MHz, CDCl_3)** $\delta = 195.9, 195.6, 155.6, 79.7, 50.1, 34.5, 33.8, 30.73, 30.71, 28.5, 25.9$; **HRMS** (ESI) calculated for $[\text{C}_{13}\text{H}_{23}\text{NO}_4\text{S}_2\text{Na}]^+$ ($\text{M}+\text{Na}^+$) requires $m/z = 344.0961$, found 344.0962.



Compound **2.3** (0.601 g, 1.87 mmol) was added to a flame-dried round-bottom flask under dry N₂(g). Anhydrous methanol (20 mL) was added, followed by 10 mL of 3 N HCl in methanol. The reaction mixture was heated at reflux for 4 h, concentrated under reduced pressure, and stored *in vacuo* with P₂O₅ and KOH for 48 h. (Scratching the bottom of the flask facilitated crystal formation.) Compound **2.4** (DTBA·HCl) was rinsed with cold toluene, and isolated by vacuum filtration as a white solid (0.320 g, quant). DTBA made in this manner was determined to be 99% pure according to Ellman's assay for sulfhydryl groups (*vide infra*).

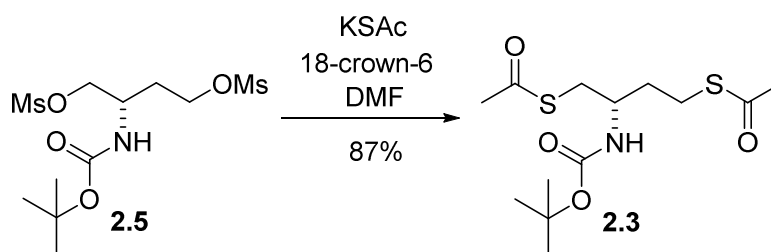
¹H NMR (400 MHz, DMSO-*d*₆) δ = 8.29 (s, 3H), 3.34–3.32 (m, 1 H), 2.96 (t, *J* = 8.7 Hz, 1H), 2.81–2.75 (m, 2H), 2.60–2.56 (m, 3H), 1.95–1.86 (m, 2H); ¹³C NMR (75 MHz, DMSO-*d*₆) δ = 51.2, 35.0, 26.0, 19.6; HRMS (ESI) calculated for [C₄H₁₂NS₂]⁺ (M⁺) requires *m/z* = 138.0406, found 138.0405.



A dry round-bottom flask was charged with **2.2** (1.178 g, 5.739 mmol) and placed under dry N₂(g). Anhydrous DCM (125 mL) was then added, and the solution was cooled to 0 °C. Triethylamine (4.0 mL, 29 mmol) was added, followed by slow drop-wise addition of

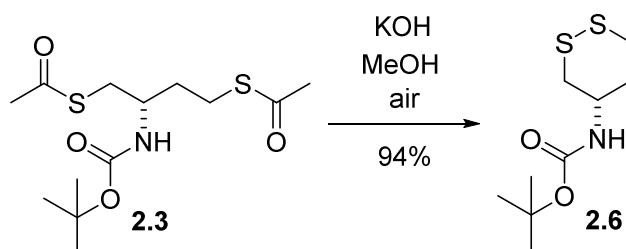
methanesulfonyl chloride (MsCl) (1.0 mL, 13 mmol). After stirring at 0 °C for 30 min, the reaction mixture was allowed to warm slowly to room temperature and left to react for an additional 30 min. The reaction mixture was quenched by the addition 100 mL of water, and extracted with DCM. The combined organic extracts were washed with brine, dried over MgSO₄(s), and concentrated under reduced pressure. Flash chromatography (60% v/v ethyl acetate in hexanes) was used to isolate **2.5** as a white solid (1.782 g, 86%).

¹H NMR (400 MHz, CDCl₃) δ = 4.81 (d, *J* = 9.7 Hz, 1H), 4.39–4.26 (m, 4H), 4.10–4.05 (m, 1H), 3.06 (s, 3H), 3.05 (s, 3H), 2.13–1.96 (m, 2H), 1.48 (s, 9H); **¹³C NMR (75 MHz, CDCl₃)** δ = 155.4, 80.6, 71.0, 66.3, 47.0, 37.7, 37.6, 31.2, 28.5; **HRMS (ESI)** calculated for [C₁₁H₂₃NO₈S₂Na]⁺ (M+Na⁺) requires *m/z* = 384.0758, found 384.0775.



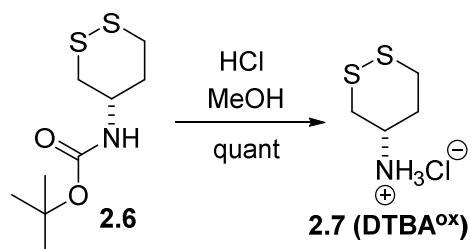
Compound **2.5** (0.610 g, 1.688 mmol), potassium thioacetate (0.482 g, 4.22 mmol), and 18-crown-6 (1.351 g, 5.111 mmol) were added to a dry round-bottom flask and dissolved with 150 mL of anhydrous DMF. The reaction mixture was stirred under dry N₂(g) for 24 h. The DMF was removed under reduced pressure. Flash chromatography (30% v/v ethyl acetate in hexanes) was used to isolate **2.3** as a white solid (0.475 g, 87%). Compound **2.3** had been prepared from L-aspartic acid by a different route.¹²⁷

¹H NMR (400 MHz, CDCl₃) δ = 4.59 (d, J = 7.9 Hz, 1H), 3.85–3.76 (m, 1H), 3.12–2.95 (m, 3H), 2.82 (ddd, J = 13.7, 8.5, 7.1 Hz, 1H), 2.36 (s, 3H), 2.33 (s, 3H), 1.84–1.75 (m, 1H), 1.74–1.64 (m, 1H), 1.44 (s, 9H); **¹³C NMR (75 MHz, CDCl₃)** δ = 195.9, 195.6, 155.6, 79.7, 50.1, 34.5, 33.8, 30.73, 30.71, 28.5, 25.9; **HRMS (ESI)** calculated for [C₁₃H₂₃NO₄S₂Na]⁺ (M+Na⁺) requires m/z = 344.0961, found 344.0962.



Compound 4 (0.482 g, 1.50 mmol) and potassium hydroxide (0.340 g, 6.06 mmol) were dissolved in 50 mL of methanol, and the resulting solution was stirred for 16 h while bubbling a light stream of air through the solution. The methanol was removed under reduced pressure, and the mixture was extracted with DCM, washed with brine, and dried over MgSO₄(s). Flash chromatography (20% v/v ethyl acetate in hexanes) was used to isolate 7 as a white solid (0.331 g, 94%).

¹H NMR (400 MHz, DMSO-*d*₆) δ = 7.08 (d, J = 7.9 Hz, 1H), 3.53–3.41 (m, 1H), 3.07–3.01 (m, 1H), 2.91–2.85 (m, 2H), 2.60 (dd, J = 13.0, 10.5 Hz, 1 H), 2.08–2.03 (m, 1H), 1.67–1.57 (m, 1H), 1.38 (s, 9H); **¹³C NMR (75 MHz, DMSO-*d*₆)** δ = 155.2, 78.7, 49.3, 37.9, 34.9, 34.5, 28.9; **HRMS (ESI)** calculated for [C₉H₁₇NO₂S₂]⁺ (M⁺) requires m/z = 258.0593, found 258.0602.



Compound **2.6** (0.402 g, 1.71 mmol) was added to a round-bottom flask. Anhydrous methanol (20 mL) was added, followed by 10 mL of 3 N HCl in methanol. The reaction mixture was heated at reflux for 4 h under N₂(g), concentrated under reduced pressure, and stored *in vacuo* with P₂O₅ and KOH for 24 h. (Scratching the bottom of the flask facilitated crystal formation.) Compound **2.7**, oxidized DTBA·HCl, was isolated as a white solid (0.289 g, quant).

¹H NMR (400 MHz, DMSO-*d*₆) δ = 8.29 (s, 3H), 3.43–3.37 (m, 1H), 3.15–3.08 (m, 2H), 3.02–2.96 (m, 1H), 2.88 (dd, *J* = 13.1, 10.6 Hz, 1H), 2.32–2.28 (m, 1H), 1.85–1.77 (m, 1H); ¹³C NMR (75 MHz, DMSO-*d*₆) δ = 48.7, 34.6, 32.8, 31.5; HRMS (ESI) calculated for [C₄H₁₀NS₂]⁺ (M⁺) requires *m/z* = 136.0250, found 136.0249.

2.7.3 Purity of DTBA assessed by Ellman's assay for sulfhydryl groups

A reaction buffer (0.10 M sodium phosphate buffer, pH 8.0, containing 1 mM EDTA) was prepared by the Pierce protocol. Ellman's reagent solution was primed by adding Ellman's reagent (4 mg) to 1 mL of the reaction buffer. A 2.50 × 10⁻⁴ M solution of DTBA was then prepared using the reaction buffer. Ellman's reagent solution (50 μL) was added to each of two vials containing 2.5 mL of reaction buffer. Reaction buffer (250 μL) was added to one of these vials, and its absorbance at 412 nm was used as a blank. DTBA solution (250 μL) was added to the other vial. After 10 min, its absorbance at 412 nm was recorded. Using Beer's law (*c* =

$A/(\epsilon \cdot l)$ with $A = 0.623$, $l = 1$ cm, and $\epsilon = 14,150 \text{ M}^{-1}\text{cm}^{-1}$) gave a thiol concentration of 4.40×10^{-5} M. Because DTBA contains two thiol groups, the assay solution had a DTBA concentration of 2.20×10^{-5} M. Accounting for dilution and using the equation $M_1 \cdot V_1 = M_2 \cdot V_2$, where $V_1 = 2.50 \times 10^{-4}$ L, $M_2 = 2.20 \times 10^{-5}$ M, and $V_2 = 2.8 \times 10^{-3}$ L, yielded $M_1 = 2.46 \times 10^{-4}$ M and thus a DTBA purity of $(2.46 \times 10^{-4} \text{ M}) / (2.50 \times 10^{-4} \text{ M}) \times 100\% = 98.4\%$. Three repetitions of this assay gave $(99 \pm 1)\%$ purity. This assay revealed that commercial DTT and BMS had $>98\%$ purity.

2.7.3 Determination of thiol pK_a values

The thiol pK_a values of DTBA were determined by measuring its absorbance at 238 nm in solutions of various pH. The deprotonated thiolate absorbs much more strongly at 238 nm than does its protonated counterpart.¹²⁹ This attribute was exploited for determining thiol pK_a values as described previously.¹¹⁶ Buffered stock solutions of K_3PO_4 , K_2HPO_4 , and KH_2PO_4 (100 mM) were degassed and flushed with $N_2(g)$ for 1 h immediately prior to use. A stock solution of DTBA (1.5 mM) in KH_2PO_4 was then prepared. Various combinations of the buffered stock solutions were combined in duplicate to give two identical sets of 1-mL solutions of pH 5.5–11. KH_2PO_4 stock solution (70 μL) was added to each replicate pair of solutions and used to set the A_{238} to zero. Dithiol solution (70 μL) was then added to its complementary 1-mL vial, and its absorbance at 238 nm was recorded. The pH of the solution was then immediately measured using a Beckman pH meter, which had been calibrated prior to use with pH 7 and pH 10 standard solutions from Fisher Scientific. This process was repeated multiple times to obtain a plot of A_{238} vs pH (**Figure 2.3**).

pK_a values were determined by fitting the data in **Figure 2.3** to eq 2.1, which is derived from Beer's law and the definition of the acid dissociation constant.¹¹⁶ In eq 2.1, C_T is total thiol concentration, ϵ_{SH}^{SH} is the extinction coefficient of the doubly protonated form, ϵ_{SH}^{S-} is the extinction coefficient of the singly protonated form, and ϵ_{S-}^{S-} is the extinction coefficient of the unprotonated form. Both pK_a values and extinction coefficients were determined from the curve fit with the program Prism 5.0 (GraphPad Software, La Jolla, CA).

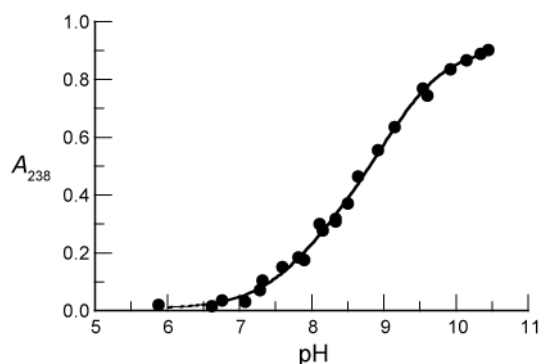


Figure 2.3 Effect of pH on absorbance at 238 nm of DTBA (0.10 mM) in 0.10 M potassium phosphate buffer. Fitting the data to equation 2.1 yielded pK_a values of 8.2 ± 0.2 and 9.3 ± 0.1 , and extinction coefficients of $\epsilon_{SH}^{SH} = 83.27 \text{ M}^{-1}\text{cm}^{-1}$, $\epsilon_{SH}^{S-} = 3436 \text{ M}^{-1}\text{cm}^{-1}$, and $\epsilon_{S-}^{S-} = 9169 \text{ M}^{-1}\text{cm}^{-1}$ with $r^2 > 0.99$.

$$A_{238} = C_T \left(\frac{\epsilon_{S-}^{S-} 10^{\text{pH}-pK_{a2}} + \epsilon_{SH}^{S-} + \epsilon_{SH}^{SH} 10^{pK_{a1}-\text{pH}}}{10^{\text{pH}-pK_{a2}} + 1 + 10^{pK_{a1}-\text{pH}}} \right) \quad (2.1)$$

2.7.4 Reduction potential of DTBA

The reduction potential (E°) of DTBA was determined by using HPLC to determine the equilibrium constant for its reaction with oxidized DTT (eq 2.2), and then inserting this value into a variation of the Nernst equation (eq 2.3).²⁹ Data were obtained by a procedure similar to that described previously.^{29,116} DTBA (10.5 mg, 0.06 mmol) and oxidized DTT (9.2 mg, 0.06 mmol) were added to a 25-mL round-bottom flask. The flask was then flushed with $N_2(g)$ for 30 min.

$$K_{eq} = \frac{[DTT][\text{oxidized DTBA}]}{[DTBA][\text{oxidized DTT}]} = \frac{[DTT]^2}{[\text{oxidized DTT}]^2} \quad (2.2)$$

$$E_{DTBA}^{o'} = E_{DTT}^{o'} - \frac{RT}{nF} \ln \frac{[DTT]^2}{[\text{oxidized DTT}]^2} \quad (2.3)$$

A 50 mM stock solution of potassium phosphate buffer (pH 7) was degassed and purged with $N_2(g)$ for 30 min immediately prior to use. Buffer (15 mL) was added, and the reaction mixture was stirred under $N_2(g)$ for 24 h at room temperature. The reaction mixture was then quenched by the addition of 3 N HCl (1:100 dilution). The reaction mixture was passed through a 4.5- μm filter, and 100 μL of the reaction mixture was analyzed immediately by HPLC using a Waters system equipped with a Waters 996 photodiode array detector, Empower 2 software, and a Varian C18 reverse-phase column. The column was eluted at 1.0 mL/min with water (5.0 mL), followed by a linear gradient (0–40% v/v) of acetonitrile/water over 40 min. Compounds were detected by their absorbance at 205 nm. Reduced and oxidized DTBA are highly polar and elute

from the column immediately (as confirmed by LC–MS). Two peaks, however, were clearly visible in the chromatogram (Figure 2.4). HPLC analysis of standards revealed that the two peaks were reduced DTT (retention time: 19 min) and oxidized DTT (retention time: 23 min). Calibration curves were generated and found to be linear over the used concentration range. From these curves, the equilibrium concentrations of reduced and oxidized DTT were determined, and a $K_{\text{eq}} = 0.469 \pm 0.131$ for the reaction was found. Assuming that DTT has $E^{\circ'} = -0.327 \text{ V}$,²⁴ eq 3 (which is a variation of the Nernst equation) was used to calculate that DTBA has $E^{\circ'} = -(0.317 \pm 0.002) \text{ V}$. This value is the mean \pm SE from seven experiments. The reverse reaction between oxidized DTBA and reduced DTT revealed that equilibrium had been established under the experimental conditions.

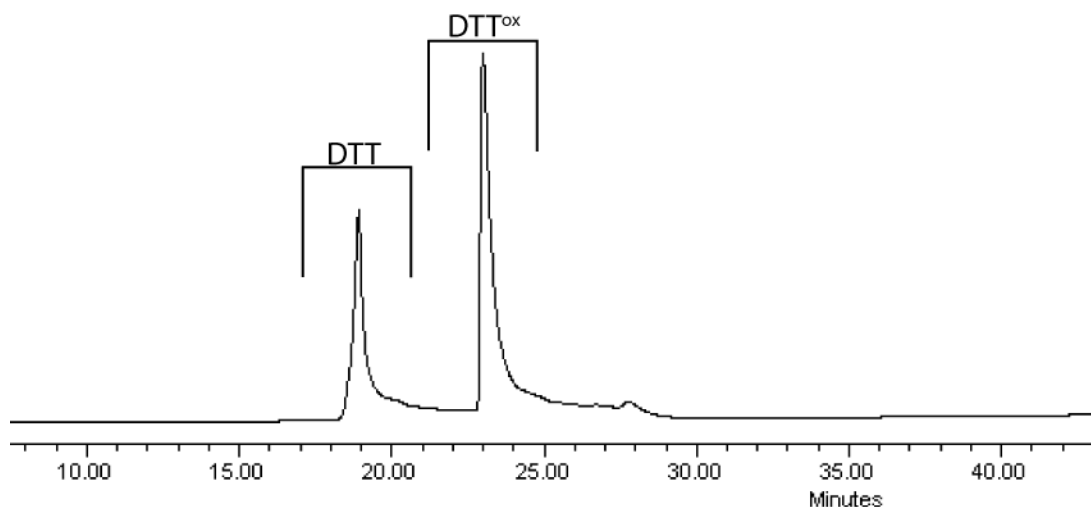


Figure 2.4 Representative HPLC chromatogram of the redox equilibrium between DTBA and DTT^{ox}. Compounds were detected by their absorbance at 205 nm.

2.7.5 Reduction potential of BMS

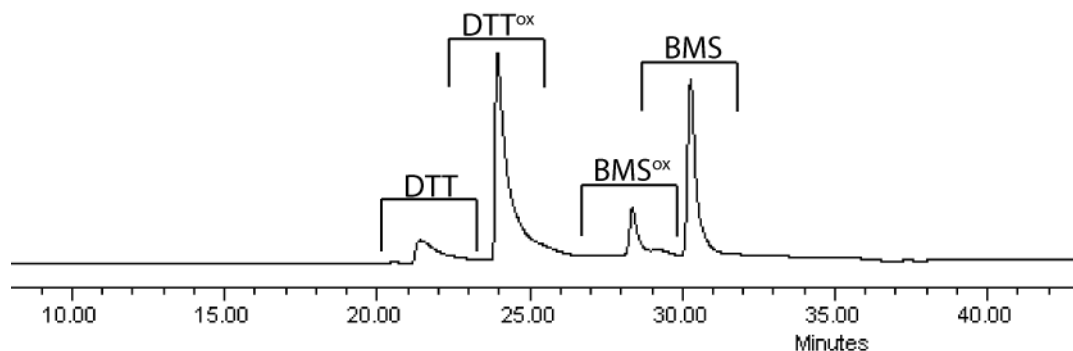


Figure 2.5 Representative HPLC chromatogram of the redox equilibrium between BMS and DTT^{ox}. Compounds were detected by their absorbance at 205 nm.

The procedure described in Section V was also performed with BMS. With $K_{eq} = 0.0517 \pm 0.0194$ and assuming $E^{\circ'} = -0.327$ V for DTT,²⁴ BMS was found to have $E^{\circ'} = (-0.291 \pm 0.002)$ V, which was again the mean \pm SE from seven experiments. The reduction potential for BMS was reported previously to be $E^{\circ'} = -0.31$ V.²⁹

2.7.6 Kinetic studies on the reduction potential of oxidized β ME

$$-\frac{\partial[\text{disulfide}]_{\text{total}}}{\partial t} = k_{\text{obs}}[\text{disulfide}]_{\text{total}}[\text{thiol}]_{\text{total}}$$

The observed second-order rate constant (k_{obs}) for a thiol–disulfide interchange reaction was determined by adapting a procedure describe previously.²⁶ For disulfide = oxidized β ME, a 50 mM stock solution of potassium phosphate buffer was degassed and purged with $\text{N}_2(\text{g})$ for 30 min immediately prior to use. A stock solution of oxidized β ME (10 mM) in 50 mM potassium phosphate buffer, pH 7.0, was purged with $\text{N}_2(\text{g})$ for 30 min immediately prior to use.

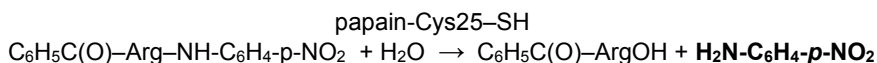
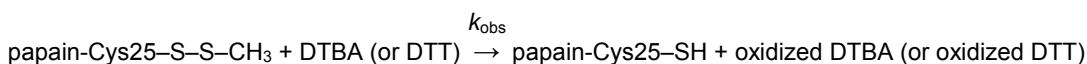
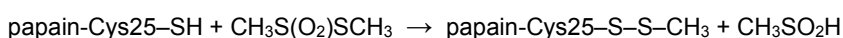
A 25-mL round-bottom flask was charged with DTBA (4.3 mg, 0.025 mmol) or DTT (3.9 mg, 0.025 mmol), and placed under $N_2(g)$. Phosphate buffer (2.5 mL) was added to the round-bottom flask containing the dithiol. Oxidized β ME stock solution (2.5 mL) was then added, and the reaction mixture was stirred at room temperature under $N_2(g)$ for 1 min. The reaction mixture was quenched by the addition of 0.10 mL of 3 N HCl. The reaction mixture was passed through a 4.5- μ m filter, and 100 μ L of the reaction mixture was analyzed immediately by HPLC using a Varian C18 reverse-phase column. The column was eluted at 1.0 mL/min with water (5.0 mL), followed by a linear gradient (0–40% v/v) of acetonitrile/water over 40 min. The extent of reduction was determined by integrating the newly formed peak corresponding to β ME at 205 nm (retention time: 8 min). This process was repeated for reaction times of 2 and 4 min. Calibration curves were generated and found to be linear over the used concentration range. The amount of residual oxidized β ME was calculated, and second-order rate constants were calculated from a linear fit of the data in Figure 2.1A (that is, $k_{\text{obs}} = [(1/c_{\text{final}}) - (1/c_{\text{initial}})]/t$). The initial values of concentration in the reaction mixture were [DTBA or DTT] = [oxidized β ME] = $c_{\text{initial}} = 5$ mM. Rate constants were the mean \pm SE from three experiments. DTBA: $k_{\text{obs}} = (0.29 \pm 0.02) \text{ M}^{-1}\text{s}^{-1}$ and DTT: $k_{\text{obs}} = (0.084 \pm 0.004) \text{ M}^{-1}\text{s}^{-1}$. The same procedure was performed for reactions at pH 5.5, giving DTBA: $k_{\text{obs}} = (0.0093 \pm 0.0003) \text{ M}^{-1}\text{s}^{-1}$ and DTT: $k_{\text{obs}} = (0.0021 \pm 0.0002) \text{ M}^{-1}\text{s}^{-1}$ (Figure 2.1A).

2.7.7 Kinetic studies on the reduction of oxidized L-glutathione

An experiment similar to above was conducted with disulfide = oxidized L-glutathione. Reactions were quenched at various time points (2, 4, 6, and 8 min) and 100 μ L was analyzed by

HPLC (1.0 mL/min with water (5.0 mL) in 0.1% v/v TFA, followed by a linear gradient (0–40% v/v) of acetonitrile in 0.1% v/v TFA over 40 min). The extent of reduction was determined by integrating the newly formed L-glutathione reduced peak at 220 nm (retention time of 7 min). Second-order rate constants were calculated from a linear fit of the data in Figure 2.1B (that is, $k_{\text{obs}} = [(1/c_{\text{final}}) - (1/c_{\text{initial}})]/t$). Rate constants were the mean \pm SE from three experiments. DTBA: $k_{\text{obs}} = (0.83 \pm 0.04) \text{ M}^{-1}\text{s}^{-1}$ and DTT: $k_{\text{obs}} = (0.16 \pm 0.02) \text{ M}^{-1}\text{s}^{-1}$.

2.7.8 Kinetic studies on the reactivation of papain



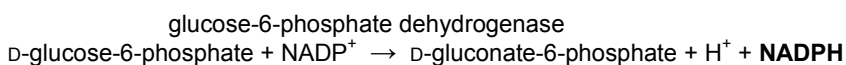
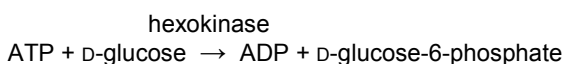
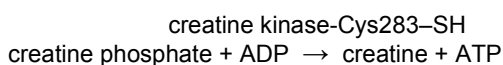
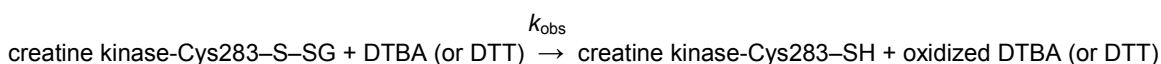
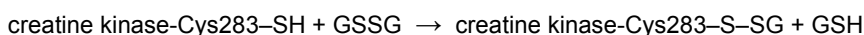
Cys25 near the active site of papaya latex papain was oxidized as a mixed disulfide by a procedure described previously.²⁷ Briefly, a stock solution of methyl methanethiosulfonate (3.5 mM) was prepared by dilution of 5 μL of methyl methanethiosulfonate with 15 mL of 0.10 M potassium phosphate buffer, pH 7.0, containing EDTA (2 mM). KCl (0.011 g, 0.15 mmol) was added to 1.5 mL of this stock solution. The solution was deoxygenated by bubbling $\text{N}_2(\text{g})$ through it for 15 min. Next, papain (5 mg, 150 units) was added, and the resulting solution was incubated at room temperature under $\text{N}_2(\text{g})$ for 12 h. Excess methyl methanethiosulfonate was removed by size-exclusion chromatography using a Sephadex G-25 column. The final concentration of papain was determined by A_{280} using $\epsilon_{280} = 5.60 \times 10^4 \text{ M}^{-1}\text{cm}^{-1}$.¹³⁹ A solution (0.26 mL) of the chromatographed protein was diluted with 4.94 mL of deoxygenated aqueous

buffer (0.10 M imidazole–HCl buffer, pH 7.0, containing 2 mM EDTA). Enzyme solution (1.25 mL) was then added to four separate vials. DTBA or DTT (10 μ L of a 1 mM solution) was added to one of the vials, and a timer was started. The initial concentrations in the reaction mixture were dithiol reducing agent: 7.9×10^{-6} M and inactive protein: 4.9×10^{-6} M. At various times, an 0.20-mL aliquot was removed from the reaction mixture and added to a cuvette of 0.8 mL of substrate solution (1.25 mM *N*-benzoyl-L-arginyl-*p*-nitroanilide in 0.10 M imidazole–HCl buffer, pH 6.0, containing 2 mM EDTA). The rate of change in absorbance at 410 nm was recorded at 25 °C. A unit of protein is defined by the amount of enzyme required to produce 1 μ mol/min of 4-nitroaniline. Using an extinction coefficient for 4-nitroaniline of $\epsilon = 8,800 \text{ M}^{-1} \text{ cm}^{-1}$ at 410 nm,¹⁴⁰ the number of units of active papain in solution at each time point was calculated. To determine the possible number of units of active papain in the reaction mixture, a large excess of DTT ($\sim 10^3$ -fold) was added to one vial and the activity was assessed. As a control, it was determined that the concentrations of DTT used had no bearing on the assay data other than activating the protein. y = enzymatic activity (%) at particular times was calculated by dividing the number of active units of enzyme by the possible number of units in the solution, and was plotted in Figure 2.2A. To determine the value of the second-order rate constant k_{obs} for the reducing agents, the second-order rate equation (eq 4) was transformed into eq 5, which was fitted to the data with the program Prism 5.0. In eq 4 and 5, $A_0 = [\text{inactive protein}]_{t=0}$, $A = [\text{inactive protein}]_t = A_0 - A_0 y$, $B_0 = [\text{reducing agent}]_{t=0}$, and $B = [\text{reducing agent}]_t = B_0 - A_0 y$. Values of k_{obs} were the mean \pm SE from three experiments. DTBA: $k_{\text{obs}} = (1275 \pm 69) \text{ M}^{-1} \text{ s}^{-1}$ and DTT: $k_{\text{obs}} = (90.4 \pm 5.2) \text{ M}^{-1} \text{ s}^{-1}$.

$$\frac{1}{B_0 - A_0} \ln \frac{A_0 B}{A B_0} = k_{\text{obs}} t \quad (2.4)$$

$$y = \frac{B_0 - B_0 e^{k_{\text{obs}} t (A_0 - B_0)}}{B_0 - A_0 e^{k_{\text{obs}} t (A_0 - B_0)}} \times 100\% \quad (2.5)$$

2.7.9 Kinetic studies on the reactivation of creatine kinase



Cys283 in the active site of rabbit muscle creatine kinase was oxidized as a mixed disulfide by a procedure described previously,²⁸ but with a slight modification in the measurement of active enzyme. A unit of enzyme was defined as the amount required to produce 1 $\mu\text{mol}/\text{min}$ of NADPH. Using an extinction coefficient for NADPH of $\varepsilon = 6.22 \text{ mM}^{-1}\text{cm}^{-1}$ at 340 nm, the units of active creatine kinase in solution at a particular time were calculated. To determine the possible number of units of active creatine kinase in the reaction mixture, a large excess of DTT ($\sim 10^3$ -fold) was added to one vial and the activity was assessed. As a control, it was determined that the concentrations of DTT used had no bearing on the assay data other than activating the protein. Enzymatic activity (%) at particular times was calculated by dividing the number of active units of enzyme by the possible number of units in the solution, and was plotted

in Figure 2.2B. Values of the second-order rate constant k_{obs} were determined by using eq 5 as described in Section IX, and were the mean \pm SE from three experiments. DTBA: $k_{\text{obs}} = (16.2 \pm 0.7) \text{ M}^{-1}\text{s}^{-1}$ and DTT: $k_{\text{obs}} = (14.7 \pm 0.4) \text{ M}^{-1}\text{s}^{-1}$.

2.7.10 Separation of DTBA using ion-exchange resin

A reaction buffer (0.10 M sodium phosphate, pH 8.0, 1 mM EDTA) was prepared. Ellman's reagent solution was prepared by adding Ellman's reagent (4 mg) to 1 mL of the reaction buffer. Next, to 25 mL of reaction buffer (0.10 M sodium phosphate, pH 8.0, 1 mM EDTA) was added DTBA (2.2 mg, 1.27×10^{-5} mol) and 1.7 g of DOWEX 50WX4-400 ion-exchange resin. The mixture was swirled for several minutes and filtered through a fritted syringe. Ellman's reagent solution (50 μL) was added to two separate vials containing 2.5 mL of reaction buffer. As a blank, 250 μL of reaction buffer was added to one of the vials, and the absorbance at 412 nm was set to zero. Filtrate (250 μL) was then added to the other vial and its absorbance was recorded. With $A_{412} = 0.012$ and using an extinction coefficient of $\epsilon = 14,150 \text{ M}^{-1}\text{cm}^{-1}$, it was calculated that >99% of DTBA was retained by the resin and thus removed from solution. The same assay was repeated with DTT, resulting in <1% being removed from solution.

2.7.11 Ultraviolet spectra of oxidized DTBA and oxidized DTT

Solutions of oxidized DTBA and DTT (1.0 mM) were prepared in Dulbecco's phosphate buffered saline (DPBS), and their ultraviolet spectra were recorded (**Figure 2.6**).

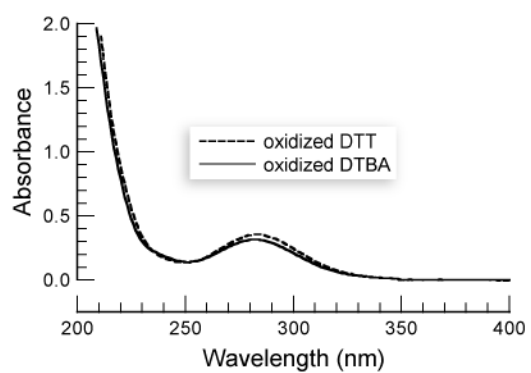
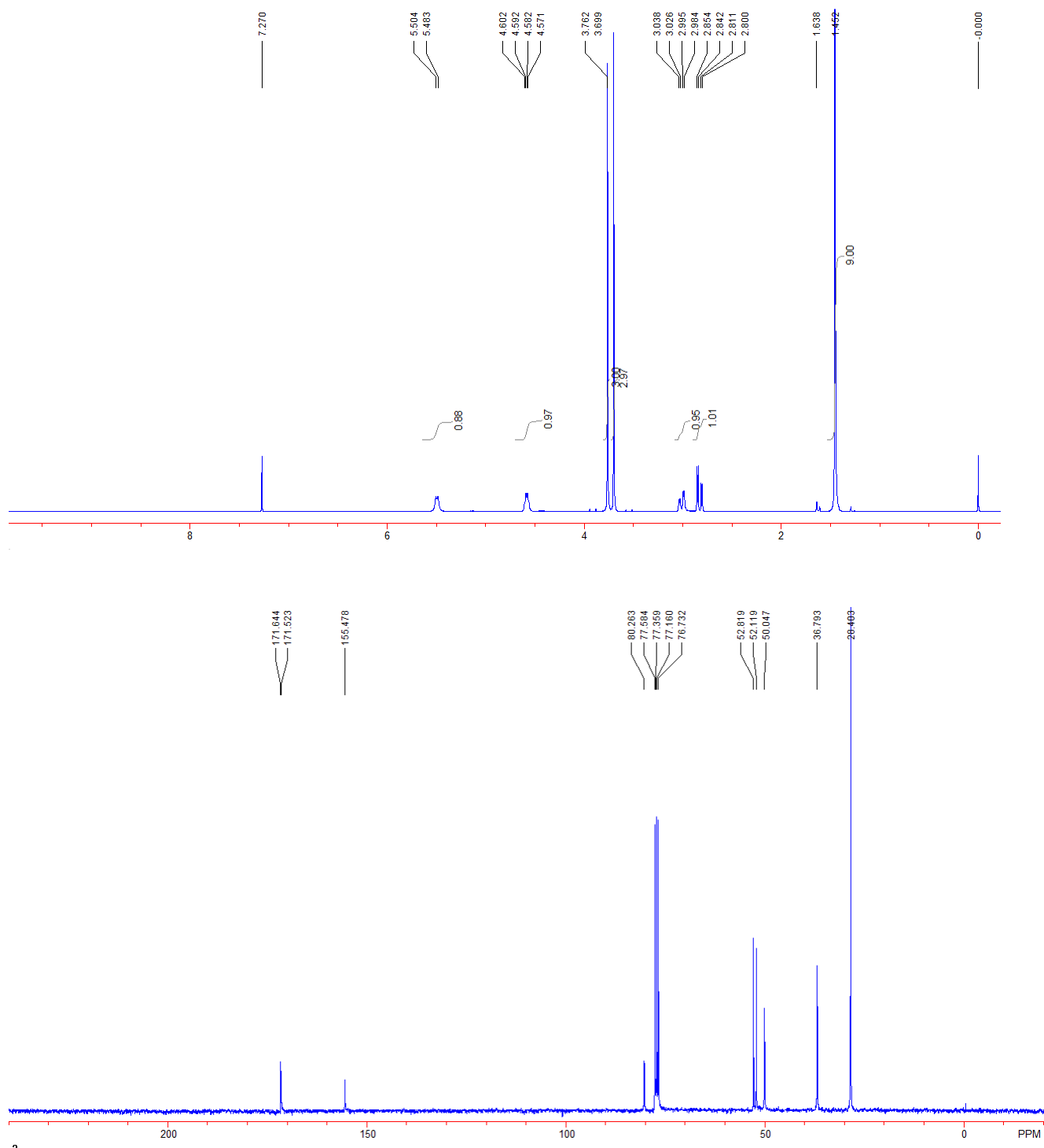
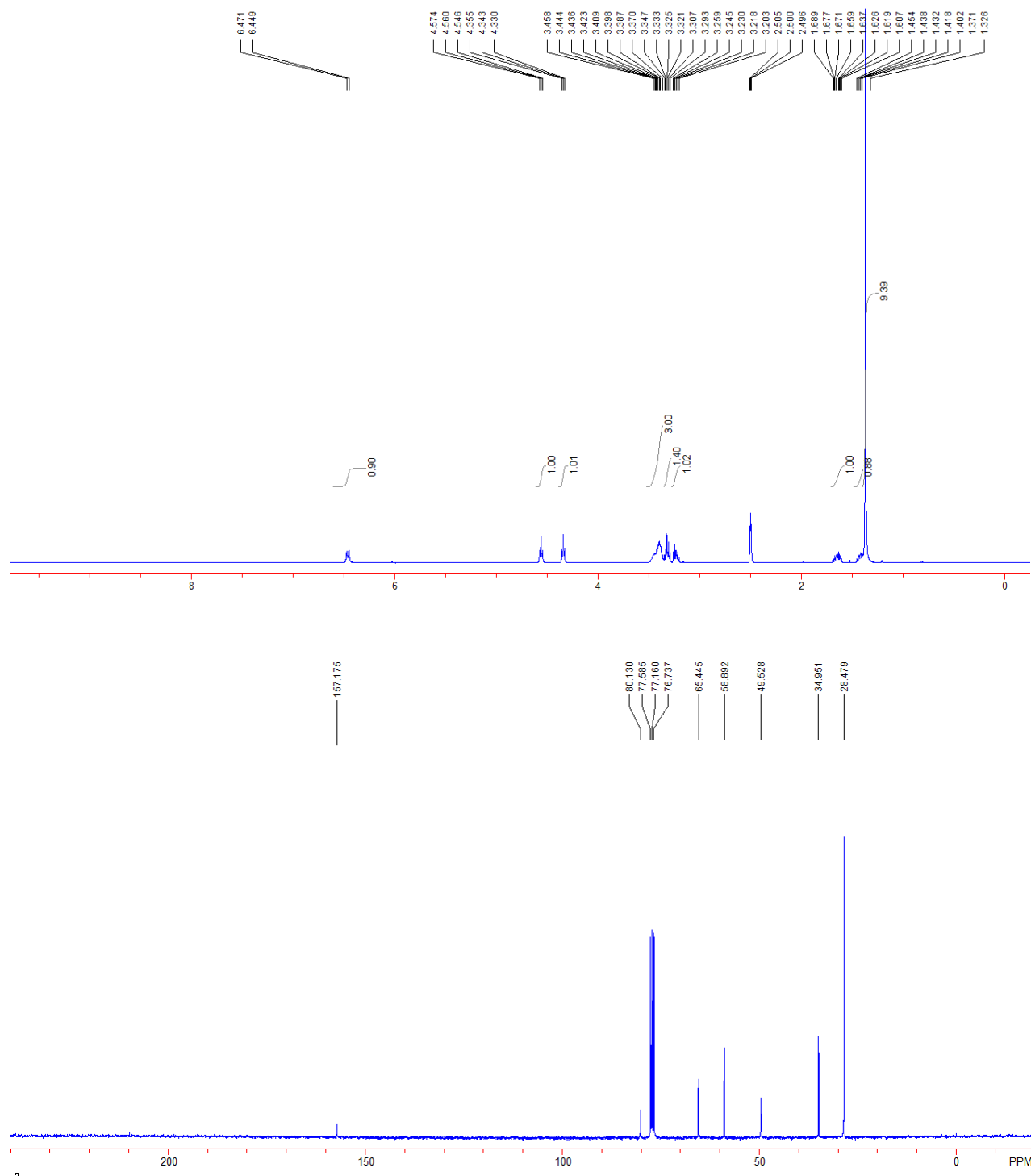


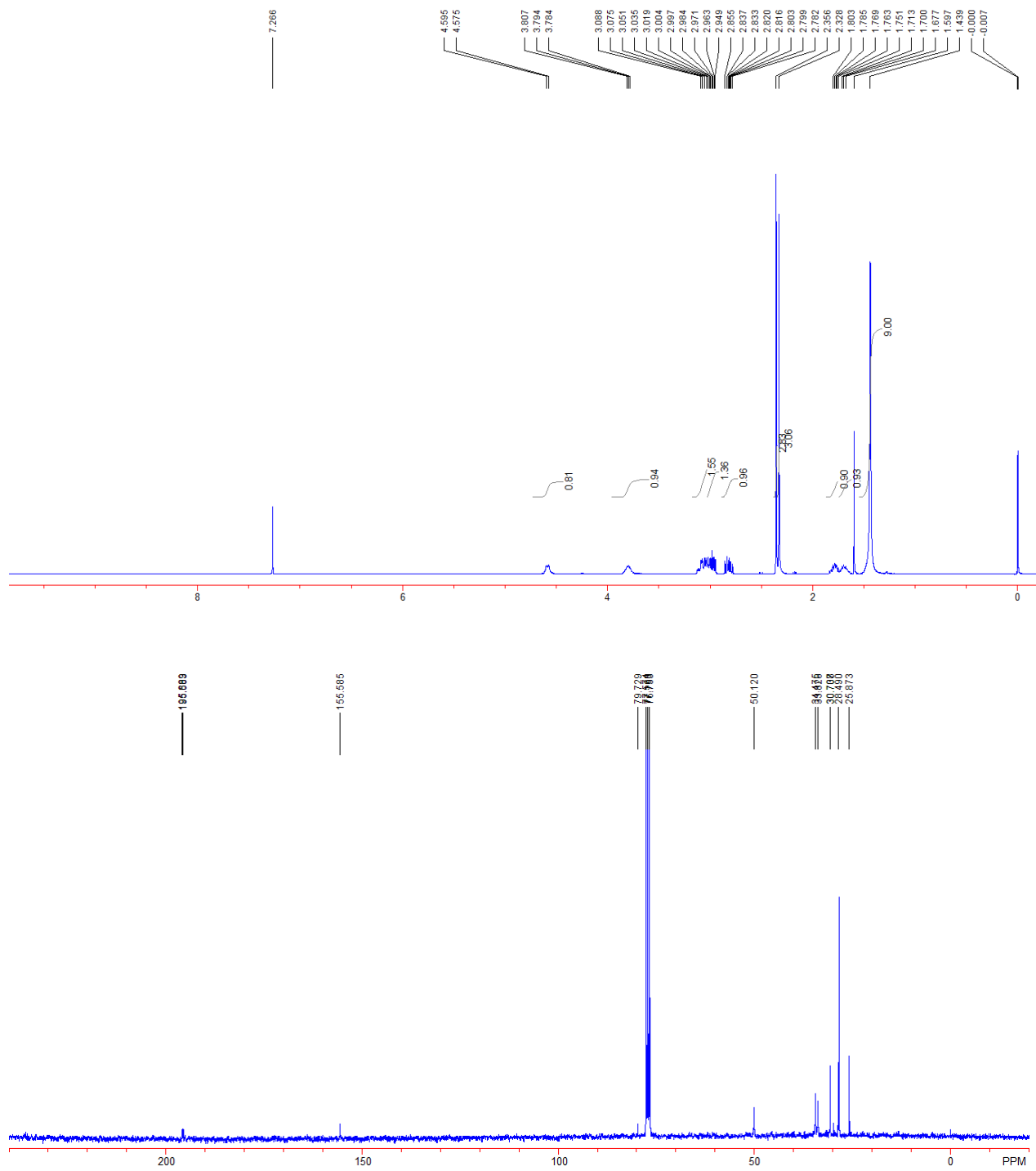
Figure 2.6 Ultraviolet spectrum of oxidized DTBA and oxidized DTT in DPBS

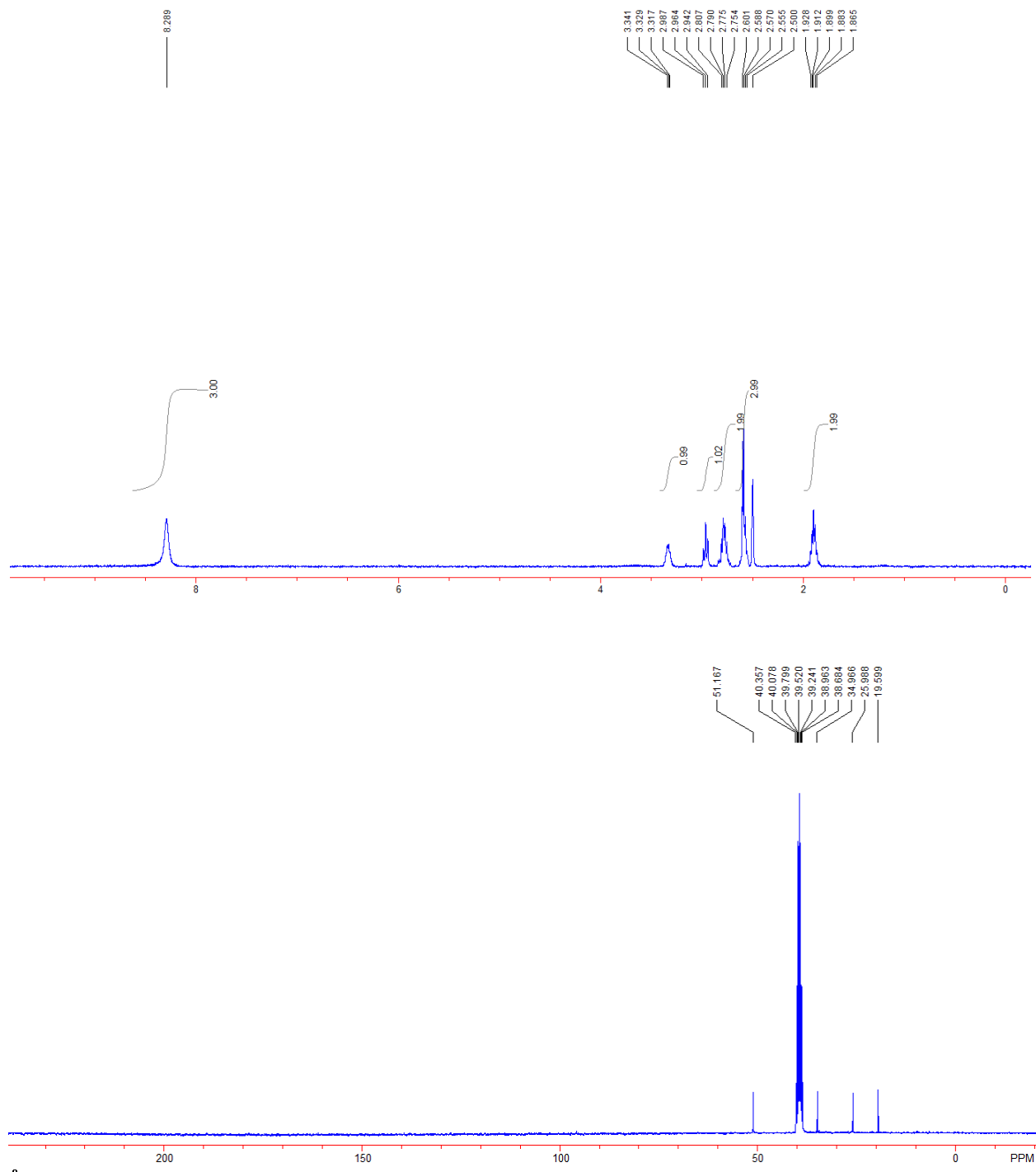
2.8 NMR Spectra

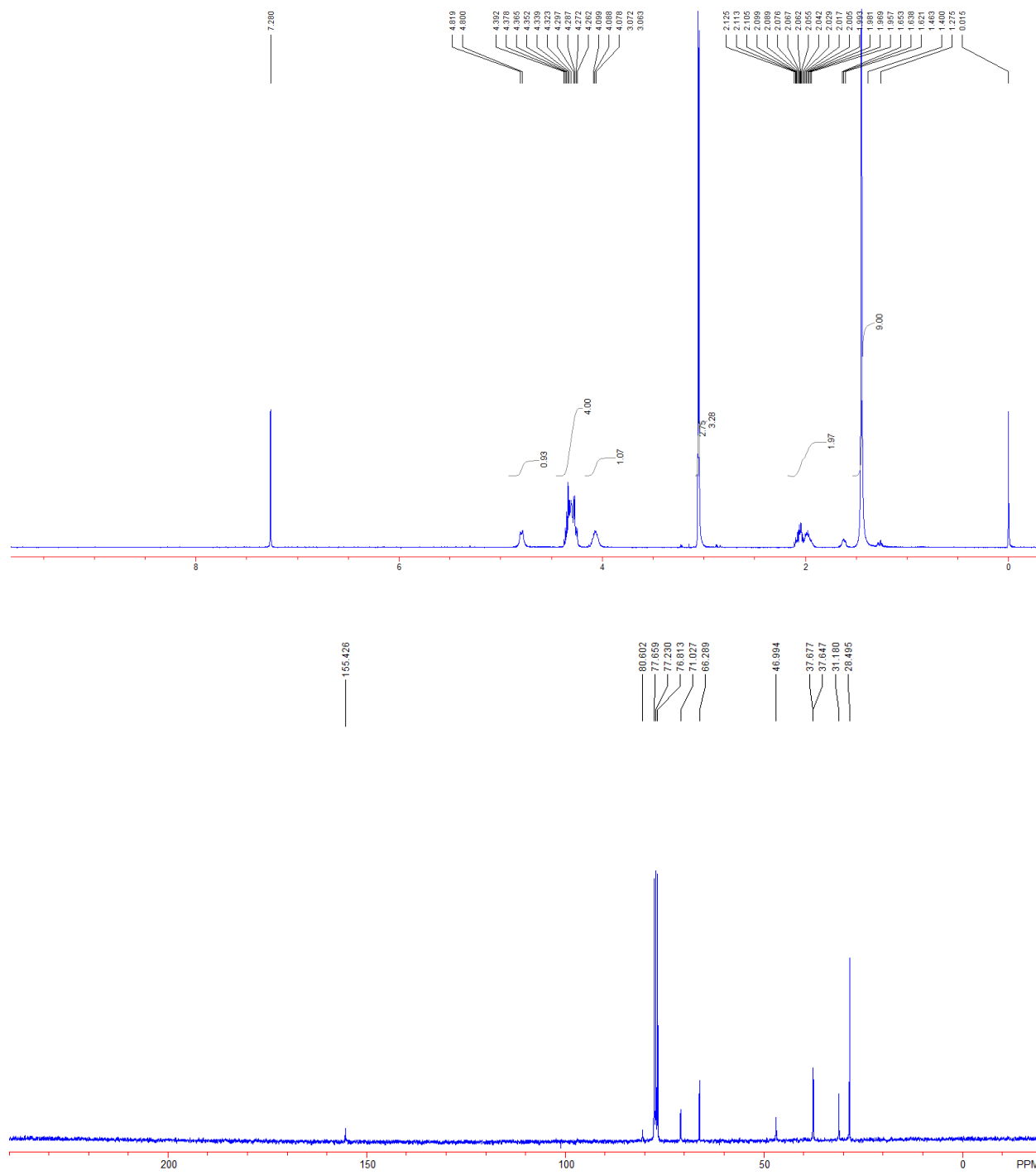
^1H NMR(CDCl_3) and ^{13}C NMR(CDCl_3) of **2.1**

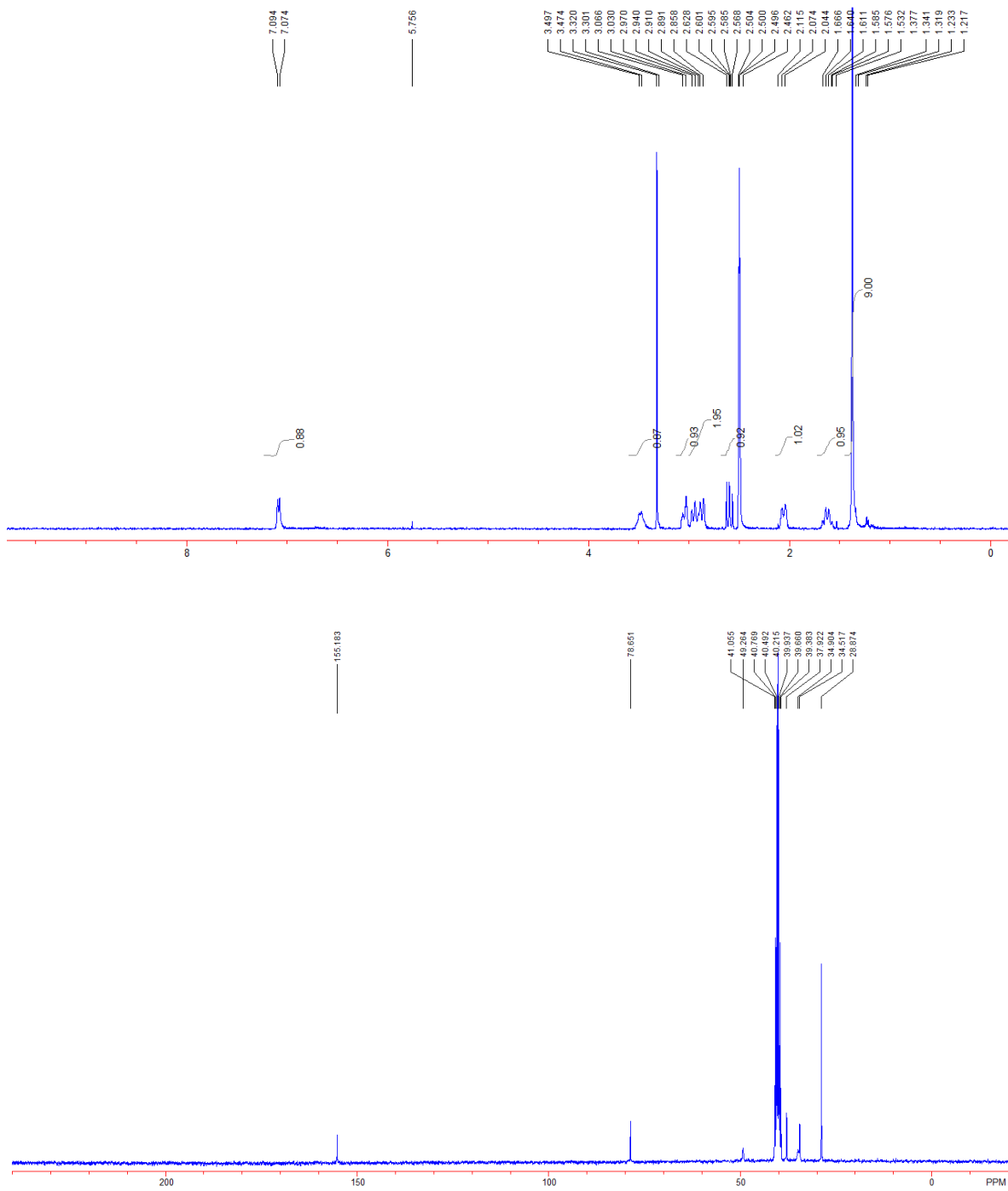


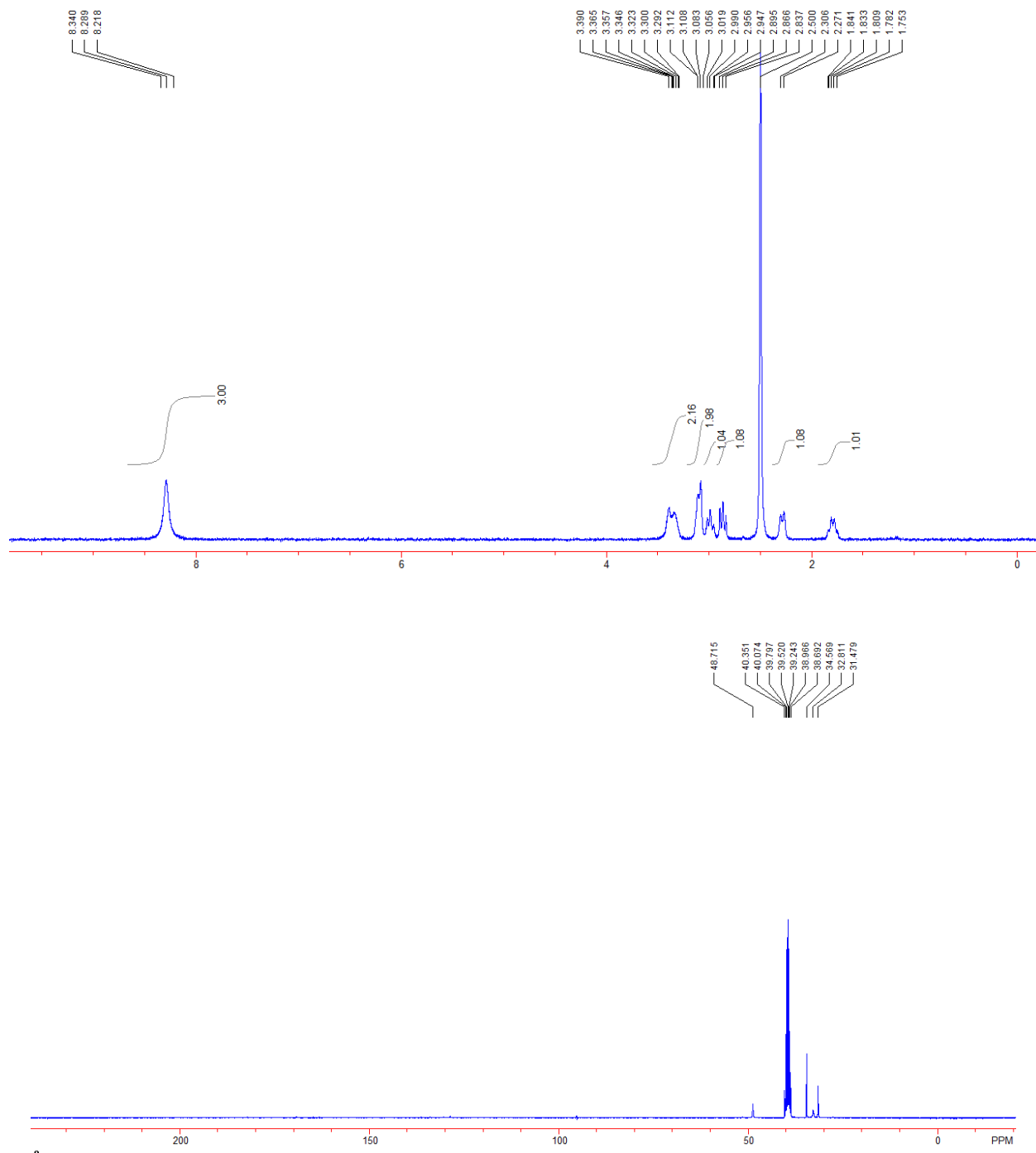
^1H NMR(DMSO- d_6) and ^{13}C NMR(CDCl_3) of **2.2**

^1H NMR(CDCl_3) and ^{13}C NMR(CDCl_3) of **2.3**

^1H NMR(DMSO- d_6) and ^{13}C NMR(DMSO- d_6) of **2.4 (DTBA)**

^1H NMR(CDCl_3) and ^{13}C NMR(CDCl_3) of **2.5**

^1H NMR(DMSO- d_6) and ^{13}C NMR(DMSO- d_6) of **2.6**

^1H NMR(DMSO- d_6) and ^{13}C NMR(DMSO- d_6) of **2.7 (DTBA^{0x})**

Chapter 3*: Thiols and Selenols as Electron-Relay Catalysts for Disulfide-Bond Reduction

3.1 Abstract

Dithiobutylamine immobilized on a resin is a useful reagent for the reduction of disulfide bonds. Its ability to reduce a disulfide bond in a protein is enhanced greatly if used along with a soluble strained cyclic disulfide or mixed diselenide that relays electrons from the resin to the protein. This electron-relay catalysis system provides distinct advantages over the use of excess soluble reducing agent alone.

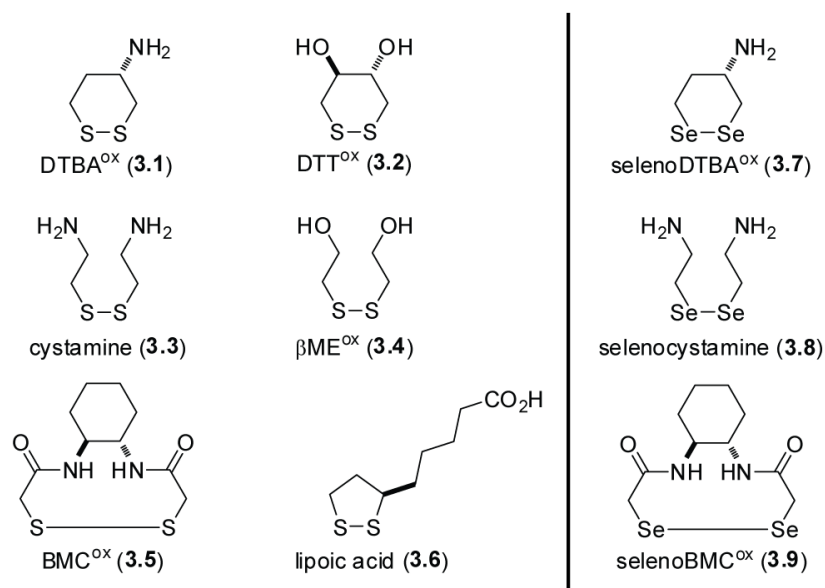
3.2 Author Contributions

J.C.L. proposed the immobilization of DTBA. J.C.L. synthesized and characterized immobilized DTBA. B.V. proposed the use of an electron relay system to aid in the reduction of protein disulfide bonds. J.C.L. proposed the use of strained cyclic disulfides and mixed diselenides in order to optimize the relay system. J.C.L. synthesized and characterized electron-relay catalysts, performed all experiments, and drafted the original manuscript and figures. J.C.L., B.V., and R.T.R. planned experiments, analyzed data, and edited the manuscript and figures.

*This chapter has been published, in part, under the same title: Reference: Lukesh, J. C., III; VanVeller, B.; Raines, R. T. *Angew. Chem., Int. Ed.* **2013**, *52*, 12901–12904 (**Cover Article**).

3.3 Introduction

For the proper function of many proteins, sulfhydryl groups need to be maintained in a reduced state or disulfide bonds need to be maintained in an oxidized state.¹⁴¹ In cells, this maintenance entails thiol–disulfide interchange reactions, often initiated by a membrane-associated protein and mediated by a soluble protein or peptide (e.g., glutathione).¹⁴²⁻¹⁴⁵ *In vitro*, small-molecule thiols and disulfides, such as those in Scheme 3.1, can accomplish this task.^{85,146,147}



Scheme 3.1 Disulfides (3.1–3.6) and diselenides (3.7–3.9) used in this work. Compounds 3.2, 3.5, 3.6, and 3.9 are racemic mixtures.

Recently, we reported on a novel disulfide-reducing agent, (2S)-2-amino-1,4-dimercaptobutane (dithiobutylamine or DTBA; reduced 3.1), derived from L-aspartic acid.⁴² As with dithiothreitol (DTT; reduced 3.2), DTBA is a dithiol capable of adopting an unstrained ring

upon oxidation.^{21,38,39} A distinct and untapped attribute of DTBA is the ability of its amino group to act as a handle for facile conjugation. Small-molecule reducing agents typically need to be maintained at millimolar concentrations, and their removal diminishes process efficiency and economy. We reasoned that attaching DTBA to a solid support would enable its removal after disulfide reduction by either filtration or centrifugation.¹⁴⁸

3.4 Results and Discussion

To test our hypothesis, we chose TentaGel resin as the solid support. This resin consists of hydrophilic poly(ethyleneglycol) units grafted onto low-cross-linked polystyrene.^{149,150} We found DTBA immobilized on TentaGel to be a potent disulfide-reducing agent with $E^{\circ'} = (-0.316 \pm 0.002)$ V, a value similar to that of soluble DTBA (Figures 3.4 and 3.5).⁴² Immobilized DTBA (10 equiv) was able to reduce cystamine (**3.3**) and oxidized β -mercaptoethanol (**3.4**) completely (Figures 3.6 and 3.7). Immobilized DTBA (10 equiv) was even able to reduce highly stable disulfides such as oxidized DTBA (**3.1**) and oxidized DTT (**3.2**) with yields of 76% and 68%, respectively (Figures 3.8 and 3.9). After each procedure, the resin was easily isolated, regenerated, and reused without any observable loss in activity. The latter are not attributes of immobilized reducing agents derived from phosphines, which form recalcitrant phosphine oxides.

Next, we assessed the ability of immobilized DTBA to reduce a disulfide bond in a folded protein, which can be a challenging task.^{43,49,50,52,54} As the target protein, we chose papain, a cysteine protease.^{132,133} Upon treatment with S-methyl methanethiosulfonate, the active-site cysteine of papain (Cys25) forms a mixed disulfide that has no detectable enzymatic activity.²³

When we incubated the oxidized enzyme with 100 equivalents of immobilized DTBA, we found that less than half of papain-Cys25-S-S-CH₃ had been reduced after 30 minutes (Figure 3.1). Moreover, the rate of reduction for this heterogeneous reaction was slow, approximately 0.1% of that provided by typical solution-phase reagents,^{27,28,42} and activation ceased after 10 minutes. When papain was treated with 1,000 equivalents of immobilized DTBA, full generation of activity was observed within 10 minutes (Figure 3.1). These data indicate that the inefficiency is likely due to a diminished ability of the protein disulfide—in comparison to small-molecule disulfides—to access the sulfhydryl groups of immobilized DTBA.^{50,54}

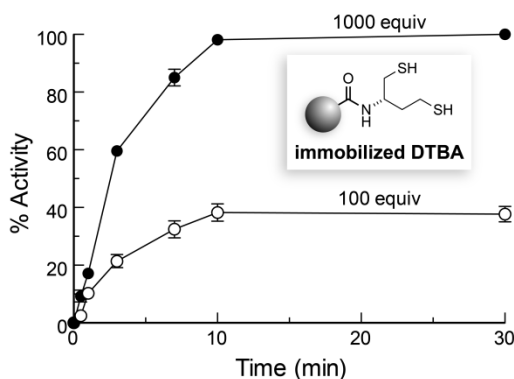
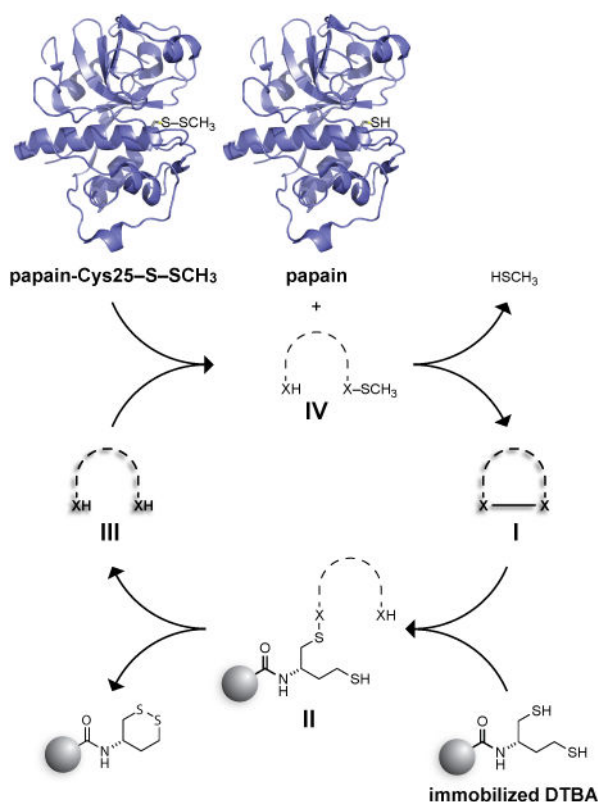


Figure 3.1 Time-course for the reactivation of papain-Cys25-S-S-CH₃ by immobilized DTBA (100 or 1000 equiv) in imidazole-HCl buffer (0.1 M, pH 7.0) containing EDTA (2 mM).

Taking inspiration from cellular thiol-disulfide interchange reactions,^{6,15,142-145,151} we reasoned that the utility of immobilized DTBA could be enhanced by a soluble molecule that could "relay" electrons from the resin to the protein (Scheme 3.2).¹⁵² To test this hypothesis, we incubated papain-Cys25-S-S-CH₃ with 100 equivalents of immobilized DTBA and 30 mol%

of disulfides **3.1–3.4** (relative to oxidized protein). Unfortunately, we observed only a slight rate enhancement (Figure 3.2A).



Scheme 3.2 Cycle for electron-relay catalysis of disulfide-bond reduction by soluble thiols (**III**, X = S) or selenols (**III**, X = Se). Papain was depicted with the program PyMOL (Schrodinger, Portland, OR) using PDB entry 1ppn.¹³³

Suspecting that the rate of the heterogeneous reaction between immobilized DTBA and unstrained disulfides **3.1–3.4** was slow (**I** to **II** in Scheme 3.2),^{153,154} we turned to disulfides **3.5** and **3.6**, believing that their incipient strain would accelerate the turnover of the soluble catalyst. BMC^{ox} (**3.5**) is a ten-membered cyclic disulfide. Rings of this size suffer transannular strain.^{39,116,155} Similarly, cyclic five-membered disulfides (i.e., 1,2-dithiolanes), such as **3.6**, place significant distortion on the preferred CSSC dihedral angle.^{39,156} Hence, the rate constant for the

reaction between 1,3-propanedithiol and 1,2-dithiolane is around 650 times greater than that for the homologated exchange reaction between 1,4-butanedithiol and 1,2-dithiane.⁴⁰

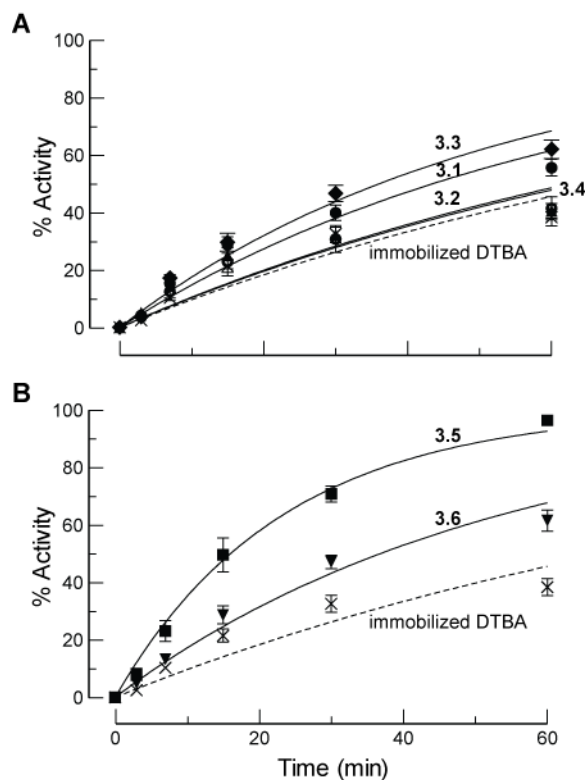


Figure 3.2 Time-course for the reactivation of papain-Cys25-S-S-CH₃ by immobilized DTBA (100 equiv) and a solution-phase disulfide catalyst (30 mol%). Reactions were performed in imidazole-HCl buffer (0.10 M, pH 7.0) containing EDTA (2 mM). (A) Unstrained disulfide catalysts. Cystamine (**3.3**): $k_{cat}^{obs}/k_{uncat}^{obs} = 1.9$; DTBA^{ox} (**3.1**): $k_{cat}^{obs}/k_{uncat}^{obs} = 1.6$; DTT^{ox} (**3.2**): $k_{cat}^{obs}/k_{uncat}^{obs} \sim 1.0$; β ME^{ox} (**3.4**): $k_{cat}^{obs}/k_{uncat}^{obs} \sim 1.0$. (B) BMC^{ox} (**3.5**): $k_{cat}^{obs}/k_{uncat}^{obs} = 4.3$; lipoic acid (**3.6**): $k_{cat}^{obs}/k_{uncat}^{obs} = 1.9$. Data for immobilized DTBA alone is shown in both panels.

Consistent with our expectations, we found that disulfide **3.5** provided a significant enhancement in the rate of papain-Cys25-S-S-CH₃ reduction. Disulfide **3.6** was somewhat less effective, as its mixed disulfide (**II** in Scheme 3.2) has a higher tendency to partition back to the disulfide (**I**).⁴⁰ Moreover, in the absence of immobilized DTBA, we found that the reduced form of DTBA regenerates activity faster than does the reduced form of BMC (Figure 3.11), affirming

that the reduction of the soluble catalyst (**I** to **III** in Scheme 3.2) limits the rate of electron-relay catalysis.

To improve catalytic efficiency further, we considered the use of selenium, which has physicochemical properties similar to those of sulfur. Yet, selenols manifest several desirable attributes as reducing agents in aqueous solution.^{11,58,69-74,76} For example, selenols have pK_a values that are typically three units lower than those of analogous thiols, significantly enhancing their nucleophilicity near neutral pH and their ability to act as a leaving group.^{57,66,67} Diselenides also have E° values that are typically 0.15 V lower than those of analogous disulfides, making selenols more potent reducing agents. In addition, reactions with selenium as the electrophile can be 10^4 times faster than those with sulfur as the electrophile, and might not require strain for efficient turnover. Indeed, there are numerous reports of small-molecule diselenides being used as catalysts for biochemical oxidation reactions.⁵⁸⁻⁶⁵ Enzymes, such as thioredoxin reductase,¹⁵⁷ are known to employ a selenol as a reducing agent. Yet, reported *in vitro* reduction reactions rarely employ small-molecule selenols, and never diselenols. A practical problem is the high reactivity of selenols with molecular oxygen. We recognized that this problem would be averted in our system, which would generate catalytic selenols *in situ* (Scheme 3.2). Because of the efficacy of disulfide **3.5** (Figure 3.2B), we were motivated to investigate its seleno congener. Accordingly, we synthesized selenoBMC^{ox} (**3.9**) as well as selenoDTBA^{ox} (**3.7**), and we obtained selenocystamine (**3.8**), which is available commercially and has demonstrated marked success in mediated thiol–disulfide interchange reactions.^{57,59,60,66,158}

We found that diselenide **3.7** is superior to its congener **3.1**, and that diselenide **3.9** performs comparably to its congener **3.5** (Figure 3.3A). These two cyclic diselenides were,

however, worse catalysts than was acyclic diselenide **3.8** (Figure 3.3B). This finding is attributable to the selenylsulfide (**II** in Scheme 3.2) generated by the reaction of **3.7** and **3.9** (but not **3.8**) with immobilized DTBA tending to partition back to the diselenide (**I**) rather than to the diselenol (**III**) needed for catalysis.^{40,159} Notably, diselenide **3.8** led to significant rate enhancements even at low loadings of catalyst.

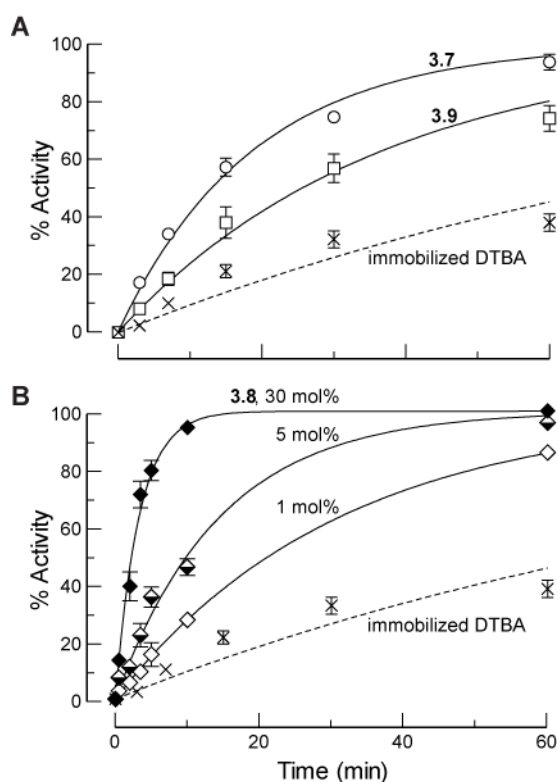


Figure 3.3 Time course for the reactivation of papain-Cys25-S-S-CH₃ by immobilized DTBA (100 equiv) and a solution-phase diselenide catalyst. Reactions were performed in imidazole-HCl buffer (0.10 M, pH 7.0) containing EDTA (2 mM). (A) Cyclic diselenide catalysts (30 mol%). selenoDTBA^{ox} (**3.7**): $k_{cat}^{obs}/k_{uncat}^{obs} = 5.3$; SelenoBMC^{ox} (**3.9**): $k_{cat}^{obs}/k_{uncat}^{obs} = 2.7$. (B) Selenocystamine (**3.8**) as a catalyst. 30 mol%: $k_{cat}^{obs}/k_{uncat}^{obs} = 30$; 5 mol%: $k_{cat}^{obs}/k_{uncat}^{obs} = 6.8$; 1 mol%: $k_{cat}^{obs}/k_{uncat}^{obs} = 3.2$. Data for immobilized DTBA alone is shown in both panels.

3.5 Conclusions

In summary, we have established that the amino group of DTBA allows for its facile conjugation to a resin. This supported reagent was effective at reducing disulfide bonds in small molecules. Unlike soluble reducing agents, immobilized DTBA was easy to recover and reuse. We also demonstrated that the rate of reducing a disulfide bond in a protein can be enhanced markedly when the reduced resin is used in conjunction with a "relay". In this biomimetic strategy, the resin acts as a repository of electrons that are relayed to a macromolecule via a small-molecule catalyst. The optimal catalysts are strained cyclic disulfides and acyclic diselenides, both of which react with excess immobilized DTBA to form a covalent intermediate that partitions toward reduced catalyst and oxidized resin.

Finally, we note that a vast excess of soluble reducing agent is typically used to preserve proteins in a reduced state.¹³⁸ Instead, maintenance could require a minute (e.g., sub-micromolar) amount of soluble catalyst along with immobilized DTBA. We anticipate that the low level of soluble reducing agent would be advantageous in common bioconjugation reactions entailing the S-alkylation of cysteine residues,¹⁶⁰ as well as in many other experimental procedures.

3.6 Acknowledgements

We are grateful to Prof. H. J. Reich for contributive discussions. B.V. was supported by postdoctoral fellowship 289613 (CIHR). This work was supported by grant R01 GM044783 (NIH). This work made use of the National Magnetic Resonance Facility at Madison, which is supported by grants P41 RR002301 and P41 GM066326 (NIH), and the Biophysics

Instrumentation Facility, which was established with grants BIR-9512577 (NSF) and S10 RR13790 (NIH).

3.7 Materials and Methods

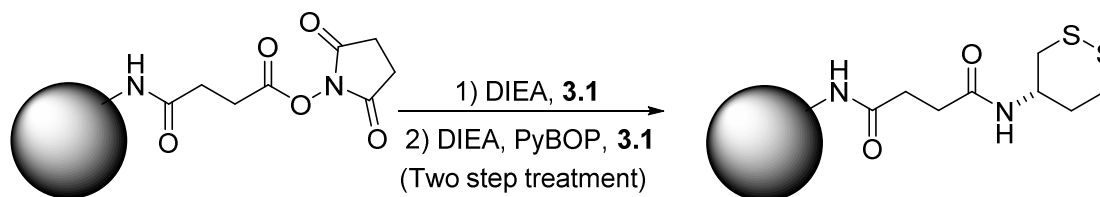
3.7.1 General

Commercial reagents were used without further purification. Dithiothreitol (DTT) was from Research Products International (Mt. Prospect, IL). Benzotriazol-1-yl-oxytripyrrolidinophosphonium hexafluorophosphate (PyBOP) was from CHEM-IMPEX INT'L INC. (Wood Dale, IL). Pre-activated succinimidyl ester TentaGel resin with a particle size of 130 μm was from Rapp Polymere (Tübingen, Germany). *N*-Methyl-2-pyrrolidone (NMP), *N,N'*-diisopropylethylamine (Hünig's base), cystamine dihydrochloride (**3.3**), selenocystamine dihydrochloride (**3.8**), racemic lipoic acid (**3.6**), 2-mercaptoethanol, 2,2'-dithiodiethanol ($\beta\text{ME}^{\text{ox}}$, **3.4**), *trans*-4,5-dihydroxy-1,2-dithiane (DTT^{ox} , **3.2**), papain (lyophilized powder from papaya latex), *N* _{α} -benzoyl-L-arginine-4-nitroanilide hydrochloride, and *S*-methyl methanethiosulfonate were from Sigma Chemical (St. Louis, MO). DTBA, DTBA^{ox} (**3.1**), BMC, and BMC^{ox} (**3.5**) were synthesized as described previously.^{42,116}

All glassware was oven or flame-dried, and reactions were performed under $\text{N}_2(\text{g})$ unless stated otherwise. Dichloromethane, diethyl ether, and tetrahydrofuran were dried over a column of alumina. Dimethylformamide and triethylamine were dried over a column of alumina and purified further by passage through an isocyanate scrubbing column. Flash chromatography was performed with columns of 40–63 Å silica, 230–400 mesh from Silicycle (Québec City, Canada). Thin-layer chromatography (TLC) was performed on plates of EMD 250- μm silica 60-F₂₅₄. The

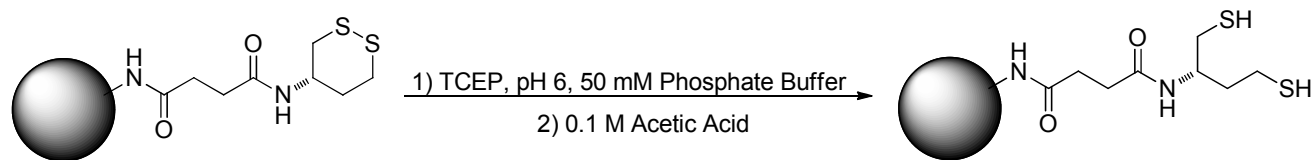
synthesis of immobilized DTBA was performed with a solid-phase peptide synthesis vessel from Chemglass (Vineland, NJ). Ellman's assay for sulfhydryl groups was performed with a Varian Cary 50 Bio UV-Vis spectrophotometer. Equilibrium and reduction potential studies were performed on an analytical HPLC (Waters system equipped with a Waters 996 photodiode array detector, Empower 2 software and a Varian C18 reverse phase column). Analytical samples of DTBA^{ox} (**3.1**), BMC^{ox} (**3.5**), selenoDTBA^{ox} (**3.7**), and selenoBMC^{ox} (**3.9**) were obtained by using a Shimadzu (Kyoto, Japan) preparative HPLC, equipped with a C18 reverse phase preparative column, a Prominence diode array detector, and fraction collector. Kinetic studies on proteins were carried out using a Varian Cary 400 Bio UV-Vis spectrometer with a Cary temperature controller at the Biophysics Instrumentation Facility at Madison (BIF). All NMR spectra were acquired at ambient temperature with a Bruker Avance III 500ii with cryoprobe spectrometer at the National Magnetic Resonance Facility at Madison (NMRFAM), and were referenced to TMS or a residual protic solvent.

3.7.2 Chemical Synthesis



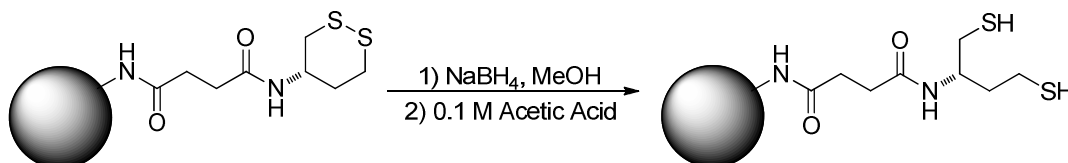
Preactivated succinimidyl ester TentaGel resin (1 g; ~0.21 mmol/g) with a particle size of 130 μm was placed in a solid-phase peptide synthesis vessel. As a pretreatment, the resin was allowed to swell in 5 mL of *N*-methyl-2-pyrrolidone (NMP) for 5 min while bubbling $\text{N}_2(\text{g})$

through the solution. The NMP was then removed by vacuum filtration and the process was repeated two more times. To the resin was then added 10 mL of NMP, 0.32 mL (1.8 mmol) of *N,N*-diisopropylethylamine (DIEA), and 0.1224 g (0.7128 mmol) of DTBA^{ox} (**1**, prepared as described previously). The resulting mixture was allowed to react for 60 min while bubbling N₂(g) through the solution. The solution was then removed by vacuum filtration, and the resin was washed with NMP (3 × 5 mL). In a second coupling step, 10 mL of NMP, 0.4701 g (0.9034 mmol) of (benzotriazol-1-yloxy)tripyrrolidinophosphonium hexafluorophosphate (PyBOP), 0.32 mL (1.8 mmol) of DIEA, and 0.1224 mg (0.7128 mmol) of DTBA^{ox} were added to the resin and allowed to react for an additional hour while bubbling N₂(g) through the solution. Then, the solution was removed by vacuum filtration. The coupling of DTBA to pre-activated TentaGel resin was performed multiple times with yields ranging from 75–93% as determined by Ellman's assay for sulfhydryl groups (see below).¹⁶¹



To 1 g of immobilized DTBA^{ox}, in a solid-phase peptide synthesis vessel, was added 0.2603 g (0.9081 mmol) of tris(2-carboxyethyl)phosphine hydrochloride (TCEP-HCl) in 10 mL of 50 mM sodium phosphate, pH 6.0. The mixture was allowed to react for 60 min while bubbling N₂(g) through the solution. Then, the solution was removed by vacuum filtration, and the resin was washed with 0.1 M acetic acid (5 × 5 mL) to ensure that the thiol groups were

protonated completely. Finally, the resin was washed methanol (3×5 mL) and dried under vacuum overnight.



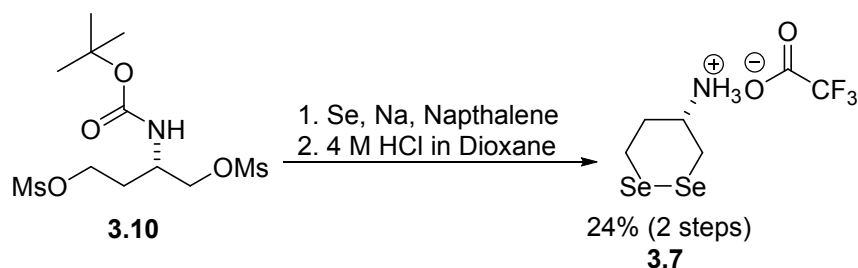
To 1 g of immobilized DTBA^{ox}, in a solid-phase peptide synthesis vessel, was added 79.41 mg (2.099 mmol) of NaBH₄ in 10 mL of methanol. The mixture was allowed to react for 60 min while bubbling N₂(g) through the solution. Then, the solvent was removed by vacuum filtration, and the resin was washed with 0.1 M acetic acid (5×5 mL) to ensure that the thiol groups were protonated completely. Finally, the resin was washed methanol (3×5 mL) and dried under vacuum overnight.

Compound **3.1** was synthesized from L-aspartic acid as described previously.

¹H NMR (500 MHz, DMSO-*d*₆) δ = 8.29 (s, 3H), 3.43–3.37 (m, 1H), 3.15–3.08 (m, 2H), 3.02–2.96 (m, 1H), 2.88 (dd, *J* = 13.1, 10.6 Hz, 1H), 2.32–2.28 (m, 1H), 1.85–1.77 (m, 1H); ¹³C NMR (125 Hz, DMSO-*d*₆) δ = 48.8, 34.6, 32.9, 31.5; HRMS (ESI) calculated for [C₄H₁₀NS₂]⁺ (M⁺) requires *m/z* = 136.0250, found 136.0249.

Compound **3.5** was synthesized from (\pm)-*trans*-1,2-diaminocyclohexane as reported previously.

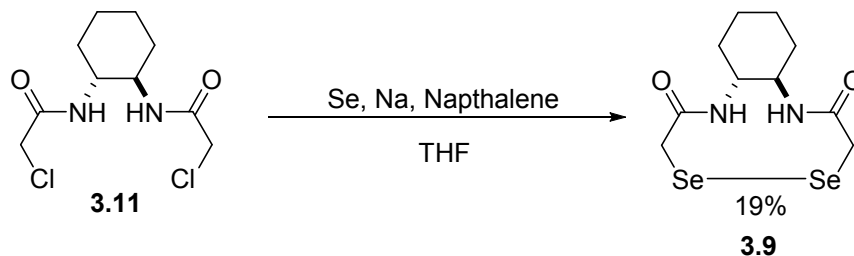
¹H NMR (500 MHz, DMSO-*d*₆) δ = 7.98 (d, *J* = 9.0 Hz, 1.63H), 7.76 (d, *J* = 8.8 Hz, 0.37H), 3.76–3.69 (m, 1.63H), 3.54–3.51 (m, 0.37H), 3.40 (d, *J* = 14.0 Hz, 1.63H), 3.32 (d, *J* = 11.4 Hz, 0.37H), 3.19 (d, *J* = 14.0 Hz, 1.63H), 3.08 (d, *J* = 11.4 Hz, 0.37H), 1.72–1.71 (m, 4H), 1.36–1.22 (m, 4H); **¹³C NMR (125 Hz, DMSO-*d*₆)** δ = 169.9, 166.1, 56.6, 54.2, 44.6, 31.12, 31.05, 25.0, 24.9; **HRMS (ESI)** calculated for [C₁₀H₁₆N₂O₂S₂Na]⁺ (M+Na⁺) requires *m/z* = 283.0546, found 283.0532.



Sodium diselenide was generated *in situ* by closely following a previously described method.¹⁶² 146.8 mg (1.859 mmol) of selenium powder and 238.3 mg (1.859 mmol) of naphthalene were placed in a flame-dried three-neck round-bottom flask. Anhydrous THF (5 mL) was added, and the resulting mixture was stirred at room temperature under N₂(g). Freshly shaved sodium metal (42.74 mg, 1.859 mmol) was then added to the mixture under N₂(g). The reaction mixture was allowed to stir for 2 h to enable consumption of all of the sodium metal. Compound **3.10** (331.0 mg, 0.9158 mmol), which was prepared as described previously,⁴² was dissolved in 10 mL of anhydrous DMF, and the resulting solution was added dropwise to the reaction mixture. After 24 h, the reaction mixture was filtered, concentrated under reduced pressure, and eluted through a silica plug with ethyl acetate (20% v/v) in hexanes. The resulting solution was then concentrated under reduced pressure, and the residue was dissolved in 4 M

HCl in dioxane. After 2 h, TLC revealed the removal of the Boc group. Compound **3.7** was purified by reverse-phase HPLC using a preparatory C18 column and a linear gradient of 10–50% v/v acetonitrile (0.1% v/v TFA) in water (0.1% v/v TFA) over 55 min. Compound **3.7** eluted at 17 min and, after lyophilization, was isolated as a yellow powder (68.13 mg, 22% over two steps)

¹H NMR (500 MHz, DMSO-*d*₆) δ = 8.02 (s, 3H), 3.43–3.36 (m, 2H), 3.25–3.21 (m, 1H), 3.14 (dd, *J* = 12.2 Hz, 1.9 Hz, 1H), 3.0 (dd, *J* = 10.9, 12.0, 1H), 2.38–2.35 (m, 1H), 1.87–1.80 (m, 1H); **¹³C NMR (125 Hz, DMSO-*d*₆)** δ = 50.5, 33.6, 24.2, 23.9; **HRMS (ESI)** calculated for [C₄H₁₀NSe₂]⁺ (M⁺) requires *m/z* = 223.9192 or 227.9154, found 223.9196 or 227.9144.



Sodium diselenide was generated *in situ* by closely following a previously described method.¹⁶² 296.0 mg (3.749 mmol) of selenium powder and 480.5 mg (3.749 mmol) of naphthalene were weighed out and placed in a flame dried three neck round bottom flask. 10 mL of anhydrous THF was added and mixture was stirred at room temperature under N₂. 86.20 mg (3.749 mmol) of freshly shaved sodium metal was then added to the mixture under N₂, and the mixture was allowed to react for 2 h to ensure that all of the sodium metal had been consumed. 497.6 mg (1.863 mmol) of **3.11** (prepared as previously described) was then dissolved in 20 mL of anhydrous THF and added drop wise to the reaction mixture. After reacting for 24 h the

reaction was filtered, concentrated, and purified by column chromatography (20% v/v methanol in ethyl acetate) resulting in **3.9** as a red/orange solid (125.3 mg, 19% yield). An analytically pure sample of **3.9** was obtained by reverse-phase HPLC using a preparatory C18 column and a linear gradient of 10-80% v/v Acetonitrile (0.1 % v/v TFA) in water (0.1% v/v TFA) over 45 min. **3.9** eluted at 23 min and, after lyophilization, was isolated as an off white powder.

¹H NMR (500 MHz, DMSO-*d*₆) δ = 7.86–7.85 (m, 1.23H), 7.62–7.60 (m, 0.77H), 3.68–3.65 (m, 2.46H), 3.54 (d, *J* = 10.2 Hz, 0.77H), 3.50–3.45 (m, 0.77H), 3.41 (d, *J* = 12.5 Hz, 1.23H), 3.19 (d, *J* = 10.2 Hz, 0.77H), 1.73–1.68 (m, 4H), 1.35–1.18 (m, 4H); **¹³C NMR (125 MHz, DMSO-*d*₆)** δ = 170.7, 167.2, 55.8, 53.5, 33.7, 31.5, 31.4, 27.6, 24.9; **HRMS (ESI)** calculated for [C₁₀H₁₆N₂O₂Se₂Na]⁺ (M+Na⁺) requires *m/z* = 374.9474, found 374.9465.

3.7.3 Coupling Yield determined by Ellman's assay for sulfhydryl groups

A reaction buffer (0.10 M sodium phosphate buffer, pH 8.0, containing 1 mM EDTA) was prepared by the Pierce protocol. A concentrated stock of Ellman's reagent (5,5'-dithio-*bis*-(2-nitrobenzoic acid) solution was prepared by adding Ellman's reagent (6 mg) to 2 mL of reaction buffer. 0.4 mL of Ellman's reagent solution was then added to two separate vials containing 10 mL of reaction buffer. One of these vials was used as a blank, and its absorbance was measured at 412 nm. Immobilized DTBA (1.3 mg) was then added to the other vial and allowed to react. After 30 min, its absorbance at 412 nm was recorded. Using Beer's law ($c = A/(\epsilon \cdot l)$ with $A = 0.690$, $l = 1.00$ cm, and $\epsilon = 14,150$ M⁻¹cm⁻¹) gave a thiol concentration of 4.88×10^{-5} M. Because DTBA contains two thiol groups, the assay mixture had an immobilized DTBA concentration of 2.44×10^{-5} M. Since the total volume of the reaction mixture was 10.4 mL,

there were 2.54×10^{-7} moles of immobilized DTBA indicative of 0.195 mmol of immobilized DTBA per gram of resin and a ~93% coupling yield.

3.7.4 Reduction potential of immobilized DTBA

The reduction potential (E°) of immobilized DTBA was determined by using ^1H NMR spectroscopy to determine the equilibrium constant (K_{eq}) for its reaction with DTT^{ox} , and then inserting that value into a variation of the Nernst equation:

$$K_{\text{eq}} = \frac{[\text{DTT}][\text{oxidized immobilized DTBA}]}{[\text{immobilized DTBA}][\text{oxidized DTT}]} = \frac{[\text{DTT}]^2}{[\text{oxidized DTT}]^2} \quad (3.1)$$

$$E_{\text{immobilized DTBA}}^{\circ'} = E_{\text{DTT}}^{\circ'} - \frac{RT}{nF} \ln \frac{[\text{DTT}]^2}{[\text{oxidized DTT}]^2} \quad (3.2)$$

Data were obtained by a procedure similar to that described previously.^{29,42} Ellman's assay was performed on immobilized DTBA immediately prior to use. What was determined to be 1.56×10^{-3} mmol of immobilized DTBA was added to a 1.5-mL LoBind Eppendorf tube, and 0.9 mL of freshly degassed 50 mM sodium phosphate buffer, pH 7.0, was then added, followed by 156 μL (1.56×10^{-3} mmol) of a 10 mM stock solution of DTT^{ox} in the same buffer. The reaction mixture was agitated with a nutator for 24 h and then quenched by the addition of 3 N HCl (1:100 dilution). The resin was separated by centrifugation, and the solution was analyzed immediately by both ^1H NMR spectroscopy and analytical HPLC, as described previously. The equilibrium concentrations of DTT and DTT^{ox} were obtained, and a value of $K_{\text{eq}} = 0.421 \pm 0.149$ was determined. Assuming that DTT has $E^{\circ'} = -0.327$ V, eq 3.2 was used to calculate $E^{\circ'} = (-0.316 \pm 0.002)$ V. This value is the mean \pm SEM.

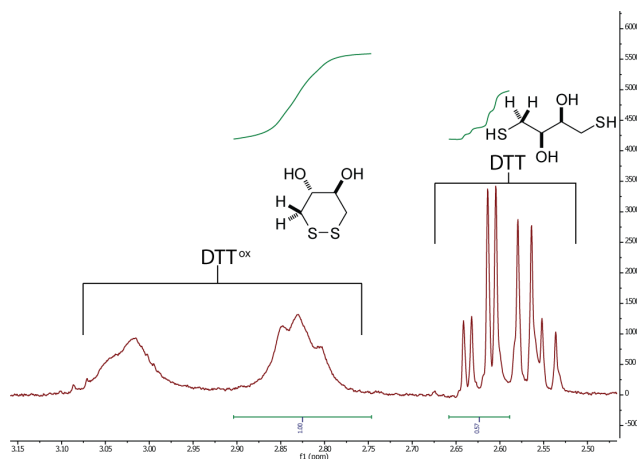


Figure 3.4 Representative ^1H NMR spectrum of the redox equilibrium between immobilized DTBA and DTT^{ox} (3.2).

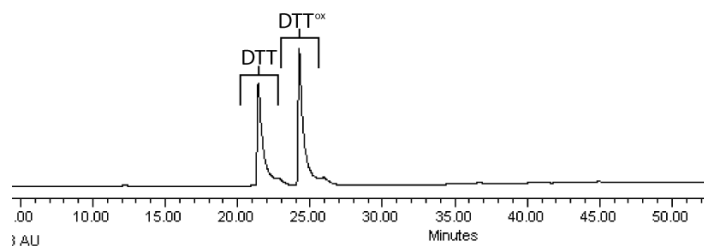


Figure 3.5 Representative HPLC chromatogram of the redox equilibrium between DTBA and DTT^{ox} . Compounds were detected by their absorbance at 205 nm.

3.7.5 Reduction of small molecules with immobilized DTBA

Reduction of 3.3

Ellman's assay was performed on immobilized DTBA immediately prior to its use. What was determined to be 13.4×10^{-3} mmol of immobilized DTBA was added to a 1.5-mL LoBind Eppendorf tube, and 0.6 mL of freshly degassed 50 mM sodium phosphate buffer, pH 7.0, was then added, followed by 134 μL (1.34×10^{-3} mmol) of a 10 mM stock solution of cystamine in the same buffer. The reaction mixture was agitated with a nutator for 24 h and then quenched by

the addition of 3 N HCl (1:100 dilution). The resin was separated by centrifugation, and the solution was analyzed immediately ^1H NMR spectroscopy. The nearly complete reduction of cystamine was observed for this reaction.

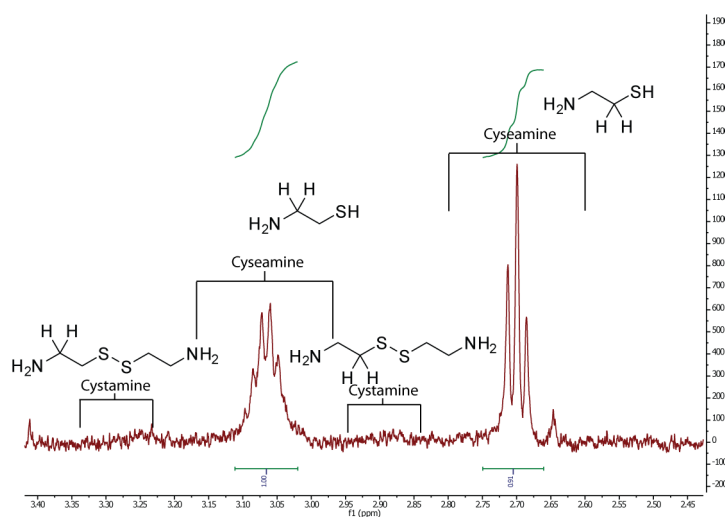


Figure 3.6 Representative ^1H NMR spectrum of the reaction between cystamine (**3.3**) and 10-fold excess of immobilized DTBA.

Reduction of 3.4

Ellman's assay was performed on immobilized DTBA immediately prior to its use. What was determined to be 5.2×10^{-3} mmol of immobilized DTBA was added to a 1.5-mL LoBind Eppendorf tube, and 0.6 mL of freshly degassed 50 mM sodium phosphate buffer, pH 7.0, was then added, followed by 52 μL (5.20×10^{-4} mmol) of a 10 mM stock solution of $\beta\text{ME}^{\text{ox}}$ in the same buffer. The reaction mixture was agitated with a nutator for 24 h and then quenched by the addition of 3 N HCl (1:100 dilution). The resin was separated by centrifugation, and the solution was analyzed immediately by analytical HPLC using a Waters system equipped with a Waters

996 photodiode array detector, Empower 2 software, and a Varian C18 reverse-phase column. The column was eluted first at 1.0 mL/min with water (5.0 mL), followed by a linear gradient (0–40% v/v) of acetonitrile/water over 40 min. Compounds were detected by their absorbance at 205 nm. A single peak at 7 min was observed (Figure 3.7). Standards of β ME and β ME^{ox} showed that this peak corresponded to β ME (β ME^{ox} has a retention time of ~23 min), confirming that nearly complete reduction of β ME^{ox} had taken place under the reaction conditions.

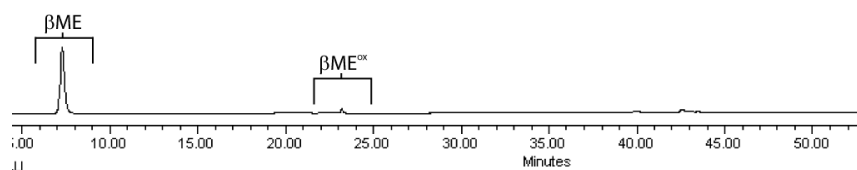


Figure 3.7 Representative HPLC chromatogram of the reaction between β ME^{ox} (**3.4**) and 10 fold excess of immobilized DTBA. Compounds were detected by their absorbance at 205 nm.

Reduction of 3.1

Ellman's assay was performed on immobilized DTBA immediately prior to its use. What was determined to be 8.44×10^{-3} mmol of immobilized DTBA was added to a 1.5-mL LoBind Eppendorf tube, and 0.6 mL of freshly degassed 50 mM sodium phosphate buffer, pH 7.0, was then added, followed by 84.4 μ L (8.44×10^{-4} mmol) of a 10 mM stock solution of DTBA^{ox} in the same buffer. The reaction mixture was agitated with a nutator for 24 h and then quenched by the addition of 3 N HCl (1:100 dilution). The resin was separated by centrifugation, and the solution was analyzed immediately with ¹H NMR spectroscopy. Concentrations of DTBA and DTBA^{ox} were determined and revealed a 76% yield of DTBA.

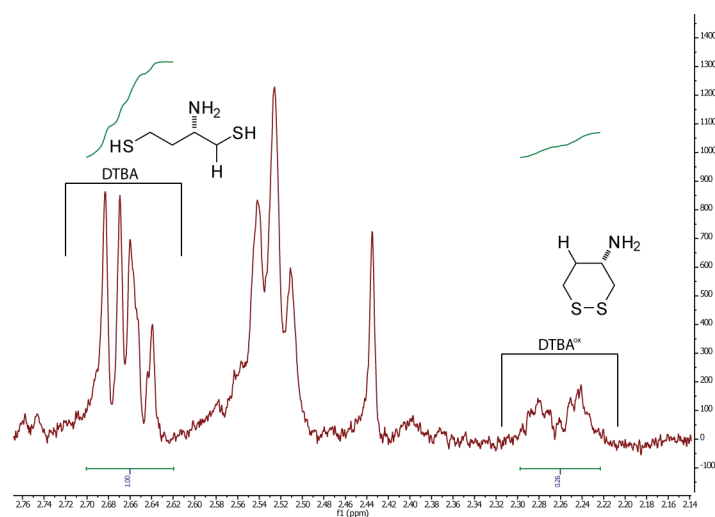


Figure 3.8 Representative ^1H NMR spectrum of the reaction between DTBA^{ox} (3.1) and a 10-fold excess of immobilized DTBA.

Reduction of 3.2

Ellman's assay was performed on immobilized DTBA immediately prior to its use. What was determined to be 8.99×10^{-3} mmol of immobilized DTBA was added to a 1.5-mL LoBind Eppendorf tube, and 0.6 mL of freshly degassed 50 mM sodium phosphate buffer, pH 7.0, was then added, followed by $89.9 \mu\text{L}$ (8.99×10^{-4} mmol) of a 10 mM stock solution of DTT^{ox} in the same buffer. The reaction mixture was agitated with a nutator for 24 h and then quenched by the addition of 3 N HCl (1:100 dilution). The resin was separated by centrifugation, and the solution was analyzed immediately by both ^1H NMR spectroscopy and analytical HPLC, as described previously. Concentrations of DTT and DTT^{ox} were determined and revealed a 68% yield of DTT.

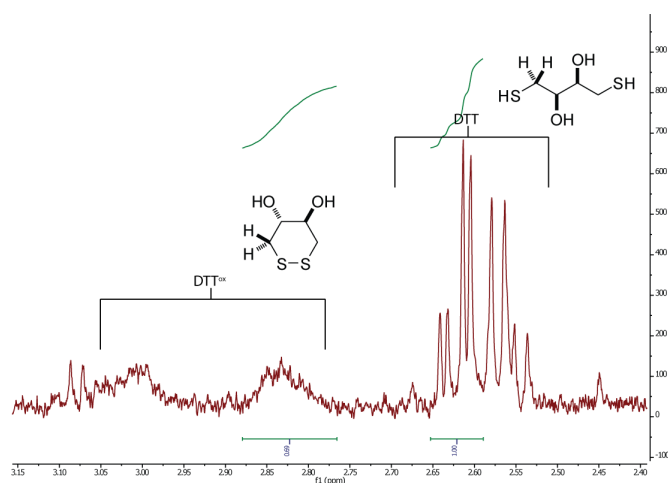


Figure 3.9 Representative ^1H NMR spectrum of the reaction between DTT^{ox} (**3.2**) and a 10-fold excess of immobilized DTBA.

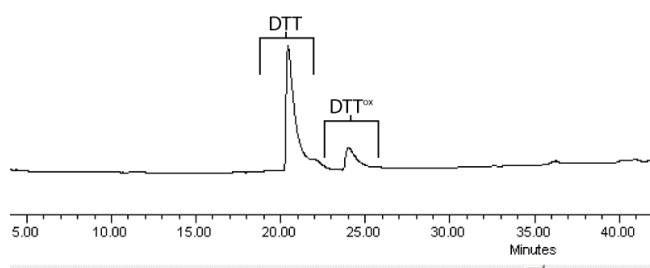
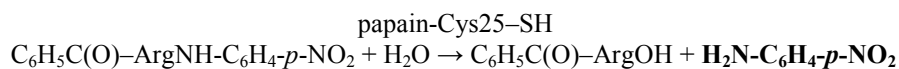
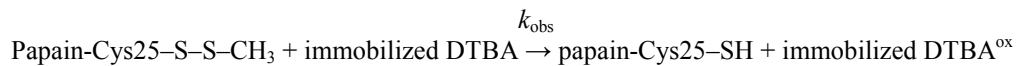
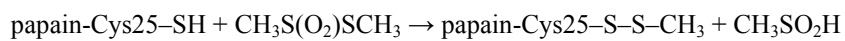


Figure 3.10 Representative HPLC chromatogram of the reaction between DTT^{ox} (**3.2**) and a 10-fold excess of immobilized DTBA. Compounds were detected by their absorbance at 205 nm.

3.7.6 Reactivation of papain with immobilized DTBA



Ellman's assay was performed on immobilized DTBA immediately prior to setting up the assay. Papain was inactivated by oxidizing its active-site cysteine (Cys25) by treatment with *S*-methyl methanethiosulfonate following a procedure described previously.⁴² A 1.25-mL solution of papain-Cys25-S-S-CH₃ (1.25×10^{-5} M, 1.56×10^{-5} mmol) in degassed 0.10 M imidazole-HCl buffer, pH 7.0, containing EDTA (2 mM) was placed in a 1.5-mL LoBind Eppendorf tube. At time $t = 0$, a ~ 100 -fold excess of immobilized DTBA (1.35×10^{-3} mmol) was added to the Eppendorf tube, which was then placed on a nutator. At various times, the resin was separated by centrifugation, and a 0.2-mL aliquot of the solution was removed and added to a cuvette containing 0.8 mL of 0.10 M imidazole-HCl buffer, pH 6.0, containing EDTA (2 mM) and *N*-benzoyl-L-arginyl-*p*-nitroanilide (1.25 mM). The rate of change in absorbance at 410 nm was recorded at 25 °C. A unit of protein is defined as the amount of enzyme required to produce 4-nitroaniline at a rate of 1 $\mu\text{mol}/\text{min}$. The units of active papain at each time point was calculated by using an extinction coefficient for 4-nitroaniline of $\epsilon = 8,800 \text{ M}^{-1}\text{cm}^{-1}$ at 410 nm. To determine the possible number of units of active papain in the reaction mixture, enzymatic activity was assessed after the addition of a large excess of DTT ($\sim 10^3$ -fold) to an Eppendorf tube. As a control, the addition of DTT was shown to have no bearing on the assay data, other than in activating the enzyme. The enzymatic activity (%) at particular times was calculated by dividing the number of active units of enzyme by the possible number of units in the solution, and was plotted in Figure 3.1. The procedure described above was also performed using $\sim 1,000$ equiv of immobilized DTBA.

3.7.7 Reactivation of papain using relay catalysts

The procedure described in Section VI was also performed in the presence of a relay catalyst. Stock solutions (1 mM) of **3.1–3.9** were prepared in degassed 0.10 M imidazole–HCl buffer, pH 7.0, containing EDTA (2 mM) or in DMSO, and 5 μ L of this solution (5×10^{-6} mmol of catalyst, 30 mol%) of was added to the reaction mixture in the Eppendorf tube. The enzymatic activity (%) at particular times was calculated by dividing the number of active units of enzyme by the possible number of units in the solution, and was plotted in Figures 3.1–3.3. To determine the value of the second-order rate constant k_{obs} , the second-order rate equation (Eq 3) was transformed into Eq 4, which was fitted to the data with the program Prism 5.0 (GraphPad Software, La Jolla, CA). In Eq 3.3 and 3.4, $A_0 = [\text{inactive protein}]_{t=0}$, $A = [\text{inactive protein}]_t = A_0 - A_0y$, $B_0 = [\text{immobilized DTBA}]_{t=0}$, and $B = [\text{immobilized DTBA}]_t = B_0 - A_0y$. Values of k_{obs} were the mean \pm SEM from at least 4 different experiments.

$$\frac{1}{B_0 - A_0} \ln \frac{A_0 B}{A B_0} = k_{\text{obs}} t \quad (3.3)$$

$$y = \frac{B_0 - B_0 e^{k_{\text{obs}} t (A_0 - B_0)}}{B_0 - A_0 e^{k_{\text{obs}} t (A_0 - B_0)}} \quad (3.4)$$

| | |
|--|--|
| immobilized DTBA | $k_{\text{obs}} = (0.16 \pm 0.01) \text{ M}^{-1} \text{ s}^{-1}$ |
| immobilized DTBA + DTBA ^{ox} (3.1) | $k_{\text{obs}} = (0.25 \pm 0.01) \text{ M}^{-1} \text{ s}^{-1}$ |
| immobilized DTBA + DTT ^{ox} (3.2) | $k_{\text{obs}} = (0.17 \pm 0.01) \text{ M}^{-1} \text{ s}^{-1}$ |
| immobilized DTBA + cystamine (3.3) | $k_{\text{obs}} = (0.30 \pm 0.02) \text{ M}^{-1} \text{ s}^{-1}$ |
| immobilized DTBA + β ME ^{ox} (3.4) | $k_{\text{obs}} = (0.17 \pm 0.01) \text{ M}^{-1} \text{ s}^{-1}$ |
| immobilized DTBA + BMC ^{ox} (3.5) | $k_{\text{obs}} = (0.67 \pm 0.01) \text{ M}^{-1} \text{ s}^{-1}$ |
| immobilized DTBA + lipoic acid (3.6) | $k_{\text{obs}} = (0.29 \pm 0.04) \text{ M}^{-1} \text{ s}^{-1}$ |
| immobilized DTBA + selenoDTBA ^{ox} (3.7) | $k_{\text{obs}} = (0.82 \pm 0.03) \text{ M}^{-1} \text{ s}^{-1}$ |
| immobilized DTBA + selenocystamine (3.8 , 1 mol%) | $k_{\text{obs}} = (0.40 \pm 0.02) \text{ M}^{-1} \text{ s}^{-1}$ |
| immobilized DTBA + selenocystamine (3.8 , 5 mol%) | $k_{\text{obs}} = (0.86 \pm 0.05) \text{ M}^{-1} \text{ s}^{-1}$ |
| immobilized DTBA + selenocystamine (3.8 , 30 mol%) | $k_{\text{obs}} = (4.7 \pm 0.2) \text{ M}^{-1} \text{ s}^{-1}$ |
| immobilized DTBA + selenoBMC ^{ox} (3.9) | $k_{\text{obs}} = (0.42 \pm 0.02) \text{ M}^{-1} \text{ s}^{-1}$ |

3.7.8 Reactivation of papain with DTBA and BMC

A procedure similar to that described previously was used to compare the rate at which DTBA and BMC reduce the active site cysteine of papain-Cys25-S-S-CH₃.⁴²

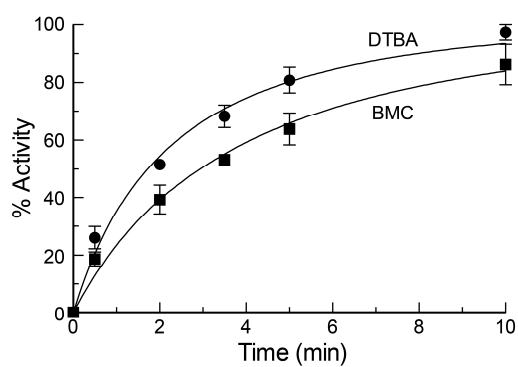
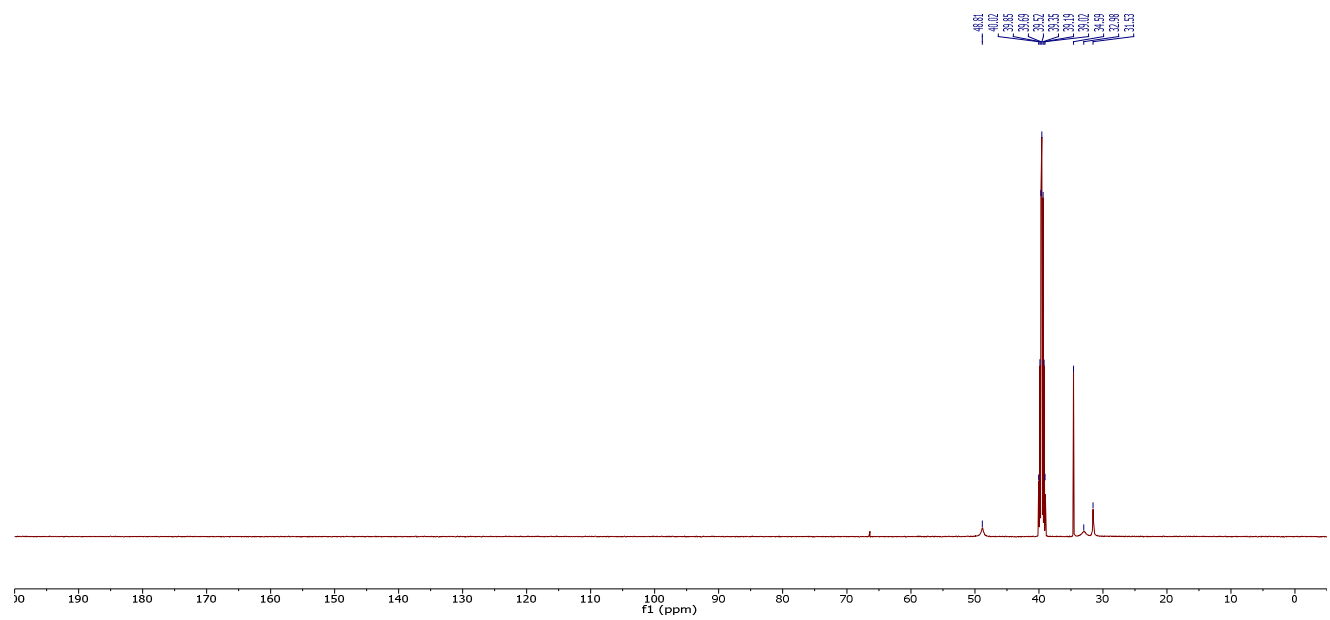
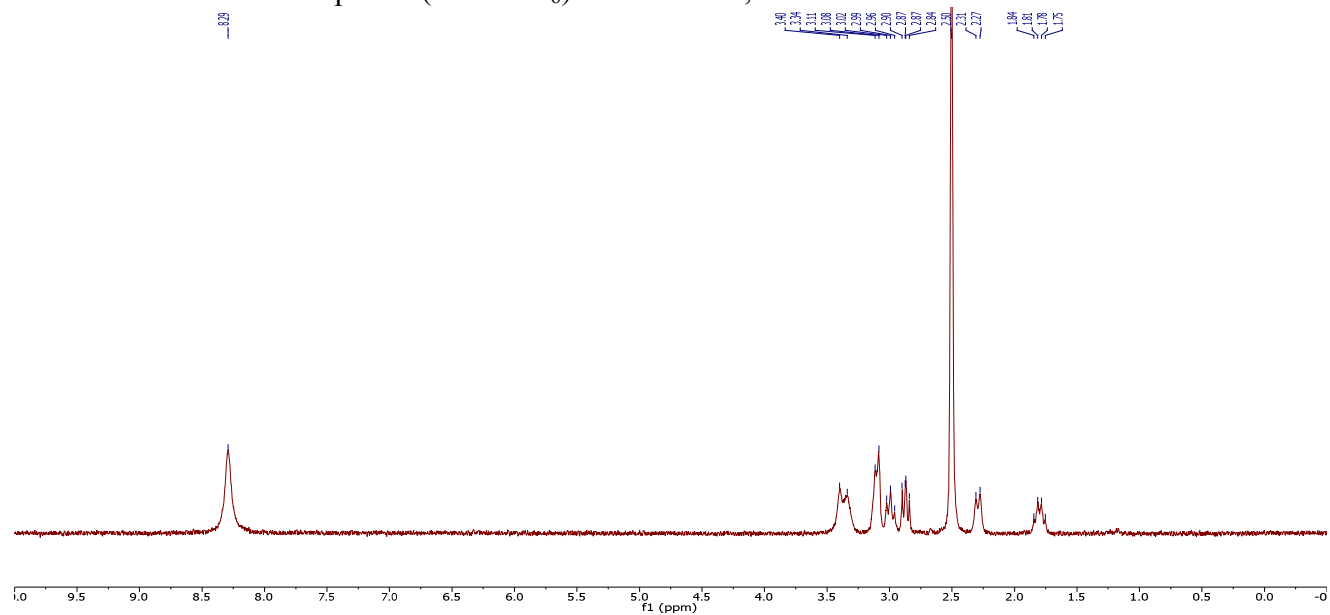


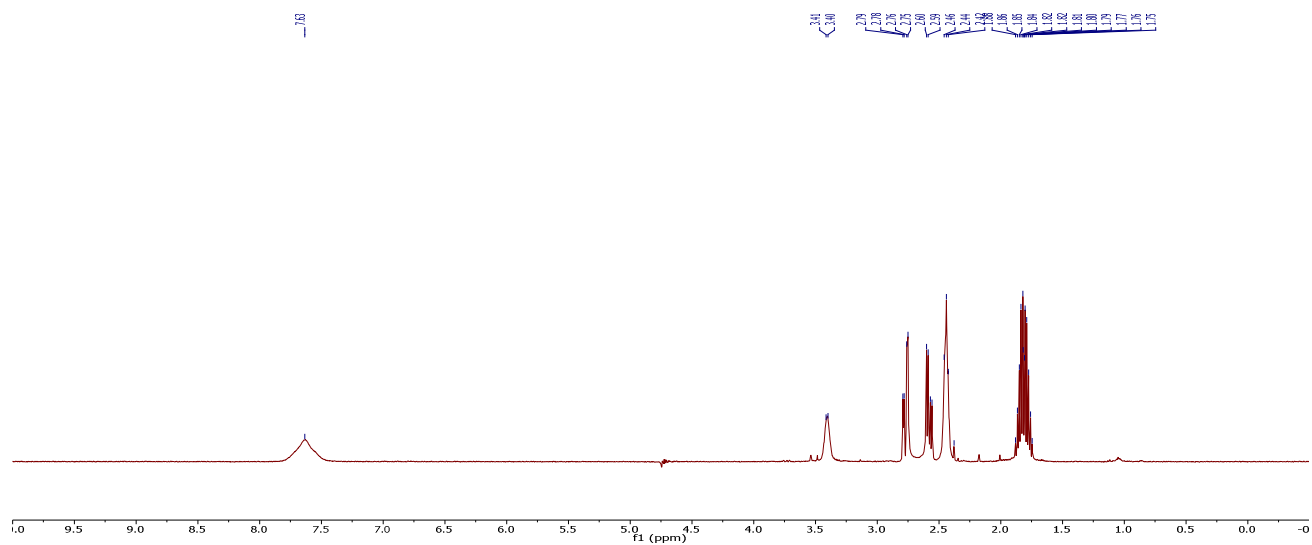
Figure 3.11 Time-course for the reactivation of papain-Cys25-S-S-CH₃ by dithiols (1.5 equiv) in 0.10 M imidazole-HCl buffer, pH 7.0, containing EDTA (2 mM). DTBA: $k_{\text{obs}} = (1067 \pm 69) \text{ M}^{-1}\text{s}^{-1}$; BMC: $k_{\text{obs}} = (609 \pm 42) \text{ M}^{-1}\text{s}^{-1}$

3.8 NMR Spectra

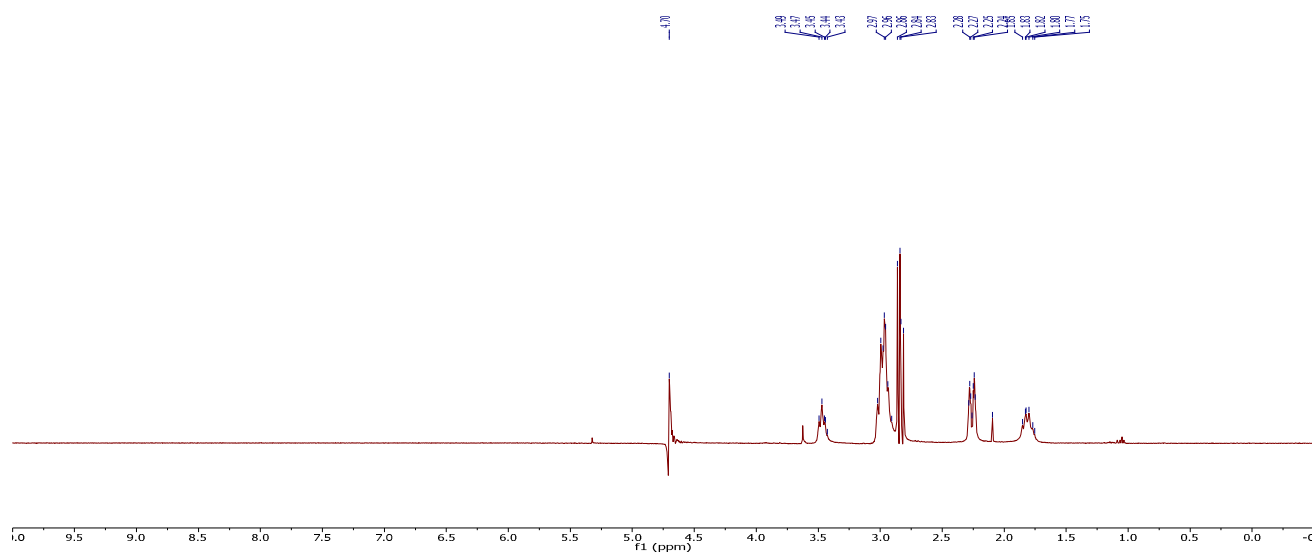
^1H NMR and ^{13}C NMR spectra (DMSO- d_6) of **3.1** with 1,4-dioxane

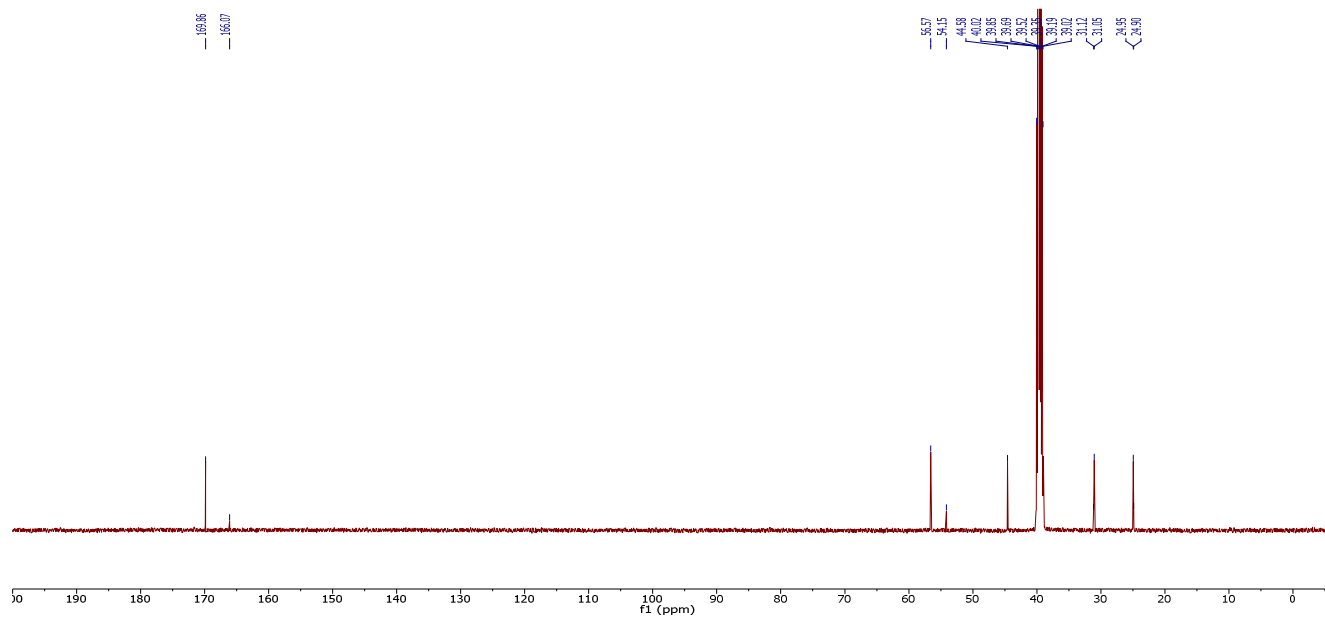
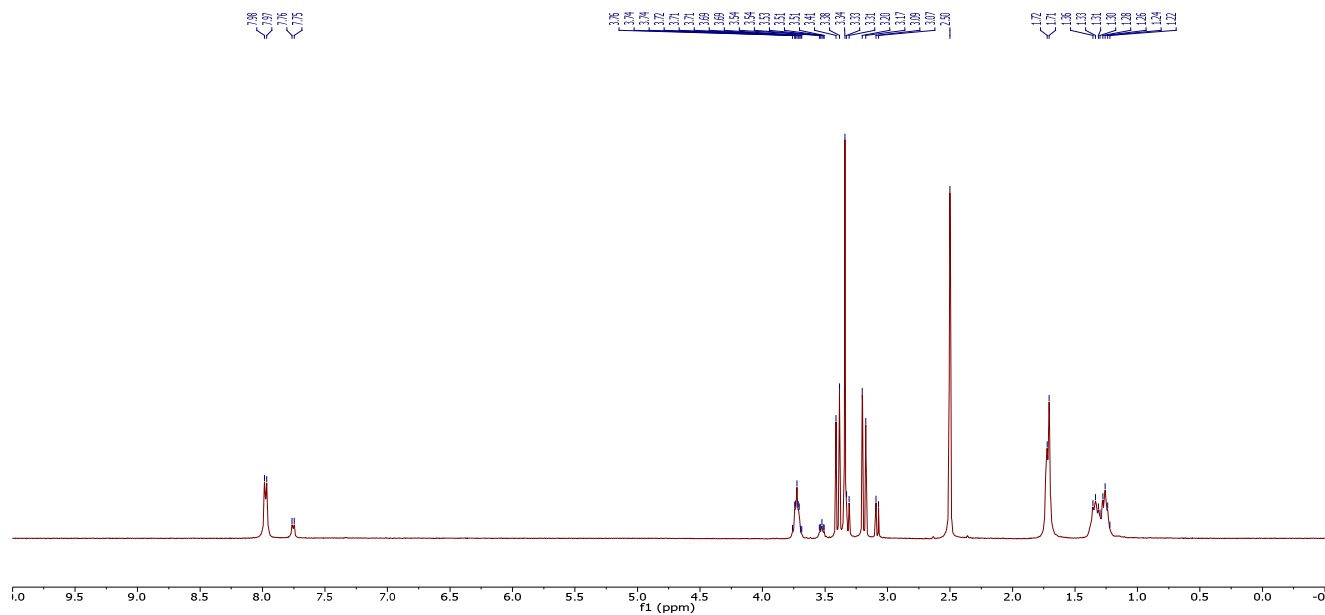


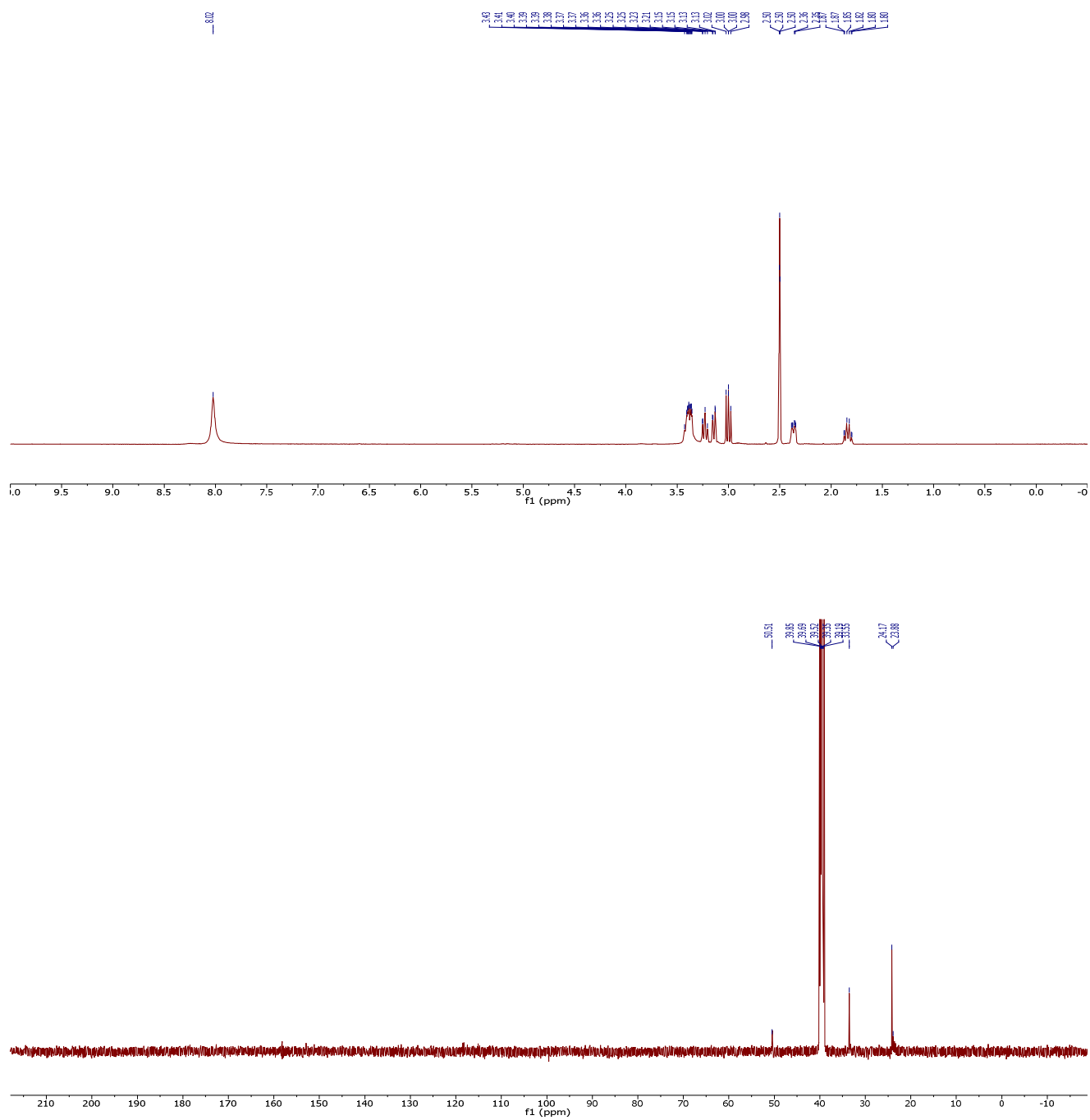
^1H NMR spectrum (50 mM sodium phosphate buffer, pH 7.0) of DTBA

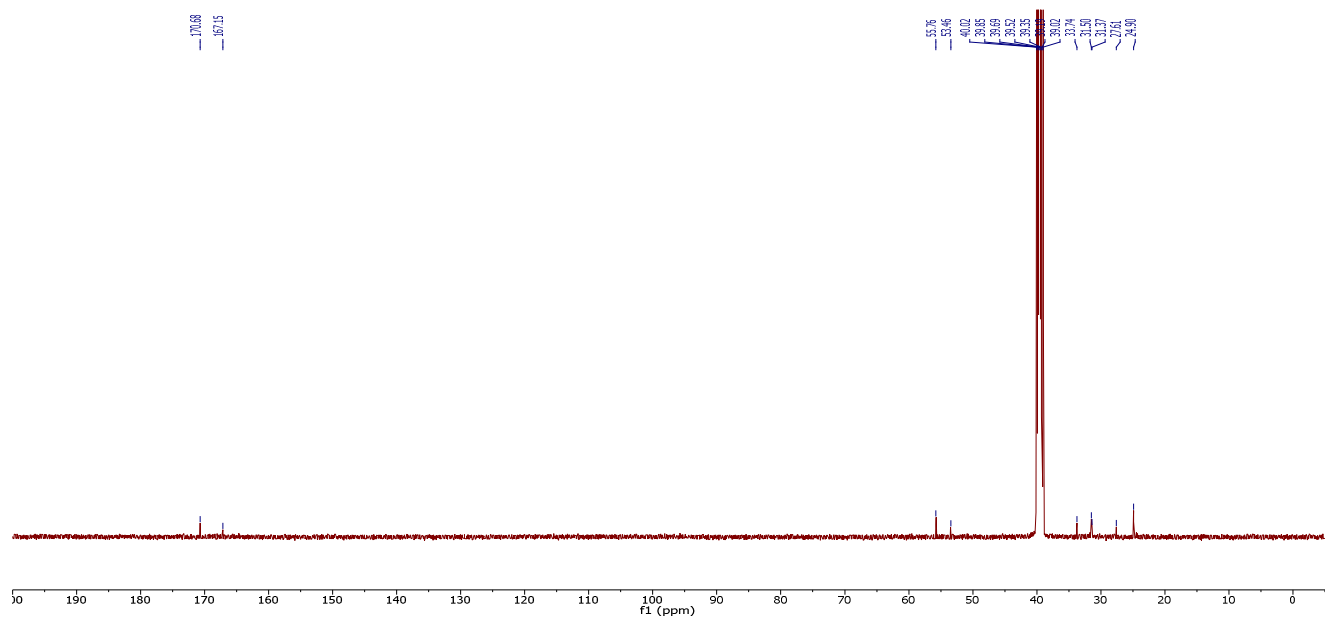
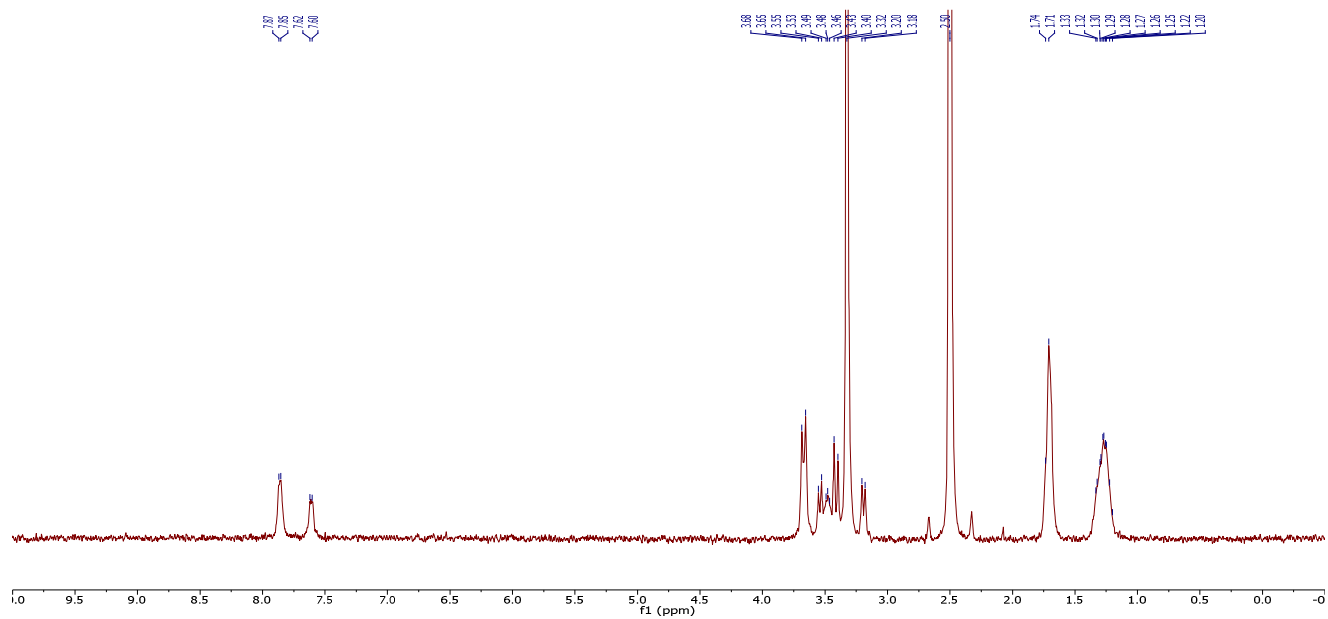


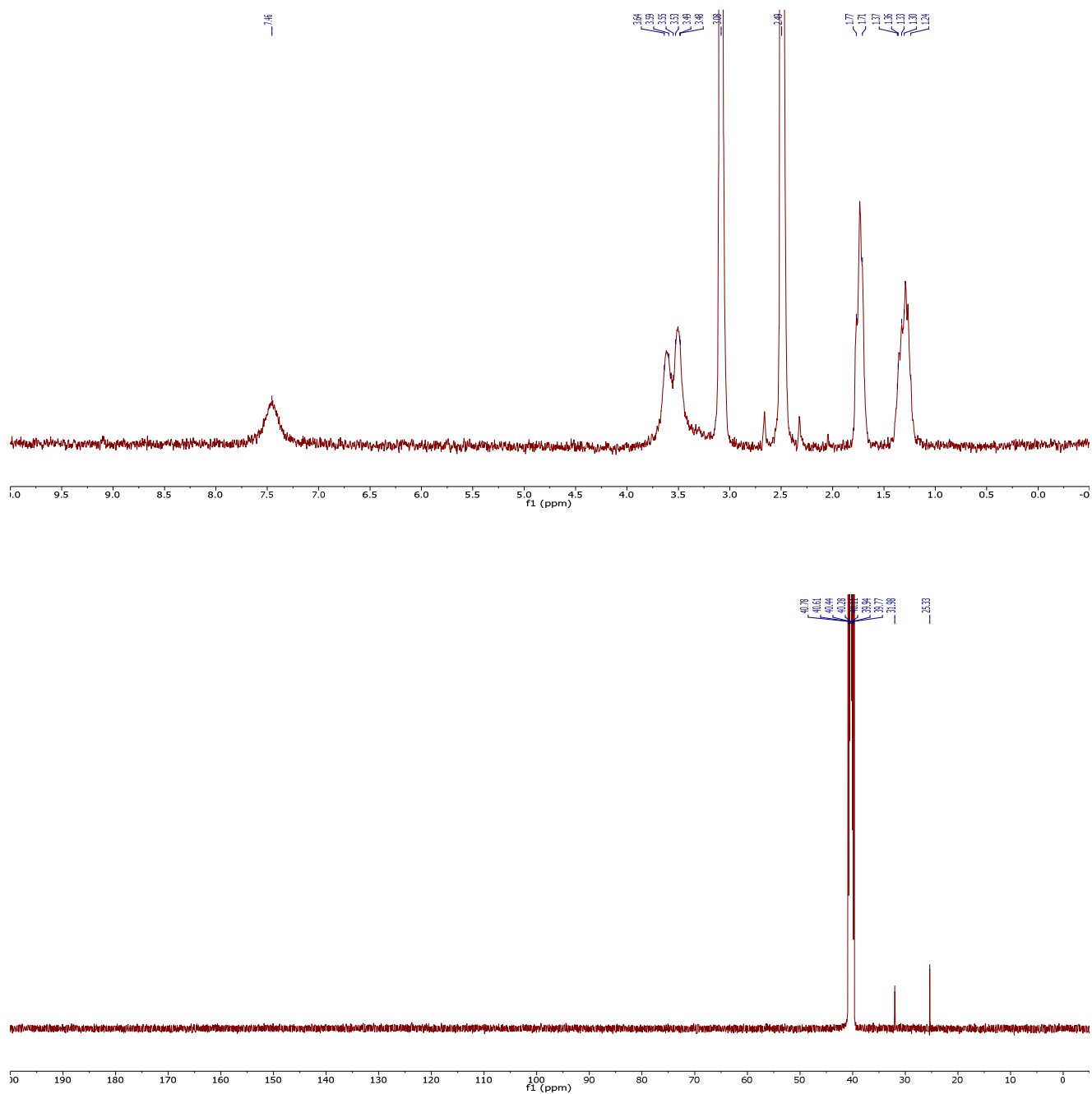
^1H NMR spectrum (50 mM sodium phosphate buffer, pH 7.0) of **3.1**



^1H NMR and ^{13}C NMR spectra (DMSO- d_6) of 3.5

^1H NMR and ^{13}C NMR spectra (DMSO- d_6) of **3.7**

^1H NMR and ^{13}C NMR spectra (DMSO- d_6) of **3.9**

^1H NMR and ^{13}C NMR spectra (DMSO- d_6 , 80 °C) spectra of **3.9**

Chapter 4*: Pyrazine-Derived Disulfide-Reducing Agent for Chemical Biology

4.1 Abstract

For fifty years, dithiothreitol (DTT) has been the preferred reagent for the reduction of disulfide bonds in proteins and other biomolecules. Herein, we report on the synthesis and characterization of 2,3-bis(mercaptomethyl)pyrazine (BMMP), a readily accessible disulfide-reducing agent with reactivity under biological conditions that is markedly superior to DTT and other known reagents.

4.2 Author Contributions

J.C.L. proposed the use of a pyrazine scaffold in order to optimize the physicochemical properties of the disulfide-reducing agent. K.K.W. assisted J.C.L. in the synthesis, characterization, and evaluation of BMMP. J.C.L. drafted the original manuscript and figures. J.C.L., K.K.W., and R.T.R. planned experiments, analyzed data, and edited the manuscript and figures.

*This chapter has been published, in part, under the same title. Reference: Lukesh, J. C., III; Wallin, K. K.; Raines, R. T. *Chem Commun.* **2014**, *50*, 9591–9594

4.3 Introduction

The redox state of cystine residues can have a profound effect on protein structure and function.^{1,5,11,141} Consequently, reagents that reduce disulfide bonds to thiols can be crucial to progress in chemical biology.^{4,5,163} Necessarily, the reduction of disulfide bonds within biomolecules must be accomplished under mild conditions: in water, at neutral pH, and at room temperature.^{5,15,24,29,37} Thiols can accomplish these goals and do so (unlike phosphines) in a reversible manner. Their reduction mechanism entails thiol–disulfide interchange initiated by the attack of a thiolate.^{17,21,34-36,122-124} The use of monothiols such as L-glutathione or β -mercaptoethanol (β ME) can lead to the trapping of the resulting intermediate as a mixed disulfide. In 1964, Cleland reported that dithiothreitol (DTT or Cleland's reagent; Table 4.1), a racemic dithiol, readily completes the reduction reaction by forming a stable six-membered ring.²⁴ The potency of DTT is evident from the low reduction potential ($E^{\circ'} = -0.327$ V) of its oxidized form.³⁸ As a result, DTT has achieved widespread use for the quantitative reduction of disulfide bonds in proteins and other biomolecules.

DTT has, however, a serious limitation. As thiolates but not thiols are nucleophilic in aqueous solution,¹⁶⁴ the observed rate of disulfide reduction is dependent on the thiol pK_a of the reducing agent. With thiol pK_a values of 9.2 and 10.1, <1% of DTT resides in the reactive thiolate form at neutral pH. As a result, several attempts have been made to create water-soluble reducing agents that sport depressed thiol pK_a values.²⁷⁻²⁹

Recently, we reported on dithiobutylamine (DTBA; Table 4.1), a dithiol reducing agent derived from L-aspartic acid.⁴² Like DTT, DTBA is a potent disulfide-reducing agent. Moreover, the amino group of DTBA confers depressed thiol pK_a values of 8.2 and 9.3 and facile

functionalization.^{42,55} That amino group, however, appeared to deter the ability of the molecule to reduce certain disulfide bonds due to unfavorable Coulombic interactions.⁴²

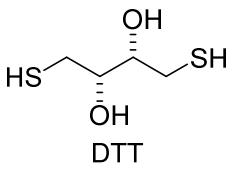
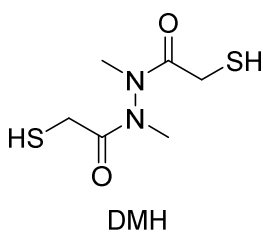
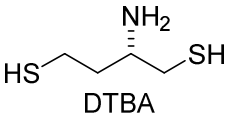
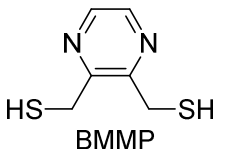
| | Thiol pK _a | Disulfide Reduction Potential (<i>E</i> ^o) |
|---|---------------------------------------|---|
|  DTT | 9.2 (10.1) ^a | -0.327 V ^a |
|  DMH | 8.0 ± 0.2 (9.1 ± 0.1) ^b | -0.262 V ^b |
|  DTBA | 8.2 (9.3) ^a | -0.317 V ^a |
|  BMMP | 7.6 ± 0.1 (9.0 ± 0.1) ^b | -0.301 ± 0.003 V ^b |

Table 4.1 Physicochemical properties of dithiol reducing agents. ^aValues are from ref. 42. ^breferences are from this work.

We were determined to improve upon DTBA. Dithiols (like DTBA and DTT) that form six-membered cyclic disulfides are potent reducing agents, reflecting a balance between the high enthalpic stability of the incipient ring and low entropic loss for its formation.^{38,39} We reasoned that the entropic loss could be diminished further by limiting rotation around of the bonds between the two sulfhydryl groups. We also sought an electron-withdrawing group that could

lower a thiol pK_a to a value close to physiological pH (which is pH 7.365 in human blood). Then, an optimal balance is achieved between the concentration of the thiolate nucleophile (low pK_a is better) and its incipient nucleophilicity (high pK_a is better).^{34,165} Accordingly, we suspected that incorporating a highly electron-deficient moiety (e.g., a pyrazine ring) that also serves to pre-organize the reagent for disulfide-bond formation could be advantageous. A compound that fits this description is 2,3-bis(mercaptomethyl)pyrazine (BMMP; Table 4.1).

4.4 Results and Discussion

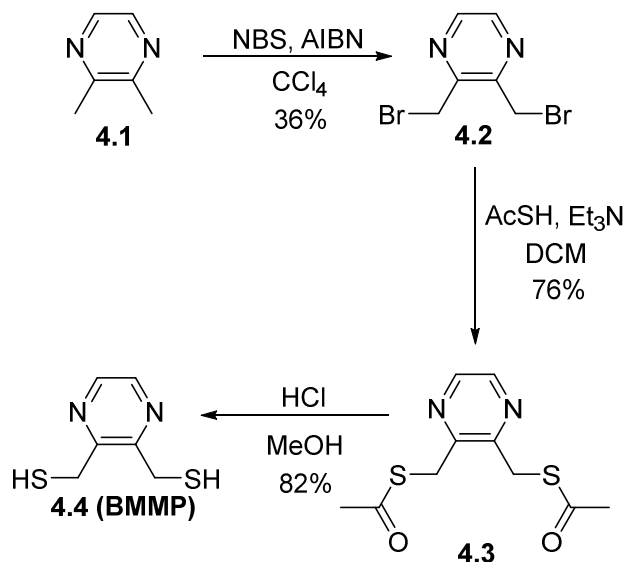
Prior to designing a synthetic route to BMMP, we calculated the free energies for the optimized geometry of reduced BMMP and oxidized BMMP and compared them to those of reduced DTT and oxidized DTT. We were aware of a prior study that predicted the stability of cyclic disulfides using molecular mechanics calculations,³⁹ and sought to assess our design at a higher level of theory (B3LYP/6-311+G(2d,p)).¹⁶⁶ The thiol pK_a values of BMMP were calculated to be substantially lower than those of DTT. Moreover, the oxidation of BMMP was calculated to be slightly more favorable than that of DTT.

Because of these encouraging computational results, we synthesized BMMP from 2,3-dimethylpyrazine (**4.1**) *via* a simple three-step route (Scheme 4.1). We isolated BMMP as an off-white/yellow powder in 22% overall yield. The compound has low odor and aqueous solubility (64 mM reduced; 8 mM oxidized) that is adequate for typical applications in chemical biology.

As predicted, BMMP has low thiol pK_a values. A pH titration monitored by UV spectroscopy revealed these values to be 7.6 ± 0.1 and 9.0 ± 0.1 . These pK_a values are significantly lower than those of DTT and DTBA (Figure 4.1).^{42,129} Moreover, the lower of its

two thiol pK_a values is closer to physiological pH than any known dithiol-based reducing agent.

(*vide infra*).^{27-29,112}



Scheme 4.1 Synthetic route to BMMP (4.4)

BMMP was also found to be a potent reducing agent, albeit slightly less than predicted by our calculations. We found that the equilibrium reaction between reduced BMMP and oxidized DTT favors those species (rather than oxidized BMMP and reduced DTT) by ~ 1.2 kcal/mol, which corresponds to a reduction potential of $E^{\circ'} = (-0.301 \pm 0.003)$ V for oxidized BMMP (Figure 4.1 and Figure; Figure 4.6). This $E^{\circ'}$ value is slightly less negative than both DTT and DTBA, and presumably results from the decreased enthalpic stability imparted by the two sp^2 -hybridized carbons in its six-membered ring.³⁹ BMMP is, however, a much more potent reducing agent than common monothiols such as β -mercaptoethanol (β ME), cysteamine, and L-glutathione.^{124,167} To probe this difference, we equilibrated oxidized β ME (β ME^{ox}) with a slight

excess of reduced BMMP for 24 h. Analysis by HPLC revealed the complete reduction of $\beta\text{ME}^{\text{ox}}$ (Figure 4.8).

Singh and Whitesides put forth *N,N'*-dimethyl-*N,N'*-bis(mercaptoacetyl)hydrazine (DMH; Fig 4.1) as a faster disulfide-reducing agent than DTT. Notably, their reported $\text{p}K_{\text{a}} = 7.6$ (8.9) and $E^{\circ'} = -0.300$ V values for DMH are indistinguishable from those of BMMP (Figure 4.1). The $E^{\circ'}$ value of DMH was corrected subsequently by Lees and Whitesides to be -0.272 V,³⁸ which is more consistent with its forming an 8-membered ring upon oxidation. To our knowledge, the $\text{p}K_{\text{a}}$ value of DMH has not been examined again. Accordingly, we synthesized DMH so as to reexamine its properties and utility. Our observed value of $E^{\circ'} = (-0.262 \pm 0.003)$ V for DMH was even higher than that of Lees and Whitesides, and confirms that DMH is a markedly weaker reducing agent than is BMMP, DTBA, or DTT (Table 4.1). Likewise, our value of $\text{p}K_{\text{a}} = 8.0 + 0.1$ (Figure 4.1) is higher than that reported by Singh and Whitesides, but consistent with values reported for mercaptoacetamido groups.^{27,29,116}

Next, we analyzed the reactivity of BMMP with relevant disulfide bonds. At pH 7.0, BMMP reduced the disulfide bond in $\beta\text{ME}^{\text{ox}}$ 11-fold faster than did DTT and 3-fold faster than did DTBA (Figure 4.1A; Table 4.2). Commensurate with their $\text{p}K_{\text{a}}$ values, DMH reduced $\beta\text{ME}^{\text{ox}}$ faster than did DTT or DTBA but slower than did BMMP. At pH 5.0, BMMP reduced $\beta\text{ME}^{\text{ox}}$ 14-fold faster than did DTT and 4-fold faster than did DTBA (Figure 4.1B; Table 4.2). These data highlight the broad pH-range at which BMMP can be utilized effectively.

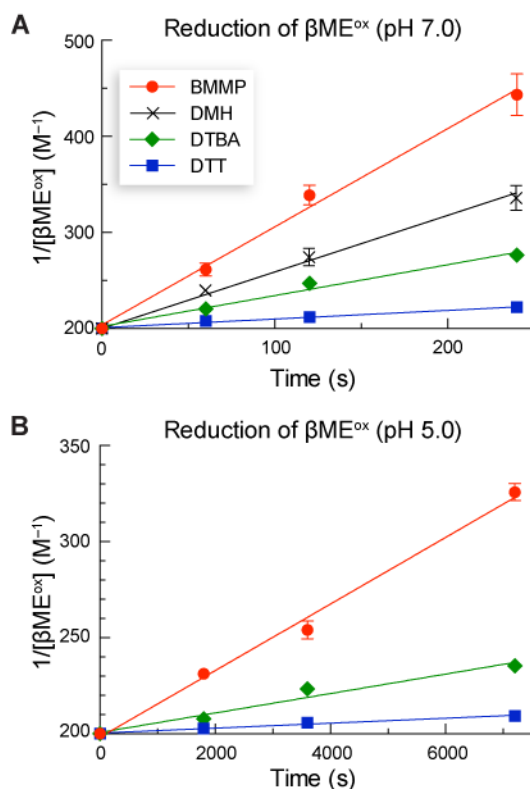


Figure 4.1 Time-course for the reduction of $\beta\text{ME}^{\text{ox}}$ (5 mM) by BMMP, DMH, DTBA, or DTT (5 mM) in buffered water. (A) In 50 mM potassium phosphate buffer, pH 7.0: $k_{\text{obs}}^{\text{BMMP}}/k_{\text{obs}}^{\text{DMH}} = 1.8$, $k_{\text{obs}}^{\text{BMMP}}/k_{\text{obs}}^{\text{DTBA}} = 3.2$, $k_{\text{obs}}^{\text{BMMP}}/k_{\text{obs}}^{\text{DTT}} = 11.4$. (B) In 50 mM sodium acetate buffer, pH 5.0: $k_{\text{obs}}^{\text{BMMP}}/k_{\text{obs}}^{\text{DTBA}} = 3.6$, $k_{\text{obs}}^{\text{BMMP}}/k_{\text{obs}}^{\text{DTT}} = 14.1$.

Finally, we assessed the ability of BMMP to reduce disulfide bonds in two proteins. Papain is a cysteine protease that contains an active-site sulfhydryl group (Cys25) that needs to be in a reduced state for catalysis.¹³² Treatment with *S*-methyl methanethiosulfonate generates an active-site mixed disulfide that results in complete loss of enzymatic activity.¹⁴ This loss in activity, however, is reversible upon treatment with a disulfide-reducing agent. We found that BMMP reduced the mixed disulfide in papain 13-fold faster than did DTT at a rate comparable to that of DTBA (Figure 4.2A; Table 4.2).⁴²

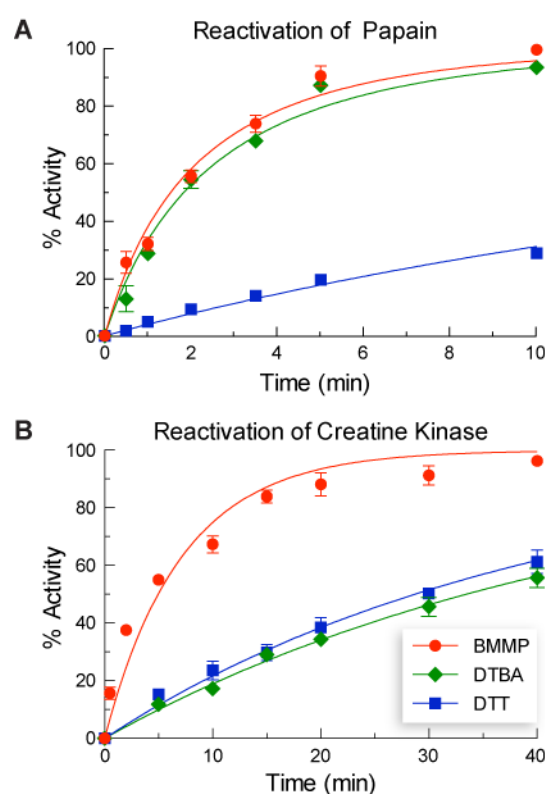


Figure 4.2 Time-course for the reduction of a mixed disulfide in proteins by BMMP, DTBA, or DTT (7.8 μM) in 0.10 M imidazole–HCl buffer, pH 7.0, containing EDTA (2 mM). (A) Papain–Cys25–S–S–CH₃ (4.4 μM): $k_{obs}^{BMMP}/k_{obs}^{DTBA} = 1.2$, $k_{obs}^{BMMP}/k_{obs}^{DTT} = 13.1$. (B) Creatine kinase–Cys283–S–S–L–glutathione (0.34 μM): $k_{obs}^{BMMP}/k_{obs}^{DTBA} = 6.8$, $k_{obs}^{BMMP}/k_{obs}^{DTT} = 5.8$.

Creatine kinase, like papain, is an enzyme that contains a thiol group (Cys283) that needs to be in a reduced state for catalytic function.¹³⁴⁻¹³⁷ When treated with oxidized L–glutathione, the resulting mixed disulfide eliminates its enzymatic activity. Previously, we reported that the ability of DTBA to reduce this disulfide bond was compromised—presumably by unfavorable Coulombic interactions—resulting in a low reaction rate comparable to that of DTT. In contrast to DTBA, BMMP is not cationic near neutral pH (For example, the pK_a of the conjugate acid of 2,5–dimethylpyrazine is 2.1¹⁶⁸). Indeed, unfavorable Coulombic interactions were not apparent

with BMMP, which was found to reduce the mixed disulfide in creatine kinase 6-fold faster than did DTT and 7-fold faster than did DTBA (Figure 4.2B; Table 4.2).

4.5 Conclusions

In conclusion, we have designed, synthesized, and characterized BMMP, a novel disulfide-reducing agent with high reactivity under biological conditions. The pyrazine ring of BMMP fuels its enhanced performance without Coulombic consequences. In a variety of relevant assays, BMMP reduces disulfide bonds ~10-fold faster than does DTT. Notably, the depressed thiol pK_a values of BMMP extended the pH range at which disulfide bonds can be reduced efficiently. These attributes render BMMP as an attractive reagent for the reduction of the disulfide bonds encountered in chemical biology.

4.6 Acknowledgements

This paper is dedicated to the memory of our colleague, W. W. (Mo) Cleland (1930-2013), on the 50th anniversary of his seminal publication on DTT (ref. 24). We are grateful to Robert W. Newberry for advice on computations. This work was supported by grant R01 GM044783 (NIH), and made use of the National Magnetic Resonance Facility at Madison, which is supported by grant P41 GM103399 (NIH).

4.7 Materials and Methods

4.7.1 General

Commercial reagents were used without further purification. Dithiothreitol (DTT) was from Research Products International (Mt. Prospect, IL). *N,N'*-dimethylhydrazine

dihydrochloride was from Santa Cruz Biotechnology, Inc (Dallas,TX). Papain (lyophilized powder from papaya latex), creatine kinase (lyophilized powder from rabbit muscle), hexokinase (lyophilized powder from *Saccharomyces cerevisiae*), glucose-6-phosphate dehydrogenase (ammonium sulfate suspension from baker's yeast), *N*_α-benzoyl-L-arginine-4-nitroanilide hydrochloride, *S*-methyl methanethiosulfonate, *trans*-4,5-dihydroxy-1,2-dithiane (oxidized DTT), 2-mercaptoethanol, oxidized 2-mercaptoethanol, and 2-butyne-1,4-diol were from Sigma–Aldrich (St. Louis, MO). DTBA and oxidized DTBA were synthesized as described previously.⁴²

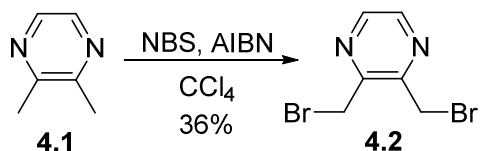
All glassware was oven or flame-dried, and reactions were performed under N₂(g) unless stated otherwise. Dichloromethane was dried over a column of alumina. Triethylamine and dimethylformamide (DMF) were dried over a column of alumina and purified further by passage through an isocyanate scrubbing column. Flash chromatography was performed with columns of 40–63 Å silica, 230–400 mesh (Silicycle, Québec City, Canada). Thin-layer chromatography (TLC) was performed on plates of EMD 250-um silica 60-F₂₅₄. The term “concentrated under reduced pressure” refers to the removal of solvents and other volatile materials using a rotary evaporator at water-aspirator pressure (<20 torr) while maintaining the water-bath temperature below 40 °C. Residual solvent was removed from samples at high vacuum (<0.1 torr). The term “high vacuum” refers to vacuum achieved by a mechanical belt-drive oil pump. Analytical samples of BMMP and BMMP^{ox} were obtained using a Shimadzu (Kyoto, Japan) preparative HPLC, equipped with a C18 reverse-phase preparative column, Prominence diode array detector, and fraction collector. Ellman’s assay for sulfhydryl groups was performed using a Varian Cary 60 Bio UV–Vis spectrophotometer. Equilibrium, reduction potential, and kinetic studies on small molecules were performed with an analytical HPLC (Waters system equipped with a Waters 996

photodiode array detector, Empower 2 software and a Varian C18 reverse-phase column). Thiol pK_a values were determined using a Varian Cary 60 UV–Vis spectrophotometer. Kinetic studies on proteins were carried out using a Varian Cary 400 Bio UV–Vis spectrometer with a Cary temperature controller at the Biophysics Instrumentation Facility at Madison (BIF). All NMR spectra were acquired at ambient temperature with a Bruker DMX-400 Avance spectrometer and a Bruker Avance III 500ii with cryoprobe spectrometer at the National Magnetic Resonance Facility at Madison (NMRFAM), and were referenced to TMS or residual protic solvent.

4.7.2 Computational procedures

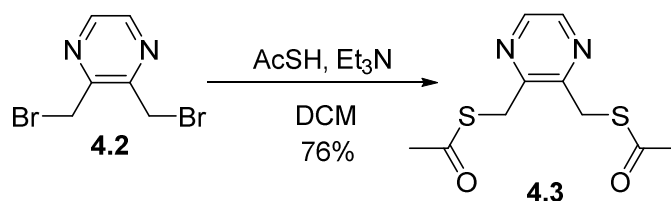
Idealized conformations of **4**, **5**, DMH, DMH^{ox}, DTT, and DTT^{ox} were determined by optimizing their geometries at the B3LYP/6-311+G(2d,p) level of theory as implemented by Gaussian 09.¹⁶⁶ The optimized structures yielded no imaginary frequencies, indicating a true energy minimum on the potential energy surface.

4.7.3 Chemical synthesis



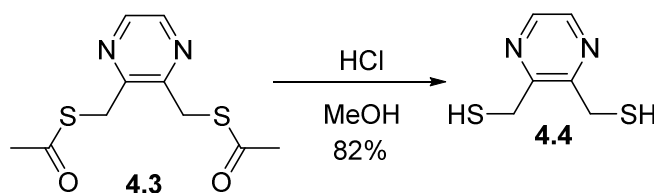
Compound **4.2** was synthesized as described previously from 2,3-dimethylpyrazine (**4.1**) resulting in comparable yields and identical NMR spectra.¹⁶⁹

¹H NMR (400 MHz, CDCl₃) δ = 8.43 (s, 2H), 4.65 (s, 4H); ¹³C NMR (125 MHz, CDCl₃) = 151.4, 143.9, 29.5.



A flame-dried round-bottom flask was charged with **4.2** (0.907 g, 3.411 mmol), dissolved with 35 mL of dichloromethane, and placed under an atmosphere of dry $\text{N}_2(\text{g})$. Triethylamine (1.50 mL, 10.76 mmol) and thioacetic acid (0.54 mL, 7.56 mmol) were then added, and the resulting solution was stirred overnight. After 16 h, the reaction was concentrated under reduced pressure and the resulting residue was purified by column chromatography (40% v/v ethyl acetate in hexanes) resulting in **4.3** (0.664 g, 76%).

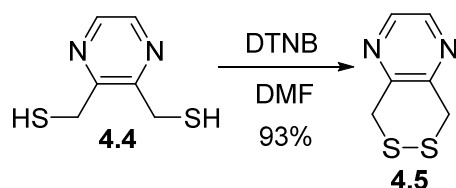
$^1\text{H NMR}$ (400 MHz, CDCl_3) δ = 8.42 (s, 2H), 4.43 (s, 4H), 2.39 (s, 6H); $^{13}\text{C NMR}$ (100 MHz, CDCl_3) δ = 194.4, 151.1, 142.8, 32.4, 30.2; HRMS (ESI) calculated for $[\text{C}_{10}\text{H}_{13}\text{N}_2\text{O}_2\text{S}_2]^+$ ($\text{M}+\text{H}^+$) requires m/z = 257.0413, found 257.0422.



To a flame-dried flask containing **4.3** (0.167 g, 0.651 mmol) was added 6 mL of anhydrous MeOH followed by 3 mL of 3 N HCl in MeOH. After reacting for 16 h under $\text{N}_2(\text{g})$, the reaction mixture was concentrated under reduced pressure, passed through a 4.5- μm filter, and purified by reverse-phase HPLC using a preparatory C18 column and a linear gradient of 10–80% v/v acetonitrile (0.1% v/v TFA) in water (0.1% v/v TFA) over 45 min. BMMP (**4.4**)

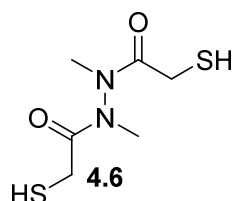
eluted at 27 min and, after lyophilization, was isolated as an off white/yellow powder (91.9 mg, 82%).

¹H NMR (400 MHz, DMSO-*d*₆) δ = 8.46 (s, 2H), 3.97 (d, *J* = 7.5 Hz, 4H), 3.05 (t, *J* = 7.5 Hz, 2H); **¹³C NMR (100 MHz, DMSO-*d*₆)** δ = 153.3, 142.5, 26.8; **HRMS (EI)** calculated for [C₆H₈N₂S₂]⁺ (M⁺) requires *m/z* = 172.0124, found 172.0125.



BMMP (**4.4**) (51.5 mg, 0.299 mmol) and 5,5'-dithio-bis(2-nitrobenzoic acid) (118.9 mg, 0.300 mmol) were placed in a 25-mL round-bottom flask. These solids were dissolved in 7 mL of anhydrous DMF, and the reaction mixture was stirred under N₂(g). After 24 h, the solvent was removed by rotary evaporation under high vacuum, passed through a 4.5- μ m filter, and purified by reverse-phase HPLC using a preparatory C18 column and a linear gradient of 10–80% v/v acetonitrile (0.1% v/v TFA) in water (0.1% v/v TFA) over 45 min. BMMP^{ox} (**4.5**) eluted at 36 min, and after lyophilization, was isolated as an off white/yellow powder (47.3 mg, 93%).

¹H NMR (400 MHz, CDCl₃) δ = 8.42 (s, 2H), 4.25 (s, 4H); **¹³C NMR (100 MHz, CDCl₃)** δ = 149.8, 142.2, 37.9; **HRMS (EI)** calculated for [C₆H₆N₂S₂]⁺ (M⁺) requires *m/z* = 169.9967, found 169.9961.



DMH (**4.6**) was synthesized from *N,N'*-dimethylhydrazine dihydrochloride as described previously.²⁸ An analytically pure sample of **6** was obtained from reverse-phase HPLC using a preparatory C18 column and a linear gradient of 10–80% v/v acetonitrile (0.1% v/v TFA) in water (0.1% v/v TFA) over 45 min. DMH eluted at 23 min and, after lyophilization, was isolated as a white solid.

¹H NMR (400 MHz, Methanol-*d*₄) (Two unresolved conformations present²⁸): δ = 3.53–3.21 (m), 3.08 (s); **¹³C NMR (100 MHz, Methanol-*d*₄) (Two conformations present)** δ = 174.5, 174.4, 172.2, 38.1, 34.8, 32.7, 26.3, 25.5, 25.4; **HRMS (ESI)** calculated for [C₆H₁₃N₂S₂]⁺ (M + H⁺) requires m/z = 209.0413, found 209.0410.

4.7.4 Determination of thiol p*K*_a values for BMMP

The thiol p*K*_a values for BMMP were determined by following closely a procedure reported previously that exploits the elevated absorbance of the deprotonated thiolate at 238 nm.^{42,116,129} A plot of A_{238} vs pH was recorded (Figure 4.3), and p*K*_a values were determined by fitting these data to eq 4.1, which is derived from both Beer's law and the definition of the acid dissociation constant.

$$A_{238} = C_T \left(\frac{\epsilon_{S^-}^{S-} 10^{(\text{pH}-\text{p}K_{a2})} + \epsilon_{SH^-}^{S-} + \epsilon_{SH}^{SH} 10^{(\text{p}K_{a1}-\text{pH})}}{10^{(\text{pH}-\text{p}K_{a2})} + 1 + 10^{(\text{p}K_{a1}-\text{pH})}} \right) \quad (4.1)$$

In eq 4.1, C_T is the total thiol concentration, ϵ_{SH}^{SH} is the extinction coefficient of the doubly protonated form of BMMP, ϵ_{SH}^{S-} is the extinction coefficient of the singly protonated form of BMMP, and ϵ_S^{S-} is the extinction coefficient of the doubly deprotonated form of BMMP.

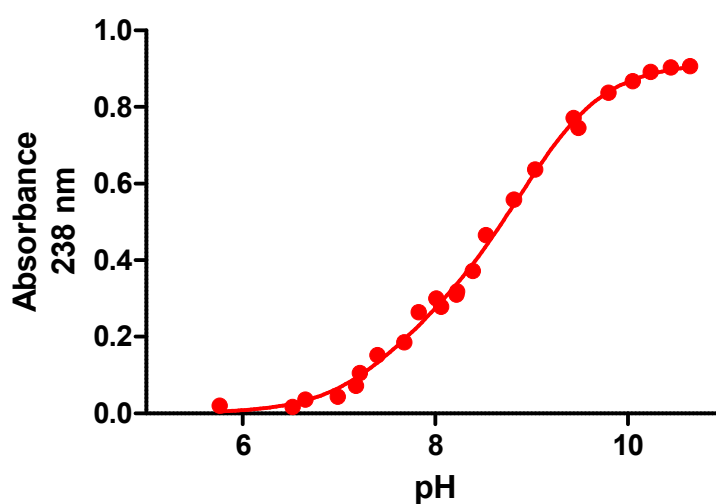


Figure 4.3 Effect of pH on absorbance by BMMP at 238 nm in a 0.10 M potassium phosphate buffer. pK_a values of 7.6 ± 0.1 and 9.0 ± 0.1 , and extinction coefficients of $\epsilon_{SH}^{SH} = 5.24$, $\epsilon_{SH}^{S-} = 3058$, $\epsilon_S^{S-} = 9159 \text{ M}^{-1}\text{cm}^{-1}$ with $r^2 > 0.99$ were determined by fitting the data to eq 4.1.

4.7.5 Determination of thiol pK_a values for DMH

The thiol pK_as of DMH were also examined using the same conditions described above.

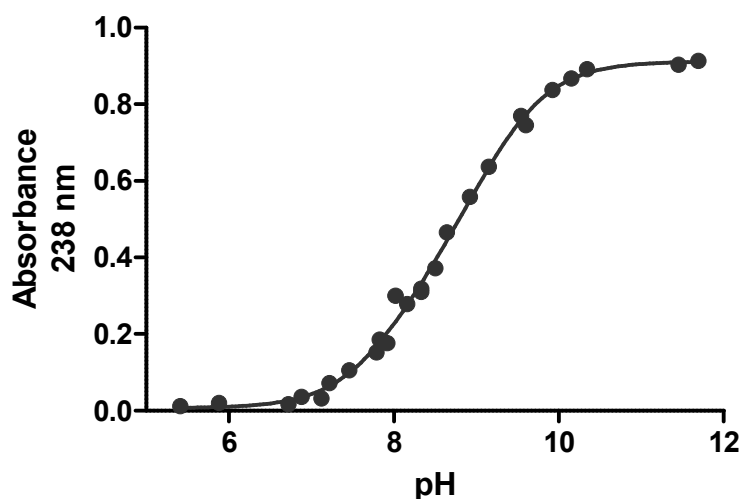


Figure 4.4 Effect of pH on absorbance by DMH at 238 nm in a 0.10 M potassium phosphate buffer. pK_a values of 8.0 ± 0.2 and 9.1 ± 0.1 , and extinction coefficients of $\epsilon_{\text{SH}}^{\text{SH}} = 67.8$, $\epsilon_{\text{SH}}^{\text{S}^-} = 3885$, $\epsilon_{\text{S}^-}^{\text{S}^-} = 9116 \text{ M}^{-1} \text{ cm}^{-1}$ with $r^2 > 0.99$ were determined by fitting the data to eq 4.1.

4.7.6 Reduction potential of BMMP

Following a procedure reported previously,^{29,42} the reduction potential of BMMP was determined by analyzing its equilibrium reaction with DTT^{ox} (eq 4.2), and measuring the amount of reduced and oxidized species in solution by analytical HPLC. Once the equilibrium constant was determined, its value was plugged into a variation of the Nernst equation (eq 4.3). BMMP (2.5 mg, 0.015 mmol) and DTT^{ox} (2.3 mg, 0.015 mmol) were placed in a 10 mL round-bottom flask, and 5 mL of degassed 50 mM potassium phosphate buffer, pH 7.0, containing EDTA (2 mM) was added. The reaction mixture was then sonicated briefly to ensure complete dissolution

of material and stirred overnight under $N_2(g)$. After reacting for 24 h, the reaction mixture was quenched by the addition of 0.1 mL of 3 N HCl, and passed through a 4.50- μ m filter. A 100- μ L aliquot of the reaction mixture was then immediately analyzed by analytical HPLC using a Waters system equipped with a Waters 996 photodiode array detector, Empower 2 software, and a Varian C18 column. The column was eluted at 1.0 mL/min with water (5.0 mL), followed by a linear gradient (0–40% v/v) of acetonitrile/water over 40 min. Four peaks were observed, corresponding to DTT (18 min), DTT^{ox} (22 min), BMMP (34 min), and BMMP^{ox} (41 min) (Figure 4.5). Calibration curves were generated and found to be linear over the concentration range analyzed. From these curves, equilibrium concentrations were determined, and a $K_{eq} = 0.137 \pm 0.036$ was determined for the reaction. Next, using this value and assuming $E^{\circ'} = -0.327$ V for DTT, a variation of the Nernst equation (eq 4.3) was used to calculate that BMMP has a reduction potential of $E^{\circ'} = (-0.301 \pm 0.003)$ V. This value is the mean \pm SE from three separate experiments.

$$K_{eq} = \frac{[DTT][oxidized\ BMMP]}{[BMMP][oxidized\ DTT]} \quad (4.2)$$

$$E_{BMMP}^{\circ'} = E_{DTT}^{\circ'} - \frac{RT}{nF} \ln \frac{[DTT][oxidized\ BMMP]}{[BMMP][oxidized\ DTT]} \quad (4.3)$$

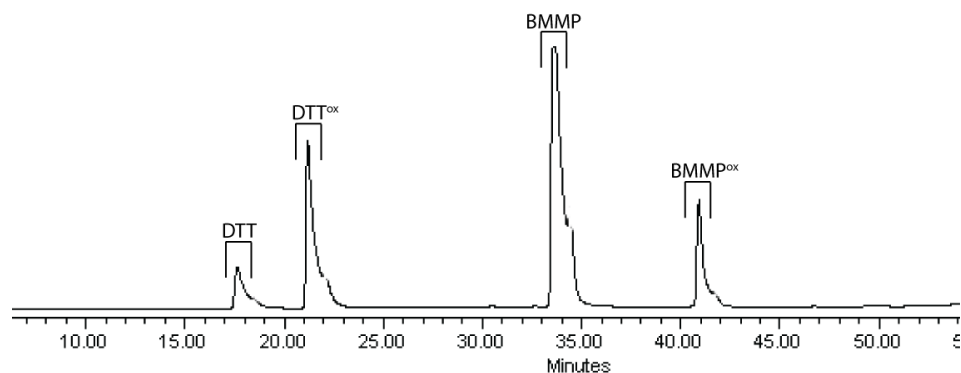


Figure 4.5 Representative HPLC chromatogram of the redox equilibrium between BMBP and DTT^{ox}. Compounds were detected by their absorbance at 205 nm.

4.7.7 Reduction potential of DMH

The reduction potential of DMH was also determined by following the same procedure described in Section 4.7.6. With $K_{\text{eq}} = 0.0065 \pm 0.0020$ and assuming $E^{\circ'} = -0.327$ V for DTT, DMH was found to have $E^{\circ'} = (-0.262 \pm 0.004)$ V.

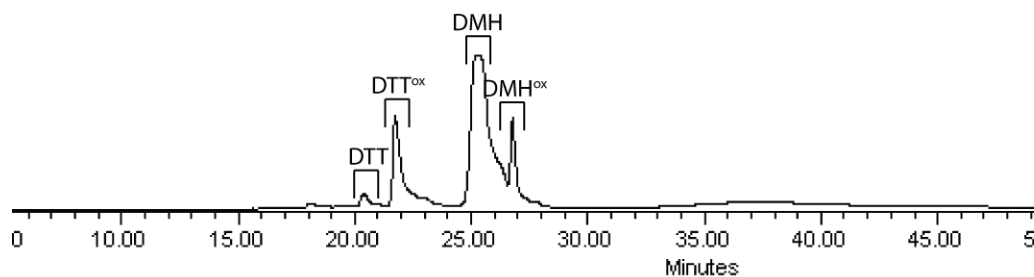


Figure 4.6 Representative HPLC chromatogram of the redox equilibrium between DMH and DTT^{ox}. Compounds were detected by their absorbance at 205 nm.

4.7.8 Equilibrium reaction with oxidized β ME

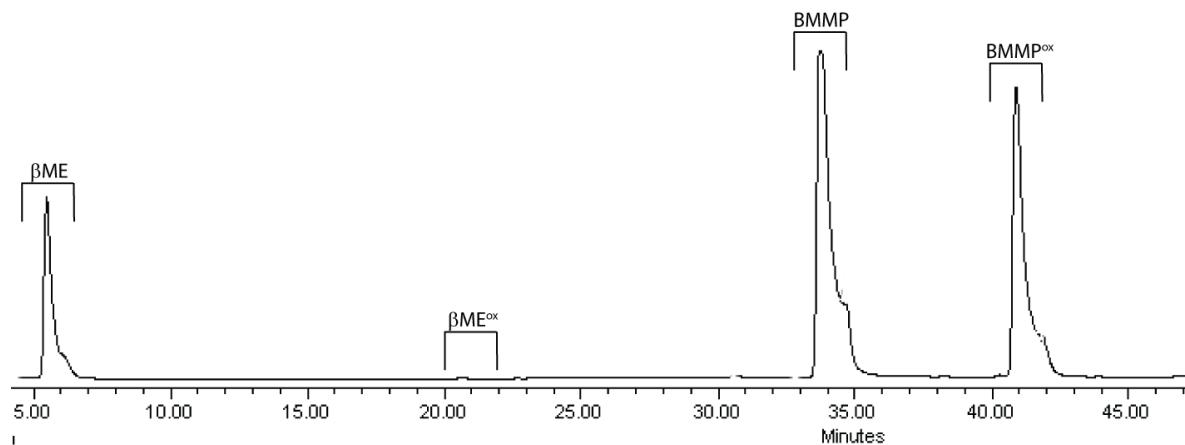


Figure 4.7 Representative HPLC chromatogram of the redox equilibrium between BMMP and β ME. Compounds were detected by their absorbance at 205 nm.

First, 4.0 mL of freshly degassed 50 mM potassium phosphate buffer, pH 7.0, containing EDTA (2 mM) was added to a round-bottom flask containing 3.0 mg (0.017 mmol) of BMMP. The flask was briefly sonicated to ensure complete dissolution of material and then stirred on under $N_2(g)$. Next, 0.6 mL (0.006 mmol) of a 10 mM stock solution of β ME^{ox} was added and the reaction was stirred overnight. After 24 h, the reaction mixture was quenched by the addition of 0.1 mL of 3 N HCl, filtered through a 4.5- μ m solution, and immediately analyzed by analytical HPLC using a Waters system equipped with a Waters 996 photodiode array detector, Empower 2 software, and a Varian C18 column. The column was eluted at 1.0 mL/min with water (5.0 mL), followed by a linear gradient (0–40% v/v) of acetonitrile/water over 40 min. Three peaks were observed, corresponding to β ME (6 min), BMMP (34 min), and BMMP^{ox} (41 min). The peak corresponding to β ME^{ox} (21 min) was not observed, indicative of the quantitative reduction of

$\beta\text{ME}^{\text{ox}}$ to form βME (Figure 4.7). This experiment was repeated three times with identical results.

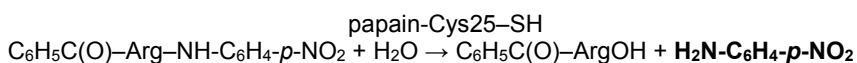
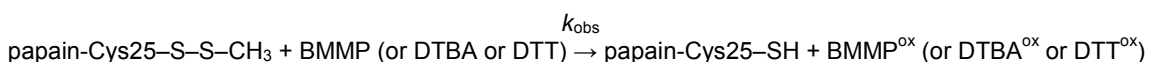
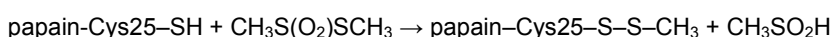
4.7.9 Reduction kinetics on oxidized βME

$$-\frac{\partial[\text{disulfide}]_{\text{total}}}{\partial t} = k_{\text{obs}}[\text{disulfide}]_{\text{total}}[\text{thiol}]_{\text{total}}$$

The observed second-order rate constant (k_{obs}) for the reduction oxidized βME by BMMP, DMH, DTBA, and DTT was determined by following a previously described procedure. A 10 mL round-bottom flask was charged with BMMP (4.3 mg, 0.025 mmol), DTBA (4.3, 0.025 mmol), or DTT (3.9 mg, 0.025 mmol). Under an atmosphere of $\text{N}_2(\text{g})$, 2.5 mL of freshly degassed 50 mM potassium phosphate buffer, pH 7.0, was then added to the reaction flask and the solution was briefly sonicated to ensure complete dissolution of reducing agent. At time $t = 0$, 2.5 mL of a 10 mM stock solution of $\beta\text{ME}^{\text{ox}}$ in 50 mM potassium phosphate buffer, pH 7.0, was then added. At various time points (1, 2, and 4 min), the reaction mixture was quenched by the addition of 0.1 mL of 3 N HCl. The reaction mixture was then passed through a 4.5- μm filter and analyzed immediately by analytical HPLC using a Varian C18 reverse-phase column. The mixture was eluted at 1.0 mL/min with water (5.0 mL), followed by a linear gradient (0–40% v/v) of acetonitrile/water over 40 min. The degree of reduction was determined by integrating the newly formed peak in the chromatogram corresponding to reduced βME (elution time of 6 min) at 205 nm. Calibration curves were generated and determined to be linear over the concentration range. The amount of residual oxidized BME was calculated, and the second-order rate constants were determined from the linear fit of the data in Figure 4.1A ($k_{\text{obs}} = [(1/C_{\text{final}}) - (1/C_{\text{initial}})]/t$).

The initial values of concentration (C_{initial}) were: BMMP, DMH, DTBA, or DTT = $\beta\text{ME}^{\text{ox}} = 5$ mM. Values of k_{obs} (Table 4.2) are the mean \pm SE from three independent experiments. The same procedure was repeated with BMMP, DTBA, and DTT in 50 mM sodium acetate buffer, pH 5.0.

4.7.10 Reactivation of papain



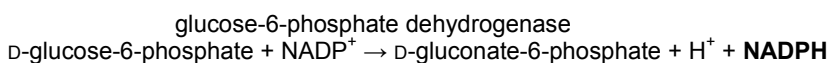
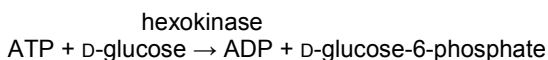
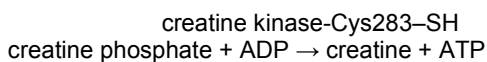
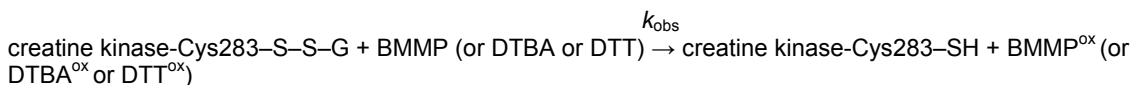
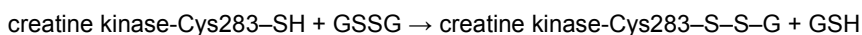
Papain was inactivated by forming a mixed disulfide upon treatment of its active-site cysteine (Cys25) with *S*-methyl methanethiosulfonate following a procedure reported previously.^{23,42} A 1.25 mL solution of papain-Cys25-S-S-CH₃ (4.4×10^{-6} M) in a degassed 0.10 M imidazole-HCl buffer, pH 7.0, containing EDTA (2 mM) was placed in a 1.5-mL LoBind Eppendorf tube. At time $t = 0$, 10 μL of a 1 mM stock solution of BMMP was added, and a timer was started. The initial concentrations of the reaction mixture were dithiol reducing agent: 7.9×10^{-6} M and inactive protein: 4.4×10^{-6} M. At various time points, a 200- μL aliquot of the reaction mixture was removed and added to a cuvette containing 800 μL of substrate solution (0.10 M imidazole-HCl buffer, pH 6.0, containing 2 mM EDTA and 1.25 mM *N*-benzoyl-L-arginyl-*p*-nitroanilide), and the rate of change in absorbance at 410 nm was recorded at 25 °C. A unit of protein is defined as the amount of enzyme required to produce 4-nitroaniline at a rate of 1 $\mu\text{mol}/\text{min}$. The units of active papain at each time point were calculated by using an extinction coefficient for 4-nitroaniline of $\epsilon = 8,800 \text{ M}^{-1}\text{cm}^{-1}$ at 410 nm. In order to determine

the possible number of units of active papain in the reaction mixture, enzymatic activity was assessed after a large excess of DTT (~100 fold) was added to an Eppendorf tube. As a control, the addition of DTT was shown to have no bearing on the assay data, other than in activating the enzyme. Y = enzymatic activity (%) at any time point was determined by dividing the number of active units of enzyme by the possible number of units in the solution, and plotted in Figure 4.2A. To determine the value of the second-order rate constant (k_{obs}) for the reducing agents, the second order rate equation (eq 4.4) was transformed into eq 5, which was fitted to the data with the program Prism 5.0. In both equations, A_0 = [inactive protein] _{$t=0$} , A = [inactive protein] _{t} = $A_0 - A_0Y$, B_0 = [reducing agent] _{$t=0$} , and B = [reducing agent] _{t} = $B_0 - A_0Y$. Values of k_{obs} (Table 4.1) are the mean \pm SE from three separate experiments.

$$\frac{1}{B_0 - A_0} \ln \frac{A_0 B}{A B_0} = k_{\text{obs}} t \quad (4.4)$$

$$y = \frac{B_0 - B_0 e^{k_{\text{obs}} t (A_0 - B_0)}}{B_0 - A_0 e^{k_{\text{obs}} t (A_0 - B_0)}} \quad (4.5)$$

4.7.11 Reactivation of creatine kinase



The oxidation and subsequent reactivation of creatine kinase with BMMP (or DTBA or DTT) was accomplished by a procedure described previously.^{28,42} Enzymatic activity (%) at particular time points was calculated by dividing the number of active units of enzyme by the possible number of units in solution, and was plotted in Figure 4.2B. Values of k_{obs} (Table 4.2) were determined using eq 4.5 and are the mean \pm SE for three separate experiments.

| Disulfide | BMMP | DMH | DTBA | DTT |
|---------------------------------------|---------------------|-----------------|---------------------|---------------------|
| $\beta\text{ME}^{\text{ox}}$, pH 7.0 | 1.02 ± 0.07 | 0.56 ± 0.04 | 0.32 ± 0.02 | 0.090 ± 0.005 |
| $\beta\text{ME}^{\text{ox}}$, pH 5.0 | 0.0183 ± 0.0007 | ND ^a | 0.0051 ± 0.0004 | 0.0013 ± 0.0001 |
| papain-Cys25-S-S-CH ₃ | 1139 ± 62 | ND ^a | 950 ± 51 | 87 ± 3 |
| creatine kinase-Cys283-S-S-G | 476 ± 34 | ND ^a | 70 ± 2 | 82 ± 3 |

^aND, not determined.

Table 4.2 Values of k_{obs} ($\text{M}^{-1}\text{s}^{-1}$) for the reduction of disulfides by dithiols

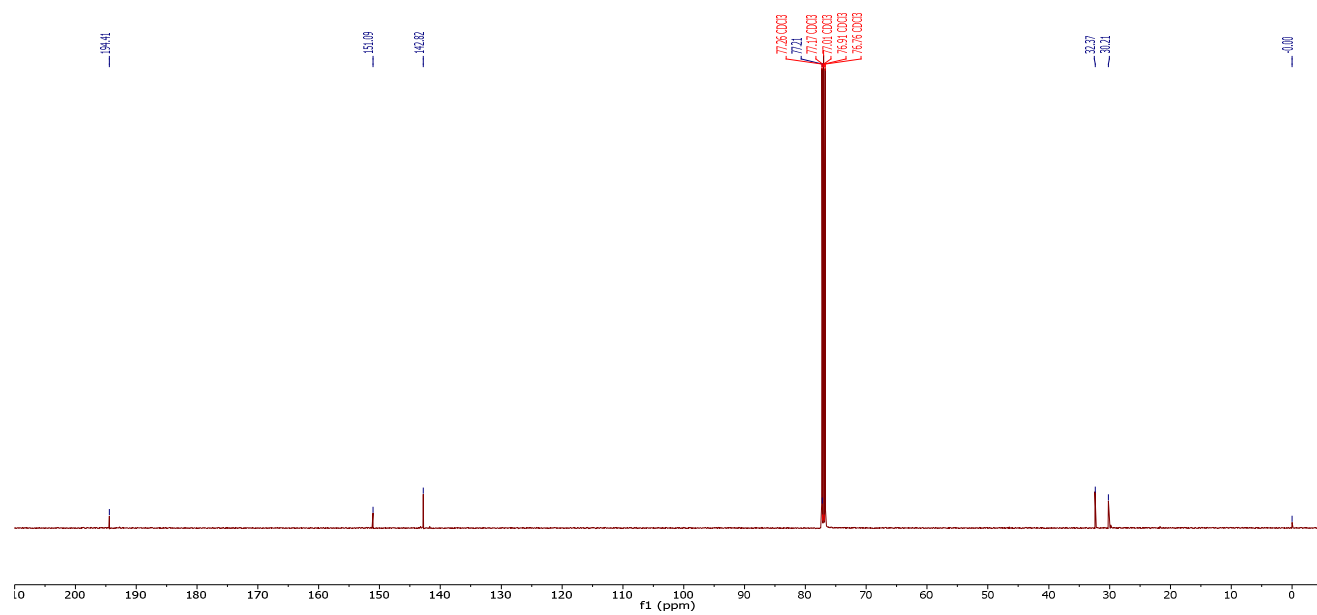
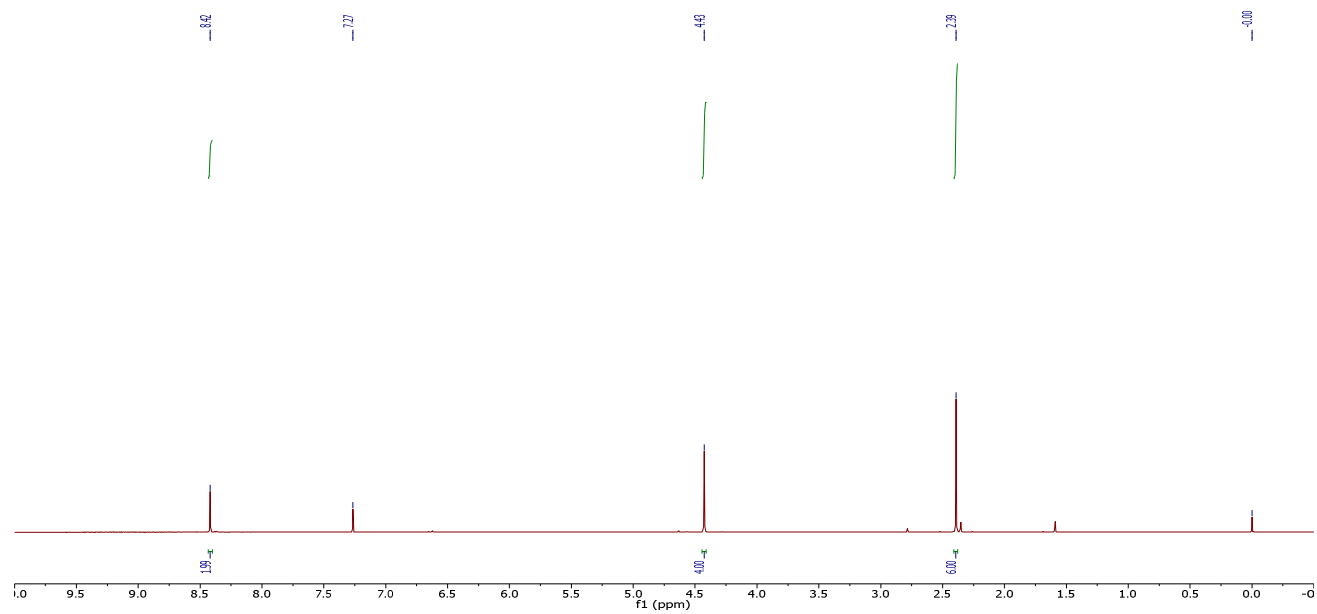
4.7.12 Determination of BMMP solubility in buffered water

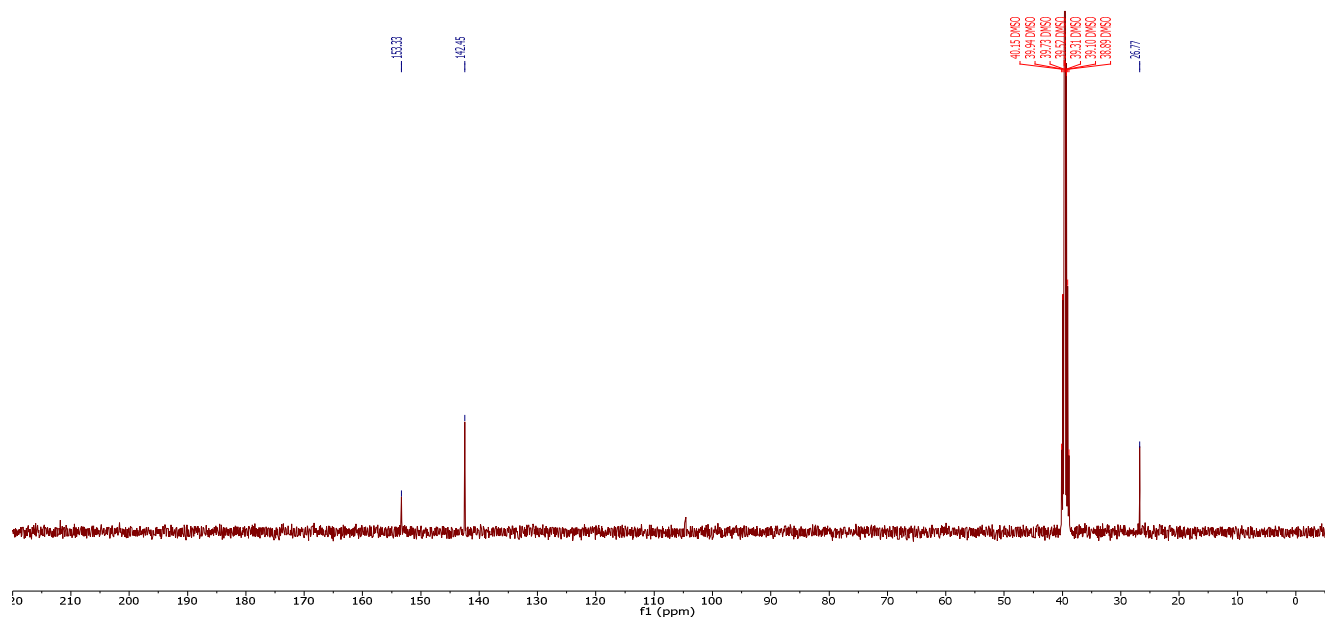
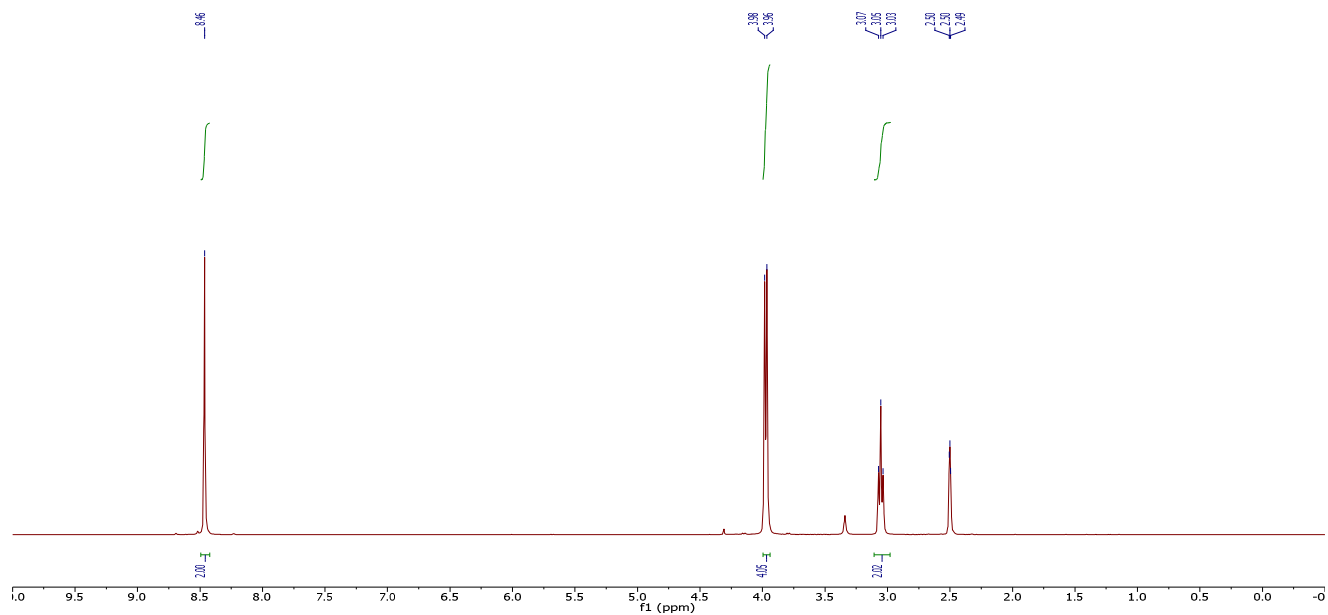
A 20 mM stock solution of 2-butyne-1,4-diol (which is an ¹H NMR standard) was prepared in 50 mM potassium phosphate buffer, pH 7.0. BMMP was added to a solution containing 1 mL of this buffer and 0.1 mL of D₂O until the solution was saturated completely. The mixture was sonicated to ensure complete dissolution and filtered into an NMR tube, and its spectrum was acquired with water suppression. The solubility of BMMP was determined to be (64 ± 14) mM by integration of the ¹H NMR peak areas for the aryl CH and methylene CH₂SH protons for BMMP and the CH₂OH protons of 2-butyne-1,4-diol. Analogously, the solubility of

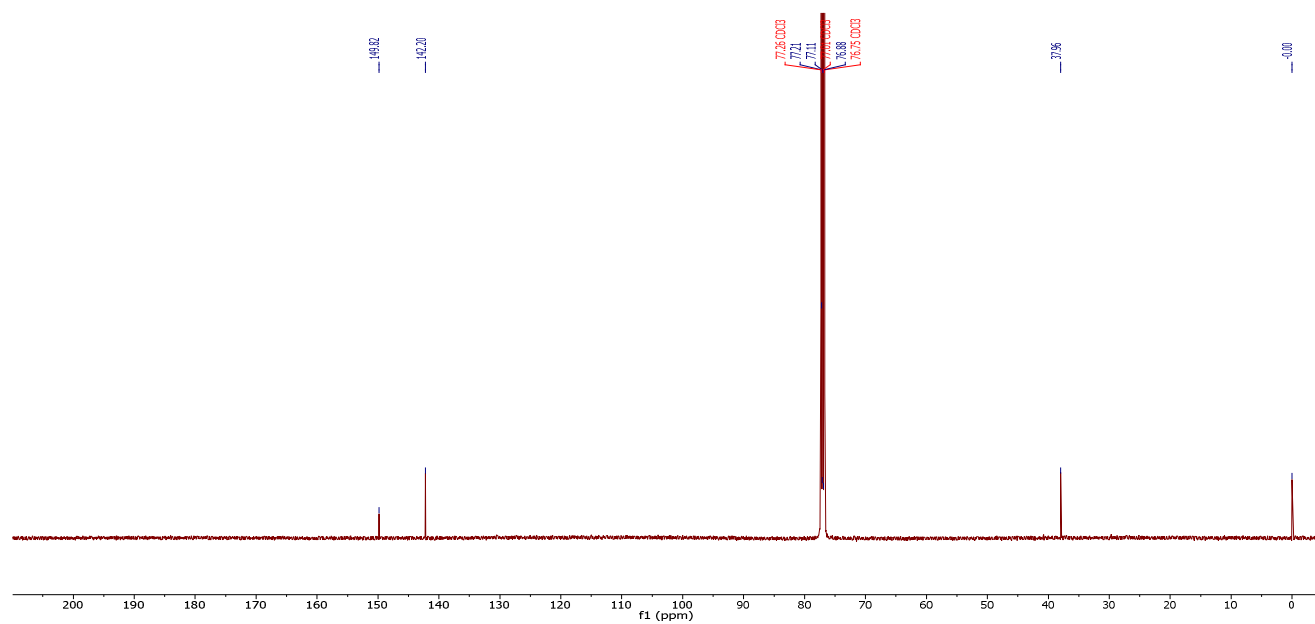
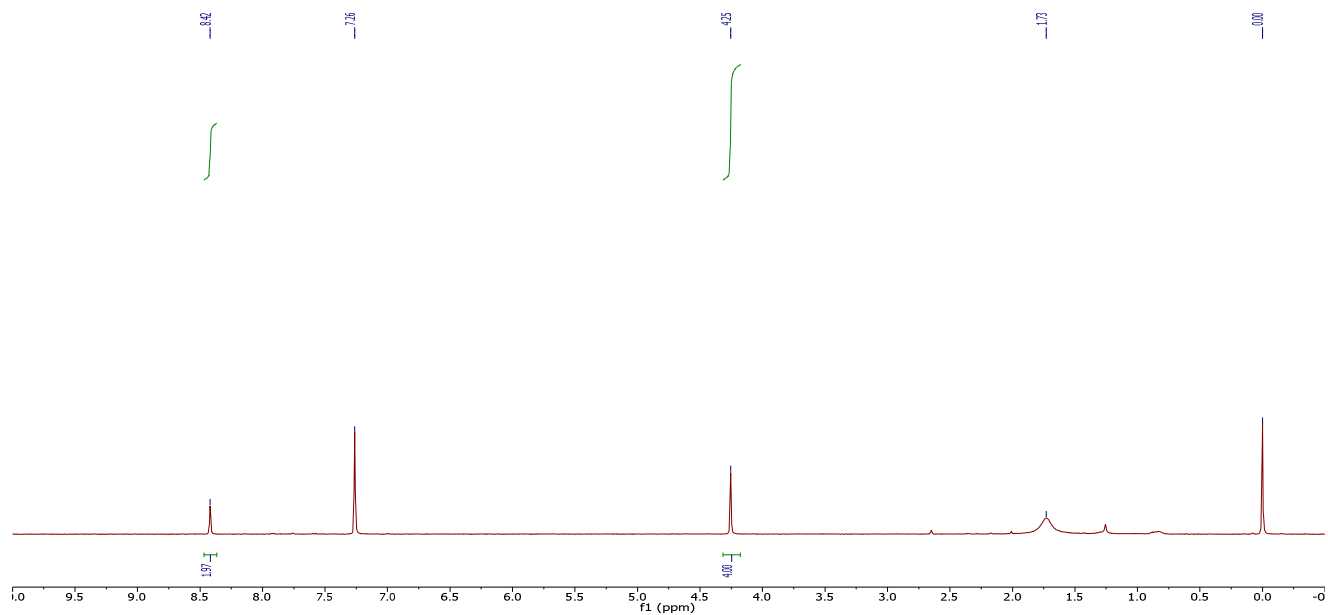
BMMP^{ox} was determined to be (7.9 ± 2.8) mM by integration of the ¹H NMR peak areas for the aryl **CH** protons of BMMP^{ox} and the **CH**₂OH protons of 2-butyne-1,4-diol.

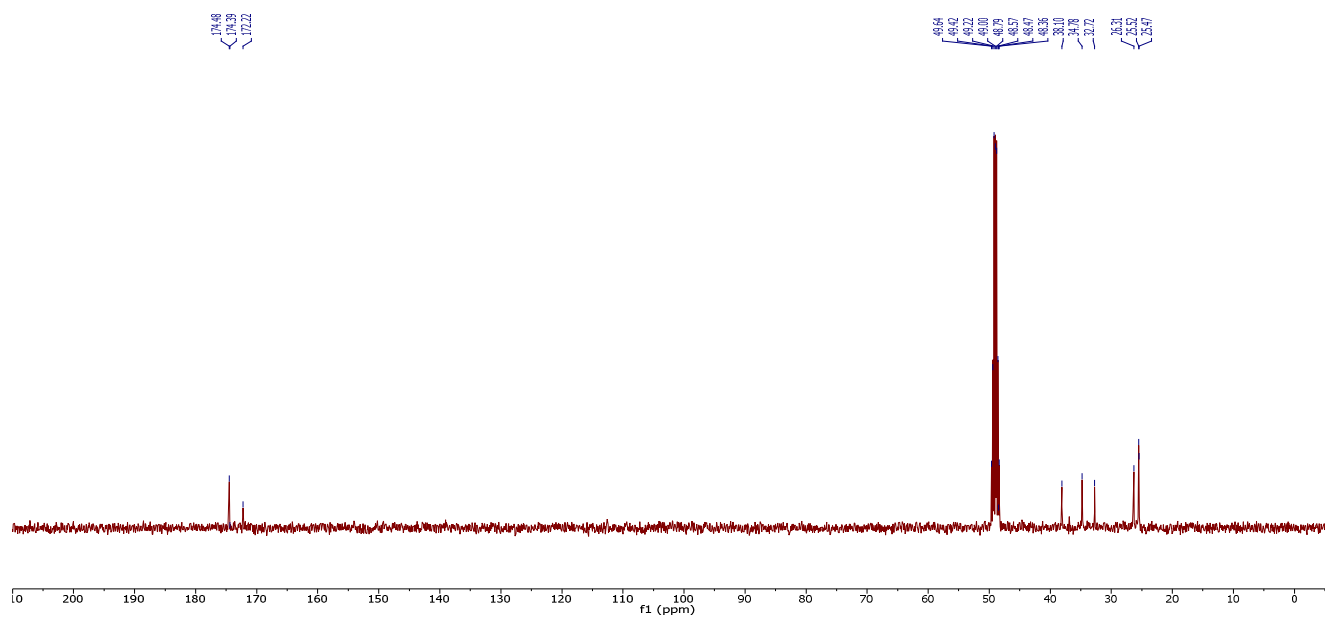
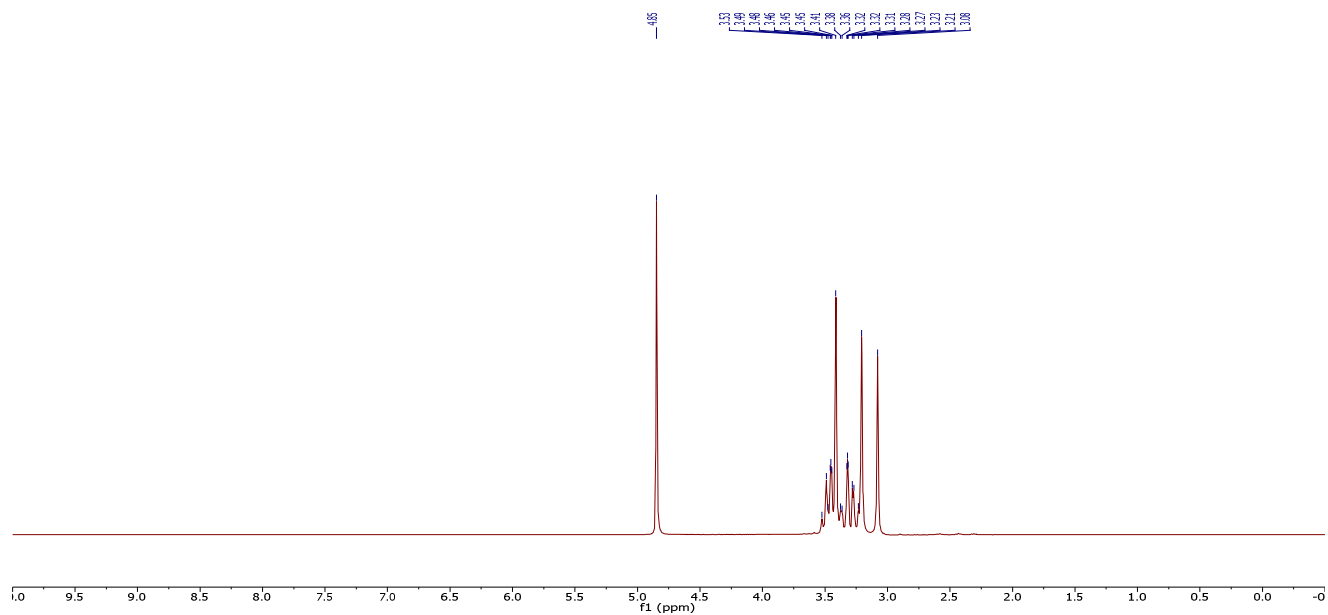
4.8 NMR Spectra

^1H NMR (CDCl_3) and ^{13}C NMR (CDCl_3) of **4.3**

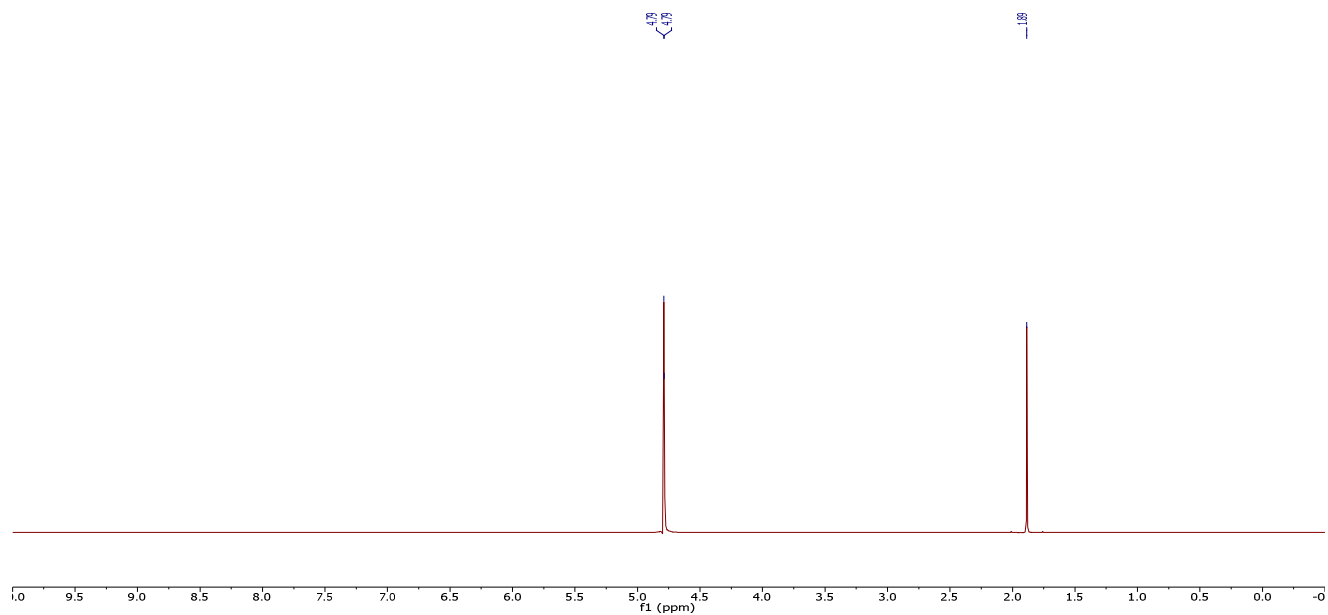


^1H NMR (DMSO- d_6) and ^{13}C NMR (DMSO- d_6) of **4.4** (BMMP)

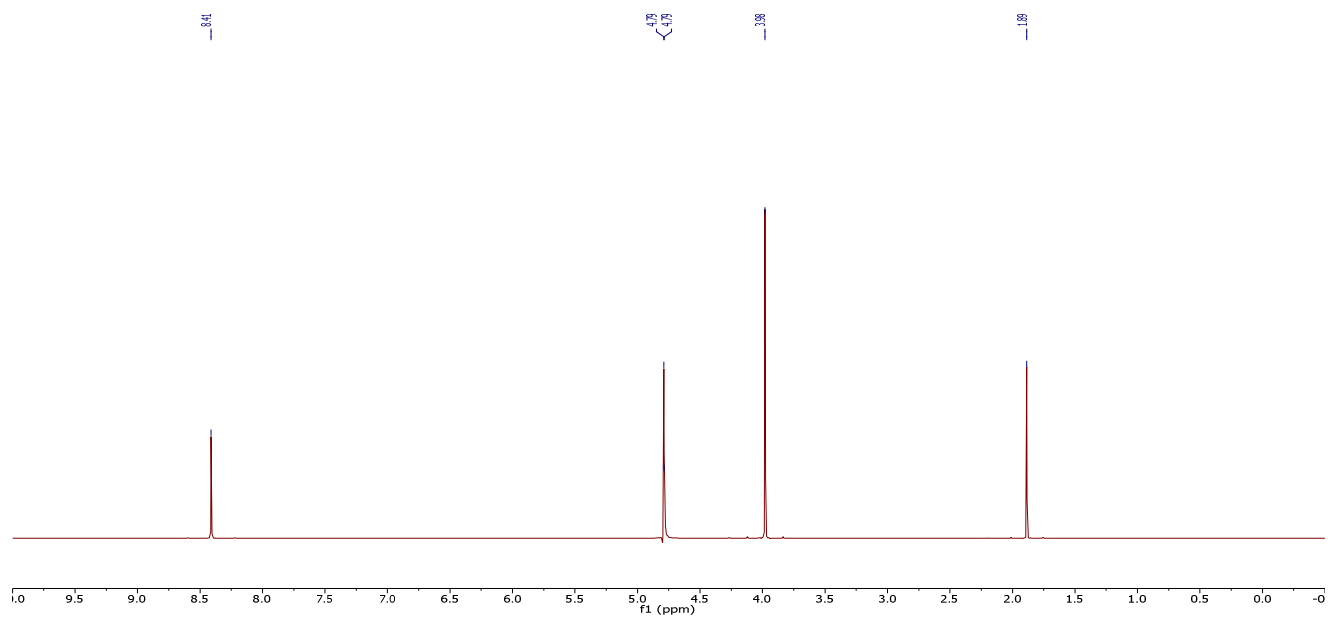
^1H NMR (CDCl_3) and ^{13}C NMR (CDCl_3) of **4.5** (BMMP^{ox})

^1H NMR (Methanol- d_4) and ^{13}C NMR (Methanol- d_4) of **4.6** (DMH)

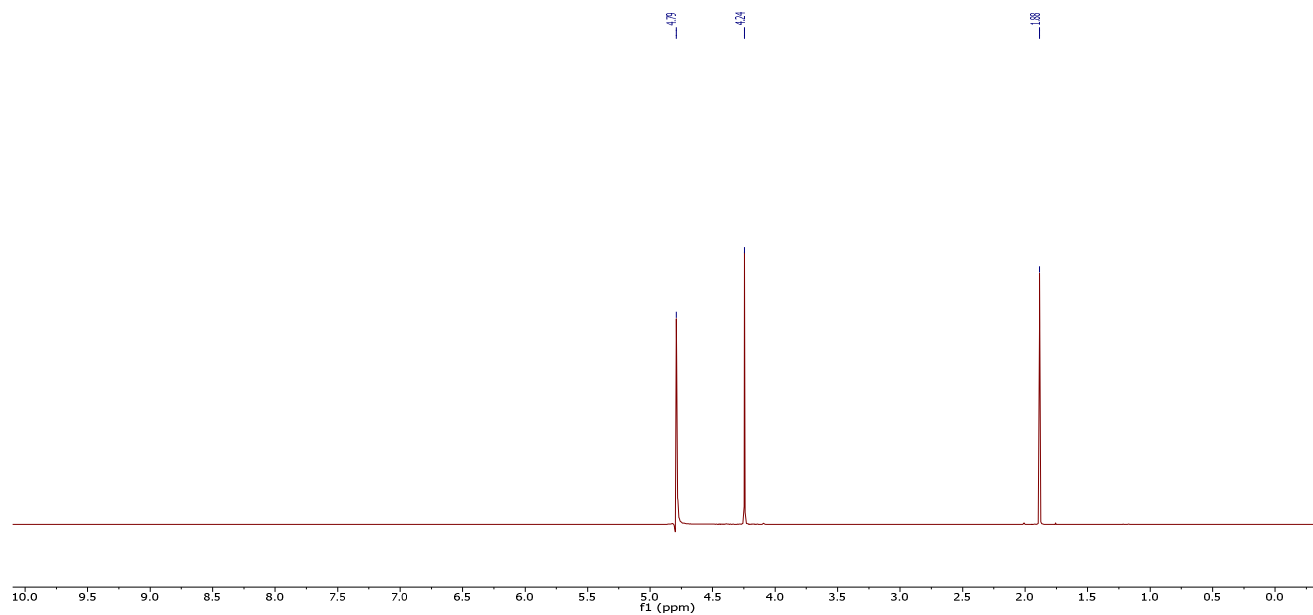
^1H NMR (50 mM potassium phosphate buffer, pH 7.0)



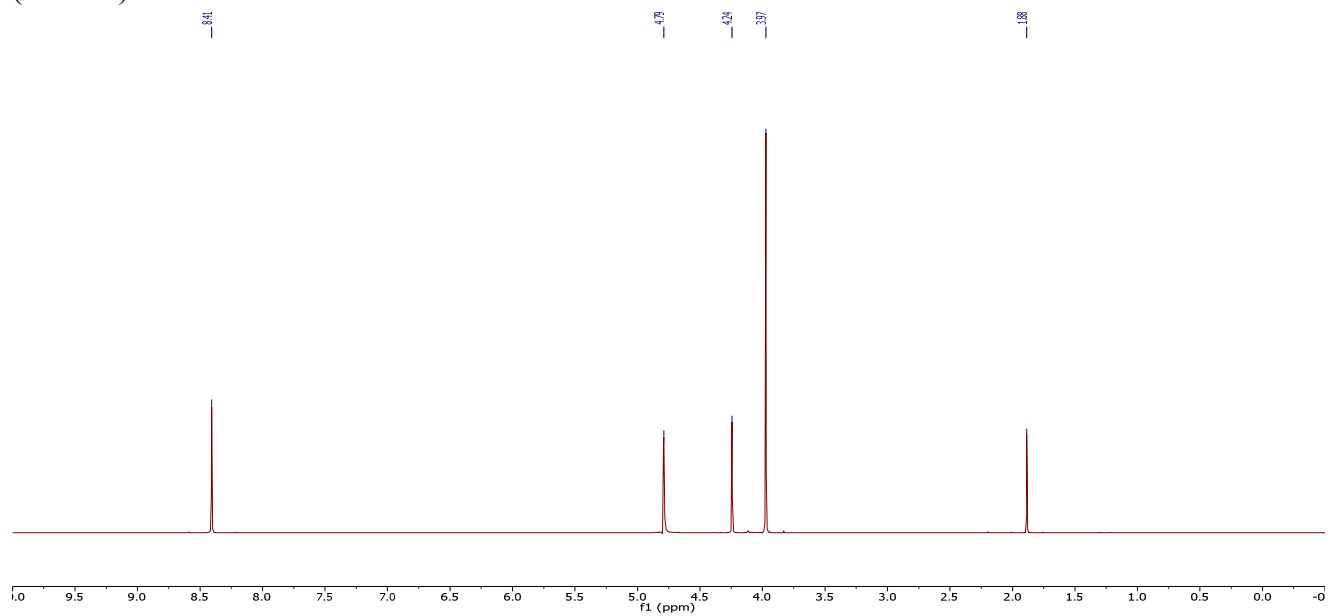
^1H NMR (50 mM phosphate buffer, pH 7.0) of **4.4** (BMMP)



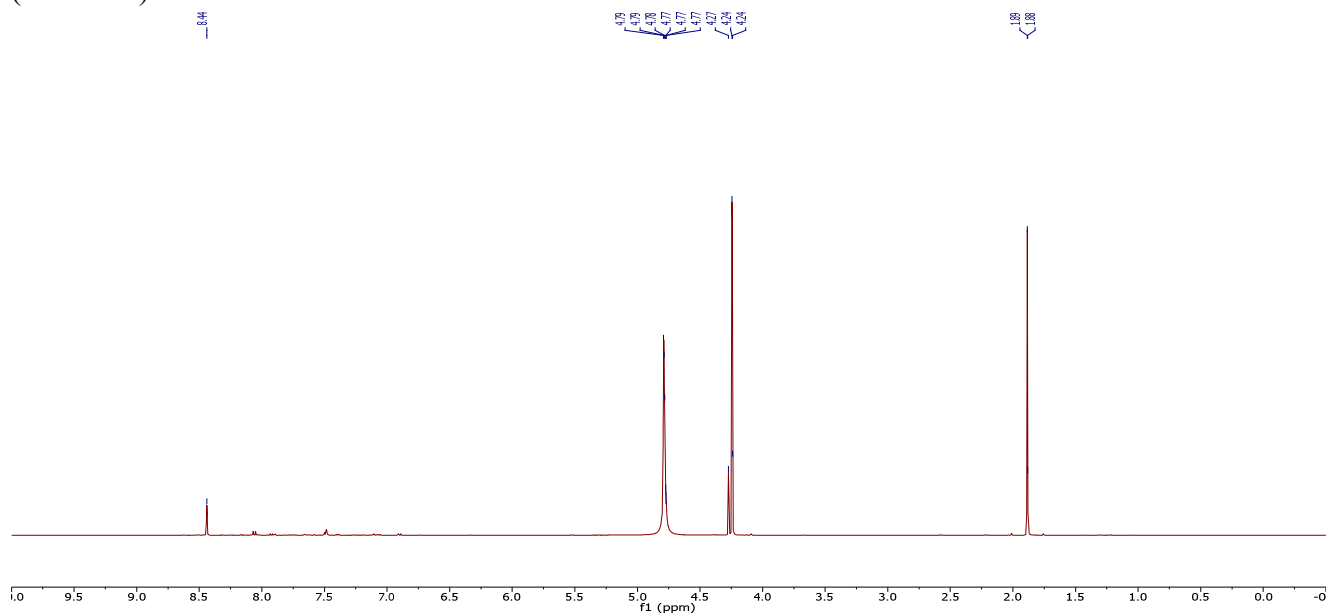
^1H NMR (50 mM potassium phosphate buffer, pH 7.0) of 2-butyne-1,4-diol



^1H NMR (50 mM potassium phosphate buffer, pH 7.0, 20 mM 2-butyne-1,4-diol) of **4.4** (BMMP)



^1H NMR (50 mM potassium phosphate buffer, pH 7.0, 20 mM 2-butyne-1,4-diol) of **4.5** (BMMP^{OX})



4.9 Cartesian Coordinates of Optimized Geometries and Partial Atomic Charges

Table 4.3 Cartesian coordinates of the optimized geometry of **4.4** (reduced BMMP); free energy = -1139.389339 Hartree.

| | | | |
|---|-------------|-------------|-------------|
| C | 0.00000000 | 0.00000000 | 0.00000000 |
| C | -0.95406700 | 1.07250700 | -0.43806000 |
| C | -2.32291100 | 0.83373200 | -0.69034200 |
| N | -3.12240600 | 1.82086200 | -1.07841100 |
| C | -2.59182700 | 3.03476500 | -1.22931700 |
| C | -1.24773000 | 3.26835200 | -0.98751200 |
| N | -0.43413900 | 2.28972000 | -0.58931400 |
| H | -0.81443200 | 4.25535900 | -1.10974500 |
| H | -3.25696800 | 3.83042800 | -1.54751800 |
| C | -2.92142600 | -0.53899100 | -0.53051100 |
| S | -4.70572000 | -0.53774300 | -0.98365800 |
| H | -4.85263500 | -1.85935000 | -0.77304500 |
| H | -2.81760500 | -0.87090500 | 0.50515100 |
| H | -2.38599000 | -1.24556300 | -1.16673800 |
| S | 0.66126500 | -0.99964900 | -1.41064300 |
| H | 1.21766000 | 0.03512700 | -2.06358900 |
| H | -0.47442700 | -0.73372000 | 0.65100300 |
| H | 0.83323800 | 0.45281700 | 0.53183300 |

Table 4.4 Partial atomic charges for the optimized geometry of **4.4** (reduced BMMP)

| Atom | Symbol | Charge |
|------|--------|-----------|
| 1 | C | -0.240841 |
| 2 | C | -0.083063 |
| 3 | C | 0.426888 |
| 4 | N | -0.162639 |
| 5 | C | 0.154077 |
| 6 | C | -0.023234 |
| 7 | N | -0.235077 |
| 8 | H | 0.106517 |
| 9 | H | 0.108367 |
| 10 | C | -0.415207 |
| 11 | S | -0.196545 |
| 12 | H | 0.081154 |
| 13 | H | 0.148652 |
| 14 | H | 0.170850 |
| 15 | S | -0.228549 |
| 16 | H | 0.100887 |
| 17 | H | 0.127196 |
| 18 | H | 0.160566 |

Table 4.5 Cartesian coordinates of the optimized geometry of **4.5** (oxidized BMMP); free energy = -1138.202460 Hartree

| | | | |
|---|-------------|-------------|-------------|
| C | 0.00000000 | 0.00000000 | 0.00000000 |
| C | -1.22554800 | -0.87538800 | -0.15546100 |
| C | -1.22555800 | -2.26904600 | -0.35947600 |
| C | -0.00002400 | -3.14443300 | -0.51498800 |
| S | 1.53191200 | -2.49364100 | 0.23405500 |
| S | 1.53184400 | -0.65070700 | -0.74924900 |
| H | 0.18165600 | -3.34186200 | -1.57335300 |
| H | -0.19950400 | -4.10073500 | -0.02744000 |
| N | -2.37735100 | -2.93831700 | -0.46398300 |
| C | -3.51420300 | -2.25834300 | -0.36282000 |
| C | -3.51419100 | -0.88601700 | -0.15237200 |
| N | -2.37733100 | -0.20608000 | -0.05106000 |
| H | -4.43949200 | -0.32573000 | -0.06635800 |
| H | -4.43950400 | -2.81857800 | -0.44914200 |

| | | | |
|---|-------------|------------|-------------|
| H | -0.19959200 | 0.95635400 | -0.48738200 |
| H | 0.18177500 | 0.19727100 | 1.05838800 |

Table 4.6 Partial atomic charges for the optimized geometry of **4.5** (oxidized BMMP)

| Atom | Symbol | Charge |
|------|--------|-----------|
| 1 | C | 0.099860 |
| 2 | C | -0.167780 |
| 3 | C | -0.167818 |
| 4 | C | 0.099972 |
| 5 | S | -0.127191 |
| 6 | S | -0.127156 |
| 7 | H | 0.164104 |
| 8 | H | 0.154199 |
| 9 | N | -0.262844 |
| 10 | C | 0.032538 |
| 11 | C | 0.032545 |
| 12 | N | -0.262836 |
| 13 | H | 0.107054 |
| 14 | H | 0.107055 |
| 15 | H | 0.154197 |
| 16 | H | 0.164102 |

Table 4.7 Cartesian coordinates of the optimized geometry of reduced DTT; free energy = -1105.325241 Hartree

| | | | |
|---|-------------|-------------|-------------|
| C | 0.00000000 | 0.00000000 | 0.00000000 |
| C | -0.79402300 | 1.30104000 | 0.06769800 |
| C | -2.30162000 | 1.13626200 | -0.18710600 |
| C | -3.00517800 | 0.22179600 | 0.81756800 |
| S | -4.77481800 | -0.05831400 | 0.41201300 |
| H | -5.08077300 | 1.24065700 | 0.25394900 |
| H | -2.56374400 | -0.77579400 | 0.80977900 |
| H | -2.91582500 | 0.62200000 | 1.82705900 |
| O | -2.90366500 | 2.42683400 | -0.20996900 |
| H | -2.56455600 | 2.90775200 | 0.55788500 |
| H | -2.43733400 | 0.73018600 | -1.19243400 |
| O | -0.66699200 | 1.93945400 | 1.33999000 |

| | | | |
|---|-------------|-------------|-------------|
| H | 0.24404300 | 2.24628600 | 1.42931100 |
| H | -0.42242700 | 1.97480000 | -0.71341700 |
| S | 1.81259900 | 0.25781000 | 0.23695700 |
| H | 1.82895600 | 0.09307300 | 1.56982000 |
| H | -0.10598400 | -0.45292300 | -0.98725300 |
| H | -0.33447400 | -0.72186200 | 0.74218100 |

Table 4.8 Partial atomic charges for the optimized geometry of reduced DTT

| Atom | Symbol | Charge |
|------|--------|-----------|
| 1 | C | -0.159791 |
| 2 | C | 0.169594 |
| 3 | C | 0.004885 |
| 4 | C | -0.000413 |
| 5 | S | -0.351191 |
| 6 | H | 0.114166 |
| 7 | H | 0.120412 |
| 8 | H | 0.155895 |
| 9 | O | -0.430165 |
| 10 | H | 0.270291 |
| 11 | H | 0.114107 |
| 12 | O | -0.483914 |
| 13 | H | 0.281039 |
| 14 | H | 0.114165 |
| 15 | S | -0.320047 |
| 16 | H | 0.103947 |
| 17 | H | 0.150258 |
| 18 | H | 0.146763 |

Table 4.9 Cartesian coordinates of the optimized geometry of oxidized DTT. Free Energy = -1104.138109 Hartree

| | | | |
|---|------------|-------------|-------------|
| C | 0.00000000 | 0.00000000 | 0.00000000 |
| S | 1.58410300 | -0.59440700 | 0.69404000 |
| S | 1.55983500 | -2.53693800 | -0.08696400 |

| | | | |
|---|-------------|-------------|-------------|
| C | -0.03960000 | -3.08756600 | 0.61824800 |
| C | -1.21551300 | -2.26174400 | 0.09301900 |
| C | -1.19874700 | -0.78897800 | 0.51946200 |
| H | -1.19783400 | -0.75674700 | 1.61707900 |
| O | -2.35428100 | -0.12919000 | 0.01488200 |
| H | -3.11187900 | -0.69176200 | 0.22379600 |
| H | -1.23177900 | -2.30038500 | -1.00189100 |
| O | -2.45056800 | -2.77838400 | 0.61772400 |
| H | -2.68506300 | -3.58556300 | 0.14759400 |
| H | -0.14886400 | -4.13017700 | 0.30556300 |
| H | 0.00642400 | -3.05617000 | 1.70707400 |
| H | 0.04305300 | -0.02076000 | -1.08909600 |
| H | -0.09487400 | 1.03891800 | 0.32344100 |

Table 4.10 Partial atomic charges for the optimized geometry of oxidized DTT.

| Atom | Symbol | Charge |
|------|--------|-----------|
| 1 | C | 0.004557 |
| 2 | S | -0.114737 |
| 3 | S | -0.116856 |
| 4 | C | -0.050649 |
| 5 | C | -0.167983 |
| 6 | C | -0.010352 |
| 7 | H | 0.106491 |
| 8 | O | -0.445927 |
| 9 | H | 0.289631 |
| 10 | H | 0.117979 |
| 11 | O | -0.462627 |
| 12 | H | 0.275991 |
| 13 | H | 0.123442 |
| 14 | H | 0.155189 |
| 15 | H | 0.149212 |
| 16 | H | 0.146639 |

Table 4.11 Cartesian coordinates of the optimized geometry of DMH. Free Energy = -1292.247888 Hartree

| | | | |
|---|-------------|-------------|------------|
| C | 0.00000000 | 0.00000000 | 0.00000000 |
| N | -0.09508500 | -0.72761800 | 1.26396700 |

| | | | |
|---|-------------|-------------|-------------|
| N | -1.36704900 | -0.72553300 | 1.84557400 |
| C | -1.44858400 | -0.08410700 | 3.15535000 |
| H | -0.93251100 | 0.87414100 | 3.10212800 |
| H | -2.48801000 | 0.10661100 | 3.41188700 |
| H | -0.98484700 | -0.70079500 | 3.92838800 |
| C | -2.25122700 | -1.67697500 | 1.36582200 |
| C | -3.55785300 | -1.81976500 | 2.12936700 |
| S | -4.63902300 | -2.99109900 | 1.21888200 |
| H | -5.66298900 | -2.86955300 | 2.08385400 |
| H | -3.34861000 | -2.20054400 | 3.13049200 |
| H | -4.05286800 | -0.85267800 | 2.22149300 |
| O | -2.00547600 | -2.33199900 | 0.37369700 |
| C | 0.75646800 | -1.73425000 | 1.68193100 |
| C | 2.05900800 | -1.87269900 | 0.89913800 |
| S | 3.29880600 | -2.92339300 | 1.74004900 |
| H | 2.39446400 | -3.55250200 | 2.51311500 |
| H | 1.81925700 | -2.29054900 | -0.08149500 |
| H | 2.52174500 | -0.89920900 | 0.74327100 |
| O | 0.47129700 | -2.44906400 | 2.62230000 |
| H | 1.04186600 | 0.15213500 | -0.26880700 |
| H | -0.51090200 | -0.53796500 | -0.80119700 |
| H | -0.46271400 | 0.97795100 | 0.13063100 |

Table 4.12 Partial atomic charges for the optimized geometry of DMH.

| Atom | Symbol | Charge |
|------|--------|-----------|
| 1 | C | -0.283588 |
| 2 | N | -0.028313 |
| 3 | N | -0.002310 |
| 4 | C | -0.287588 |
| 5 | H | 0.136125 |
| 6 | H | 0.131272 |
| 7 | H | 0.175265 |
| 8 | C | 0.240271 |
| 9 | C | -0.091617 |
| 10 | S | -0.224413 |
| 11 | H | 0.083872 |
| 12 | H | 0.159114 |
| 13 | H | 0.144822 |
| 14 | O | -0.434543 |

| | | |
|----|---|-----------|
| 15 | C | 0.206672 |
| 16 | C | -0.031179 |
| 17 | S | -0.308059 |
| 18 | H | 0.132124 |
| 19 | H | 0.168848 |
| 20 | H | 0.135352 |
| 21 | O | -0.463912 |
| 22 | H | 0.128362 |
| 23 | H | 0.178108 |
| 24 | H | 0.135314 |

Table 4.13 Cartesian coordinates of the optimized geometry of oxidized DMH. Free Energy = – 1291.051740 Hartree

| | | | |
|---|-------------|-------------|-------------|
| C | 0.00000000 | 0.00000000 | 0.00000000 |
| S | -0.78787300 | -1.69121900 | -0.04339800 |
| S | 0.46337800 | -2.91302600 | 1.08652400 |
| C | 1.89945700 | -3.27718600 | -0.01717500 |
| C | 3.27024000 | -2.59799100 | 0.11909100 |
| N | 3.39844600 | -1.28041600 | 0.50354300 |
| N | 2.27540200 | -0.49909200 | 0.73704600 |
| C | 1.45879300 | -0.20879800 | -0.34031700 |
| O | 1.84108000 | -0.30980500 | -1.48968300 |
| C | 2.06345600 | -0.09614500 | 2.12630500 |
| H | 1.45238500 | 0.80254500 | 2.16717300 |
| H | 1.59473600 | -0.88982400 | 2.71072400 |
| H | 3.03187000 | 0.14598100 | 2.56449800 |
| C | 4.66927600 | -0.58386100 | 0.31361500 |
| H | 4.82008100 | 0.12533900 | 1.12841100 |
| H | 5.46720900 | -1.32023500 | 0.32085600 |
| H | 4.66827200 | -0.05089700 | -0.63952700 |
| O | 4.24845000 | -3.25556100 | -0.18285300 |
| H | 2.10181700 | -4.34007400 | 0.10741600 |
| H | 1.56379400 | -3.12250600 | -1.04432600 |
| H | -0.48608500 | 0.54280400 | -0.80862800 |
| H | -0.20314300 | 0.47491800 | 0.95448900 |

Table 4.14 Partial atomic charges for the optimized geometry of oxidized DMH.

| Atom | Symbol | Charge |
|------|--------|-----------|
| 1 | C | -0.307967 |

| | | |
|----|---|-----------|
| 2 | S | -0.122816 |
| 3 | S | 0.130840 |
| 4 | C | -0.193910 |
| 5 | C | 0.211784 |
| 6 | N | 0.059248 |
| 7 | N | -0.203296 |
| 8 | C | 0.334650 |
| 9 | O | -0.404489 |
| 10 | C | -0.350976 |
| 11 | H | 0.133997 |
| 12 | H | 0.172818 |
| 13 | H | 0.141434 |
| 14 | C | -0.269997 |
| 15 | H | 0.117610 |
| 16 | H | 0.175912 |
| 17 | H | 0.153596 |
| 18 | O | -0.464211 |
| 19 | H | 0.178585 |
| 20 | H | 0.201215 |
| 21 | H | 0.175584 |
| 22 | H | 0.130389 |

Chapter 5*: Organocatalysts of Oxidative Protein Folding Inspired by Protein Disulfide Isomerase

5.1 Abstract

Organocatalysts derived from diethylenetriamine are effective catalysts for the isomerization of non-native protein disulfide bonds to native ones. These catalysts contain a pendant hydrophobic moiety to encourage interaction with the non-native state, and thiol groups with low pK_a values that form a disulfide bond with a high E°' value.

5.2 Author Contributions

J.C.L. proposed the use of hydrophobic moieties to improve efficiency of small molecule PDI mimics. K.K.W. assisted J.C.L. in the synthesis and characterization of small molecule PDI mimics. K.A.A. prepared and purified sRNase A. K.A.A. performed and analyzed RNase A refolding experiments. J.C.L. drafted the original manuscript and figures. J.C.L., K.A.A, and R.T.R. planned experiments, analyzed data, and edited the manuscript and figures.

*This chapter will be published, in part, under the same title. Reference: Lukesh, J. C., III[#]; Andersen, K. A.[#]; Wallin, K. K.; Raines, R. T., *manuscript in preparation*

[#] These authors contributed equally

5.3 Introduction

The formation of native disulfide bonds is at the core of oxidative protein folding.^{1,5,9,141} In oxidizing environments, reduced proteins with multiple cysteine residues tend to oxidize rapidly and nonspecifically. To attain a proper three-dimensional fold, any nonnative disulfide bonds must isomerize to the linkages found in the native protein.¹⁷⁰ In eukaryotic cells, this process is mediated by the enzyme protein disulfide isomerase (PDI; EC 5.3.4.1).^{9,84-87,91,96,99,100}

Catalysis of disulfide-bond isomerization by PDI involves thiol–disulfide interchange chemistry (Figure 5.1). The mechanism commences with the nucleophilic attack by a thiolate on a non-native protein-disulfide bond, generating a mixed disulfide and a new substrate thiolate. This thiolate can then attack another non-native disulfide bond, inducing further rearrangements until the proper fold is achieved (Figure 5.1).

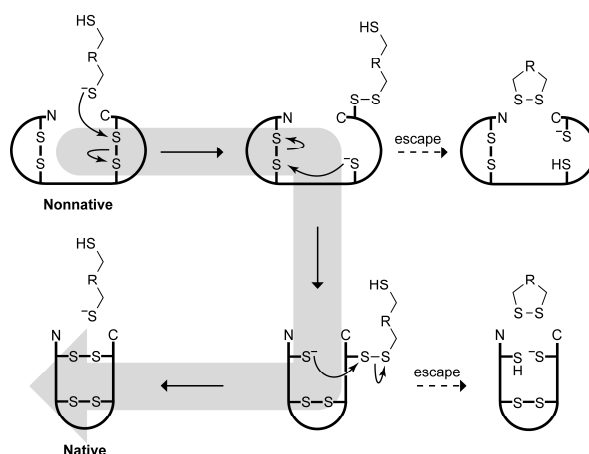


Figure 5.1 Putative mechanism for catalysis of protein-disulfide isomerization by protein disulfide isomerase (PDI).

PDI is abundant in the endoplasmic reticulum (ER) of eukaryotic cells. The enzyme contains four domains: a, a', b, and b'.⁸⁷ The a and a' domains each contain one active-site CGHC

motif—a pattern analogous to that in many other oxidoreductases, whereas the b and b' domains appear to mediate substrate binding.^{87,171,172} The physicochemical properties of its active-site make PDI an ideal catalyst for the reshuffling of disulfide bonds in misfolded proteins. In its catalytic mechanism (Figure 5.1), the deprotonated thiolate of the N-terminal active-site cysteine (CGHC) initiates catalysis.¹⁷³ The amount enzymatic thiolate present is dependent on two factors.^{4,101} One is the pK_a of the active-site cysteine residue; the other is the reduction potential (E°) of the disulfide bond formed between the two active-site cysteine residues. In PDI, the cysteine pK_a is 6.7, and the disulfide E° is -0.18 V.^{104,105} Given the properties of the ER (pH 7.0; $E_{\text{solution}} = -0.18$ V), 33% of PDI active sites will contain a reactive thiolate.^{6,102} Moreover, the high (less negative) reduction potential of PDI, renders the protein as a weak disulfide-reducing agent, ensuring that ample time is available for the catalyst to rearrange all of the disulfide bonds before reducing its protein substrate to "escape" (Figure 5.1). Still, the second active-site cysteine residue can rescue the enzyme from non-productive mixed disulfide intermediates (Figure 5.1).^{96,174,175}

The production of proteins that contain disulfide bonds via recombinant DNA technology often leads to the aggregation of misfolded proteins. These aggregates must then be reduced, denatured, and solubilized to enable proper folding.^{106,107} Many pharmaceutically relevant proteins containing disulfide bonds.^{108,109} For example, antibodies contain at least 12 intrachain and 4 interchain disulfide bonds,¹⁷⁶ and there are now 338 distinct antibodies in clinical development. Accordingly, increasing the yield of properly folded proteins has never been more critical to the biotechnology industry.

Efficient oxidative protein folding requires a redox environment that supports thiol oxidation and disulfide-bond isomerization. *In vivo* and *in vitro*, this environment can be provided by a redox buffer consisting of reduced and oxidized glutathione. For example, the oxidative folding of ribonuclease A (RNase A) occurs readily in the presence of 1 mM glutathione (GSH) and 0.2 mM oxidized glutathione (GSSG).¹⁷⁷ Adding PDI accelerates this process, but the large-scale use of PDI as a catalyst for folding proteins *in vitro* is impractical due to its high cost and instability, and the complexity of its separation from the newly folded protein of interest. As a result, the development and use of small-molecule PDI mimics has become a high priority.

To date, most PDI mimics have focused on replicating the physicochemical properties of the CGHC active site—low thiol pK_a and high disulfide E°' . Previously, we reported on (\pm)-*trans*-1,2-bis(mercaptoacetamido)cyclohexane (BMC; Figure 5.2), a small molecule that catalyzes the formation of native disulfide bonds in proteins, both *in vitro* and *in vivo*.¹¹⁶ Though effective, BMC has shortcomings. For example, its low disulfide E°' render the compound too reducing for optimal catalysis of disulfide-bond isomerization. Subsequently, various CXXC and CXC peptides, aromatic thiols, and selenium-based catalysts have been employed by us and others with some success.^{54,61,63,64,110-115,117,118} In addition to non-optimal thiol pK_a and disulfide E°' values, these organocatalysts failed to mimic a hallmark of enzymatic catalysts—binding to the substrate. A recent crystal structure of PDI revealed that the b and b' domains of PDI contain an exposed hydrophobic patch, forming a continuous hydrophobic surface between the two catalytic active sites (a and a').^{86,87,90-92} Unfolded or misfolded proteins tend to have more hydrophobic residues exposed than do proteins in their native fold.¹⁷⁸ Accordingly, we

hypothesized that the hydrophobic nature of PDI is essential for its efficiency and selectively in binding to unfolded or misfolded proteins. We were encouraged by the demonstrated ability of small-molecule oxidants with hydrophobic moieties to accelerate the oxidation of reduced proteins.^{119,179}

With this in mind, we set out to design small-molecule PDI mimics with low thiol pK_a and high disulfide E°' values that also emulate the hydrophobic binding site (b and b' domains) of PDI. We hypothesized that dithiol **5.2** (Figure 5.2) would provide a scaffold for the development of useful catalysts. We were drawn to dithiol **5.2** for three reasons. First, its mercaptoacetamido groups are known to have low thiol pK_a values.¹¹⁶ Secondly, its oxidized form resides in a large, 13-membered ring, which we reasoned would lead to a high reduction potential. Finally, dithiol **5.2** has an amino group that can be modified readily with hydrophobic moieties that mimic the b and b' domains of PDI.

5.4 Results and Discussion

Our study commenced by synthesizing dithiol **5.2** from diethylenetriamine in a few high-yielding steps. To determine its thiol pK_a values, we monitored its $A_{238\text{ nm}}$ as a function of pH.¹²⁹ We found pK_a values of 8.0 ± 0.2 and 9.2 ± 0.1 . These values are slightly less than those of BMC, presumably due to the introduction of an additional electronegative nitrogen atom. To determine its reduction potential, we equilibrated equimolar amounts of **5.2** and oxidized β -mercaptoethanol, and determined the amount of reduced and oxidized species with analytical HPLC.^{29,116} We found a disulfide E°' value of (-0.192 ± 0.003) V. This value indicates that dithiol **5.2** is a weaker reducing agent than BMC, which is consistent with BMC being more

preorganized for disulfide-bond formation. Finally, in order to probe the effect of increasing hydrophobicity on catalyzing the formation of native disulfide bonds in proteins, we synthesized dithiols **5.3–5.8**.

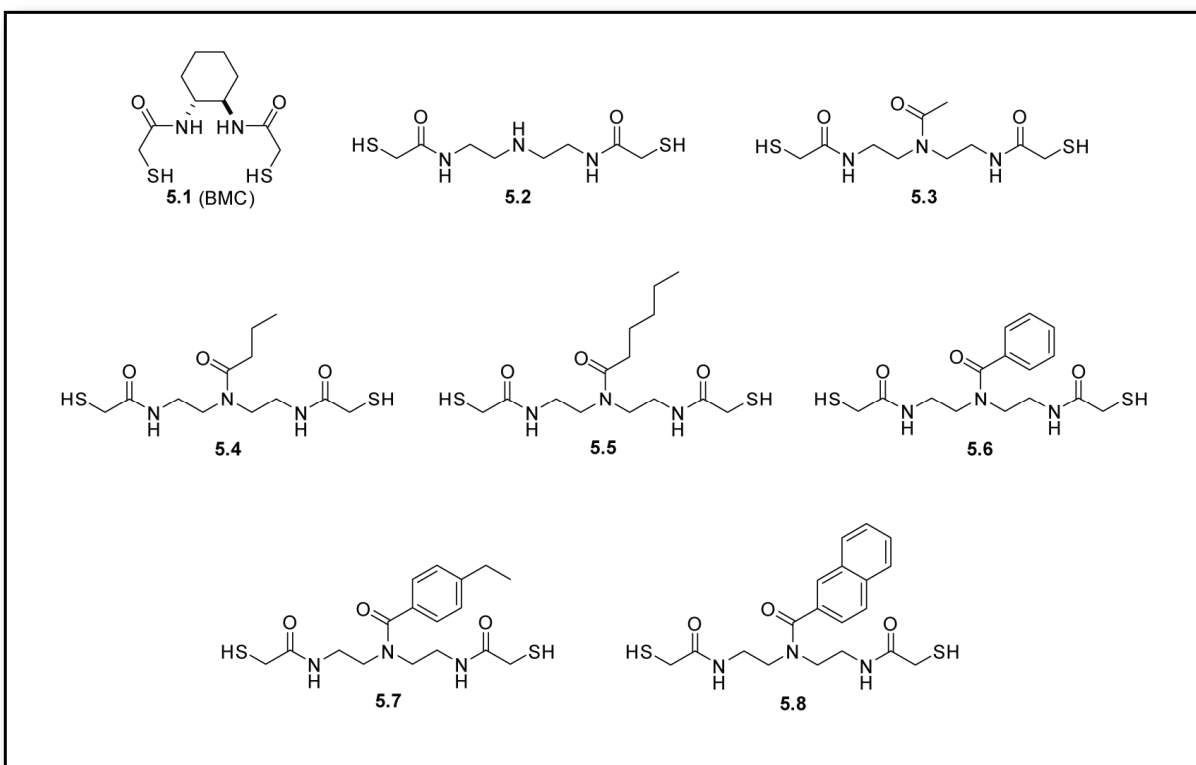


Figure 5.2 Small molecule PDI mimics assessed in this study.

Enzymatic catalysis provides an extremely sensitive measure of native protein structure. RNase A contains eight cysteine residues, which could form 105 ($= 7 \times 5 \times 3 \times 1$) distinct fully oxidized species, only one of which gives rise to enzymatic activity (Figure 5.3).¹⁸⁰ Accordingly, we tested the efficacy of this panel of compounds to catalyze the isomerization of "scrambled"

RNase A (sRNase A), which is a mixture of oxidized species, to its native state (RNase A) The reshuffling of nonnative disulfide bonds of sRNase A in RNase A was monitored by measuring the gain of catalytic activity.¹⁸¹ Dithiol **5.8** was excluded from the analysis due to its low solubility in aqueous solution.

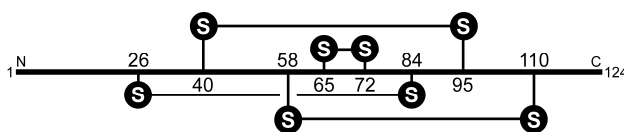


Figure 5.3 Scheme showing the connectivity of the four disulfide bonds in native RNase A. There are 104 other fully oxidized forms.

Some, but not all, of the PDI mimics led to a significant increase in the yield of oxidative protein folding (Figure 5.4). This finding contrasts with adding monothiols (*e.g.*, glutathione), which have been shown to reduce the yield of properly folded protein by favoring the accumulation of mixed disulfide species.^{5,177} Most notably, the data with dithiols **5.2–5.7** revealed an overall trend toward higher yield with increasing hydrophobicity of the pendant carboxamide. This trend culminated with dithiol **2.7**, which increased the yield of folded RNase A by 21% versus the uncatalyzed reaction.

The apparent correlation of catalytic efficacy with hydrophobicity could be due to a physicochemical property other than hydrophobicity. Accordingly, we determined the thiol pK_a and disulfide $E^{\circ'}$ values of the most efficacious dithiols containing alkyl (**5.5**) and aryl (**5.7**) carboxamide. We found dithiol **5.5** to have thiol pK_a values of 8.1 and 9.3 and a disulfide $E^{\circ'}$ value of -0.203 V (table 5.1). We found dithiol **5.7** to have similar physicochemical properties, with thiol pK_a values of 8.1 and 9.4 and a disulfide $E^{\circ'}$ value of -0.206 V. Both of these

compounds possess thiol acidity and disulfide stability to those of parent dithiol **5.2**, indicating that hydrophobicity was indeed likely correlated with catalytic efficacy.

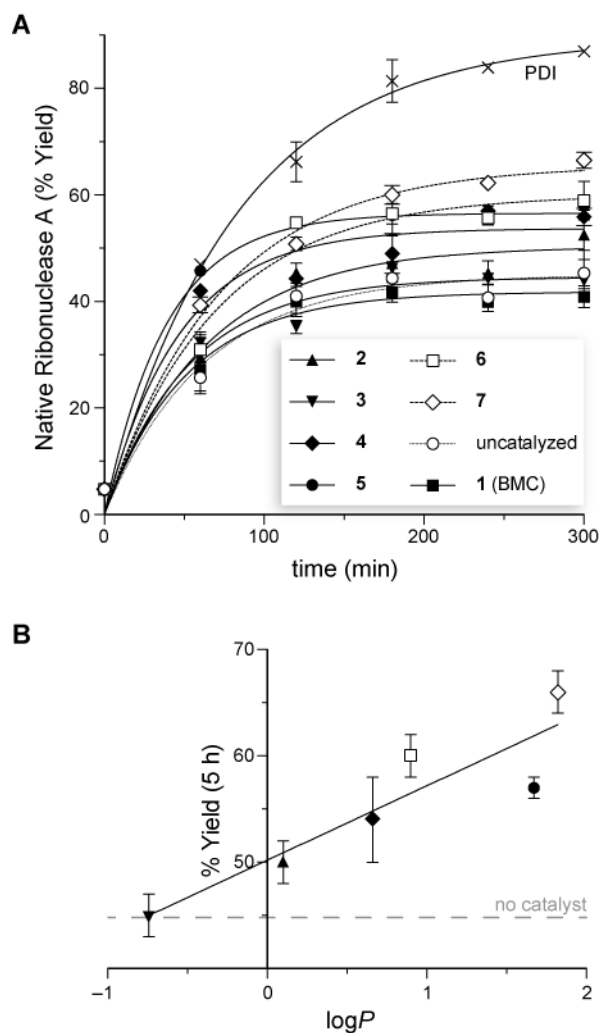


Figure 5.4 Catalysis of disulfide-bond isomerization by PDI and PDI mimics **5.1–5.7**. (A) Graph of the time-course for the unscrambling of sRNase A to give native RNase A. All assays were performed at 30 °C in 50 mM Tris–HCl buffer, pH 7.6, containing GSH (1.0 mM), GSSG (0.2 mM), and dithiol catalyst (1.0 mM) or PDI (1.0 mM). (B) Graph of the yield of native RNase A achieved by PDI mimics **5.2–5.7** after 5 h as a function of the $\log P$ value of its side chain (Table 5.1).

Our data are the first to indicate that increasing hydrophobicity of a small-molecule PDI mimic can have a profound effect on its efficacy as a catalyst. Still, none of the small-molecule catalysts were as efficacious as PDI itself. The molecular mass of PDI (57 kDa) is, however, $>10^2$ -fold greater than any of its mimics, enabling optimization of substrate binding and turnover beyond that attainable with small-molecule catalysts.

Table 5.1 Properties of PDI and mimics **5.1–5.8**

| Catalyst | p <i>K</i> _a | Disulfide <i>E</i> ' | log <i>P</i> ^a | Folding yield (%) ^b |
|------------|-------------------------|----------------------|---------------------------|--------------------------------|
| (None) | — | — | — | 45 ± 2 |
| PDI | 6.7 ^c | −0.180 V | — | 87 ± 2 |
| BMC | 8.3; 9.9 ^d | −0.232 V | — | 42 ± 2 |
| 5.2 | 8.0; 9.2 | −0.192 V | 0.10 | 50 ± 2 |
| 5.3 | ND | ND | −0.74 | 45 ± 2 |
| 5.4 | ND | ND | 0.66 | 54 ± 4 |
| 5.5 | 8.1; 9.3 | −0.203 V | 1.67 | 57 ± 1 |
| 5.6 | ND | ND | 0.90 | 60 ± 2 |
| 5.7 | 8.1; 9.4 | −0.206 V | 1.82 | 66 ± 2 |
| 5.8 | ND | ND | 2.06 | ND |

^aValues were calculated for dimethylamine in dithiol **5.2** and tertiary amide moiety in dithiols **5.3–5.8** (e.g., *N,N*-dimethylacetamide for dithiol **5.3**) with software from Molinspiration (Slovenský Grob, Slovak Republic), and are similar to known experimental values.¹⁸²

^bValues are for the unscrambling of sRNase A to give native RNase A by 1 mM catalyst in 5 h, as in Figure 5.4.

^cValues for the N-terminal cysteine in the active site of PDI.⁶

^dValues from ref. 116

ND, not determined.

Like the substrate-binding domains of PDI, the hydrophobicity of dithiols **5.4–5.7** likely encourages their interaction with unfolded or misfolded proteins.^{86,87,90-92,98,183,184} Dithiols having

moieties with higher $\log P$ values perform better, and aromatic moieties seem to be especially efficacious (Figure 5.4B). We note that a more hydrophobic catalyst could also increase the rate of the underlying thiol-disulfide interchange chemistry, as nonpolar environments are known to lower the free energy of activation for this reaction.¹⁷

5.5 Conclusions

In conclusion, we have designed, synthesized, and characterized novel organocatalysts that enhance the efficiency of oxidative protein folding. Moreover, we demonstrated that increasing the hydrophobicity of catalysts has a marked effect on their catalytic efficacy. Our findings could have a favorable impact on the folding of antibodies and other pharmaceutically relevant proteins, and inspire the design of a new genre of organocatalysts for oxidative protein folding.

5.6 Acknowledgements

This work made use of the National Magnetic Resonance Facility at Madison, which is supported by grant P41 GM103399 (NIH).

5.7 Materials and Methods

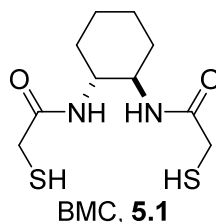
5.7.1 General

Commercial reagents were used without further purification. PDI (from bovine liver), β -Mercaptoethanol (β ME), oxidized β -mercaptoethanol (β ME^{ox}), and diethylenetriamine were from Sigma-Aldrich (St. Louis, MO). RNase A was from Sigma-Aldrich and was purified further by cation-exchange chromatography. The RNase A substrate 6-FAM–dArUdAdA–6-TAMRA

was from Integrated DNA Technologies (Coralville, IA). All glassware was oven- or flame-dried, and reactions were performed under $N_2(g)$ unless stated otherwise. Dichloromethane (DCM) and tetrahydrofuran (THF) were dried over a column of alumina. Triethylamine was dried over a column of alumina and purified further by passage through an isocyanate scrubbing column. Flash chromatography was performed with columns of 40–63 Å silica, 230–400 mesh from (Silicycle, Québec City, Canada). Thin-layer chromatography (TLC) was performed on plates of EMD 250- μm silica 60-F₂₅₄. The term "concentrated under reduced pressure" refers to the removal of solvents and other volatile materials using a rotary evaporator at water aspirator pressure (<20 torr) while maintaining the water-bath temperature below 40 °C. Residual solvent was removed from samples at high vacuum (<0.1 torr). The term "high vacuum" refers to vacuum achieved by a mechanical belt-drive oil pump. Analytical samples of all protein folding catalysts were obtained with a preparative HPLC, instrument from Shimadzu (Kyoto, Japan), which was equipped with a C18 reverse-phase preparative column, a Prominence diode array detector, and fraction collector. Equilibrium and reduction potential assays were performed using an analytical HPLC instrument from Waters (Milford, MA), which was equipped with a Waters 996 photodiode array detector, Empower 2 software, and a Varian C18 reverse-phase column. Thiol pK_a values were determined with a Varian Cary 60 UV-Vis spectrophotometer. Fluorescence was measured with an Infinite M1000 plate reader from Tecan (Männedorf, Switzerland). Calculations and rate constants were performed with Prism 6 software from GraphPad (La Jolla, CA). All NMR spectra were acquired at ambient temperature with a Bruker DMX-400 Avance spectrometer and Bruker III 500ii with cryoprobe spectrometer at the

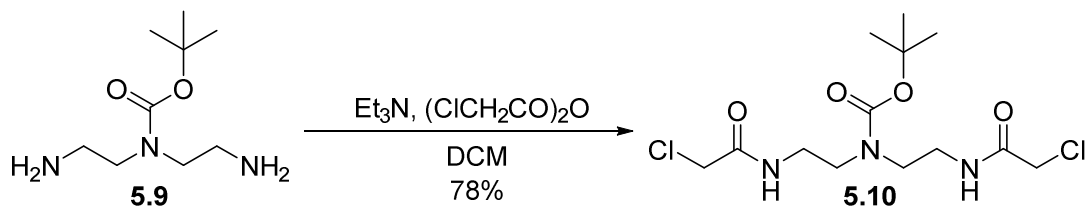
National Magnetic Resonance Facility at Madison (NMRFAM), and were referenced to TMS or residual solvent.

5.7.2 Chemical Synthesis



BMC (**5.1**) was synthesized as a racemate from (\pm)-*trans*-1,2-diaminocyclohexane as described previously.¹¹⁶ An analytically pure sample of BMC was obtained by reverse-phase HPLC using a preparatory C18 column and a linear gradient of 10–80% v/v acetonitrile (0.1% v/v TFA) in water (0.1% v/v TFA) over 45 min. BMC eluted at 23 min and, after lyophilization, was isolated as a white powder.

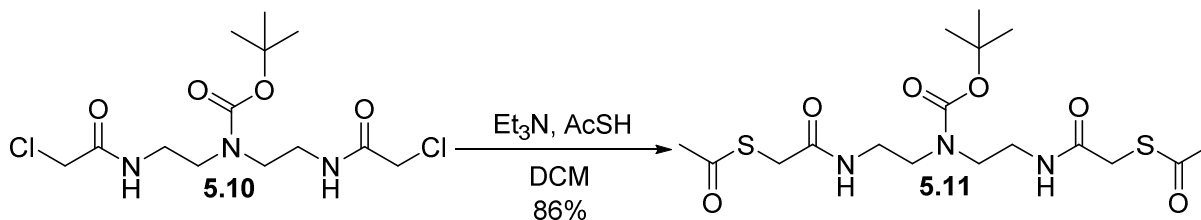
¹H NMR (400 MHz, DMSO-*d*₆) δ = 7.83 (d, *J* = 5.3 Hz, 2H), 3.52–3.48 (m, 2H), 3.09–2.99 (m, 4H), 2.60 (t, *J* = 7.9 Hz, 2H), 1.79–1.77 (m, 2H), 1.66–1.65 (m, 2H), 1.24–1.20 (m, 4H); ¹³C NMR (100 MHz, CDCl₃) δ = 169.2, 52.2, 31.7, 27.3, 24.3; HRMS (ESI) calculated for [C₁₀H₁₉N₂O₂S₂]⁺ (M + H⁺) requires *m/z* = 263.0883, found 263.0895.



To a flame-dried round-bottom flask was added **5.9** (0.847 g, 4.166 mmol), which was synthesized as described previously.¹⁸⁵ Fifty mL of dichloromethane was then added and the

solution was cooled to 0 °C under an atmosphere of N₂(g). Next, triethylamine (2.3 mL, 16.667 mmol) and chloroacetic anhydride (1.567 g, 9.167 mmol) were added, and the reaction mixture was stirred for 30 min before being quenched by the addition of 50 mL of saturated NaHCO₃. The organic layer was extracted and washed with water (2 x 25 mL). The organic extract was then dried over MgSO₄(s), filtered, and concentrated under reduced pressure, and the product was purified by column chromatography (silica, EtOAc), yielding **5.10** as a colorless oil (1.154 g, 78%).

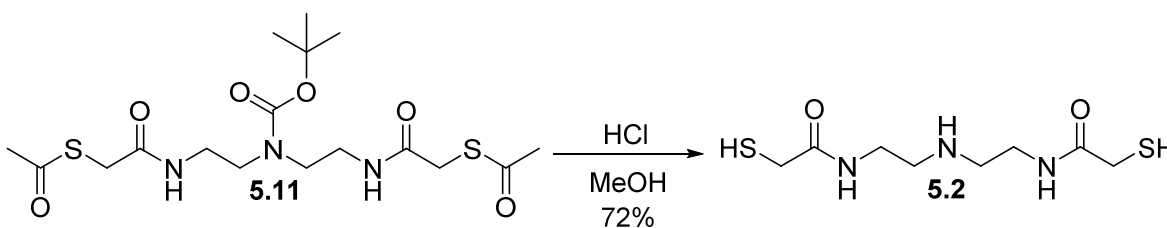
¹H NMR (400 MHz, CDCl₃) δ = 7.36 (br, s, 1H), 6.99 (br, s, 1H), 4.09–3.98 (m, 4H), 3.48–3.38 (m, 8H), 1.49 (s, 9H); **¹³C NMR (100 MHz, CDCl₃)** δ = 166.9, 166.4, 156.6, 81.0, 47.1, 46.1, 42.5, 39.8, 38.8, 28.3; **HRMS (ESI)** calculated for [C₁₃H₂₃Cl₂N₃O₄Na]⁺ (M + Na⁺) requires m/z = 378.0958, found 378.0938.



Compound **5.10** (1.154 g, 3.239 mmol) was placed in a round-bottom flask and, dissolved with 30 mL of dichloromethane, and the resulting solution was placed under an atmosphere of N₂(g). Triethylamine (2.3 mL, 16.208 mmol) and thioacetic acid (0.5 mL, 7.131 mmol) were then added, and the resulting solution was stirred under N₂(g). After 16 h, the reaction mixture

was concentrated, and the product was purified by column chromatography (silica, EtOAc), giving **5.11** as a colorless oil (2.792 g, 86%).

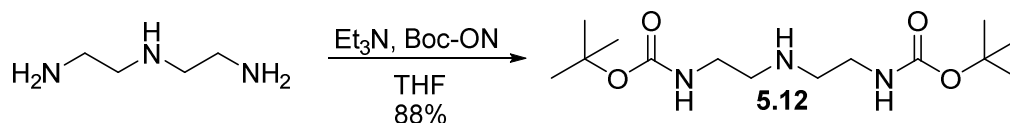
$^1\text{H NMR}$ (400 MHz, CDCl_3) δ = 6.81 (br, s, 2H), 3.56 (s, 4H), 3.42–3.29 (m, 8H), 2.41 (s, 6H), 1.49 (s, 9H); $^{13}\text{C NMR}$ (100 MHz, CDCl_3) δ = 195.1, 194.7, 168.2, 156.3, 80.3, 47.9, 47.1, 39.7, 38.9, 32.9, 30.1, 28.3; **HRMS** (ESI) calculated for $[\text{C}_{17}\text{H}_{29}\text{N}_3\text{O}_6\text{S}_2\text{Na}]^+$ ($\text{M} + \text{Na}^+$) requires m/z = 458.1390, found 458.1405.



A flame-dried round-bottom flask was charged with **5.11** (0.178 g, 0.409 mmol) and placed under an atmosphere of $\text{N}_2(\text{g})$. Four mL of anhydrous methanol followed by 2 mL of 3 N HCl in methanol were then added, and the reaction mixture was stirred under $\text{N}_2(\text{gas})$. Upon confirmation by TLC that the Boc group had been removed, the reaction mixture was concentrated under reduced pressure, and the product was purified by reverse-phase HPLC using a preparatory C18 column and a linear gradient of 10–50% v/v acetonitrile (0.1% v/v TFA) in water (0.1% v/v TFA) over 55 min. Dithiol **5.2** eluted as its TFA salt at 12.5 min and, after lyophilization, was isolated as a white solid (0.108 g, 72%).

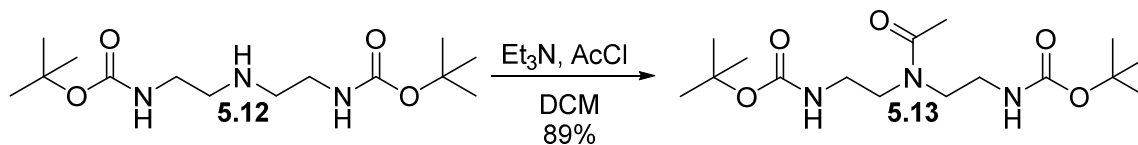
$^1\text{H NMR}$ (400 MHz, $\text{DMSO}-d_6$) δ = 8.76 (br, s, 2H), 8.33 (br, s, 2H), 3.5203.35 (m, 8H), 3.15 (d, J = 7.7 Hz, 4H), 2.88 (t, J = 7.7 Hz, 2H); $^{13}\text{C NMR}$ (100 MHz, $\text{DMSO}-d_6$) δ = 170.4,

46.1, 35.5, 27.2; **HRMS** (ESI) calculated for $[\text{C}_8\text{H}_{18}\text{N}_3\text{O}_2\text{S}_2]^+$ ($\text{M} + \text{H}^+$) requires $m/z = 252.0835$, found 252.0839.



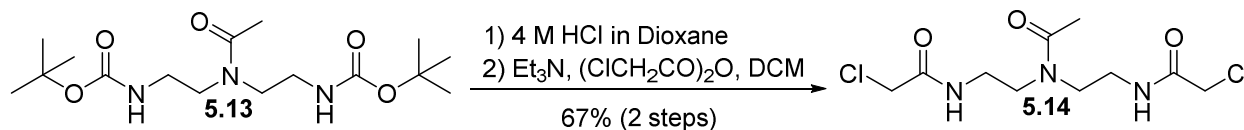
Synthesis of compound **5.12** was accomplished by closely following a procedure reported previously.¹⁸⁶ Specifically, diethylenetriamine (2.003 g, 19.415 mmol) and triethylamine (8.1 mL, 58.245 mmol) were dissolved in 100 mL of THF, and the resulting solution was cooled to 0 °C in an ice bath, and placed under an atmosphere of $\text{N}_2(\text{g})$. Next, a solution of 2-(boc-oxyimino)-2-phenylacetonitrile (Boc-ON) (9.563 g, 38.832 mmol), in 40 mL of THF, was added dropwise. The reaction mixture was stirred for 1 h on ice and then for another 1 h at room temperature. The solvent was removed under reduced pressure and the residue was dissolved in 200 mL of dichloromethane and washed with 5% w/v NaOH. The organic extract was then dried with $\text{MgSO}_4(\text{s})$, filtered, concentrated under reduced pressure, and the product was purified by column chromatography (silica, 10% v/v methanol in dichloromethane, 1% ammonium hydroxide), yielding **5.12** as a colorless oil (5.184 g, 88%).

^1H NMR (400 MHz, CDCl_3) $\delta = 4.95$ (br, s, 2H), 3.22 (q, $J = 5.9$ Hz, 4H), 2.73 (t, $J = 5.9$ Hz, 4 H), 1.45 (s, 18H); **^{13}C NMR (100 MHz, CDCl_3)** $\delta = 156.3$, 79.4, 49.0, 40.5, 28.6; **HRMS** (ESI) calculated for $[\text{C}_{14}\text{H}_{30}\text{N}_3\text{O}_4]^+$ ($\text{M} + \text{H}^+$) requires $m/z = 304.2231$, found 304.2230.



Compound **5.12** (0.419 g, 1.381 mmol) was placed in a flame-dried round-bottom flask, dissolved in 15 mL of anhydrous dichloromethane, and cooled to 0 °C in an ice bath under an inert atmosphere. Triethylamine (0.72 mL, 5.17 mmol) and acetyl chloride (0.16 mL, 2.29 mmol) were then added, and the resulting solution was stirred at 0 °C for 1 h and at room temperature for another 2 h. The reaction mixture was then concentrated under reduced pressure, and the product was purified by column chromatography (silica, EtOAc), yielding **5.13** as a colorless oil (0.425 g, 89%).

¹H NMR (400 MHz, CDCl₃) δ = 5.20 (br, s, 1H), 5.11 (br, s, 1H), 3.47-3.43 (m, 4H), 3.32–3.25 (m, 4H), 2.12 (s, 3H), 1.43 (s, 18H); **¹³C NMR (100 MHz, CDCl₃)** δ = 172.2, 156.6, 156.2, 79.8, 79.5, 49.4, 45.8, 39.7, 39.3, 28.6, 28.5, 21.6; **HRMS (ESI)** calculated for [C₁₆H₃₂N₃O₅]⁺ (M + H⁺) requires m/z = 346.2337, found 346.2338.



Forty mL of 4 M HCl in dioxane was added to a round-bottom flask containing **5.13** (0.425 g, 1.230 mmol). The solution was stirred overnight and then concentrated under reduced pressure. The product was then partially dissolved in 20 mL of dichloromethane, and the resulting slurry was cooled to 0 °C in an ice bath, and placed under an atmosphere of N₂(g).

Triethylamine (1.1 mL, 7.9 mmol) and chloroacetic anhydride (0.463 g, 2.706 mmol) were then added, and the reaction mixture was stirred for 30 min before being quenched by the addition of 50 mL of saturated NaHCO₃(aq). The organic layer was extracted and washed with water (2 x 25 mL). The organic extract was then dried with MgSO₄(s), filtered, and concentrated under reduced pressure. The product was purified by column chromatography (silica, 10% v/v methanol in dichloromethane), yielding **5.14** as a colorless oil (0.245 g, 67%).

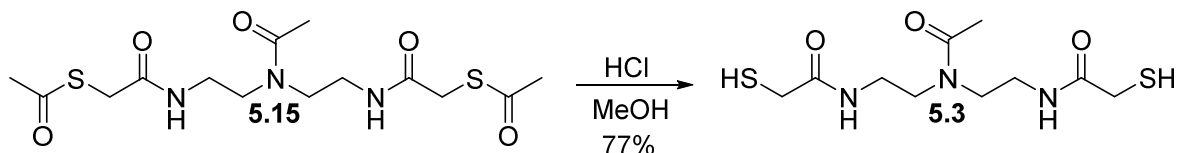
¹H NMR (400 MHz, CDCl₃) δ = 7.33 (br, s, 1H), 7.06 (br, s, 1H), 4.06 (s, 2H), 4.02 (s, 2H), 3.60–3.56 (m, 2H), 3.52–3.47 (m, 6H), 2.15 (s, 3H); ¹³C NMR (100 MHz, CDCl₃) δ = 172.5, 167.2, 166.9, 48.7, 45.4, 42.6, 39.6, 38.8, 21.5; HRMS (ESI) calculated for [C₁₀H₁₈Cl₂N₃O₃]⁺ (M + H⁺) requires *m/z* = 298.0713, found 298.0720.



A round-bottom flask was charged with **5.14** (0.246 g, 0.824 mmol), dissolved in 15 mL of dichloromethane and placed under an atmosphere of N₂(g). Triethylamine (0.57 mL, 4.12 mmol) and thioacetic acid (0.13 mL, 1.81 mmol) were then added and, the reaction mixture was stirred overnight. After 16 h, the mixture was concentrated under reduced pressure, and the product was purified by column chromatography (silica, 10% v/v methanol in dichloromethane), providing **5.15** as a yellow oil (0.286 g, 92%).

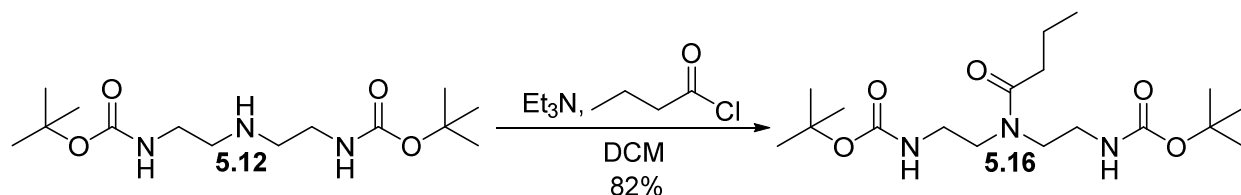
¹H NMR (400 MHz, CDCl₃) δ = 6.91 (br, s, 2H), 3.58 (s, 2H), 3.54 (s, 2H), 3.52–3.35 (m, 8H), 2.44 (s, 3H), 2.41 (s, 3H), 2.09 (s, 3H); ¹³C NMR (100 MHz, CDCl₃) δ = 195.8, 195.2,

172.6, 168.9, 168.7, 48.8, 45.1, 39.4, 38.9, 33.1, 33.0, 30.5, 30.4, 21.6; **HRMS** (ESI) calculated for $[\text{C}_{14}\text{H}_{24}\text{N}_3\text{O}_5\text{S}_2]^+$ ($\text{M} + \text{H}^+$) requires $m/z = 378.1152$, found 378.1150.



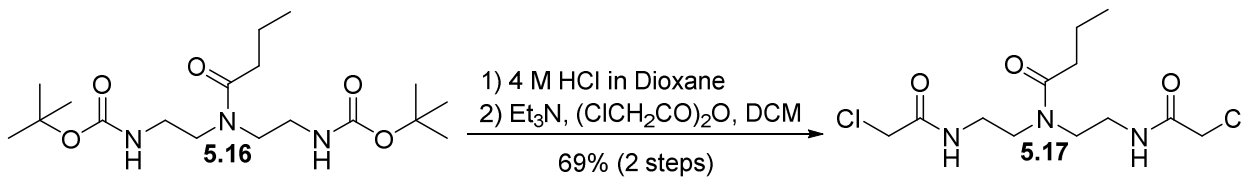
A flame-dried round-bottom flask was charged with **5.15** (0.159 g, 0.421 mmol) and placed under an atmosphere of $\text{N}_2(\text{g})$. Four mL of anhydrous methanol followed by 2 mL of 3 N HCl in methanol were then added and, the resulting solution was stirred under $\text{N}_2(\text{g})$. After 16 h, the reaction mixture was concentrated under reduced pressure, and the product was purified by reverse-phase HPLC using a preparatory C18 column and a linear gradient of 10–80% v/v acetonitrile (0.1% v/v TFA) in water (0.1% v/v TFA) over 45 min. Dithiol **5.3** eluted at 17 min and, after lyophilization, was isolated as a colorless oil (95.11 mg, 77%).

^1H NMR (400 MHz, $\text{DMSO}-d_6$) $\delta = 8.19$ (t, $J = 6.0$ Hz, 1H), 8.07 (t, $J = 5.9$ Hz, 1H), 3.33–3.26 (m, 4H), 3.24–3.16 (m, 4H), 3.11 (d, $J = 8.6$ Hz, 2H), 3.06 (d, $J = 8.6$ Hz, 2H), 2.74 (t, $J = 8.6$ Hz, 1H), 2.71 (t, $J = 8.6$ Hz, 1H), 1.99 (s, 3H); **^{13}C NMR (100 MHz, $\text{DMSO}-d_6$)** $\delta = 170.1$, 170.0, 169.9, 47.8, 44.65, 37.7, 36.9, 27.1, 27.0, 21.3; **HRMS** (ESI) calculated for $[\text{C}_{10}\text{H}_{20}\text{N}_3\text{O}_3\text{S}_2]^+$ ($\text{M} + \text{H}^+$) requires $m/z = 294.0942$, found 294.0941.



Compound **5.12** (0.619 g, 2.040 mmol) was placed in a flame-dried round-bottom flask and dissolved in 20 mL of anhydrous dichloromethane, and the resulting solution was cooled to 0 °C in an ice bath under an atmosphere of N₂(g). Triethylamine (1.4 mL, 10.2 mmol) and butyryl chloride (0.25 mL, 2.45 mmol) were then added, and the reaction mixture was stirred at 0 °C for 1 h and at room temperature for another 2 h. The reaction mixture was then concentrated under reduced pressure, and the product was purified by column chromatography (silica, EtOAc), yielding **5.16** as a colorless oil (0.625 g, 82%).

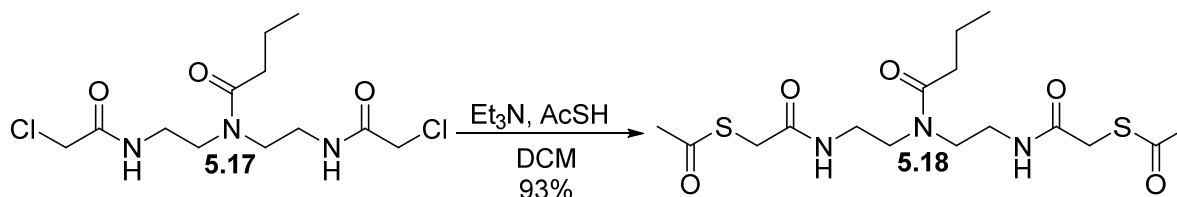
¹H NMR (400 MHz, CDCl₃) δ = 5.39 (br, s, 1H), 5.30 (br, s, 1H), 3.48–3.42 (m, 4H), 3.32–3.25 (m, 4H), 2.32 (t, *J* = 7.5 Hz, 2H), 1.65 (sex, *J* = 7.5 Hz, 2H), 1.43 (s, 9H), 1.42 (s, 9H), 0.95 (t, *J* = 7.5 Hz, 3H); ¹³C NMR (100 MHz, CDCl₃) δ = 174.7, 156.6, 156.1, 79.6, 79.3, 48.4, 45.7, 39.6, 39.3, 34.9, 28.4, 18.8, 13.9; HRMS (ESI) calculated for [C₁₈H₃₆N₃O₅]⁺ (M + H⁺) requires *m/z* = 374.2650, found 374.2655.



Fifty mL of 4 M HCl in dioxane was added to a round-bottom flask containing **5.16** (0.625 g, 1.673 mmol). The reaction mixture was left to stir overnight and then concentrated

under reduced pressure. The compound was then partially dissolved in 20 mL of dichloromethane, cooled to 0 °C in an ice bath, and placed under an atmosphere of N₂(g). Triethylamine (1.2 mL, 8.4 mmol) and chloroacetic anhydride (0.629 g, 3.681 mmol) were then added, and the reaction mixture was stirred for 30 min before being quenched by the addition of 50 mL of saturated NaHCO₃(aq). The organic layer was extracted and washed twice with 25 mL of water. The organic extract was then dried with anhydrous MgSO₄, filtered, concentrated under reduced pressure, and the product was purified by column chromatography (silica, 10% v/v methanol in dichloromethane), yielding **5.17** as a colorless oil (0.377 g, 69%).

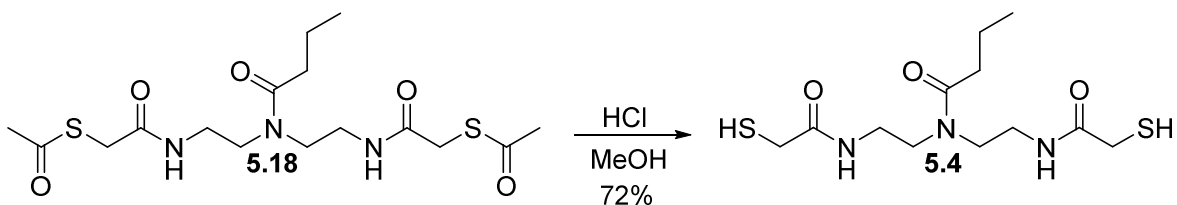
¹H NMR (400 MHz, CDCl₃) δ = 7.48 (br, s, 1H), 7.26 (br, s, 1H), 4.06 (s, 2H), 4.00 (s, 2H), 3.58 (t, *J* = 6.1 Hz, 2H), 3.52–3.46 (m, 6H), 2.34 (t, *J* = 7.4 Hz, 2H), 1.66 (sex, *J* = 7.4 Hz, 2H), 0.96 (t, *J* = 7.4 Hz, 3H); **¹³C NMR (100 MHz, CDCl₃)** δ = 175.0, 167.1, 166.9, 47.6, 45.2, 42.5, 39.5, 38.7, 34.9, 18.9, 14.0; **HRMS (ESI)** calculated for [C₁₂H₂₂Cl₂N₃O₃]⁺ (M + H⁺) requires *m/z* = 326.1033, found 326.1036.



A round-bottom flask was charged with **5.17** (0.377 g, 1.154 mmol), dissolved with 20 mL of dichloromethane, and placed under an atmosphere of N₂(g). Triethylamine (0.80 mL, 5.77 mmol) and thioacetic acid (0.18 mL, 2.54 mmol) were then added, and the resulting solution was stirred under N₂(g). After 16 h, the reaction mixture was concentrated under reduced pressure,

and the product was purified by column chromatography (silica, 10% v/v methanol in dichloromethane), providing **5.18** as a yellow oil (0.435 g, 93%).

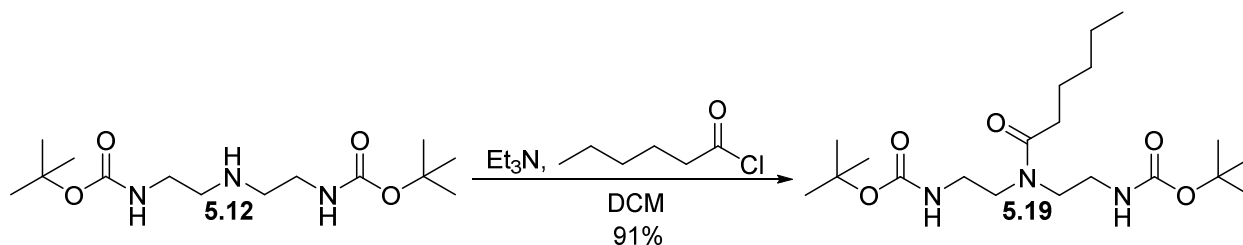
¹H NMR (400 MHz, CDCl₃) δ = 7.13 (br, s, 2H), 3.59 (s, 2H), 3.56 (s, 2H), 3.51–3.37 (m, 8H), 2.42 (s, 3H), 2.41 (s, 3H), 2.32 (t, J = 7.5 Hz, 2H), 1.64 (sex, J = 7.5 Hz, 2H), 0.96 (t, J = 7.5 Hz, 3H); **¹³C NMR (100 MHz, CDCl₃)** δ = 195.6, 195.0, 174.9, 168.8, 168.6, 47.6, 45.1, 39.4, 38.8, 34.9, 33.0, 30.3, 30.2, 18.8, 13.9; **HRMS (ESI)** calculated for [C₁₆H₂₈N₃O₅S₂]⁺ (M + H⁺) requires m/z = 406.1465, found 406.1459.



A flame-dried round-bottom flask was charged with **5.18** (0.111 g, 0.274 mmol) and placed under an atmosphere of N₂(g). Six mL of anhydrous methanol followed by 3 mL of 3 N HCl in methanol were then added, and the resulting solution was stirred under N₂. After 16 h, the reaction mixture was concentrated under reduced pressure, and the product was purified by reverse-phase HPLC using a preparatory C18 column and a linear gradient of 10–80% v/v acetonitrile (0.1% v/v TFA) in water (0.1% v/v TFA) over 45 min. Dithiol **5.4** eluted at 22 min and, after lyophilization, was isolated as a colorless oil (63.42 mg, 72%).

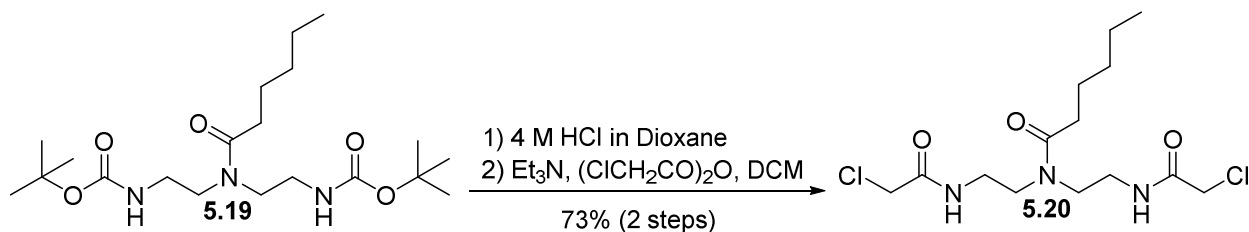
¹H NMR (400 MHz, DMSO-*d*₆) δ = 8.19 (t, J = Hz, 1H), 8.05 (t, J = Hz, 1H), 3.34–3.28 (m, 4H), 3.23–3.15 (m, 4H), 3.09 (d, J = 8.0 Hz, 2H), 3.06 (d, J = 8.0 Hz, 2H), 2.74 (t, J = 8.0 Hz, 1H), 2.71 (t, J = 8.0 Hz, 1H), 2.27 (t, J = 7.4 Hz, 2H), 1.51 (sex, J = 7.4 Hz, 2H), 0.87 (t, J =

7.4 Hz, 3H); ^{13}C NMR (100 MHz, $\text{DMSO-}d_6$) δ = 172.3, 170.0, 169.7, 46.8, 45.0, 37.8, 37.0, 34.0, 27.1, 27.0, 18.3, 13.8; HRMS (ESI) calculated for $[\text{C}_{12}\text{H}_{24}\text{N}_3\text{O}_3\text{S}_2]^+$ ($\text{M} + \text{H}^+$) requires m/z = 322.1254, found 322.1258.



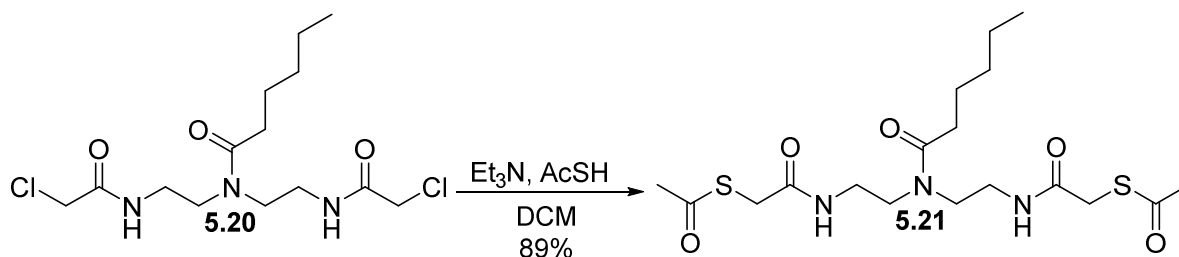
Compound **5.12** (1.534 g, 5.056 mmol) was placed in a flame-dried round-bottom flask and dissolved in 50 mL of anhydrous dichloromethane, and the resulting solution was cooled to 0 °C in an ice bath under an atmosphere of $\text{N}_2(\text{g})$. Triethylamine (2.1 mL, 15.2 mmol) and hexanoyl chloride (0.78 mL, 5.56 mmol) were then added, and the reaction mixture was stirred at 0 °C for 1 h and at room temperature for another 2 h. The reaction mixture was then concentrated under reduced pressure, and the product was purified by column chromatography (silica, 50% v/v EtOAc in hexanes), yielding **5.19** as a colorless oil (1.848 g, 91%).

^1H NMR (400 MHz, CDCl_3) δ = 5.12 (br, s, 1H), 5.06 (br, s, 1H), 3.48–3.43 (m, 4H), 3.32–3.24 (m, 4H), 2.32 (t, J = 7.6 Hz, 2H), 1.62 (quin, J = 7.6 Hz, 2H), 1.43 (s, 18H), 1.34–1.26 (m, 4H), 0.90 (t, J = 6.7 Hz, 3H); ^{13}C NMR (100 MHz, CDCl_3) δ = 174.7, 156.4, 156.0, 79.5, 79.2, 48.3, 45.6, 39.5, 39.2, 32.9, 31.5, 28.3, 25.0, 22.5, 13.9; HRMS (ESI) calculated for $[\text{C}_{20}\text{H}_{40}\text{N}_3\text{O}_5]^+$ ($\text{M} + \text{H}^+$) requires m/z = 402.2963, found 402.2966.



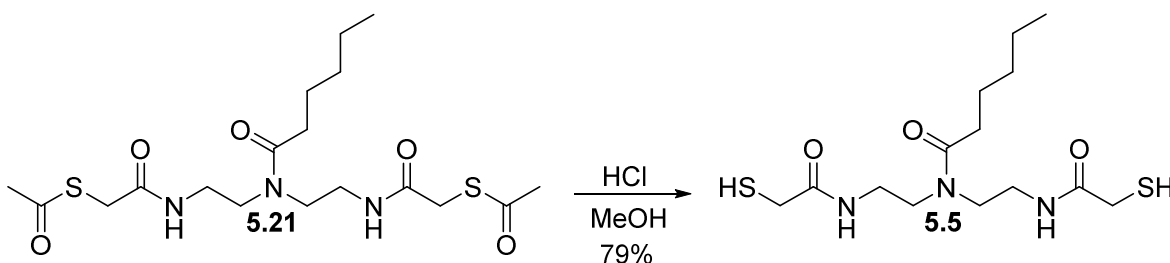
Fifty mL of 4 M HCl in dioxane was added to a round-bottom flask containing **5.19** (0.867 g, 2.159 mmol). The resulting solution was stirred overnight and then concentrated under reduced pressure. The product was then partially dissolved in 40 mL of dichloromethane, and the resulting slurry was cooled to 0 °C in an ice bath, and placed under an atmosphere of N₂(g). Triethylamine (1.8 mL, 12.9 mmol) and chloroacetic anhydride (0.923 g, 5.398 mmol) were then added and the reaction mixture was stirred for 30 min before being quenched by the addition of 50 mL of saturated NaHCO₃(aq). The organic layer was extracted and washed with water (2 x 30 mL). The organic extract was then dried over anhydrous MgSO₄(s), filtered, and concentrated under reduced pressure, and the product was purified by column chromatography (silica, 10% v/v methanol in dichloromethane), yielding **5.20** as a colorless oil (0.558 g, 73%).

¹H NMR (400 MHz, CDCl₃) δ = 7.36 (br, s, 1H), 7.08 (br, s, 1H), 4.06 (s, 2H), 4.00 (s, 2H), 3.58 (t, J = 6.1 Hz, 2H), 3.52–3.46 (m, 6H), 2.35 (t, J = 7.4 Hz, 2H), 1.63 (quin, J = 7.4 Hz, 2H), 1.34–1.26 (m, 4H), 0.90 (t, J = 6.7 Hz, 3H); **¹³C NMR (100 MHz, CDCl₃)** δ = 175.2, 167.1, 166.9, 47.7, 45.3, 42.6, 39.7, 38.8, 33.1, 31.7, 25.3, 22.7, 14.1; **HRMS (ESI)** calculated for [C₁₄H₂₆Cl₂N₃O₃]⁺ (M + H⁺) requires m/z = 354.1346, found 354.1342.



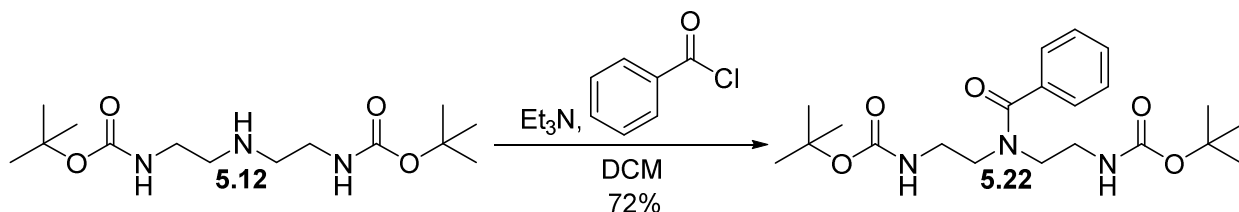
A round-bottom flask charged with **5.20** (0.558 g, 1.575 mmol) was dissolved with 20 mL of dichloromethane and placed under $N_2(g)$. Triethylamine (1.1 mL, 7.9 mmol) and thioacetic acid (0.25 mL, 3.47 mmol) were then added, and the resulting solution was stirred under $N_2(g)$. After 16 h, the reaction mixture was concentrated under reduced pressure, and the product was purified by column chromatography (silica, 10% v/v methanol in dichloromethane), providing **5.21** as a colorless oil (0.608 g, 89%).

1H NMR (400 MHz, $CDCl_3$) δ = 7.03–6.98 (m, 2H), 3.57 (s, 2H), 3.55 (s, 2H), 3.51–3.36 (m, 8H), 2.42 (s, 2H), 2.41 (s, 2H), 2.32 (t, J = 7.4 Hz, 2H), 1.61 (quin, J = 7.4 Hz, 2H), 1.36–1.28 (m, 4H), 0.90 (t, J = 6.7 Hz, 3H); ^{13}C NMR (100 MHz, $CDCl_3$) δ = 195.7, 195.1, 175.2, 168.8, 168.6, 47.8, 45.3, 39.6, 38.9, 33.1, 33.0, 32.9, 31.6, 30.4, 30.3, 25.2, 22.6, 14.1; HRMS (ESI) calculated for $[C_{18}H_{32}N_3O_5S_2]^+$ ($M + H^+$) requires m/z = 434.1778, found 434.1780.



A flame-dried round-bottom flask was charged with **5.21** (0.149 g, 0.344 mmol) and placed under an atmosphere of N₂(g). Six mL of anhydrous methanol followed by 3 mL of 3 N HCl in methanol were then added and, the reaction mixture was stirred under N₂(g). After 24 h, the reaction mixture was concentrated under reduced pressure, and the product was purified by reverse-phase HPLC using a preparatory C18 column and a linear gradient of 10–80% v/v acetonitrile (0.1% v/v TFA) in water (0.1% v/v TFA) over 45 min. Dithiol **5.5** eluted at 28 min and, after lyophilization, was isolated as a colorless oil (94.98 mg, 79%).

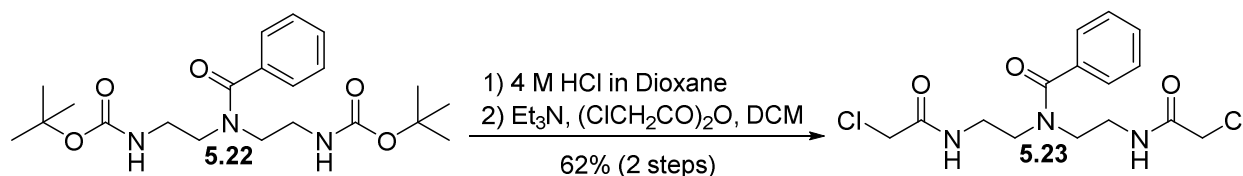
¹H NMR (400 MHz, DMSO-*d*₆) δ = 8.21 (t, *J* = 5.8 Hz, 1H), 8.07 (t, *J* = 5.8 Hz, 1H), 3.31 (t, *J* = 6.6 Hz, 2H), 3.29 (t, *J* = 6.6 Hz, 2H) 3.22=3.15 (m, 4H), 3.08 (d, *J* = 8.0 Hz, 2H), 3.06 (d, *J* = 8.0 Hz, 2H), 2.75 (t, *J* = 8.0 Hz, 1H), 2.72 (t, *J* = 8.0 Hz, 1H), 2.27 (t, *J* = 7.5 Hz, 2H), 1.48 (quin, *J* = 7.5 Hz, 2H), 1.32-1.20 (m, 4H), 0.86 (t, *J* = 6.9 Hz, 3H); **¹³C NMR (100 MHz, DMSO-*d*₆)** δ = 172.5, 170.0, 169.7, 46.8, 44.7, 37.8, 37.0, 32.0, 31.1, 27.2, 27.1, 24.6, 22.1, 14.0; **HRMS (ESI)** calculated for [C₁₄H₂₈N₃O₃S₂]⁺ (M + H⁺) requires *m/z* = 350.1567, found 350.1565.



Compound **5.12** (1.391 g, 4.585 mmol) was placed in a flame-dried round-bottom flask and dissolved in 50 mL of anhydrous dichloromethane, and the resulting solution was cooled to 0 °C in an ice bath under an atmosphere of N₂(g). Triethylamine (1.9 mL, 13.8 mmol) and benzoyl

chloride (0.64 mL, 5.50 mmol) were then added, and the reaction mixture was stirred at 0 °C for 1 h and at room temperature for another 2 h. The reaction mixture was then concentrated under reduced pressure, and the product was purified by column chromatography (silica, EtOAc), yielding **5.22** as a colorless oil (1.848 g, 91%).

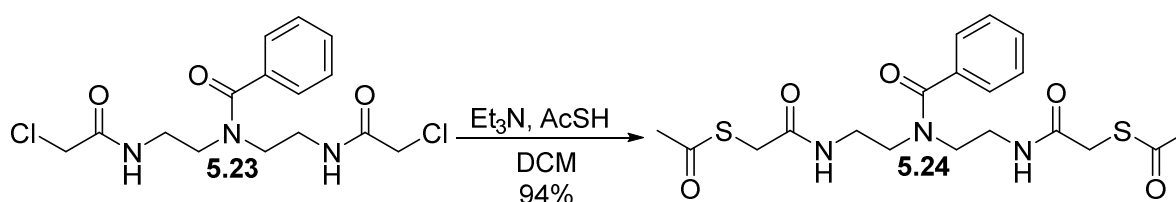
¹H NMR (400 MHz, CDCl₃) δ = 7.40–7.35 (m, 5H), 5.12 (br, s, 1H), 5.06 (br, s, 1H), 3.67–3.24 (m, 8H), 1.44 (s, 18H); **¹³C NMR (100 MHz, CDCl₃)** δ = 173.4, 156.7, 155.8, 136.4, 129.6, 128.7, 126.8, 50.0, 45.0, 39.5, 38.9, 28.6, 28.4; **HRMS (ESI)** calculated for [C₂₁H₃₄N₃O₅]⁺ (M + H⁺) requires m/z = 408.2493, found 408.2491.



Fifty mL of 4 M HCl in dioxane was added to a round-bottom flask containing **5.22** (0.713 g, 1.750 mmol). The resulting solution was stirred under N₂(g) overnight and then concentrated under reduced pressure. The product was then partially dissolved in 55 mL of dichloromethane, and the resulting slurry was cooled to 0 °C in an ice bath, and placed under an atmosphere of N₂(g). Triethylamine (1.5 mL, 10.5 mmol) and chloroacetic anhydride (0.748 g, 4.375 mmol) were then added and the reaction mixture was stirred for 30 min before being quenched by the addition of 55 mL of saturated NaHCO₃(aq). The organic layer was extracted and washed with water (2 x 40 mL). The organic extract was then dried with anhydrous MgSO₄(s), filtered, and concentrated under reduced pressure, and the product was purified by

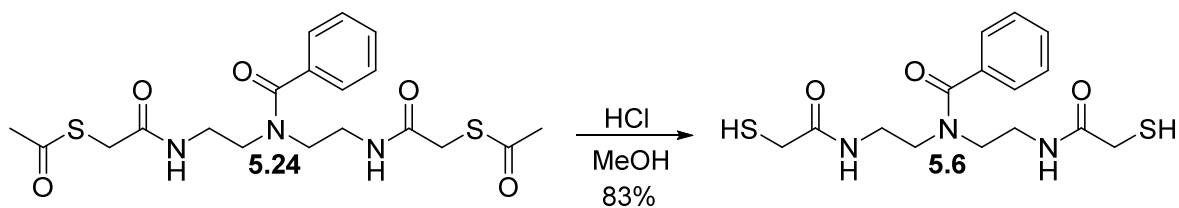
column chromatography (silica, 10% v/v methanol in dichloromethane), yielding **5.23** as a colorless oil (0.391 g, 62%).

$^1\text{H NMR}$ (400 MHz, CDCl_3) δ = 7.44–7.41 (m, 3H), 7.37–7.35 (m, 2H), 6.90 (br, s, 2H), 4.05 (s, 2H), 3.98 (s, 2H), 3.80–3.41 (m, 8H); $^{13}\text{C NMR}$ (100 MHz, CDCl_3) δ = 173.4, 167.1, 166.3, 135.6, 129.9, 128.8, 126.5, 48.9, 44.6, 42.5, 39.0, 38.3; **HRMS** (ESI) calculated for $[\text{C}_{15}\text{H}_{20}\text{Cl}_2\text{N}_3\text{O}_3]^+$ ($\text{M} + \text{H}^+$) requires m/z = 360.0877, found 360.0888.



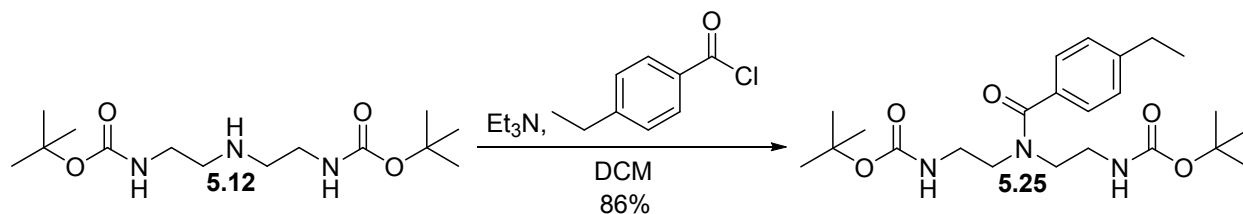
A round-bottom flask charged with **5.23** (0.391 g, 1.085 mmol) was dissolved with 15 mL of dichloromethane and placed under $\text{N}_2(\text{g})$. Triethylamine (0.76 mL, 5.43 mmol) and thioacetic acid (0.17 mL, 2.39 mmol) were then added, and the reaction mixture was stirred under $\text{N}_2(\text{g})$. After 24 h, the reaction mixture was concentrated under reduced pressure, and the product was purified by column chromatography (silica, 10% v/v methanol in dichloromethane), providing **5.24** as a colorless oil (0.448 g, 94%).

$^1\text{H NMR}$ (400 MHz, CDCl_3) δ = 7.43–7.42 (m, 3H), 7.37–7.35 (m, 2H), 6.98 (br, s, 1H), 6.80 (br, s, 1H), 3.72–3.32 (m, 12H), 2.37 (s, 6H); $^{13}\text{C NMR}$ (100 MHz, CDCl_3) δ = 195.6, 195.4, 173.4, 168.9, 168.4, 135.8, 129.8, 128.6, 126.6, 49.3, 44.8, 39.2, 38.5, 32.9, 30.3; **HRMS** (ESI) calculated for $[\text{C}_{19}\text{H}_{26}\text{N}_3\text{O}_5\text{S}_2]^+$ ($\text{M} + \text{H}^+$) requires m/z = 440.1309, found 440.1310.



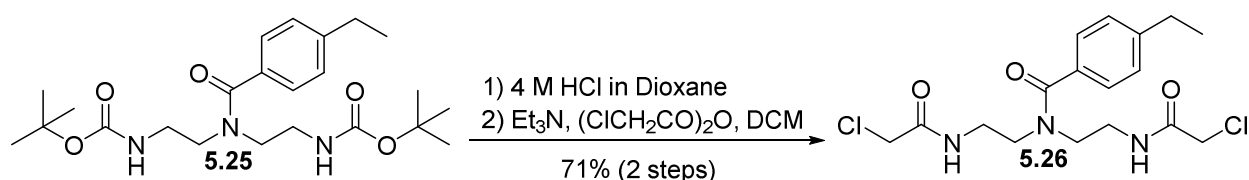
A flame-dried round-bottom flask was charged with **5.24** (0.131 g, 0.298 mmol) and placed under an atmosphere of $N_2(g)$. Six mL of anhydrous methanol followed by 3 mL of 3 N HCl in methanol were then added, and the reaction mixture was stirred under $N_2(g)$. After 24 h, the reaction mixture was concentrated under reduced pressure, and the product was purified by reverse-phase HPLC using a preparatory C18 column and a linear gradient of 10–80% v/v acetonitrile (0.1% v/v TFA) in water (0.1% v/v TFA) over 45 min. Dithiol **5.6** eluted at 25 min and, after lyophilization, was isolated as a colorless oil (87.92 mg, 83%).

1H NMR (400 MHz, $DMSO-d_6$) δ = 8.23 (br, s, 1H), 8.08 (br, s, 1H), 7.42–7.40 (m, 3H), 7.36–7.34 (m, 2H), 3.52–3.50 (m, 2H), 3.36–3.34 (m, 2H), 3.28–3.25 (m, 2H), 3.14–3.10 (m, 4H), 3.01 (d, J = 8.0 Hz, 2H), 2.76 (t, J = 8.0 Hz, 1H), 2.68 (t, J = 8.0 Hz, 1H); ^{13}C NMR (100 MHz, $DMSO-d_6$) δ = 171.1, 169.9, 169.6, 136.9, 129.0, 128.3, 126.6, 48.3, 44.1, 37.3, 36.7, 27.2, 27.0; HRMS (ESI) calculated for $[C_{15}H_{22}N_3O_3S_2]^+$ ($M + H^+$) requires m/z = 356.1098, found 356.1096.



Compound **5.12** (1.592 g, 5.247 mmol) was placed in a flame-dried round-bottom flask and dissolved in 60 mL of anhydrous dichloromethane, and cooled to 0 °C in an ice bath under an atmosphere of N₂(g). Triethylamine (2.2 mL, 15.7 mmol) and 4-ethylbenzoyl chloride (0.93 mL, 6.30 mmol) were then added and the reaction mixture was stirred at 0 °C for 1 h and at room temperature for another 2 h. The reaction mixture was then concentrated under reduced pressure, and the product was purified by column chromatography (silica, 50 % EtOAc v/v in hexanes), yielding **5.25** as a white solid (1.965 g, 86%).

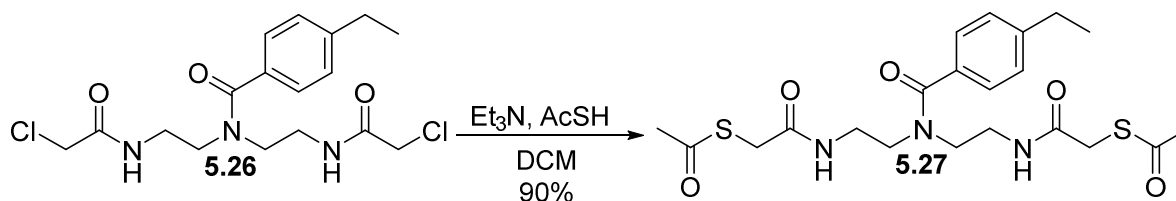
¹H NMR (400 MHz, CDCl₃) δ = 7.29 (d, *J* = 7.7 Hz, 2H), 7.20 (d, *J* = 7.7 Hz, 2H), 5.15 (br, s, 1H), 5.07 (br, s, 1H), 3.65–3.25 (m, 8H), 2.65 (q, *J* = 7.6 Hz, 2H), 1.44 (s, 18H), 1.23 (t, *J* = 7.6 Hz, 3H); ¹³C NMR (100 MHz, CDCl₃) δ = 173.6, 156.6, 155.9, 133.7, 128.1, 126.9, 79.6, 50.0, 45.0, 39.4, 39.1, 28.8, 28.5, 15.4; HRMS (ESI) calculated for [C₂₃H₃₈N₃O₅]⁺ (M + H⁺) requires *m/z* = 436.2806, found 436.2806.



Fifty mL of 4 M HCl in dioxane was added to a round-bottom flask containing **5.25** (0.689 g, 1.584 mmol). The resulting solution was stirred overnight and then concentrated under reduced pressure. The product was then partially dissolved in 60 mL of dichloromethane, and the resulting solution was cooled to 0 °C in an ice bath, and placed under an atmosphere of N₂(g). Triethylamine (1.1 mL, 7.9 mmol) and chloroacetic anhydride (0.677 g, 3.960 mmol) were then added and the reaction mixture was stirred for 30 min before being quenched by the addition of

60 mL of saturated $\text{NaHCO}_3(\text{aq})$. The organic layer was extracted and washed with water (2 x 40 mL). The organic extract was then dried with anhydrous $\text{MgSO}_4(\text{s})$, filtered, and concentrated under reduced pressure, and the product was purified by column chromatography (silica, 10% v/v methanol in dichloromethane), yielding **5.26** as a colorless oil (0.437 g, 71%).

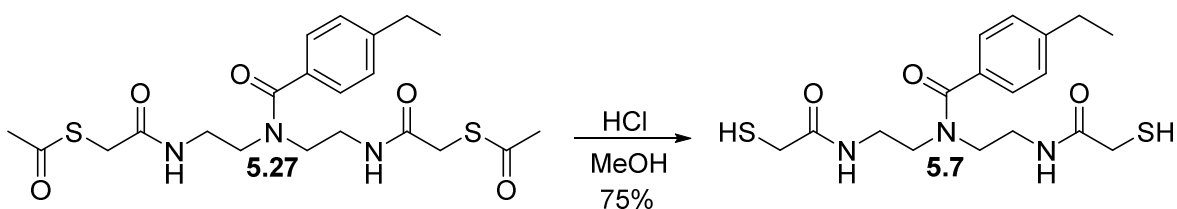
$^1\text{H NMR}$ (400 MHz, CDCl_3) δ = 7.61 (br, s, 1H), 7.28 (d, J = 7.8 Hz, 2H), 7.23 (d, J = 7.8 Hz, 2H), 7.10 (br, s, 1H), 3.97 (s, 4H), 3.73–3.41 (m, 8H), 2.67 (q, J = 7.7 Hz, 2H), 1.24 (t, J = 7.7 Hz, 3H); $^{13}\text{C NMR}$ (100 MHz, CDCl_3) δ = 173.6, 167.1, 166.5, 146.3, 132.9, 128.2, 126.7, 48.9, 44.6, 42.5, 38.5, 28.7, 15.4; **HRMS** (ESI) calculated for $[\text{C}_{17}\text{H}_{24}\text{Cl}_2\text{N}_3\text{O}_3]^+$ ($\text{M} + \text{H}^+$) requires m/z = 388.1190, found 388.1192.



A round-bottom flask was charged with **5.26** (0.437 g, 1.125 mmol), dissolved with 15 mL of dichloromethane, and placed under an atmosphere of $\text{N}_2(\text{g})$. Triethylamine (0.78 mL, 5.62 mmol) and thioacetic acid (0.18 mL, 2.48 mmol) were then added, and the reaction mixture was stirred under $\text{N}_2(\text{g})$. After 24 h, the reaction mixture was concentrated under reduced pressure, and the product was purified by column chromatography (silica, 10% v/v methanol in dichloromethane), providing **5.27** as a yellow solid (0.473 g, 90%).

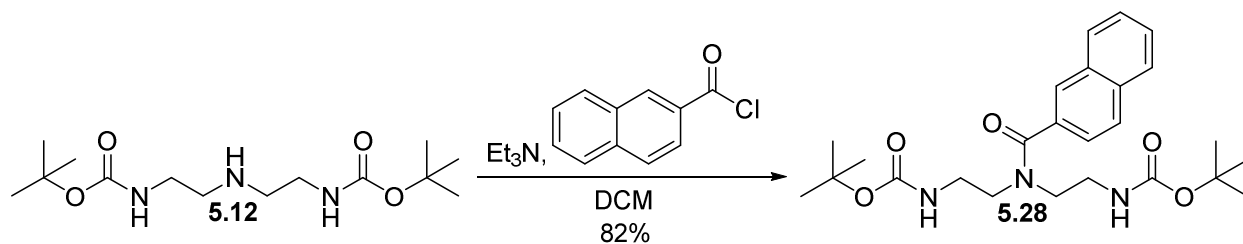
$^1\text{H NMR}$ (400 MHz, CDCl_3) δ = 7.29 (d, J = 8.0 Hz, 2H), 7.23 (d, J = 8.0 Hz, 2H), 7.02 (br, s, 1H), 6.84 (br, s, 1H), 3.68–3.33 (m, 12H), 2.68 (q, J = 7.6 Hz, 2H), 2.37 (s, 6H), 1.25 (t, J

= 7.6 Hz, 3H); ^{13}C NMR (100 MHz, CDCl_3) δ = 195.6, 173.7, 169.0, 168.5, 146.3, 133.2, 128.2, 126.9, 49.5, 44.9, 39.3, 38.7, 33.0, 30.4, 28.8, 15.5; HRMS (ESI) calculated for $[\text{C}_{21}\text{H}_{30}\text{N}_3\text{O}_5\text{S}_2]^+$ ($\text{M} + \text{H}^+$) requires m/z = 468.1622, found 468.1626.



A flame-dried round-bottom flask was charged with **5.27** (0.147 g, 0.314 mmol) and placed under an atmosphere of $\text{N}_2(\text{g})$. Six mL of anhydrous methanol followed by 3 mL of 3 N HCl in methanol were then added, and the reaction mixture was stirred under $\text{N}_2(\text{g})$. After 24 h, the reaction mixture was concentrated under reduced pressure, and the product was purified by reverse-phase HPLC using a preparatory C18 column and a linear gradient of 10–80% v/v acetonitrile (0.1% v/v TFA) in water (0.1% v/v TFA) over 45 min. Dithiol **5.7** eluted at 30 min and, after lyophilization, was isolated as a white solid (90.32 mg, 75%).

^1H NMR (400 MHz, $\text{DMSO}-d_6$) δ = 8.20 (br, s, 1H), 8.06 (br, s, 1H), 7.28 (d, J = 7.8 Hz, 2H), 7.24 (d, J = 7.8 Hz, 2H), 3.54–3.46 (m, 2H), 3.35–3.29 (m, 4H), 3.14–3.02 (m, 6H), 2.74–2.60 (m, 4H), 1.19 (t, J = 7.5 Hz, 3H); ^{13}C NMR (100 MHz, $\text{DMSO}-d_6$) δ = 171.2, 169.8, 169.6, 144.6, 134.2, 127.6, 126.7, 48.4, 44.1, 37.3, 36.8, 28.0, 27.1, 15.4; HRMS (ESI) calculated for $[\text{C}_{17}\text{H}_{26}\text{N}_3\text{O}_3\text{S}_2]^+$ ($\text{M} + \text{H}^+$) requires m/z = 384.1411, found 384.1411.



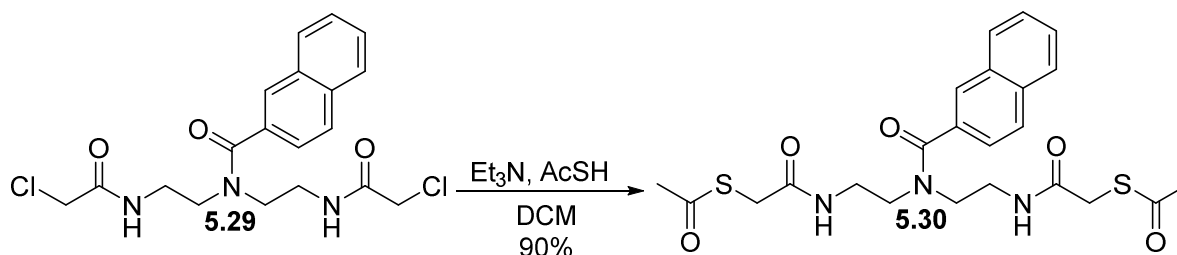
Compound **5.12** (0.203 g, 0.669 mmol) was placed in a flame-dried round-bottom flask and dissolved in 10 mL of anhydrous dichloromethane, and cooled to 0 °C in an ice bath under an atmosphere of N₂(g). Triethylamine (0.28 mL, 2.01 mmol) and 2-naphthoyl chloride (0.153 g, 0.803 mmol) were then added and the reaction mixture was stirred at 0 °C for 1 h and at room temperature for another 2 h. The reaction mixture was then concentrated under reduced pressure, and the product was purified by column chromatography (silica, 50 % EtOAc v/v in hexanes), yielding **5.28** as a white solid (0.251 g, 82%).

¹H NMR (400 MHz, CDCl₃) δ = 7.90–7.87 (m, 1H), 7.85–7.82 (m, 3H), 7.53–7.49 (m, 2H), 7.47–7.47 (d, *J* = 8.5 Hz, 1H), 5.35 (br, s, 1H), 5.11 (br, s, 1H), 3.73–3.65 (m, 2H), 3.51–3.40 (m, 4H), 3.27–3.19 (m, 2H), 1.45 (s, 9H), 1.39 (s, 9H); ¹³C NMR (100 MHz, CDCl₃) δ = 173.1, 156.6, 155.8, 133.6, 133.5, 132.7, 128.4, 127.8, 127.0, 126.7, 126.5, 124.1, 79.4, 49.9, 45.1, 39.2, 38.8, 28.5, 28.4; HRMS (ESI) calculated for [C₂₅H₃₆N₃O₅]⁺ (M + H⁺) requires *m/z* = 458.2650, found 458.2642.



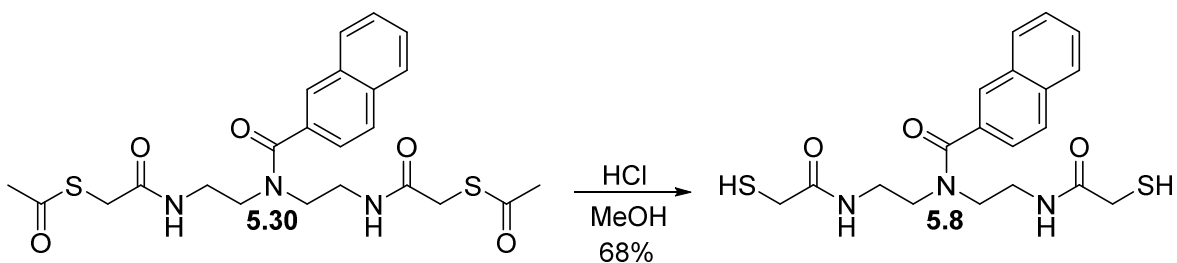
15 mL of 4 M HCl in dioxane was added to a round-bottom flask containing **5.28** (0.251 g, 0.549 mmol). The resulting solution was stirred overnight and then concentrated under reduced pressure. The product was then partially dissolved in 20 mL of dichloromethane, and the resulting slurry was cooled to 0 °C in an ice bath, and placed under an atmosphere of N₂(g). Triethylamine (0.46 mL, 3.28 mmol) and chloroacetic anhydride (0.235 g, 1.373 mmol) were then added and the reaction mixture was stirred for 30 min before being quenched by the addition of 20 mL of saturated NaHCO₃(aq). The organic layer was extracted out and washed with water (2 x 20 mL). The organic extract was then dried with anhydrous MgSO₄(s), filtered, and concentrated under reduced pressure, and the product was purified by column chromatography (silica, 10% v/v methanol in dichloromethane), yielding **5.29** as a colorless oil (0.171 g, 76%).

¹H NMR (400 MHz, CDCl₃) δ = 7.91–7.86 (m, 4H), 7.58–7.53 (m, 2H), 7.45–7.43 (m, 2H), 6.90 (br, s, 1H), 4.06–3.43 (m, 12H); **¹³C NMR (100 MHz, CDCl₃)** δ = 173.4, 167.1, 166.5, 133.6, 133.0, 132.7, 128.8, 128.4, 128.0, 127.4, 127.1, 126.5, 123.7, 49.0, 44.7, 42.6, 38.8, 38.4; **HRMS (ESI)** calculated for [C₁₉H₂₂Cl₂N₃O₃]⁺ (M + H⁺) requires m/z = 410.1033, found 410.1033.



A round-bottom flask was charged with **5.29** (0.171 g, 0.417 mmol), dissolved with 5 mL of dichloromethane, and placed under an atmosphere of N₂(g). Triethylamine (0.29 mL, 2.08 mmol) and thioacetic acid (0.1 mL, 1.40 mmol) were then added, and the reaction mixture was stirred overnight. After 24 h, the reaction mixture was concentrated under reduced pressure, and the product was purified by column chromatography (silica, 10% v/v methanol in dichloromethane) providing **5.30** as a yellow solid (0.184 g, 90%).

¹H NMR (400 MHz, CDCl₃) δ = 7.87–7.82 (m, 4H), 7.53–7.49 (m, 2H), 7.44 (d, *J* = 8.4 Hz, 1H), 7.35 (br, s, 1H), 7.10 (br, s, 1H), 3.69–3.28 (m, 12H), 2.30 (s, 6H); ¹³C NMR (100 MHz, CDCl₃) δ = 195.5, 173.3, 168.9, 168.4, 133.5, 133.1, 132.6, 128.5, 127.9, 127.2, 126.9, 126.5, 123.9, 49.3, 44.8, 39.2, 38.5, 32.9, 30.3; HRMS (ESI) calculated for [C₂₃H₂₈N₃O₅S₂]⁺ (M + H⁺) requires *m/z* = 490.1465, found 490.1464.



A flame-dried round-bottom flask was charged with **5.30** (0.184 g, 0.376 mmol) and placed under an atmosphere of N₂(g). Six mL of anhydrous methanol followed by 3 mL of 3 N HCl in methanol were then added, and the reaction mixture was stirred under N₂(g) overnight. After 24 h, the reaction mixture was concentrated under reduced pressure, and the product was purified by reverse-phase HPLC using a preparatory C18 column and a linear gradient of 10–

80% v/v acetonitrile (0.1% v/v TFA) in water (0.1% v/v TFA) over 45 min. Dithiol **5.8** eluted at 32 min and, after lyophilization, was isolated as a white solid (103.69 mg, 68%).

¹H NMR (400 MHz, DMSO-*d*₆) δ = 8.29 (t, J = 5.7 Hz, 1H), 8.06 (t, J = 5.7 Hz, 1H), 7.97–7.93 (m, 4H), 7.59–7.55 (m, 2H), 7.50 (dd, J = 8.5, 1.6 Hz, 1H), 3.59–3.57 (m, 2H), 3.43–3.34 (m, 4H), 3.16 (m, 4H), 3.00 (d, J = 8.0 Hz, 2H), 2.80 (t, J = 8.0 Hz, 1H), 2.66 (t, J = 8.0 Hz, 1H); **¹³C NMR (100 MHz, DMSO-*d*₆)** δ = 171.1, 170.0, 169.7, 134.3, 132.9, 132.3, 128.3, 128.0, 127.8, 126.9, 126.7, 125.9, 124.5, 48.5, 44.2, 37.3, 36.8, 27.3, 27.1; **HRMS (ESI)** calculated for [C₁₉H₂₄N₃O₃S₂]⁺ (M + H⁺) requires m/z = 406.1254, found 406.1256.

5.7.3 Determination of thiol p*K*_a Values

The thiol p*K*_a values for **5.2**, **5.5**, and **5.7** were determined by following closely a procedure reported previously that exploits the elevated absorbance of the deprotonated thiolate at 238 nm.^{42,116,129} A plot of A_{238} vs pH was recorded (Figure 5.4), and p*K*_a values were determined by fitting these data to eq 5.1, which was derived from Beer's law and the definition of the acid dissociation constant.

$$A_{238} = C_T \left(\frac{\epsilon_{S^-} 10^{(\text{pH}-\text{p}K_{a2})} + \epsilon_{SH^-} + \epsilon_{SH}^{SH} 10^{(\text{p}K_{a1}-\text{pH})}}{10^{(\text{pH}-\text{p}K_{a2})} + 1 + 10^{(\text{p}K_{a1}-\text{pH})}} \right) \quad (5.1)$$

In eq 5.1, C_T is the total thiol concentration, ϵ_{SH}^{SH} is the extinction coefficient of the doubly protonated form of **5.2**, **5.5**, or **5.7**, ϵ_{SH^-} is the extinction coefficient of the singly protonated form of **5.2**, **5.5**, or **5.7**, and ϵ_{S^-} is the extinction coefficient of the doubly deprotonated form of **5.2**, **5.5**, or **5.7**.

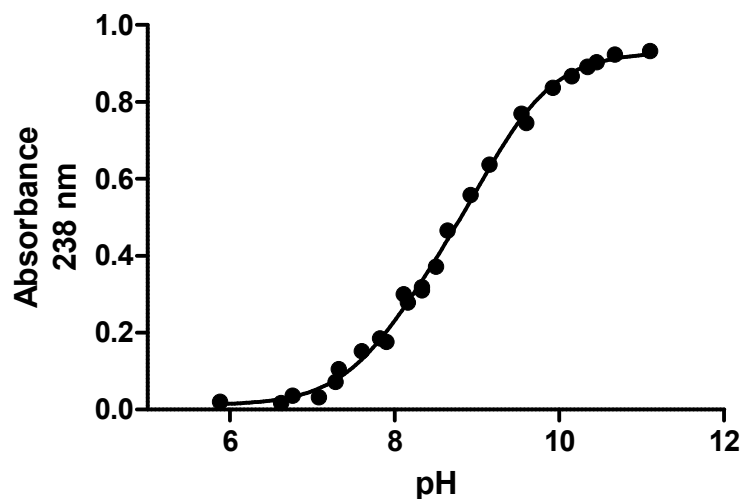


Figure 5.5 Effect of pH on absorbance by **5.2** at 238 nm in 0.10 M potassium phosphate buffer. pK_a values of 8.0 ± 0.2 and 9.2 ± 0.1 , and extinction coefficients of $\epsilon_{SH}^{SH} = 9.20$, $\epsilon_{SH}^{S-} = 3996$, $\epsilon_{S-}^{S-} = 9296 \text{ M}^{-1}\text{cm}^{-1}$ with $r^2 > 0.99$ were determined by fitting the data to eq 5.1.

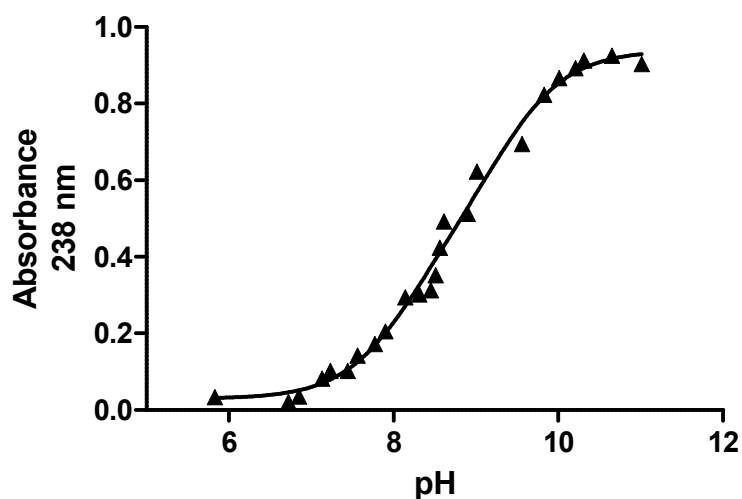


Figure 5.6 Effect of pH on absorbance by **5.5** at 238 nm in 0.10 M potassium phosphate buffer. pK_a values of 8.1 ± 0.3 and 9.3 ± 0.3 , and extinction coefficients of $\epsilon_{SH}^{SH} = 10.23$, $\epsilon_{SH}^{S-} = 4610$, $\epsilon_{S-}^{S-} = 9386 \text{ M}^{-1}\text{cm}^{-1}$ with $r^2 > 0.99$ were determined by fitting the data to eq 5.1.

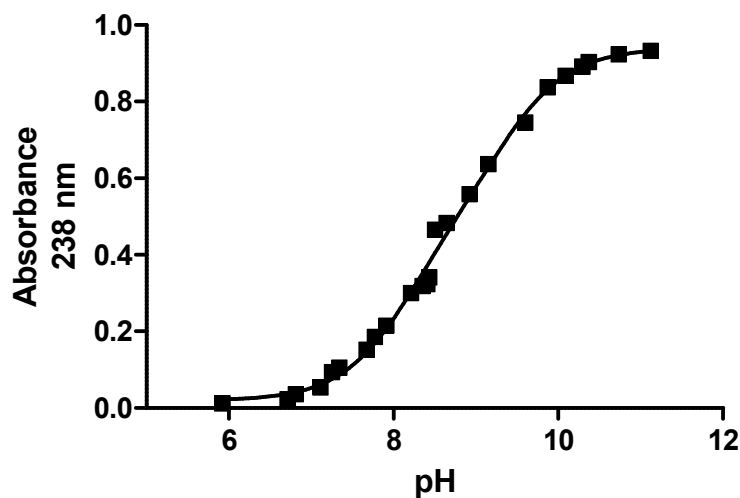


Figure 5.7 Effect of pH on absorbance by **5.7** at 238 nm in 0.10 M potassium phosphate buffer. pK_a values of 8.1 ± 0.2 and 9.4 ± 0.2 , and extinction coefficients of $\epsilon_{SH}^{SH} = 8.13$, $\epsilon_{SH}^{S-} = 4940$, $\epsilon_{S-}^{S-} = 9390 \text{ M}^{-1}\text{cm}^{-1}$ with $r^2 > 0.99$ were determined by fitting the data to eq 5.1.

5.7.4 Determination of reduction potential

The reduction potentials of BMC, **5.2**, **5.5** and **5.7** were determined as described previously.^{29,116} Briefly, an equilibrium was established between reduced BMC (or **5.2**, or **5.5**, or **5.7**) and $\beta\text{ME}^{\text{ox}}$ and analyzed with analytical HPLC. The equilibrium concentrations were determined by integration of the peaks corresponding to βME and $\beta\text{ME}^{\text{ox}}$. From these concentrations, the K_{eq} for the reaction was determined and the reduction potential of BMC (or **5.2**, or **5.5**, or **5.7**) was then calculated using the Nernst equation and $E_{\beta\text{ME}^{\text{oxo}'}} = -0.260 \text{ V}$. The values reported are the mean ($\pm\text{SE}$) of three separate measurements for each compound

5.7.5 Assay for isomerase activity

sRNase was prepared as described previously.¹⁸⁷ The activation of sRNase A in the presence of refolding catalysts was determined as described previously. Refolding reactions were performed at 30 °C in 50 mM Tris–HCl buffer (pH 7.6), containing GSH (1.0 mM), GSSG (0.2 mM), and catalyst (1 mM). Catalysts were delivered from 100-fold concentrated stock solutions in DMSO. The reactions were initiated by the addition of sRNase A to a final concentration of 5 µg/mL. Reaction progress was monitored by quantifying the cleavage of the RNase A substrate 6-FAM–dArUdAdA–6-TAMRA at 493 nm/515 nm, as described previously.¹⁸¹ Assays were performed in triplicate at ambient temperature in a black polystyrene 96-well plate, in 200 µL of 0.10 M MES-NaOH buffer, pH 6.0, containing NaCl (0.10 M). The resulting fluorescence data were fitted to the equation $k_{\text{cat}}/K_M = (\Delta I/\Delta t)/(I_f - I_0)[E]$, in which $\Delta I/\Delta t$ is the initial reaction velocity, I_0 is the fluorescence intensity before addition of any ribonuclease, I_f is the fluorescence intensity after complete substrate hydrolysis, and $[E]$ is the total ribonuclease concentration. Reaction progress was monitored every hour until the increase in activity leveled off (~5 h). In Figure 5.4A, data were fitted to eq 5.2.

$$[\text{active RNase A}] = [\text{sRNase A}]_{t=0}(1 - e^{[\text{catalyst}]tk_{\text{obs}}}) \quad (5.2)$$

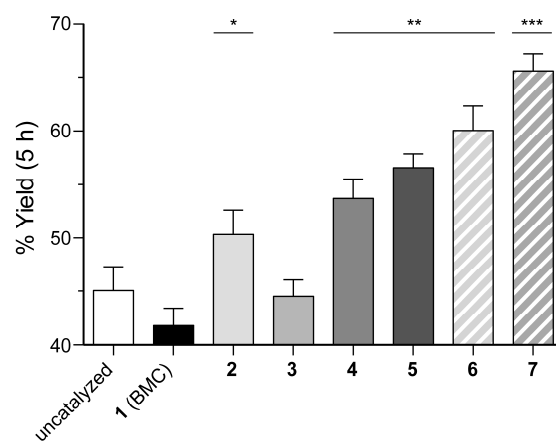
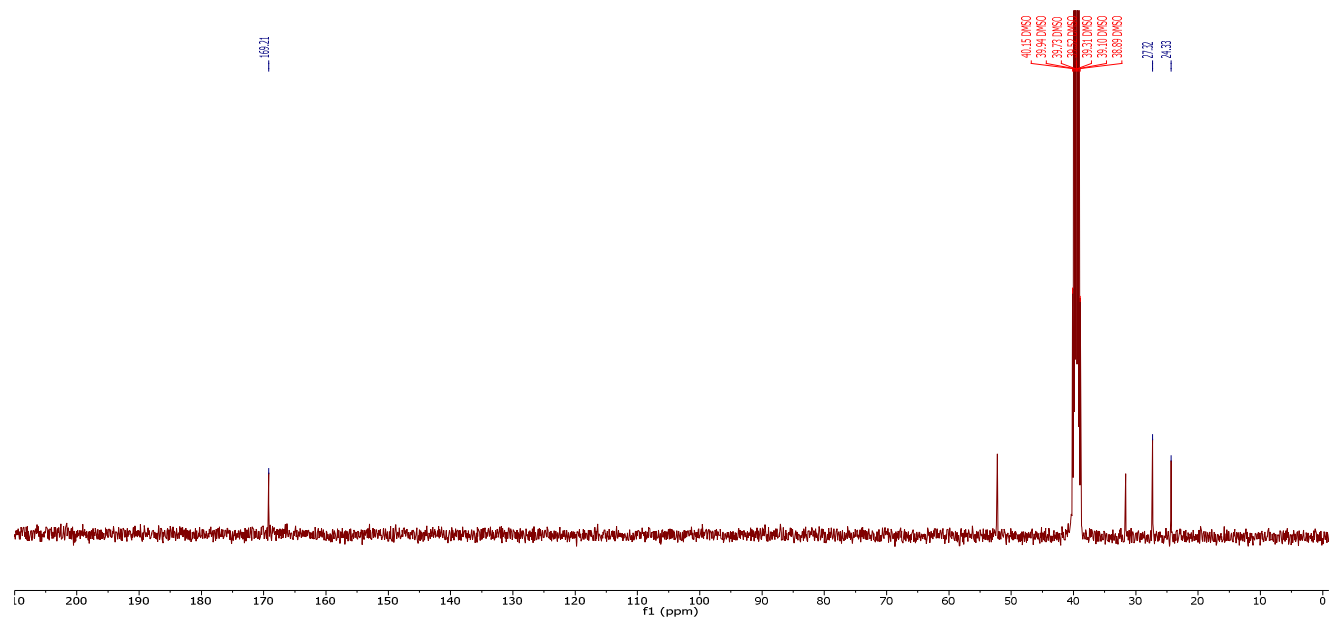
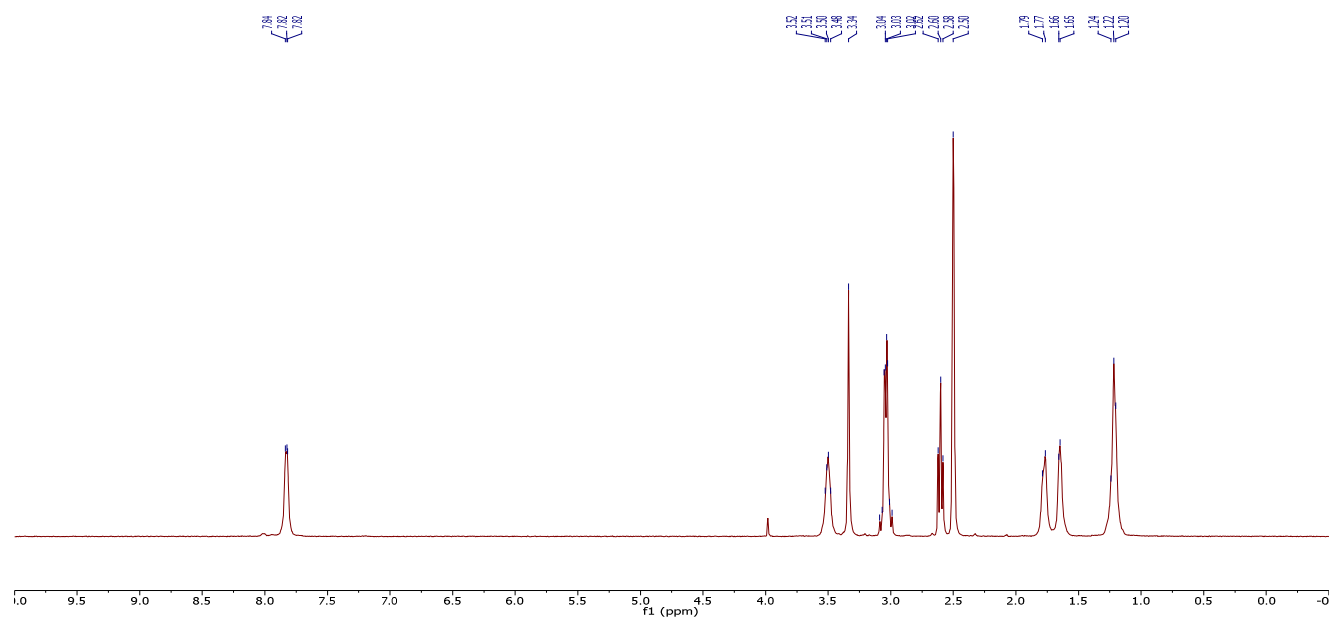


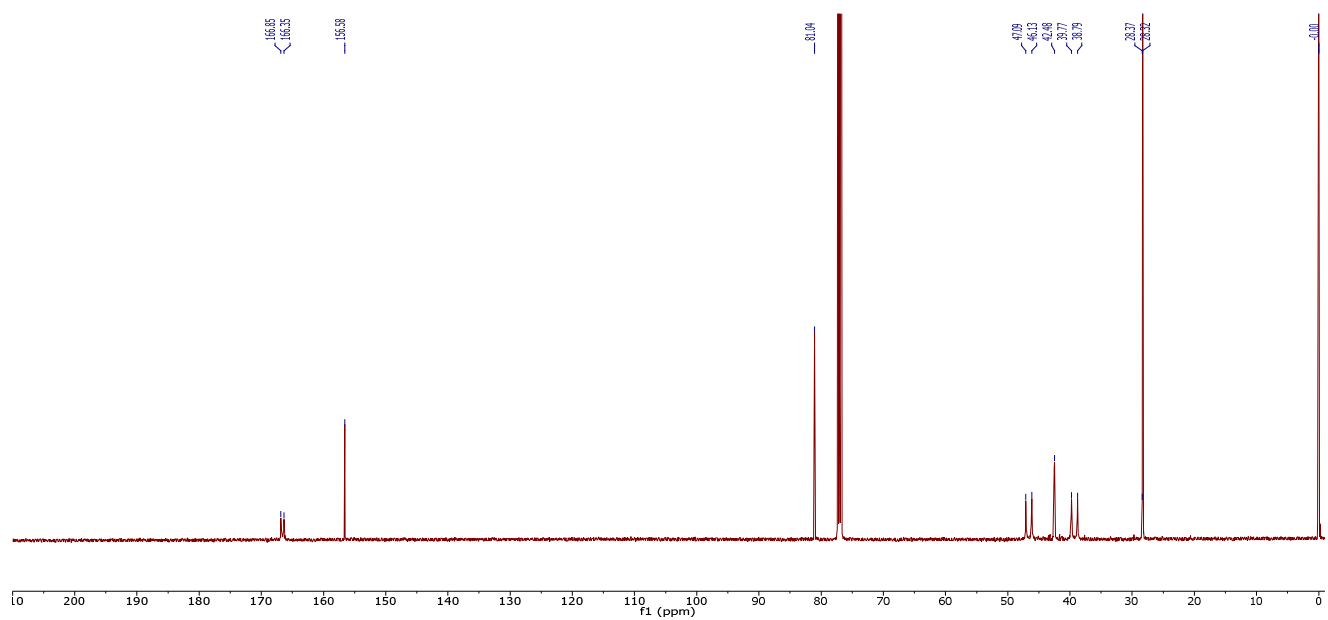
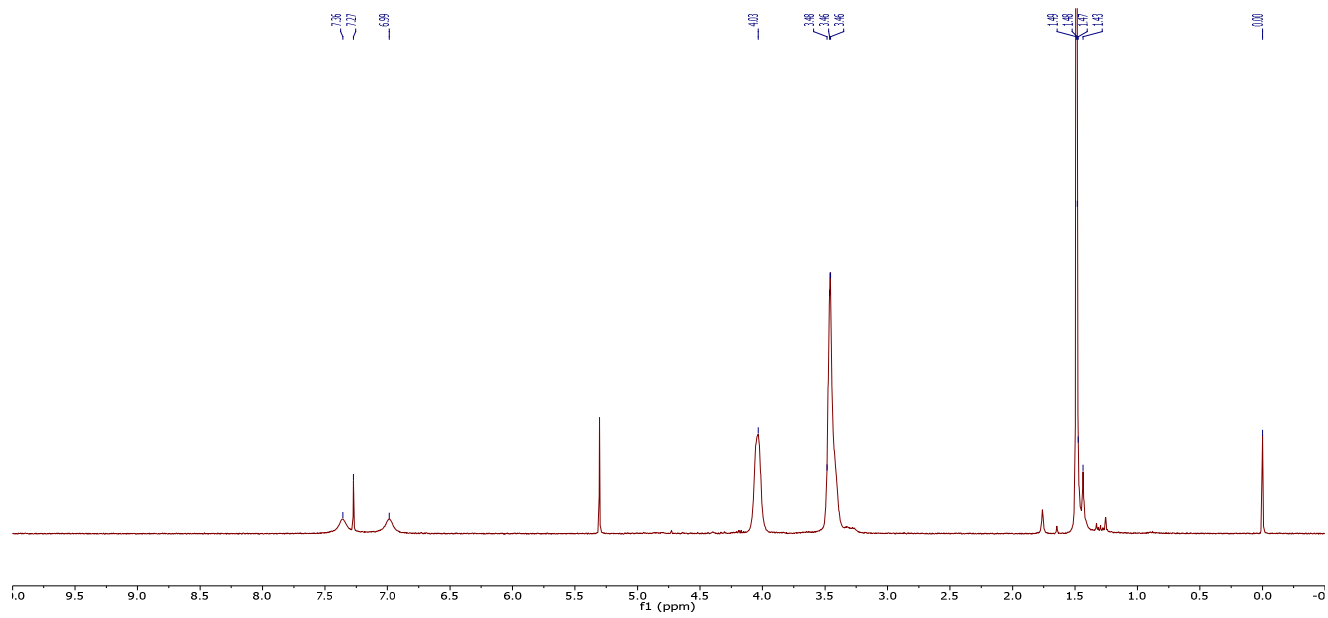
Figure 5.8 Yield of native RNase A achieved by PDI mimics 5.1-5.7 after 5 h (* $p < 0.05$, ** $p < 0.01$, *** $p < 0.005$). Values are listed in Table 5.1.

5.8 NMR Spectra

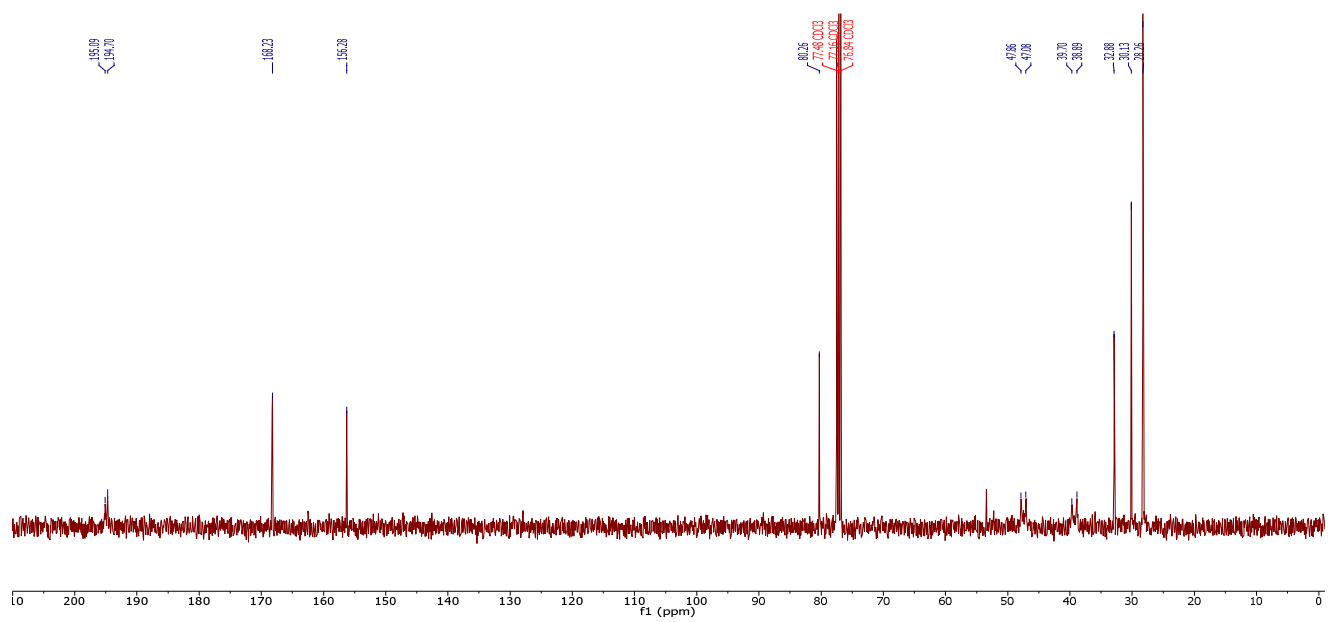
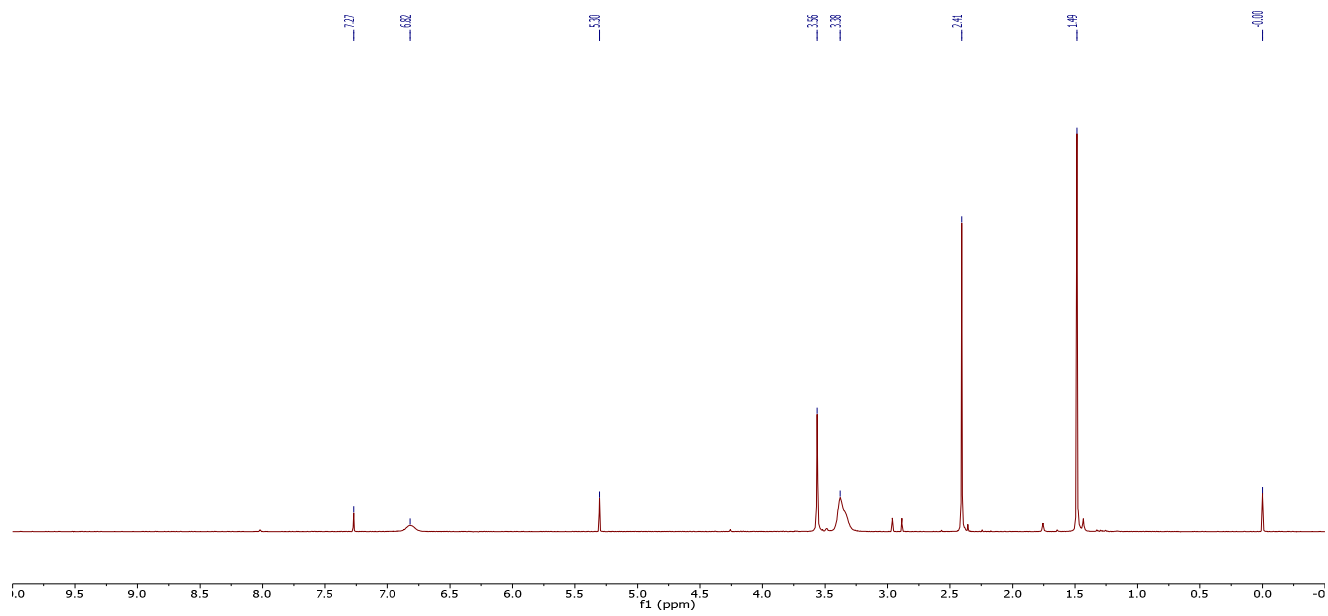
^1H NMR (DMSO- d_6) and ^{13}C NMR (DMSO- d_6) of **5.1** (BMC)

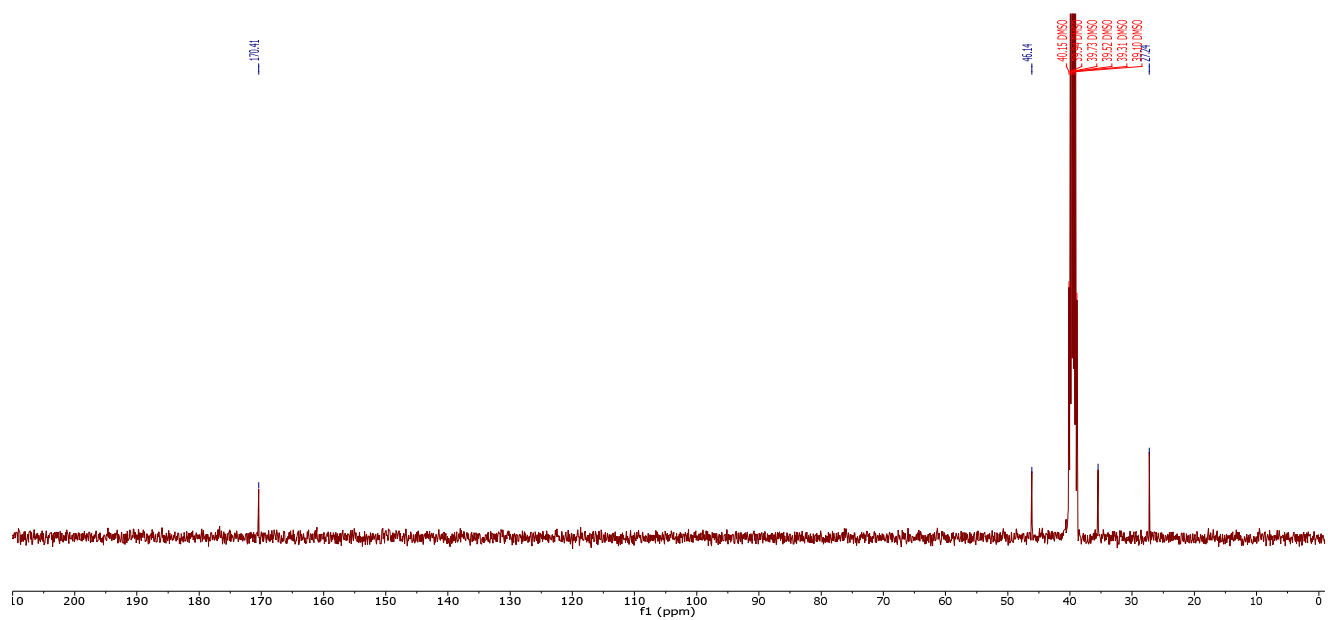
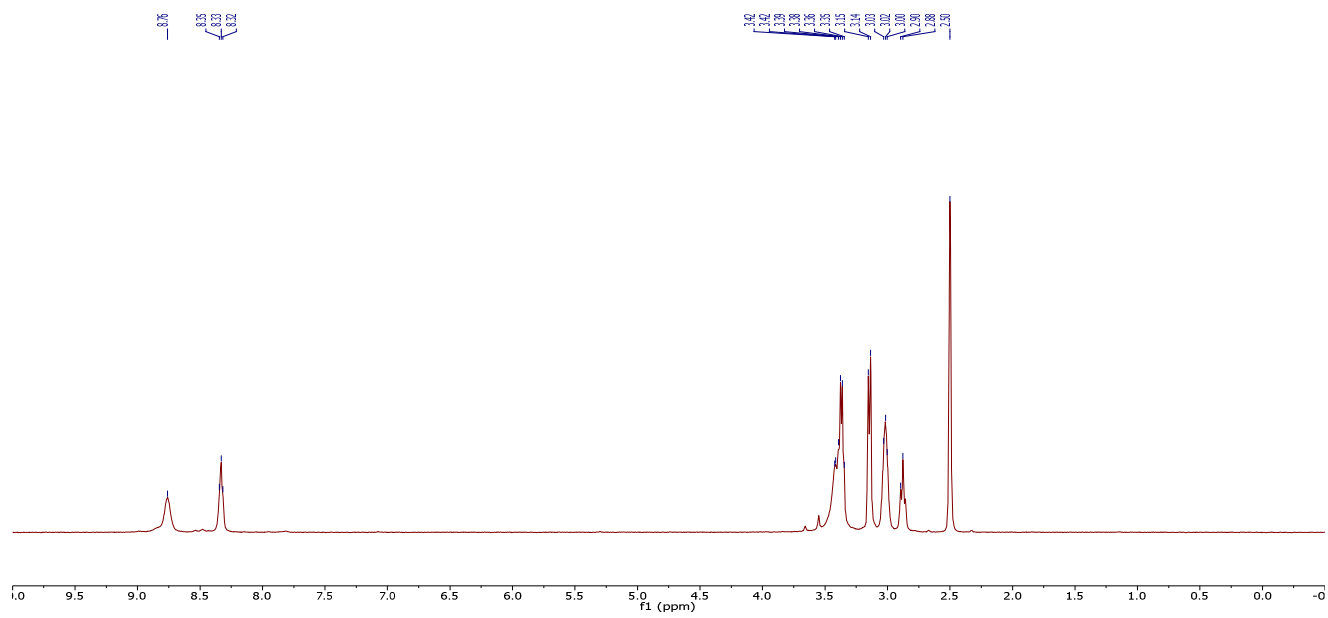


^1H NMR (CDCl_3) and ^{13}C NMR (CDCl_3) of **5.10** in dichloromethane

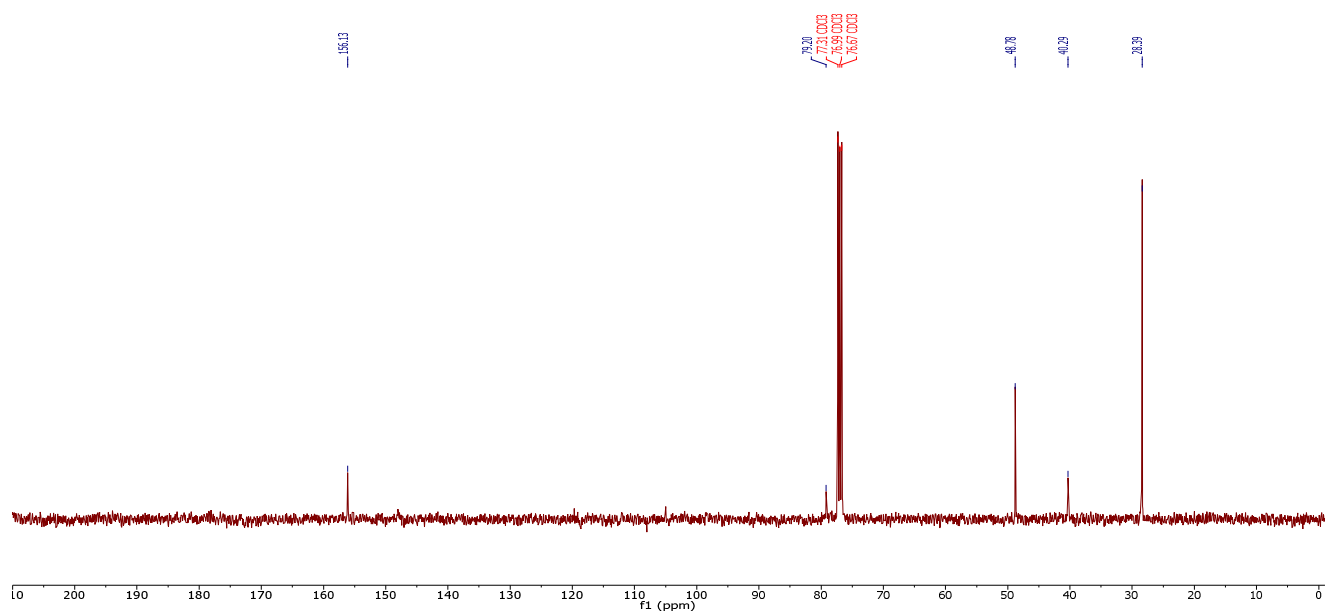
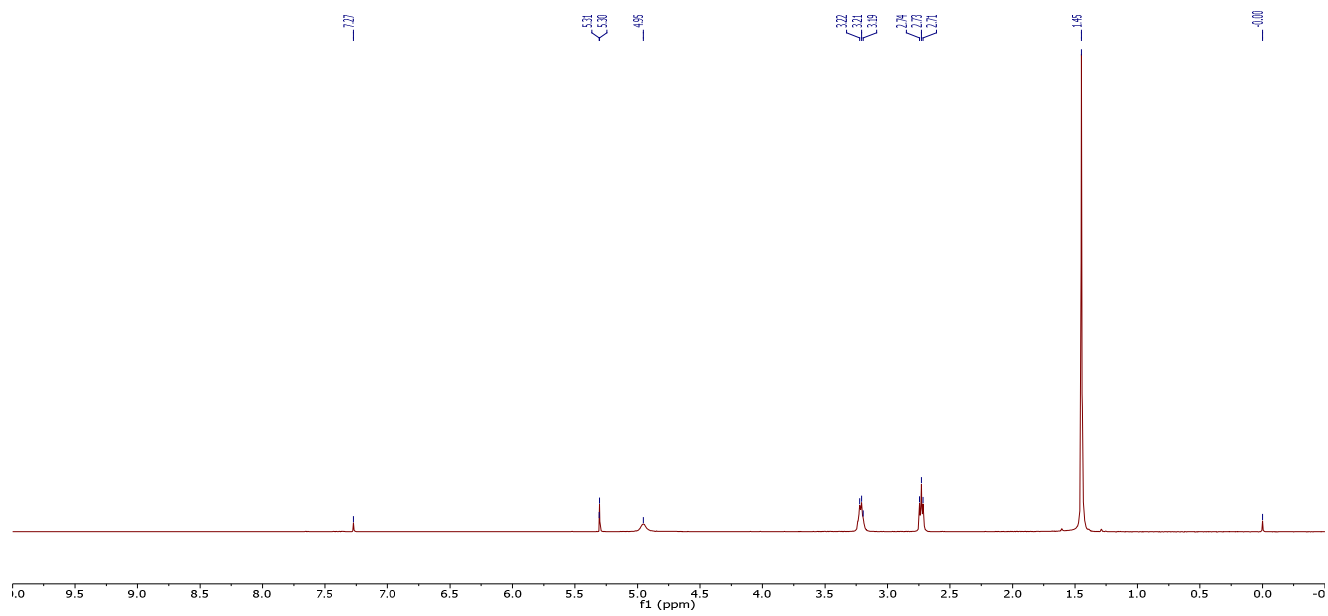


^1H NMR (CDCl_3) and ^{13}C NMR (CDCl_3) of **5.11** in dichloromethane

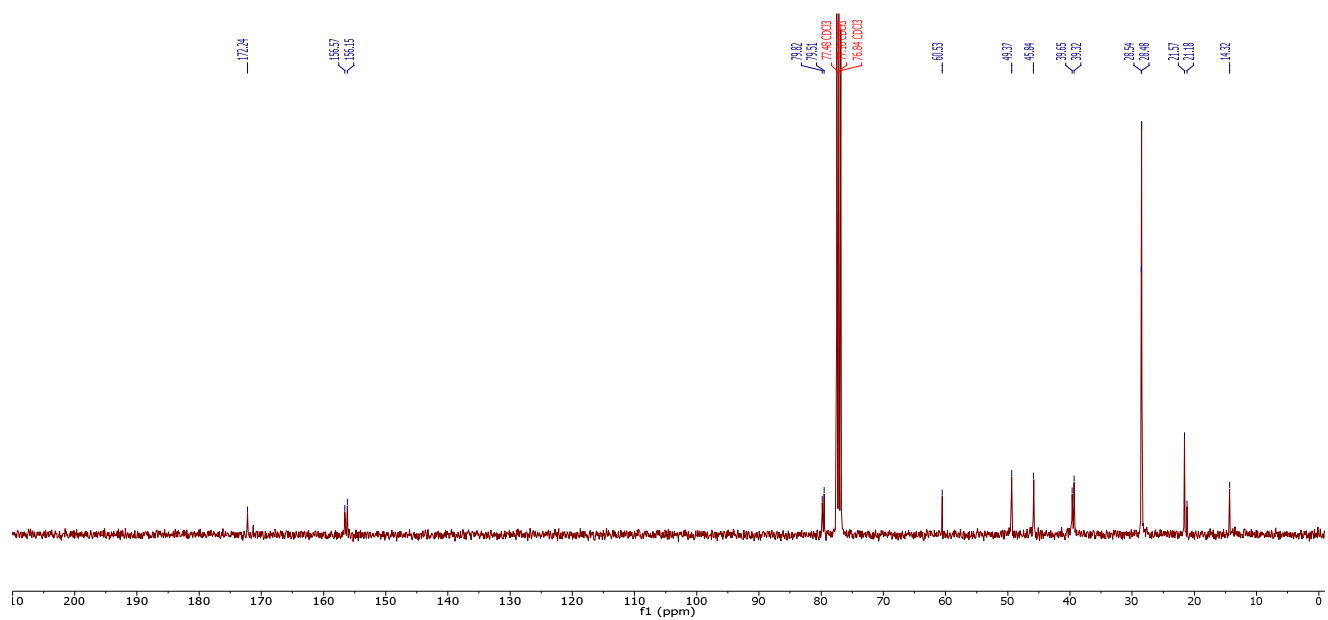
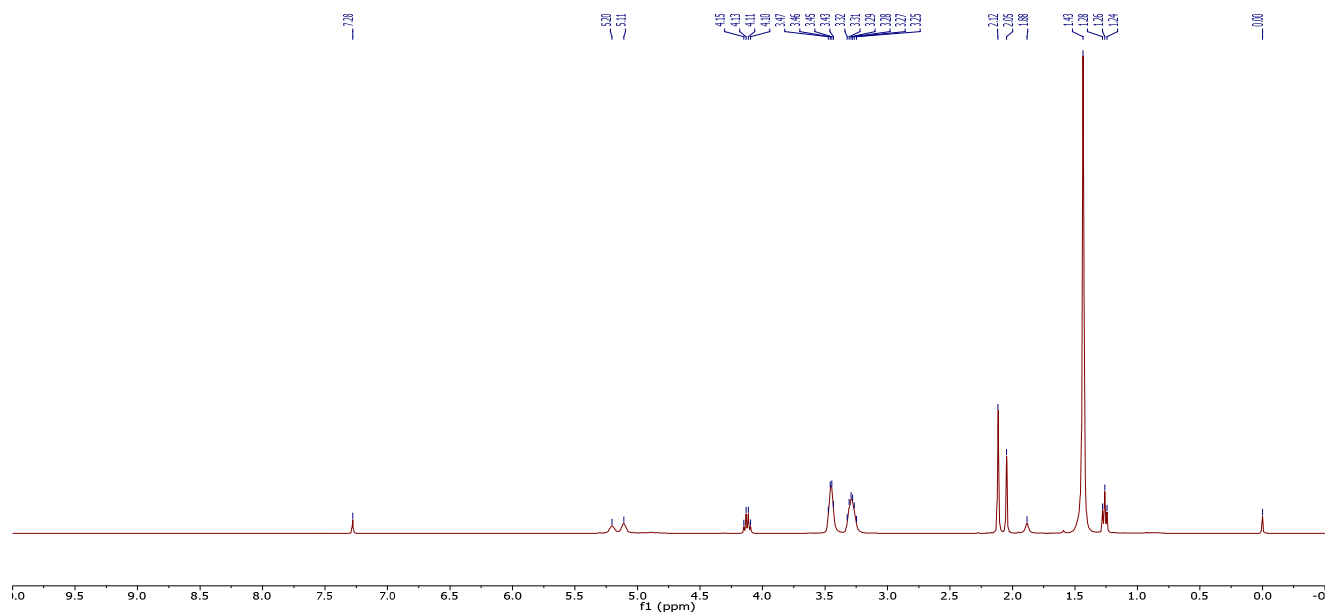


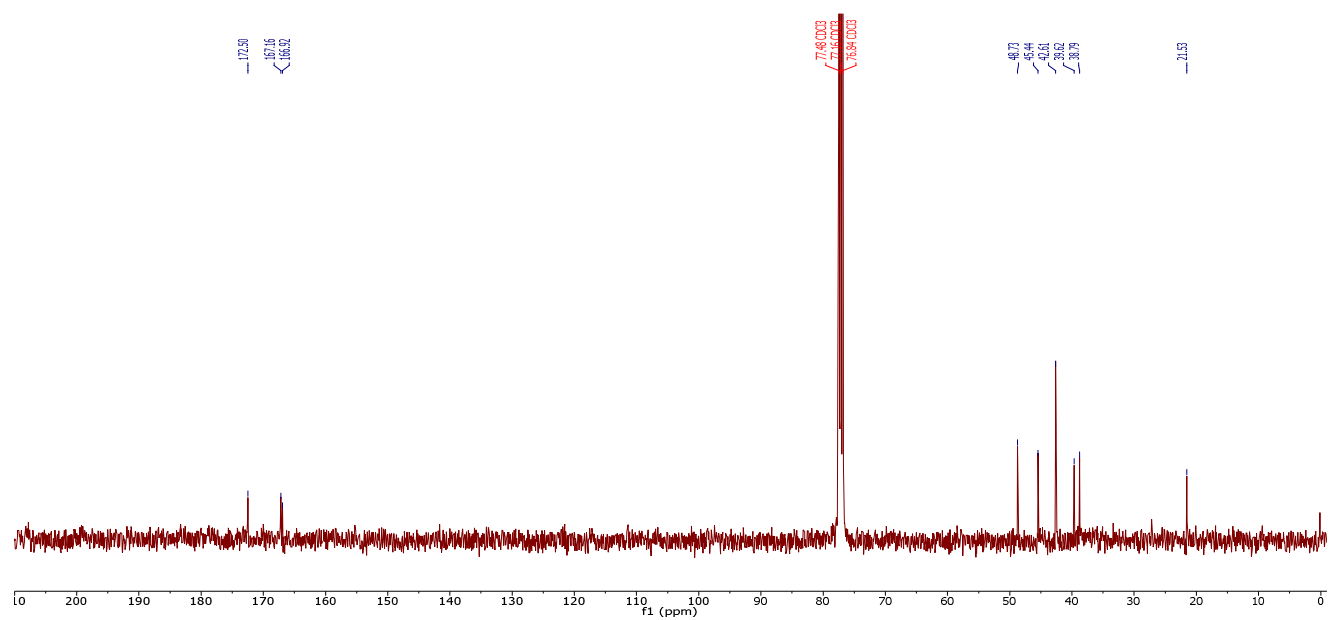
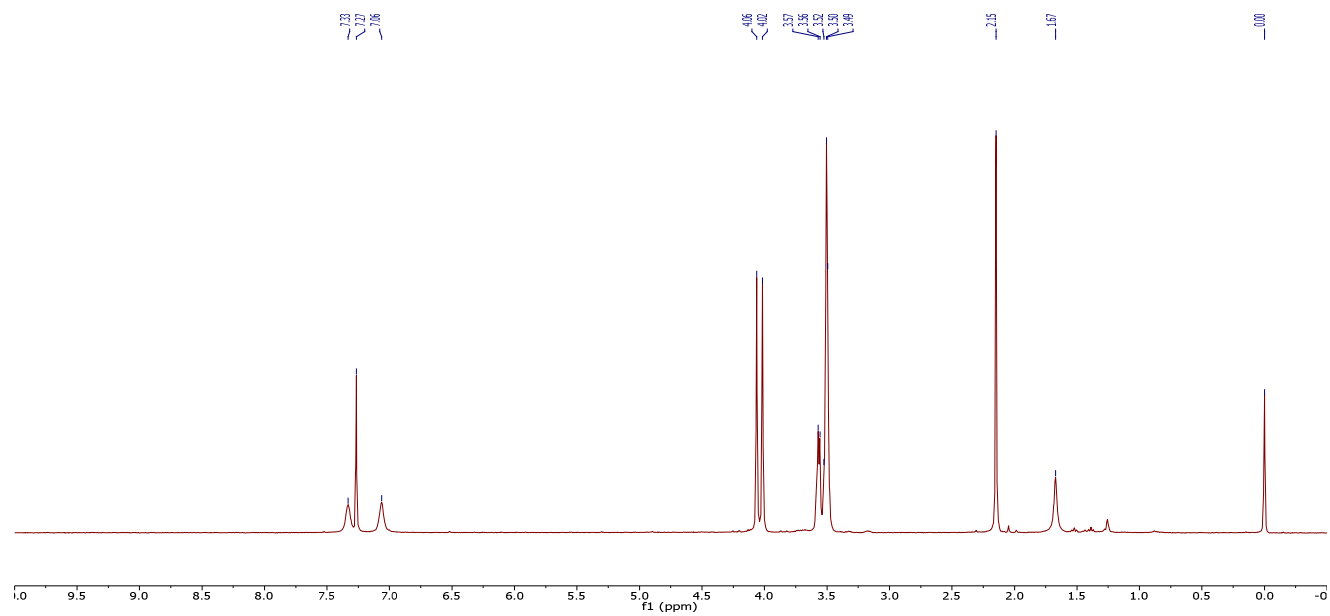
^1H NMR (DMSO- d_6) and ^{13}C NMR (DMSO- d_6) of **5.2**

^1H NMR (CDCl_3) and ^{13}C NMR (CDCl_3) of **5.12** in dichloromethane

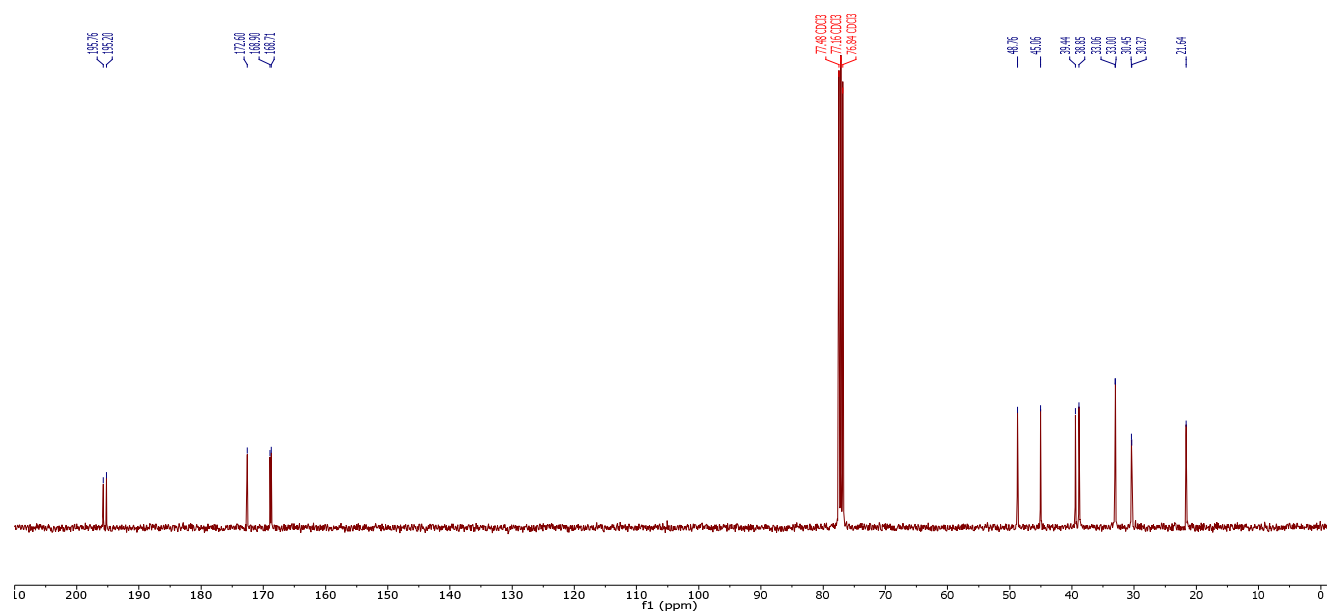
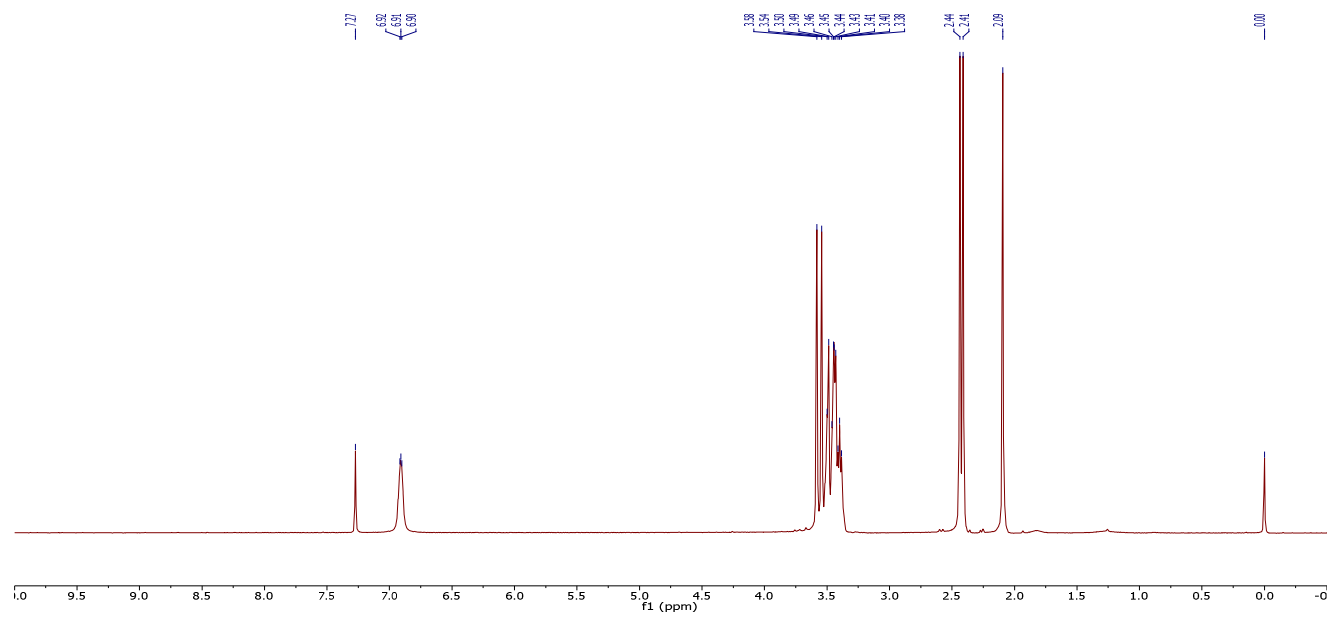


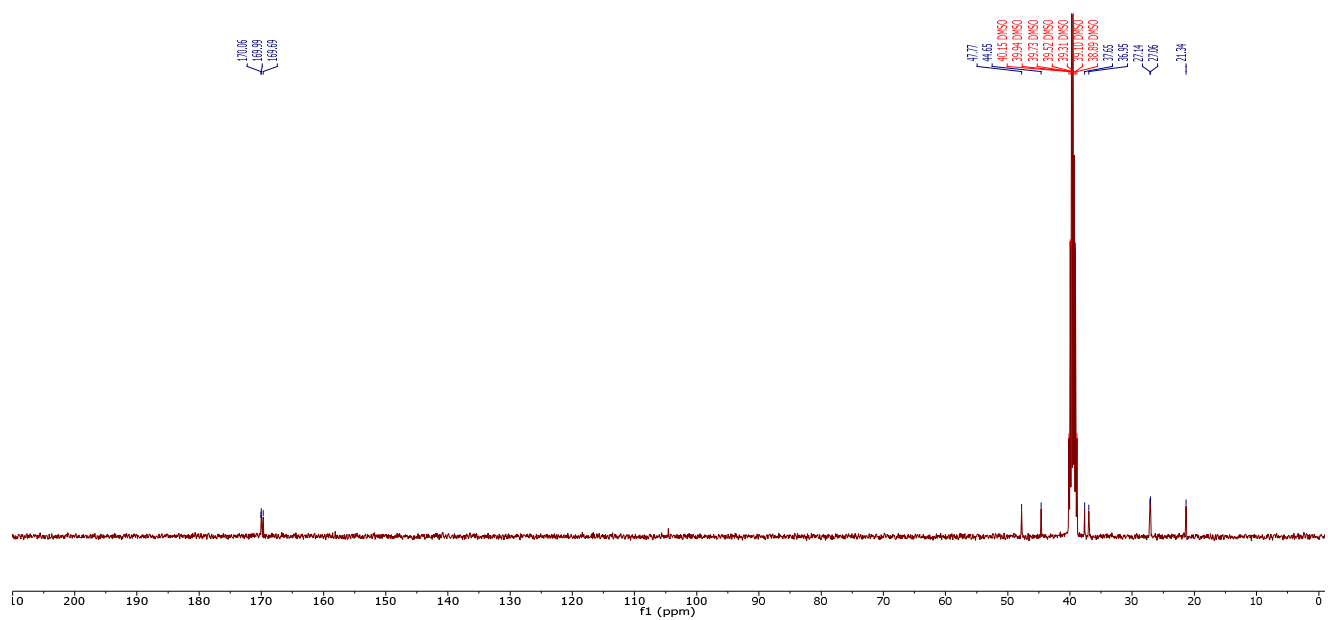
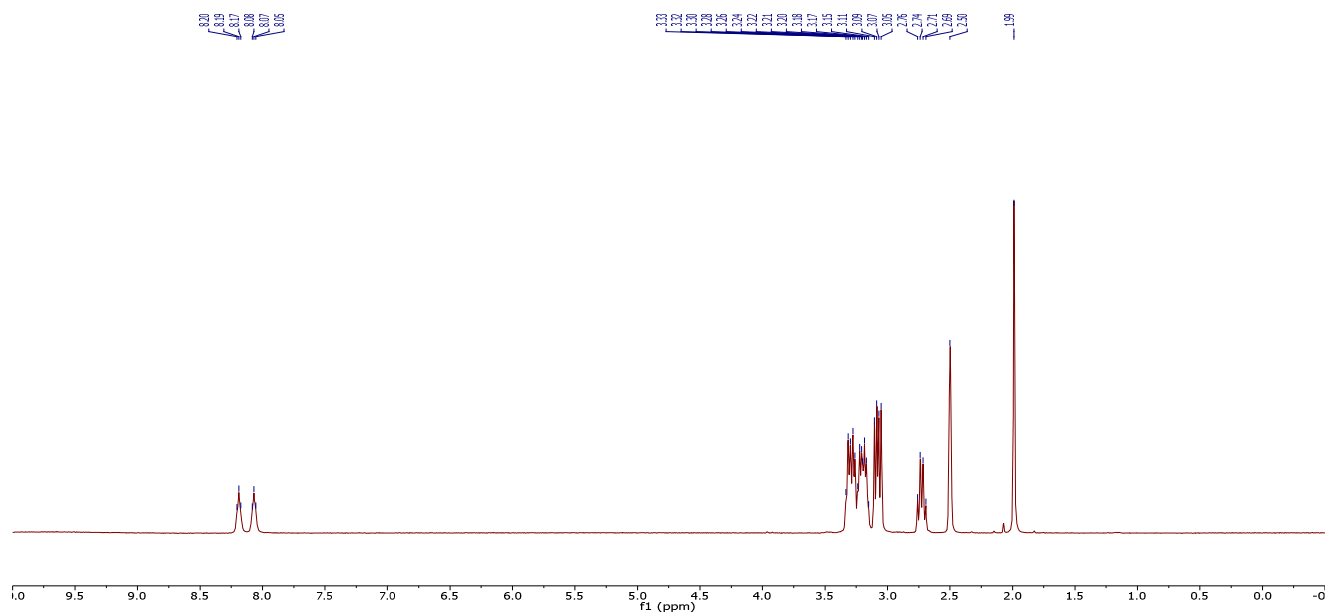
^1H NMR (CDCl_3) and ^{13}C NMR (CDCl_3) of **5.13** in ethyl acetate

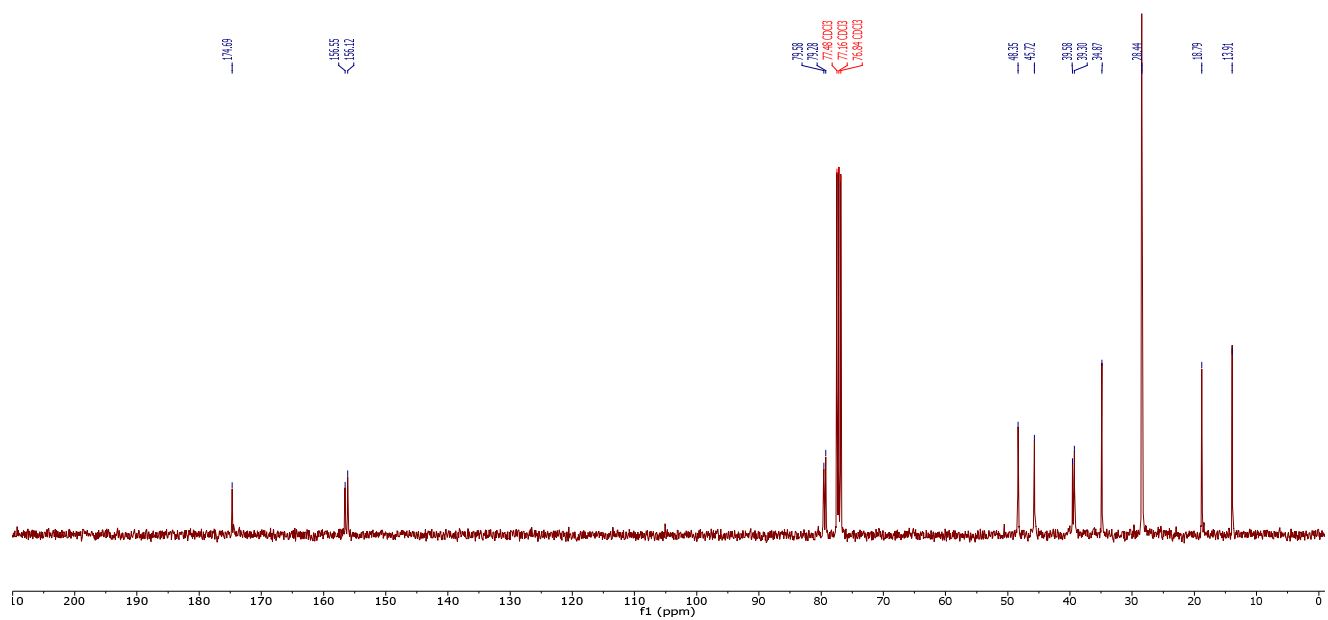
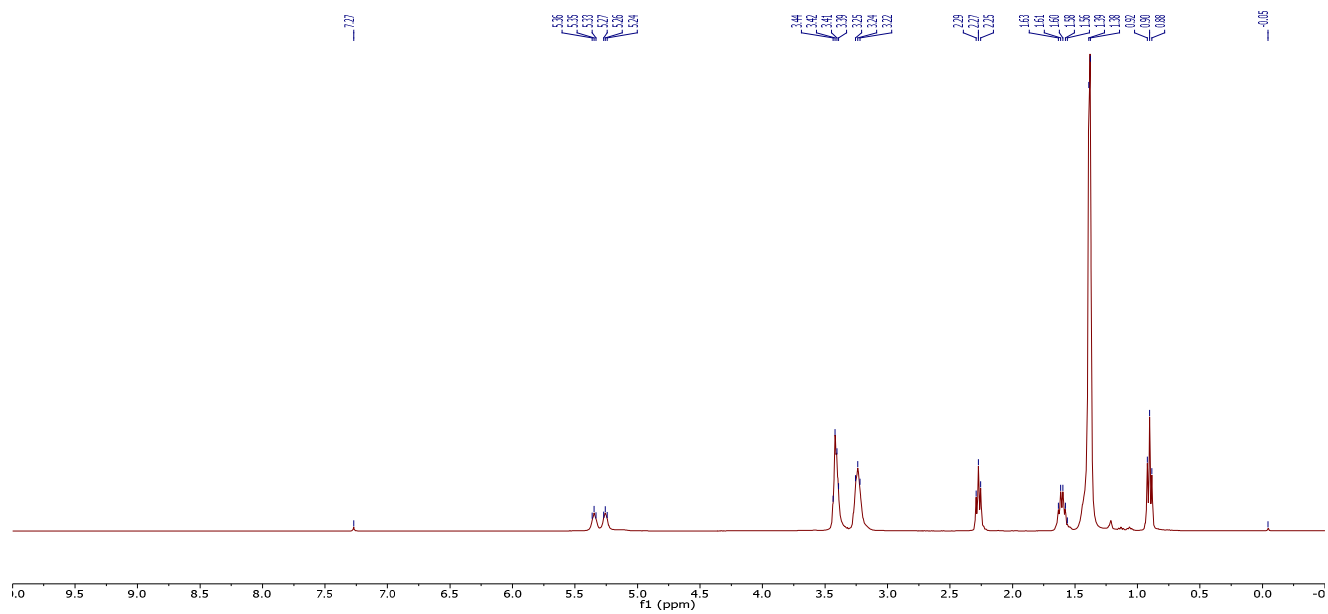


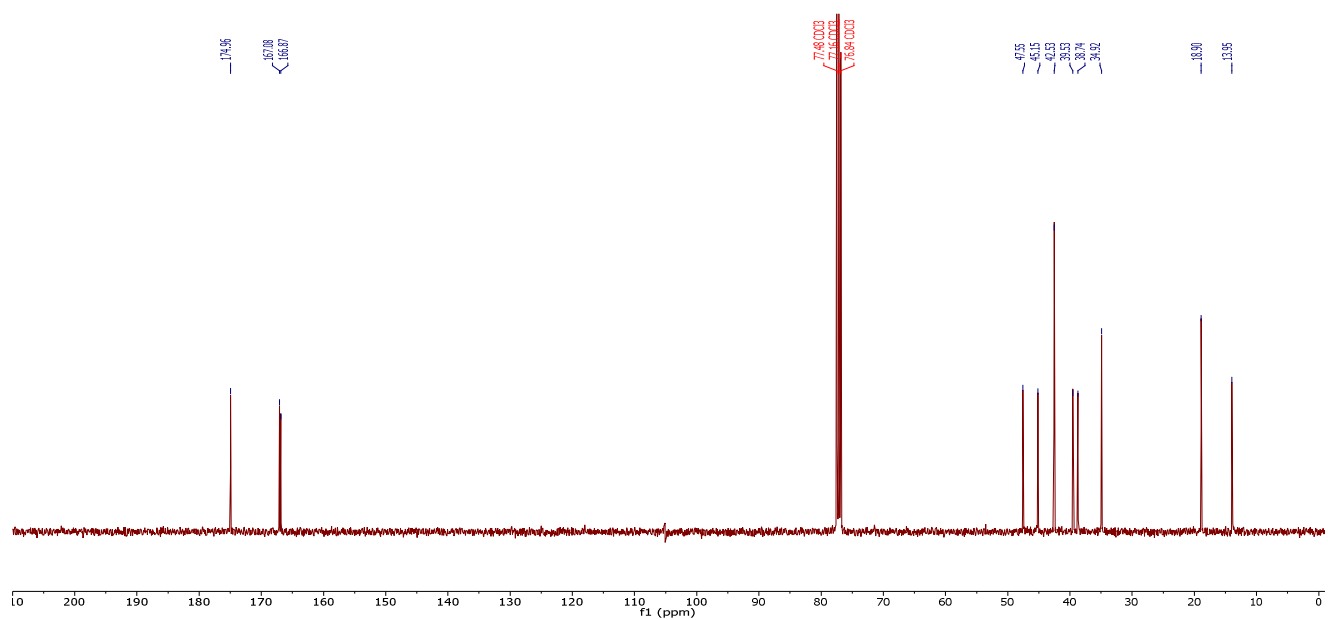
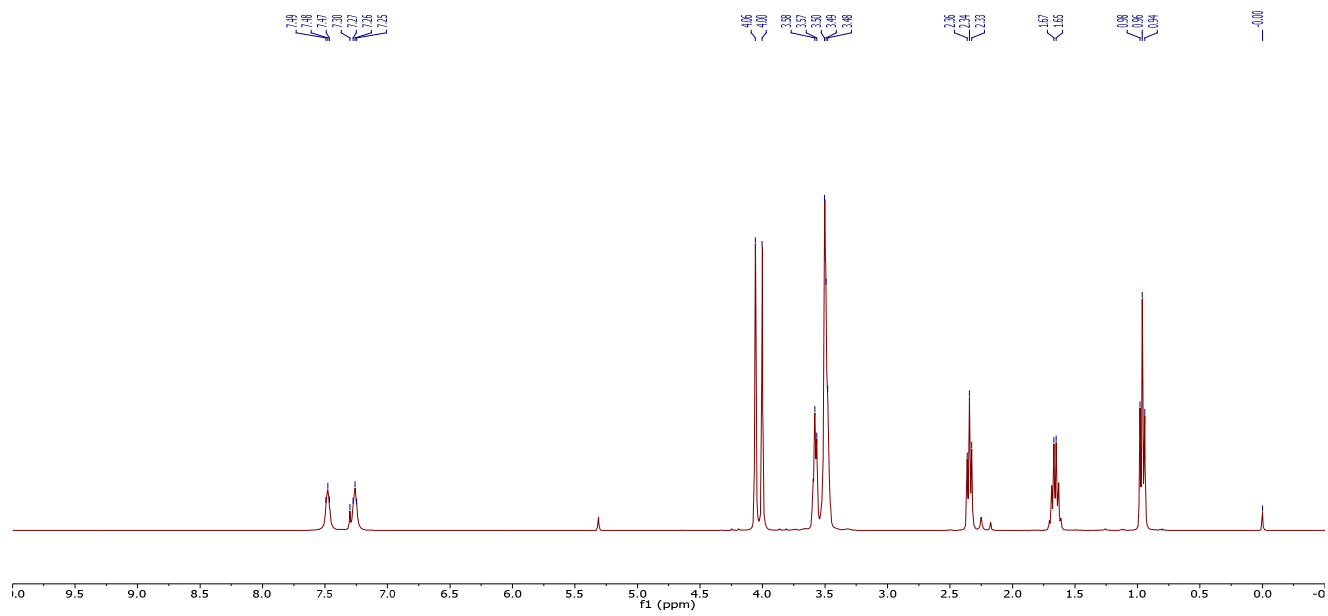
^1H NMR (CDCl_3) and ^{13}C NMR (CDCl_3) of **5.14**

^1H NMR (CDCl_3) and ^{13}C NMR (CDCl_3) of **5.15**

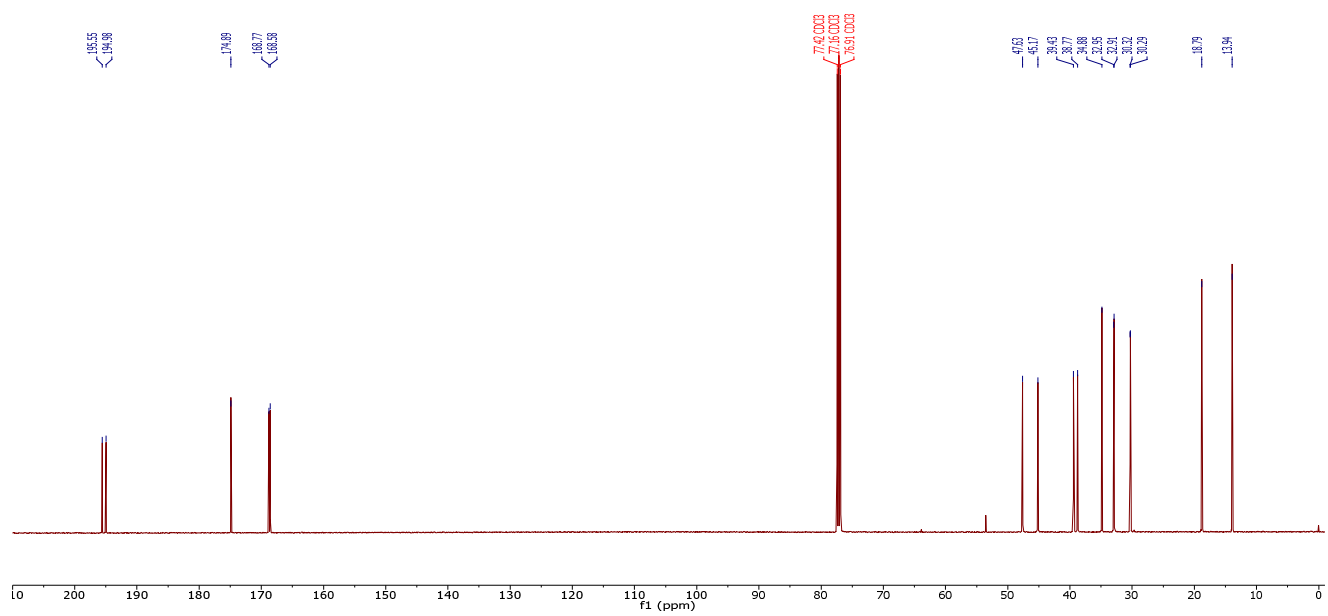
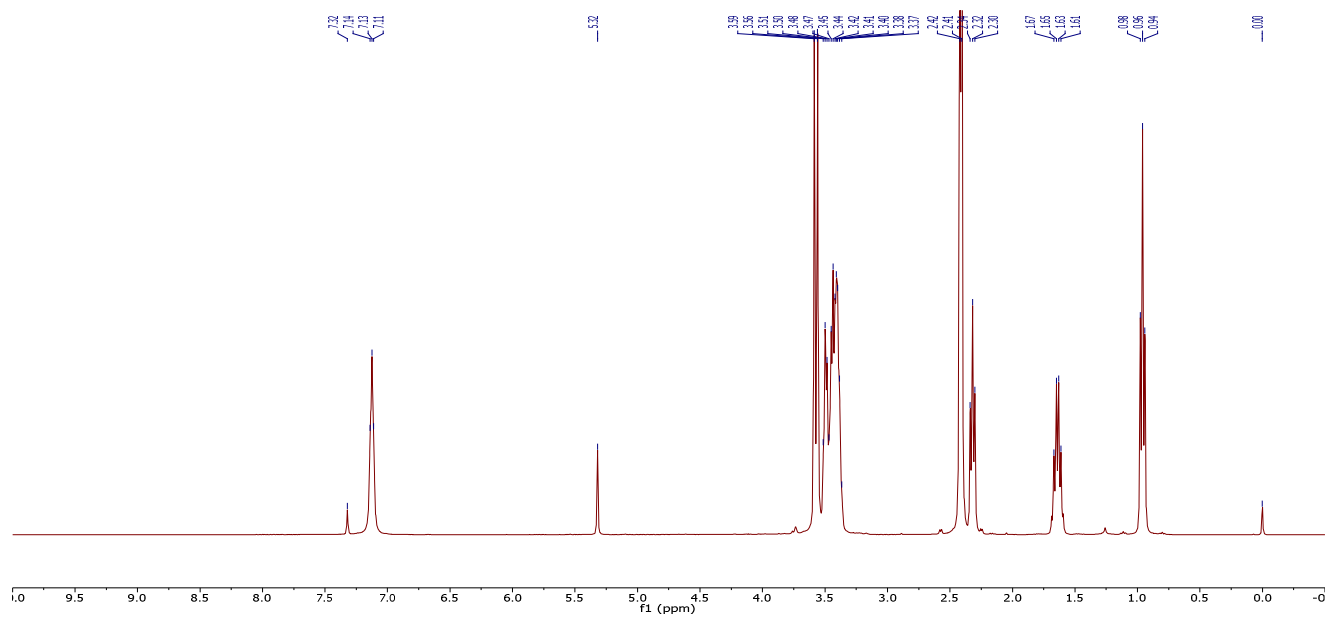


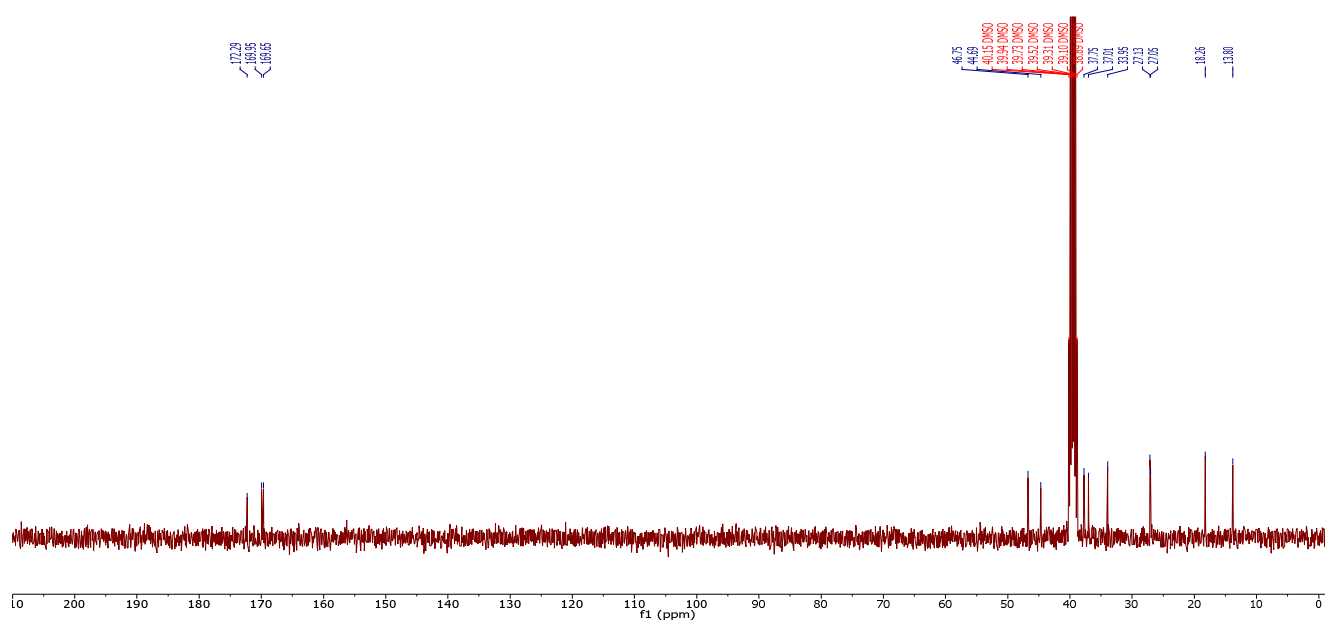
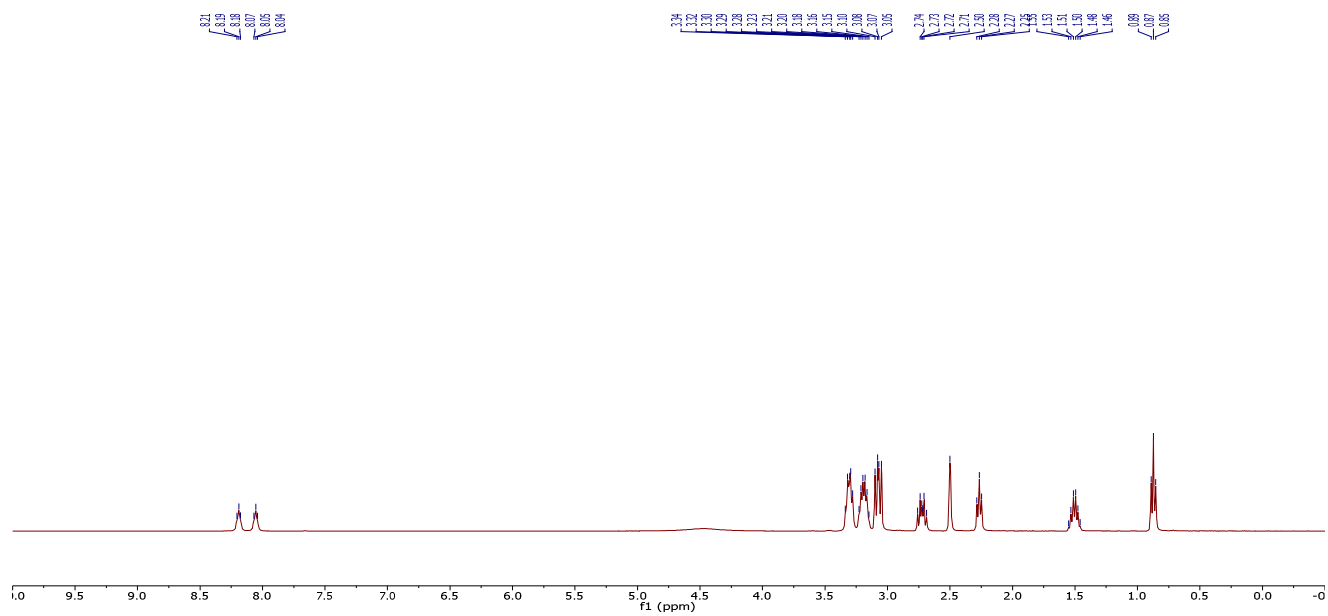
^1H NMR (DMSO- d_6) and ^{13}C NMR (DMSO- d_6) of **5.3**

^1H NMR (CDCl_3) and ^{13}C NMR (CDCl_3) of **5.16**

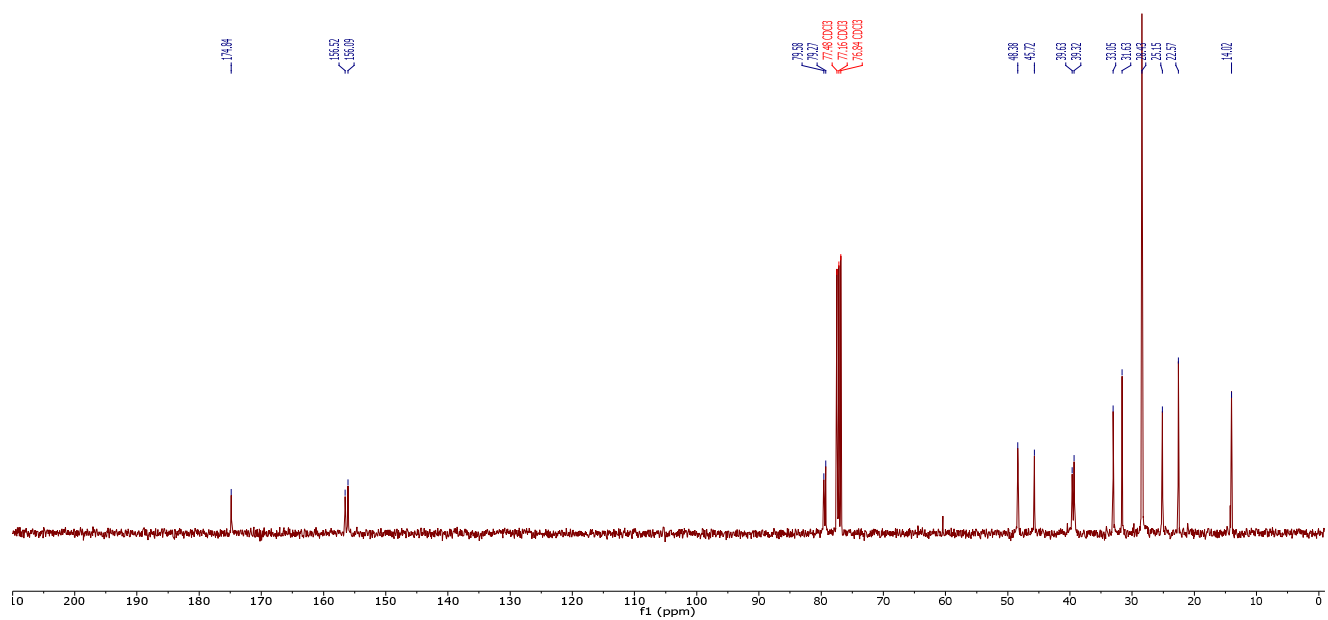
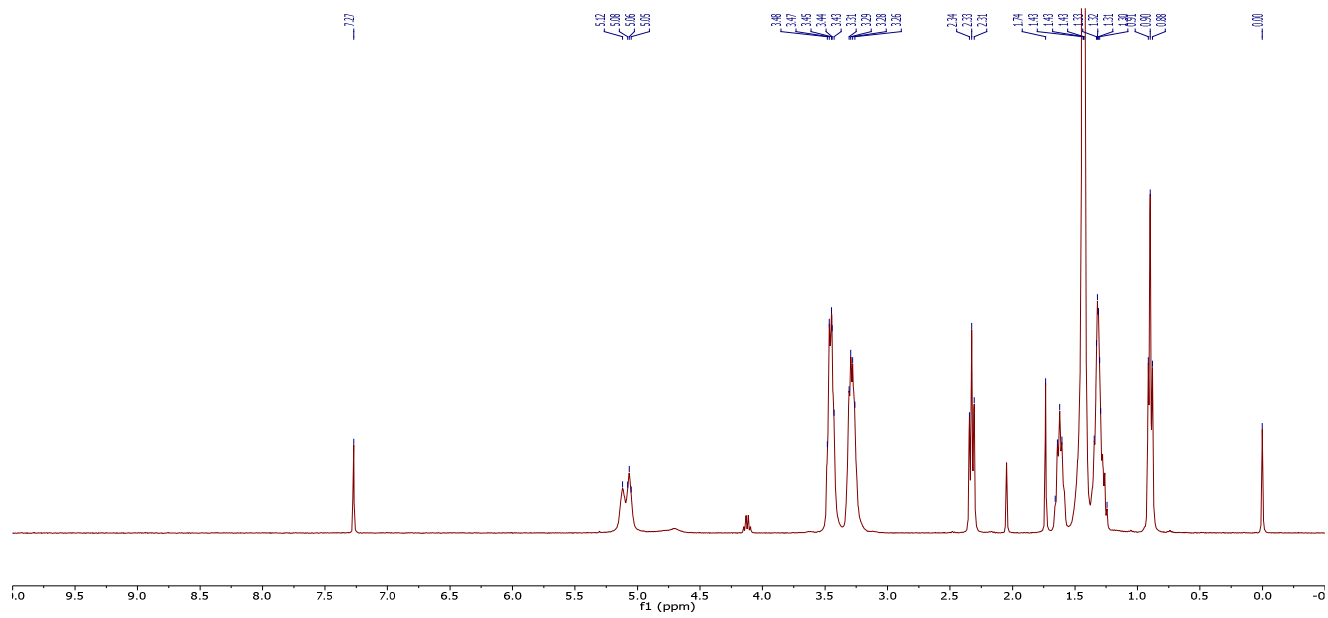
^1H NMR (CDCl_3) and ^{13}C NMR (CDCl_3) of **5.17**

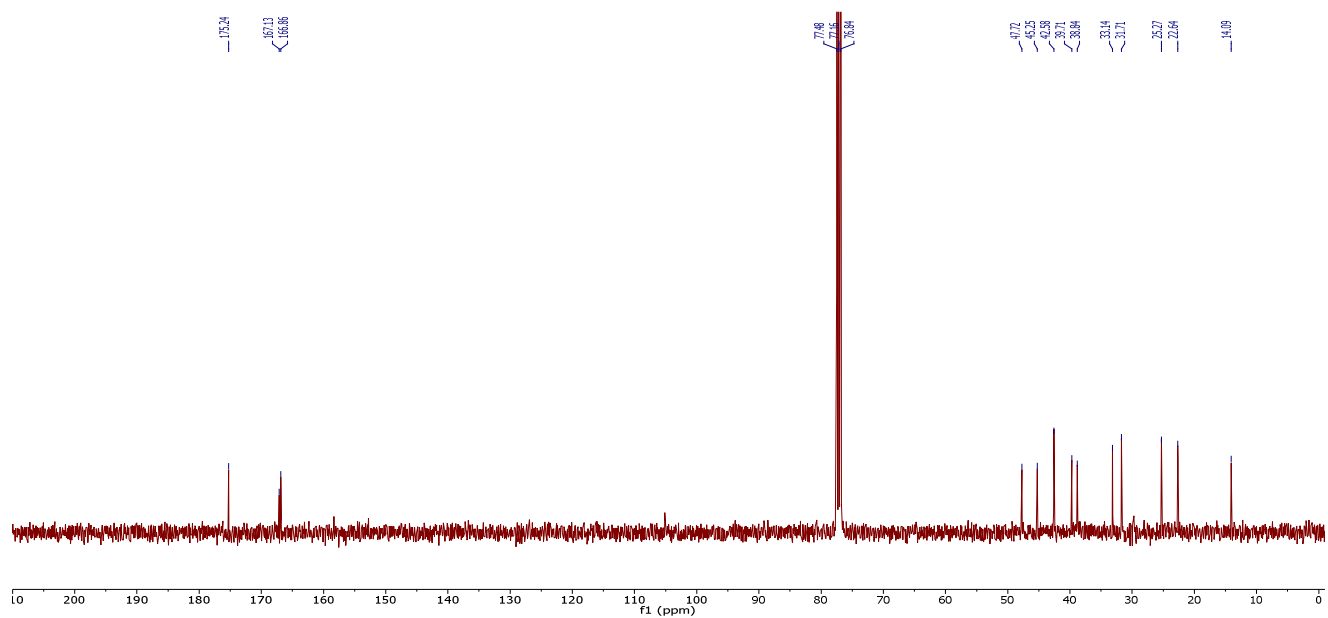
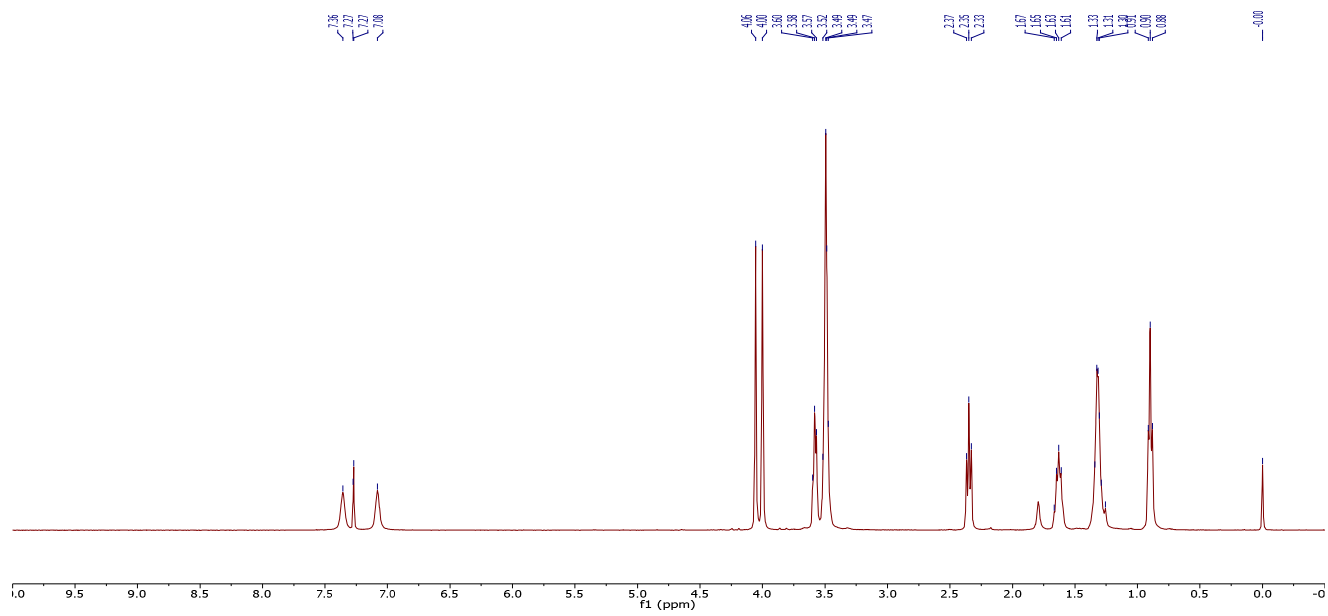
^1H NMR (CDCl_3) and ^{13}C NMR (CDCl_3) of **5.18** in dichloromethane

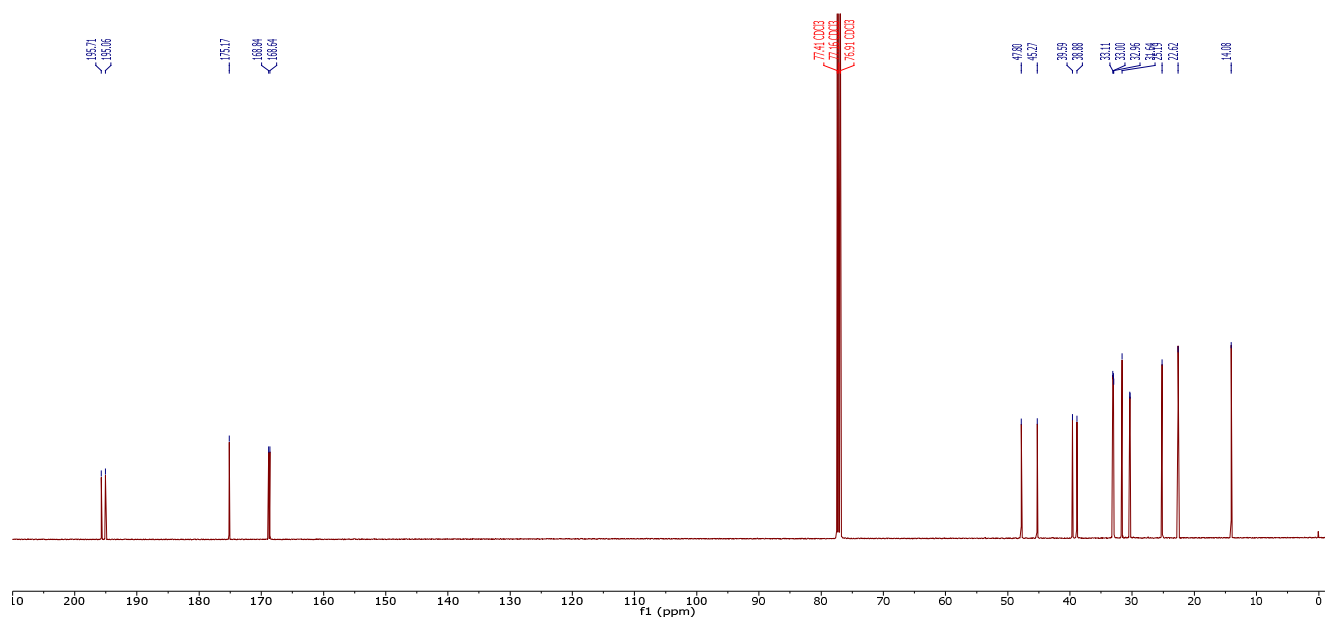
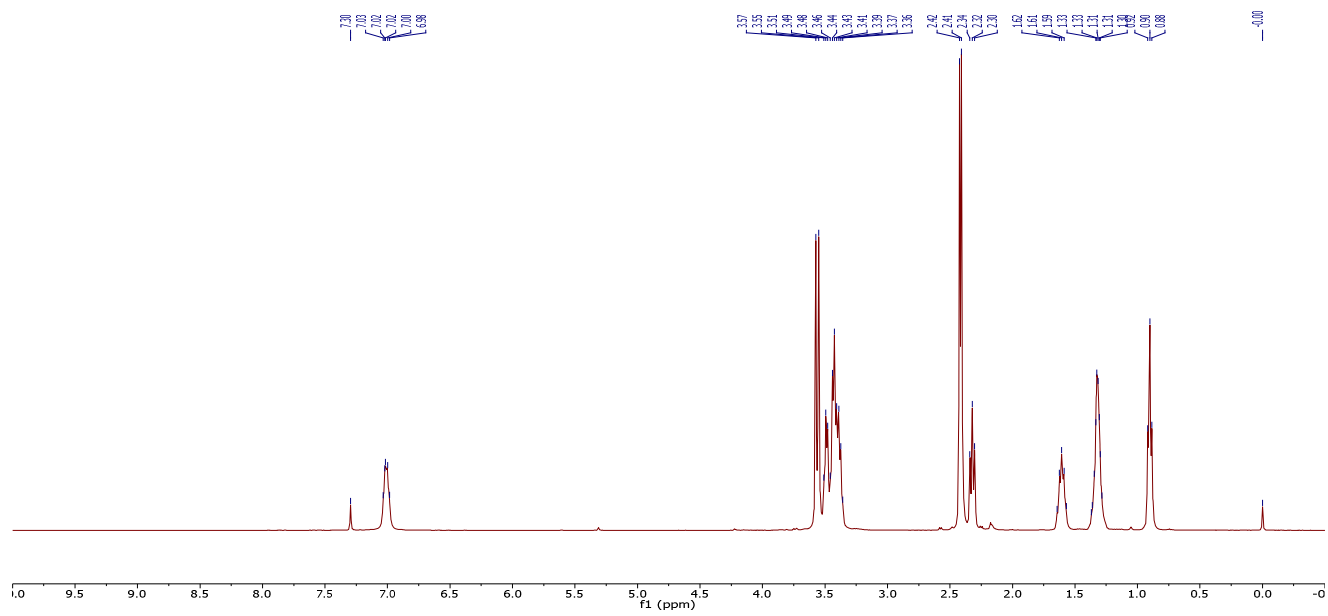


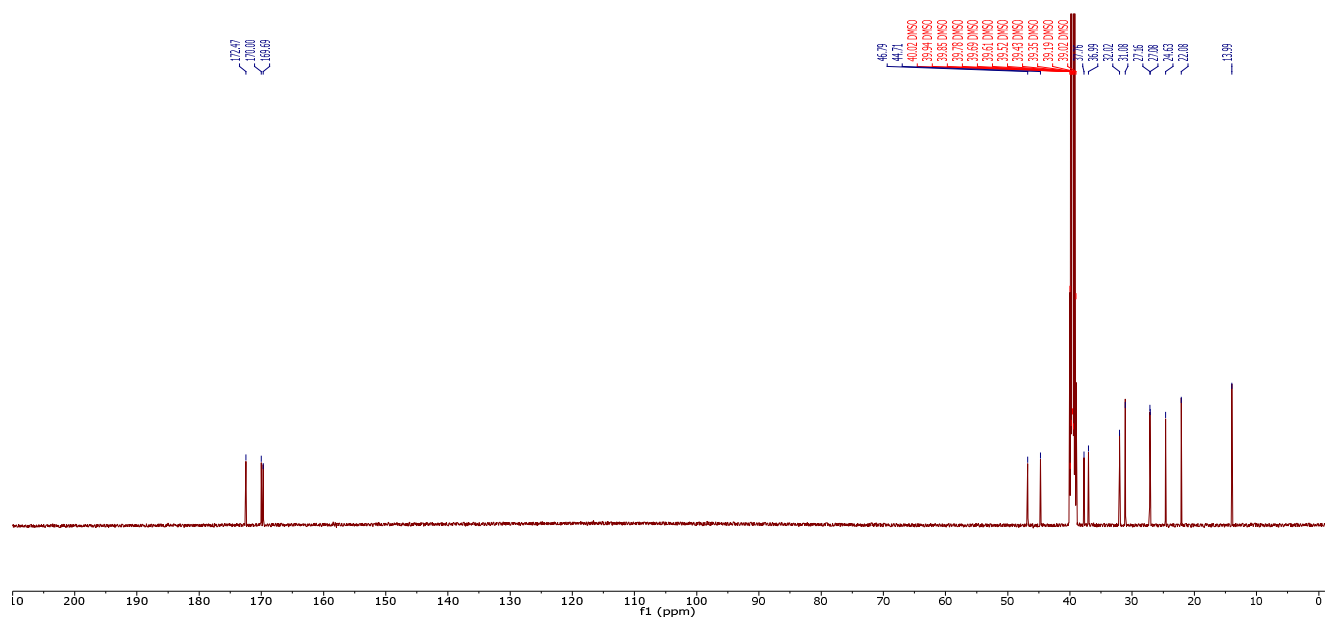
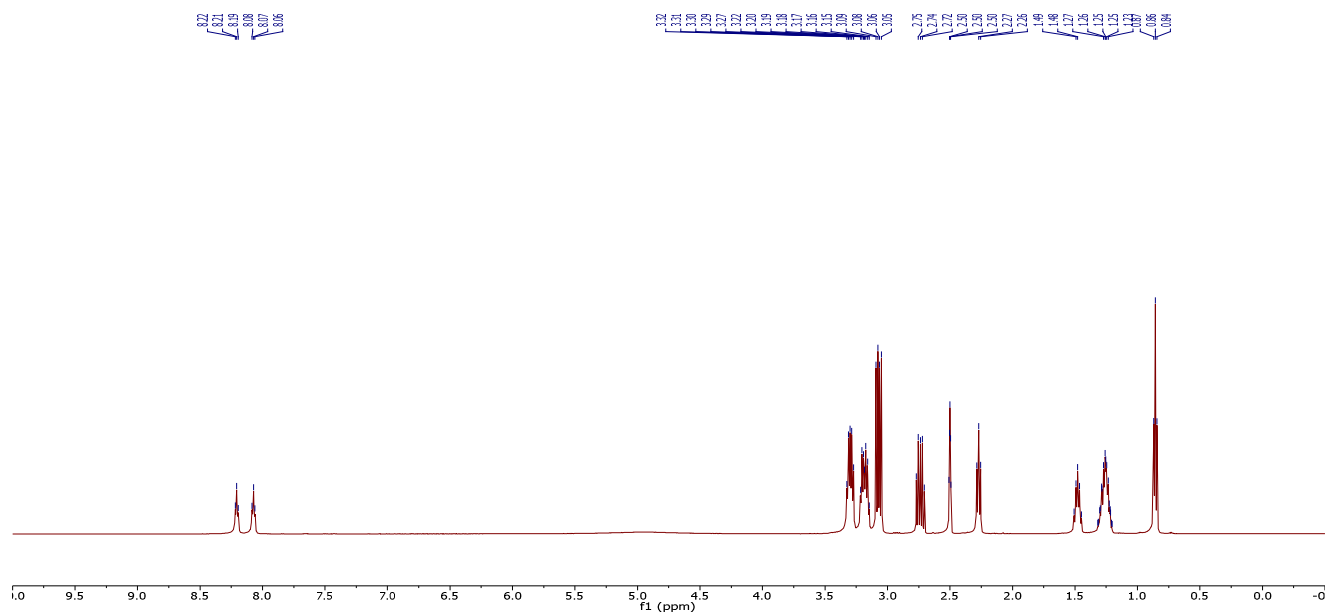
^1H NMR (DMSO- d_6) and ^{13}C NMR (DMSO- d_6) of **5.4**

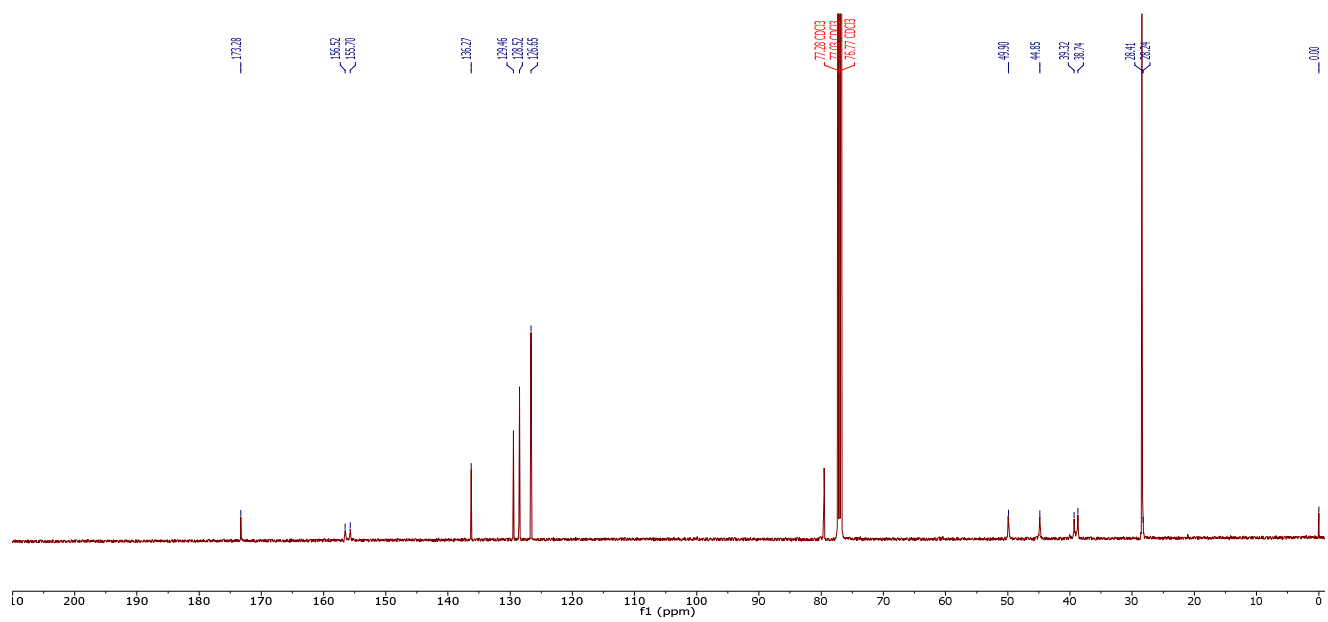
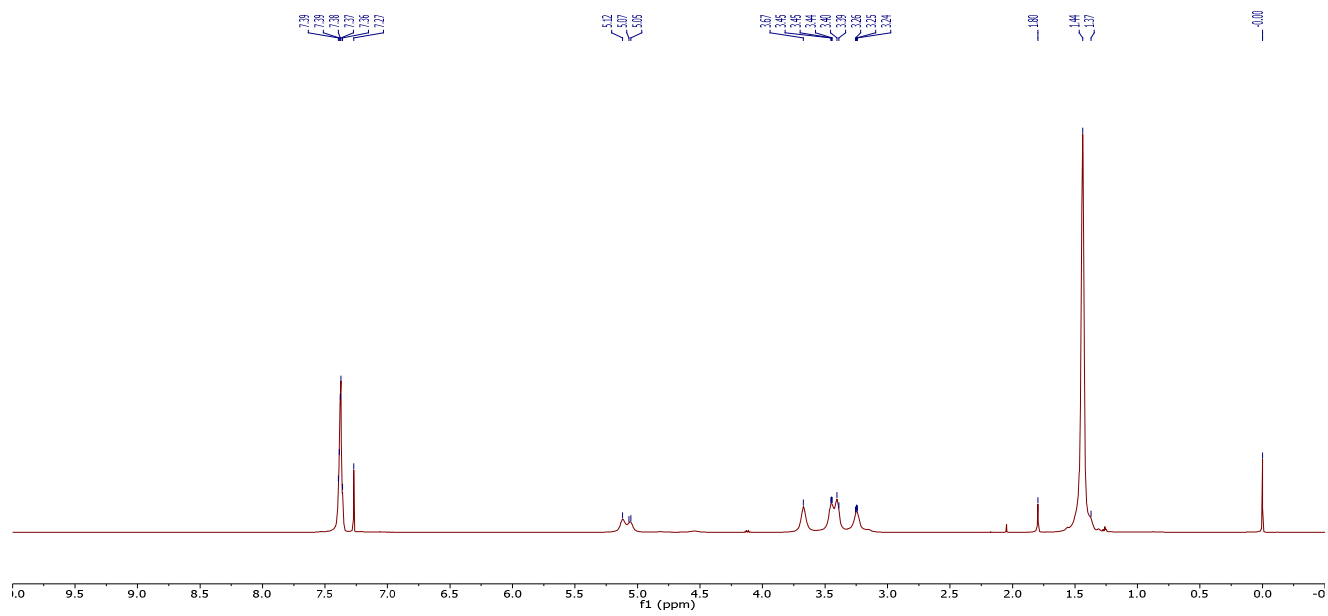
^1H NMR (CDCl_3) and ^{13}C NMR (CDCl_3) of **5.19** in ethyl acetate

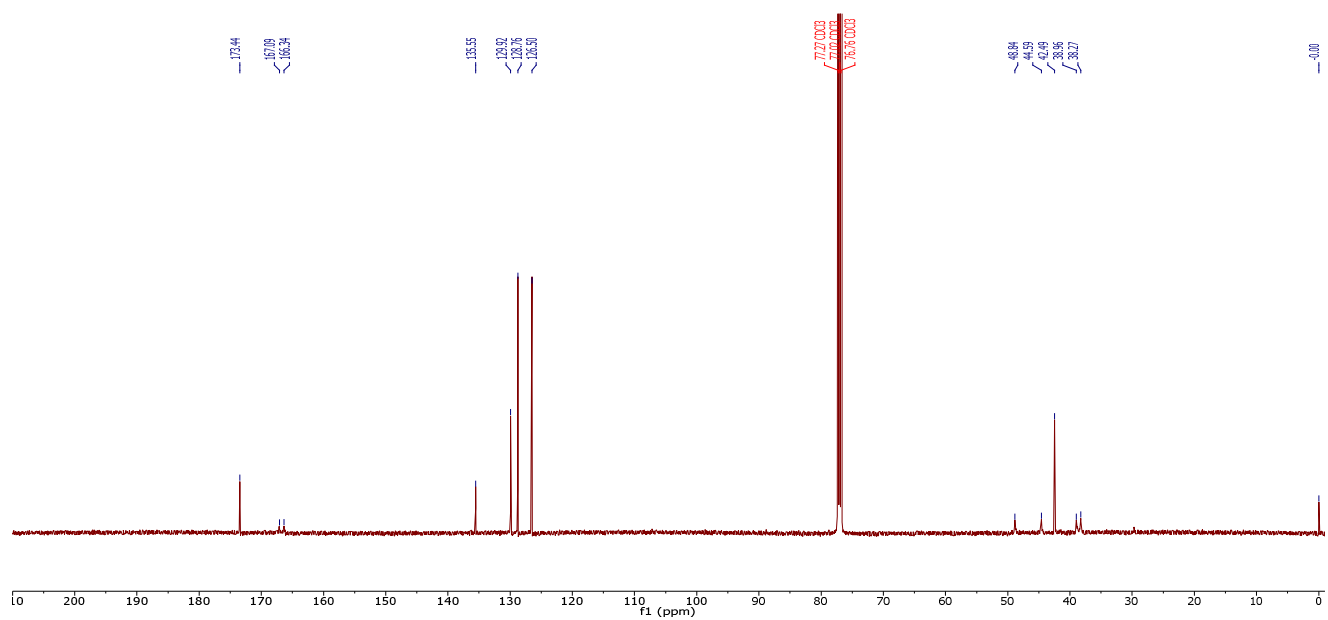
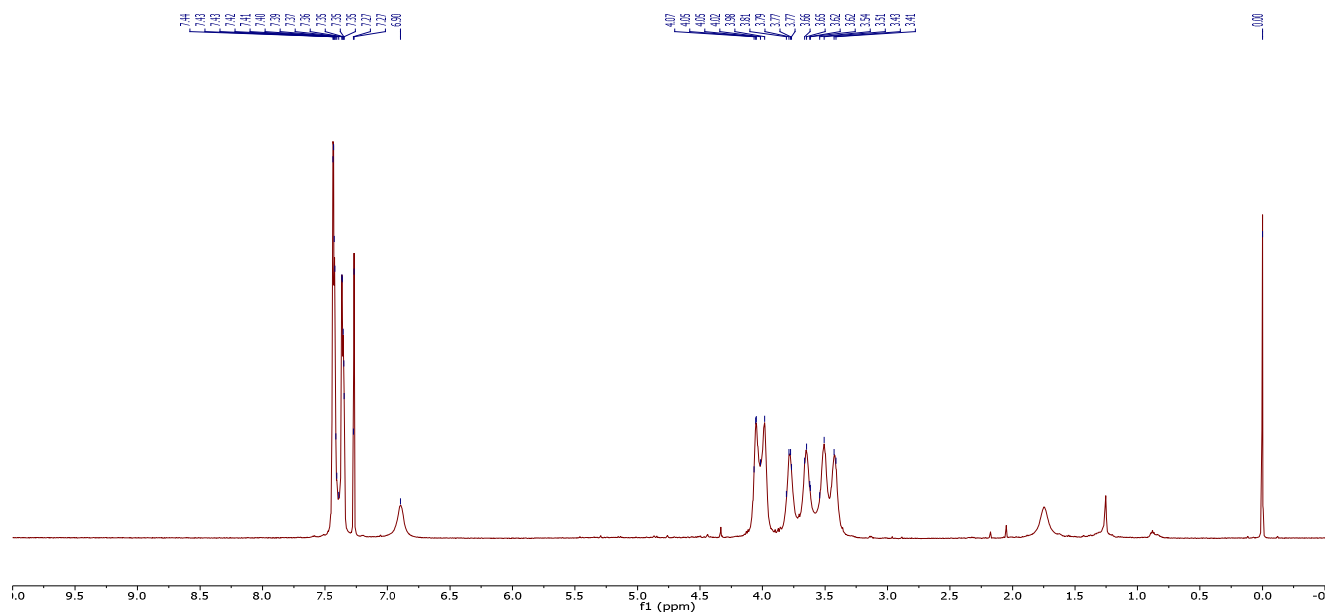


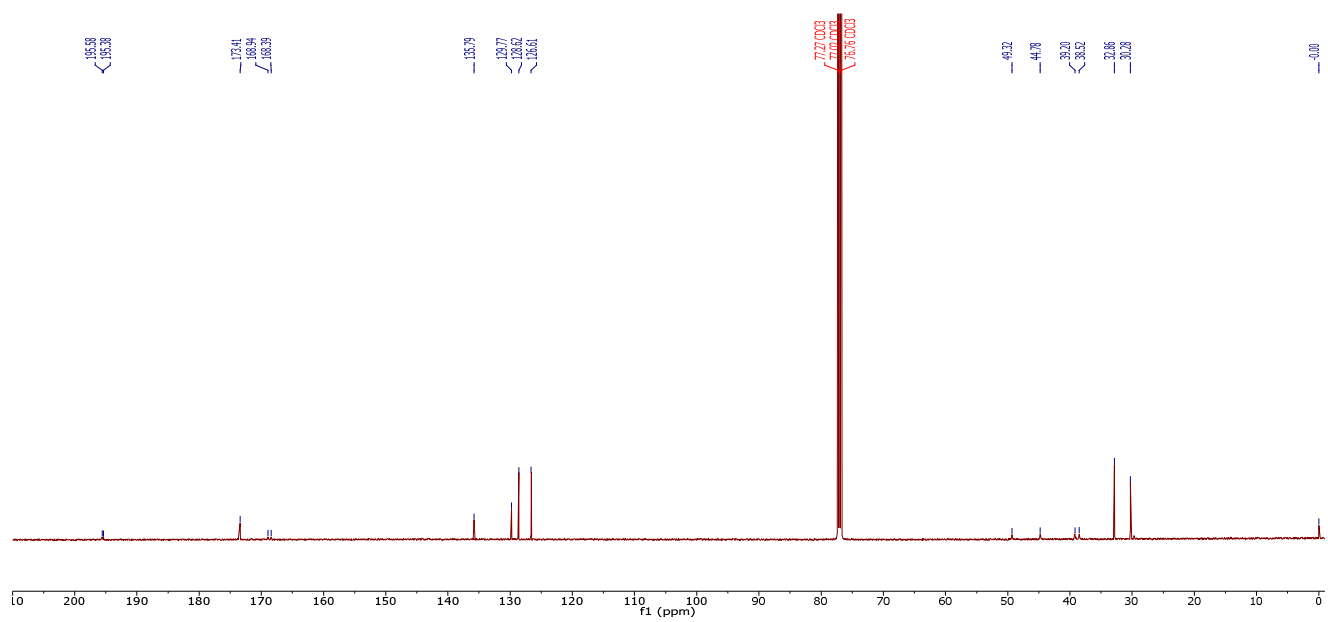
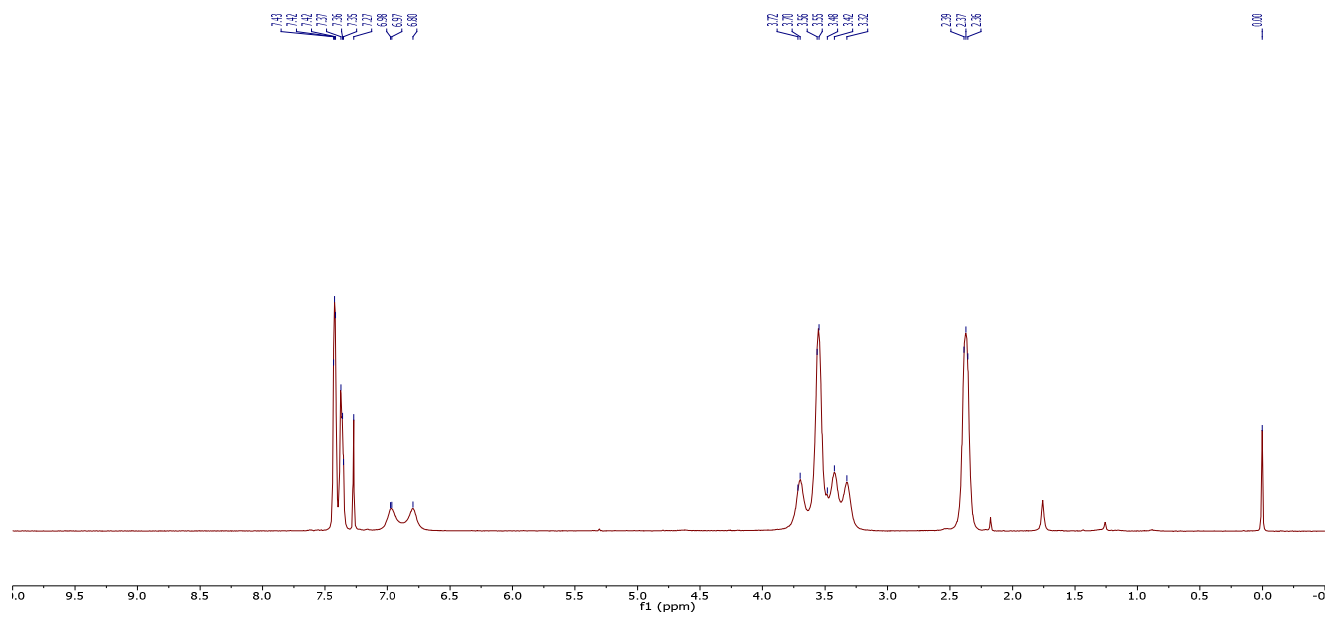
^1H NMR (CDCl_3) and ^{13}C NMR (CDCl_3) of **5.20**

^1H NMR (CDCl_3) and ^{13}C NMR (CDCl_3) of **5.21**

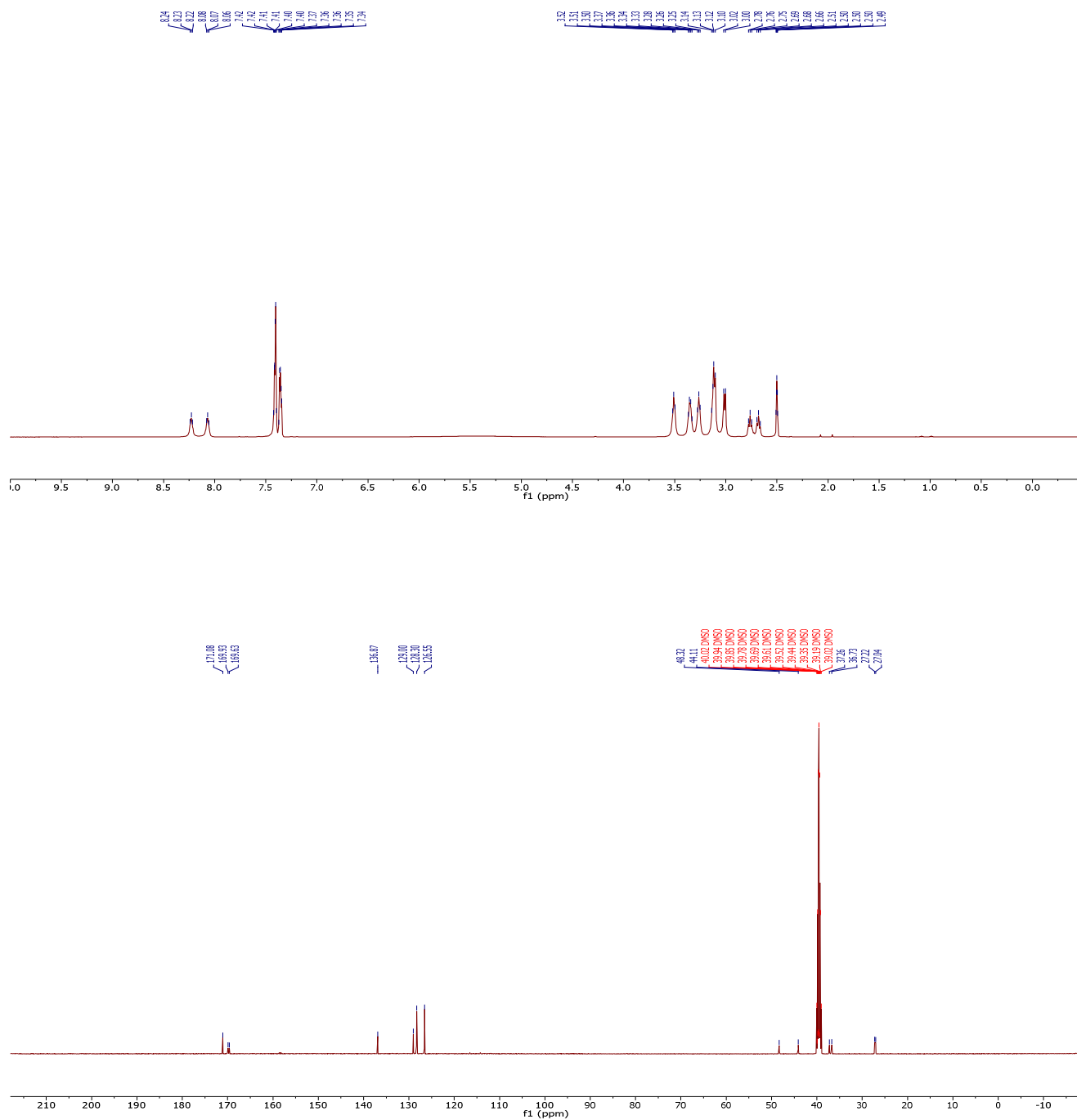
^1H NMR (DMSO- d_6) and ^{13}C NMR (DMSO- d_6) of **5.5**

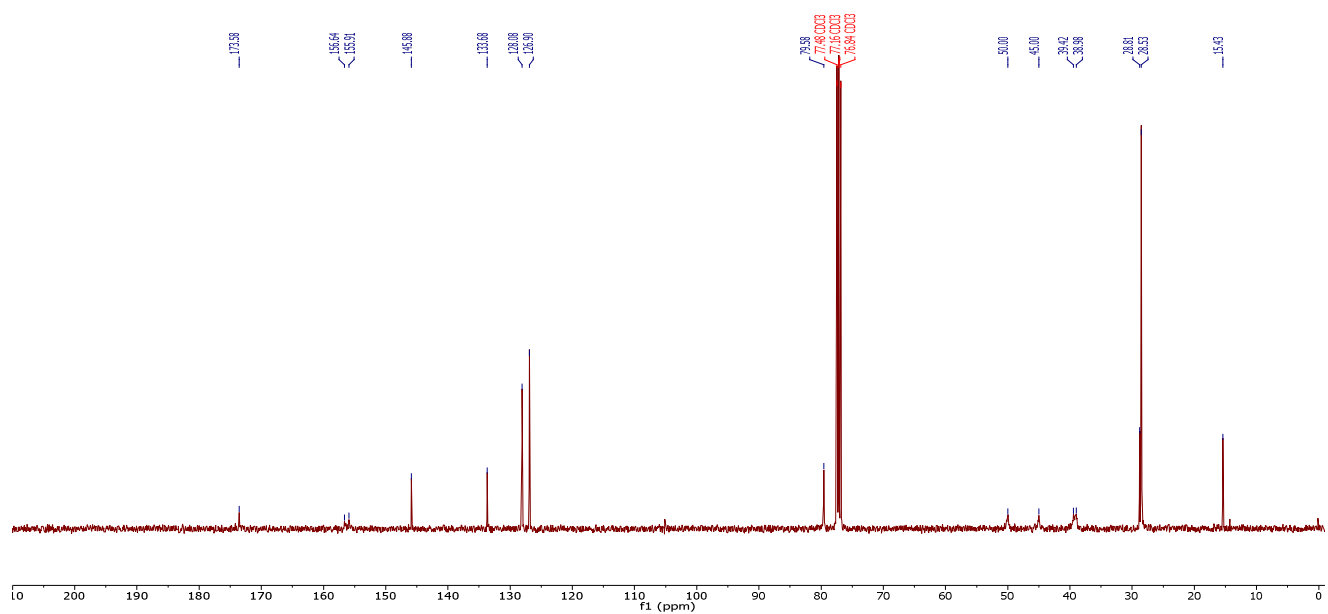
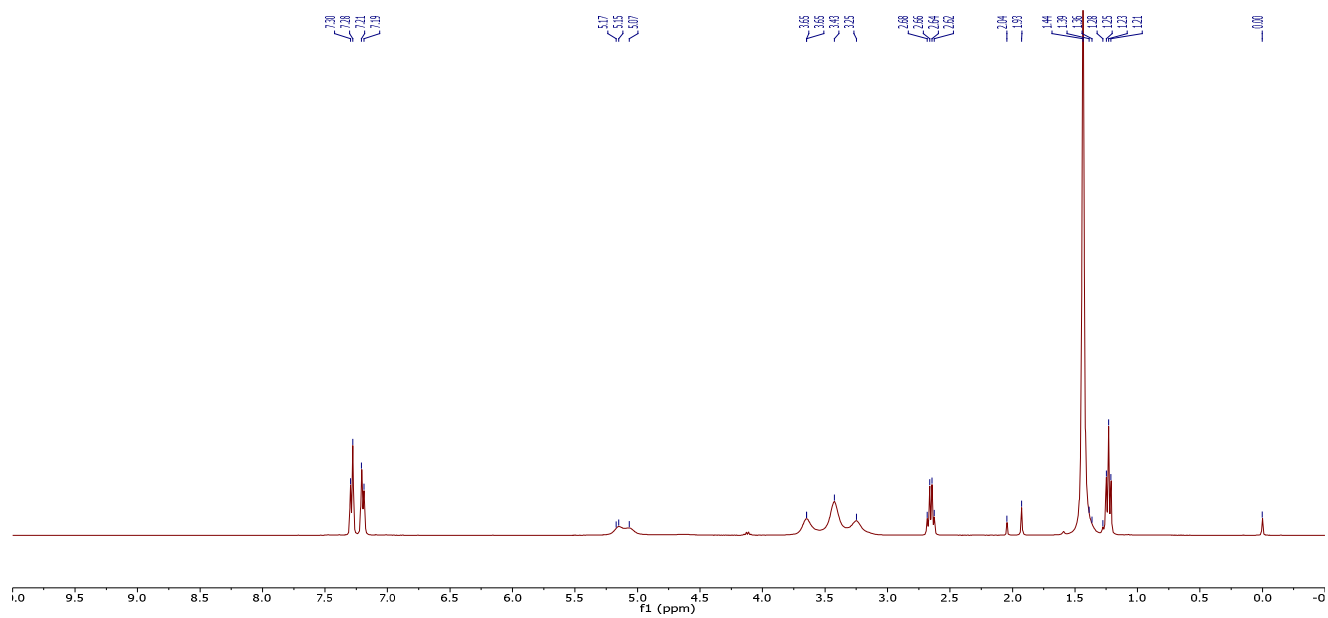
^1H NMR (CDCl_3) and ^{13}C NMR (CDCl_3) of **5.22**

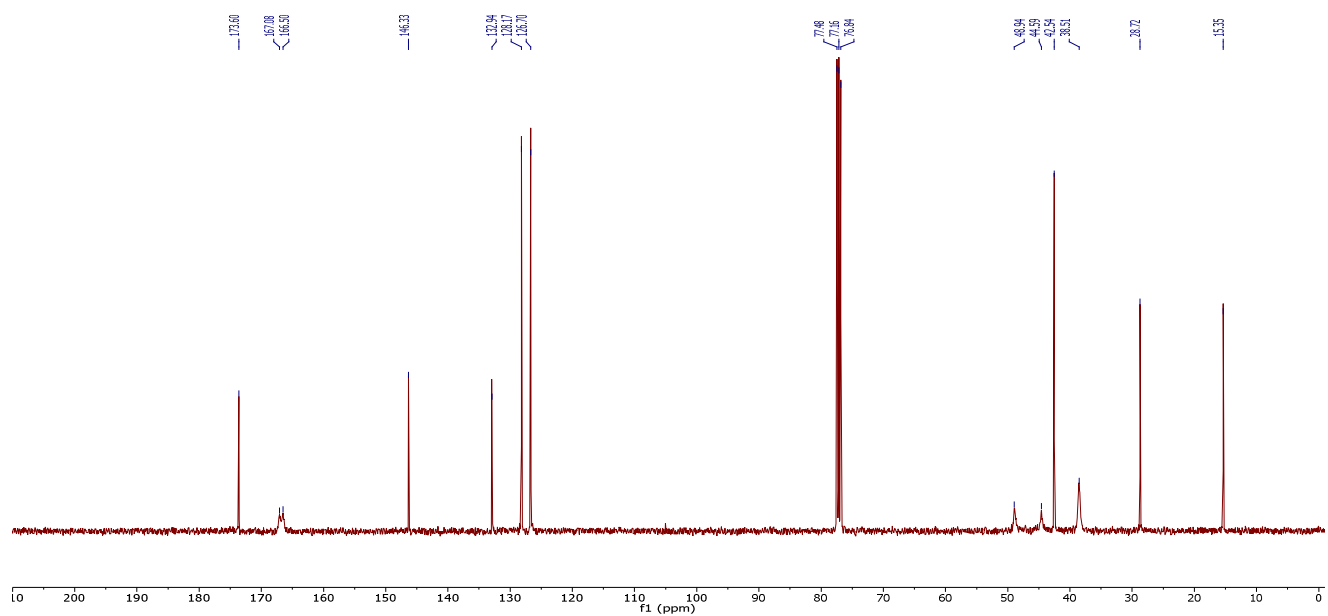
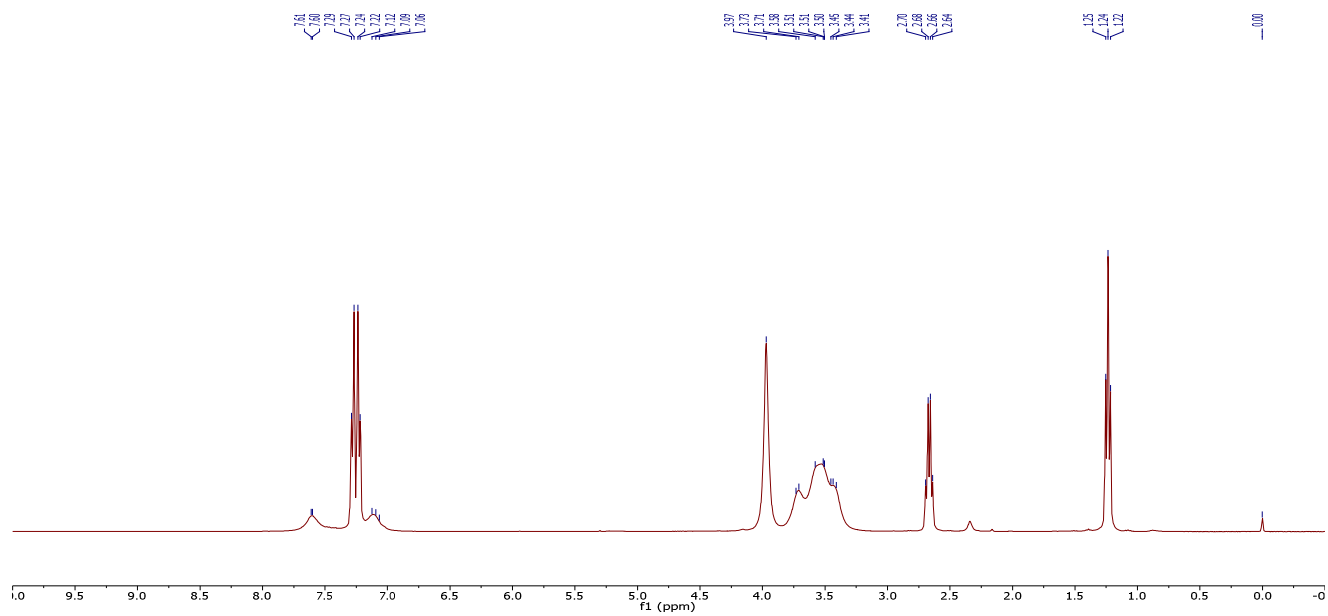
^1H NMR (CDCl_3) and ^{13}C NMR (CDCl_3) of **5.23**

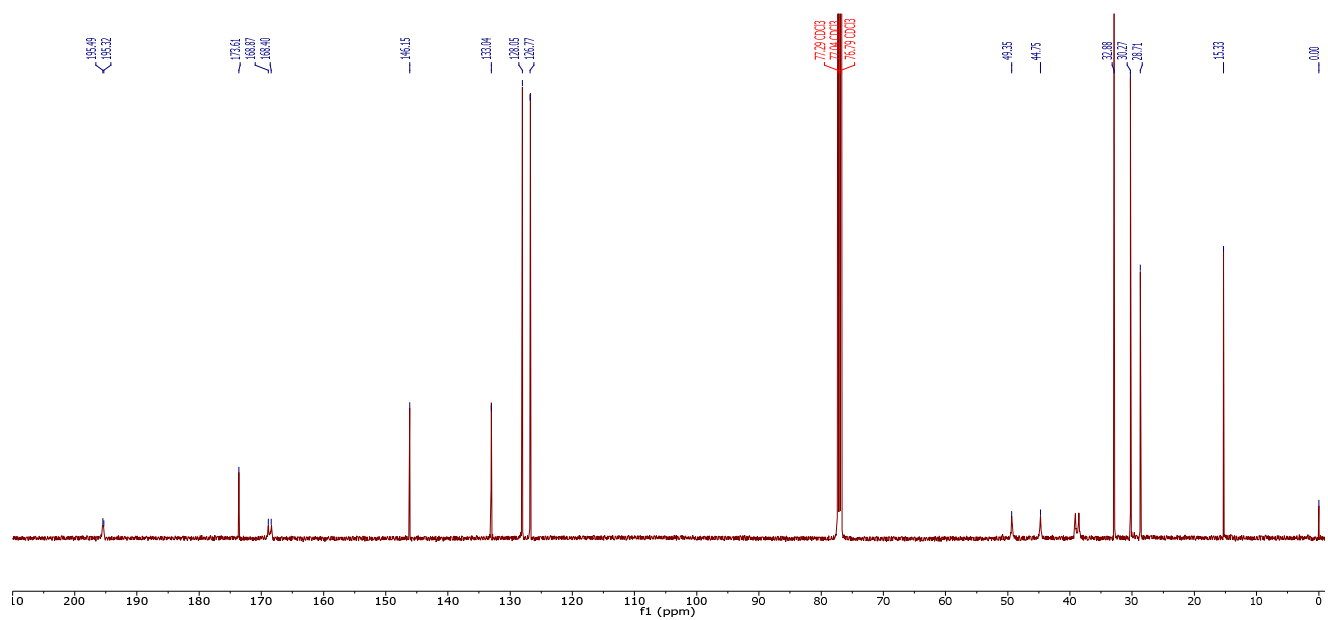
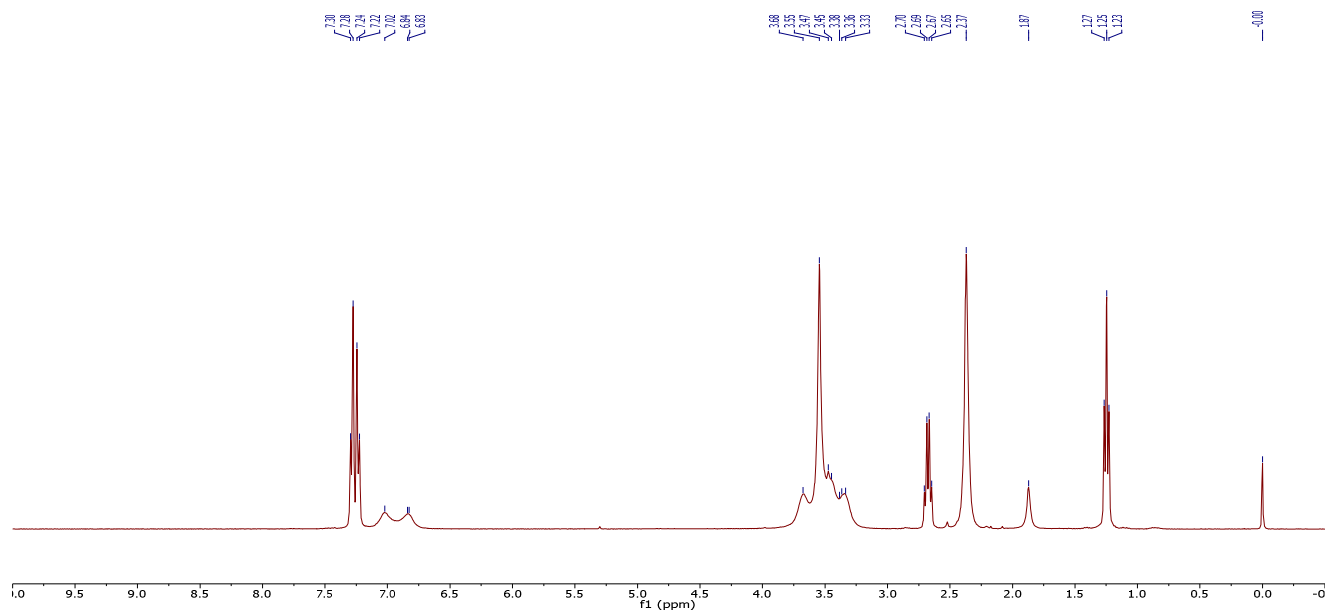
^1H NMR (CDCl_3) and ^{13}C NMR (CDCl_3) of **5.24**

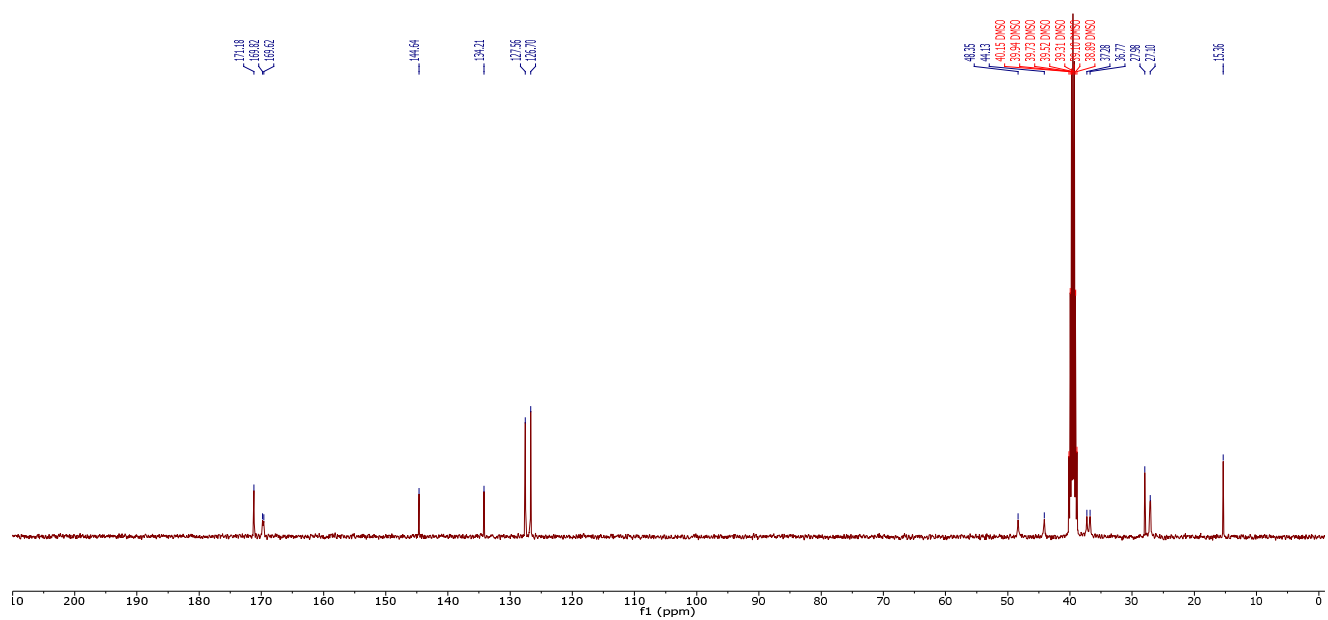
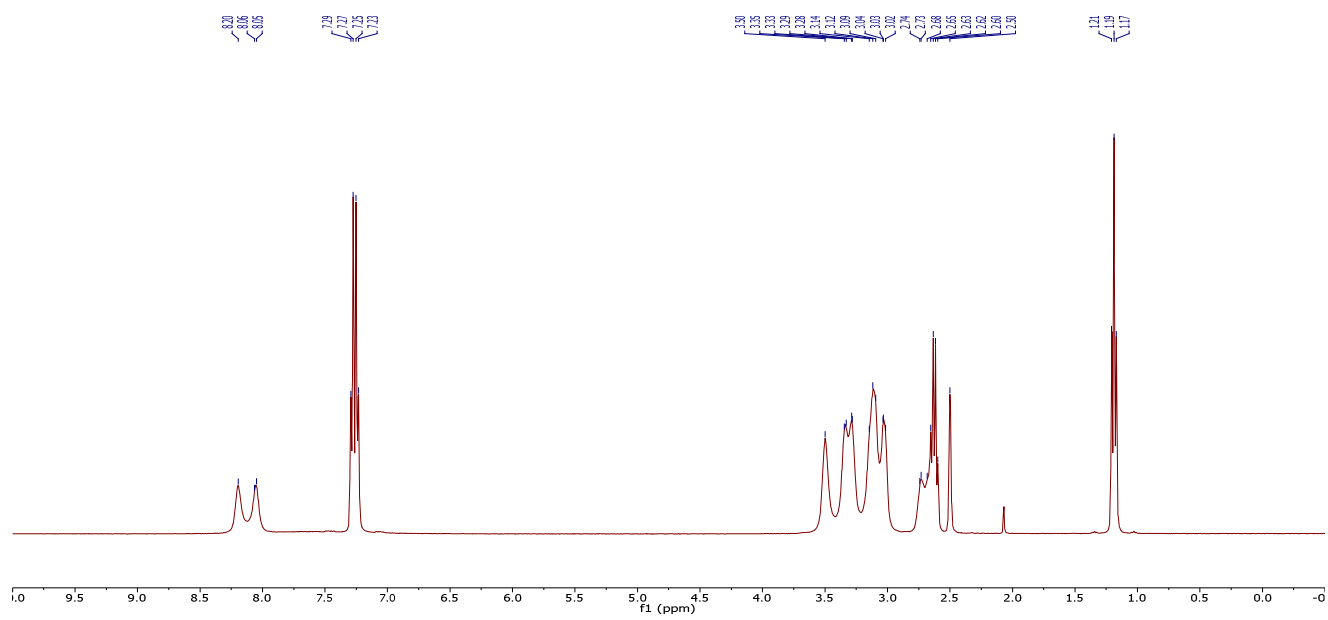
^1H NMR (DMSO- d_6) and ^{13}C NMR (DMSO- d_6) of **5.6**



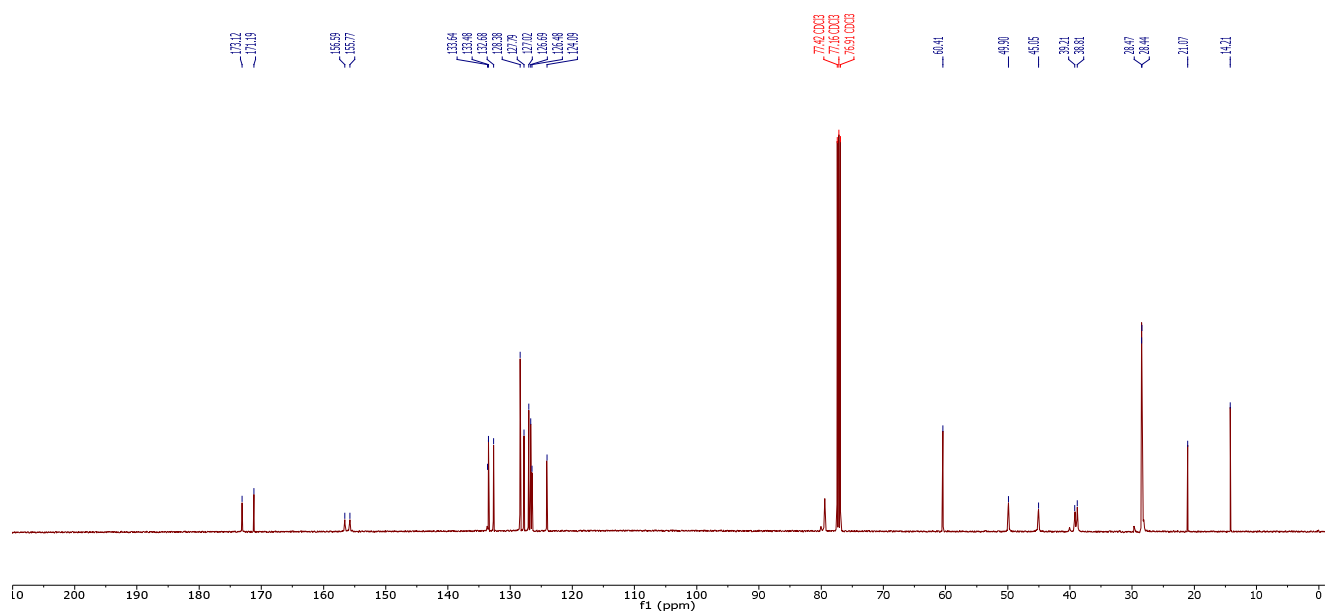
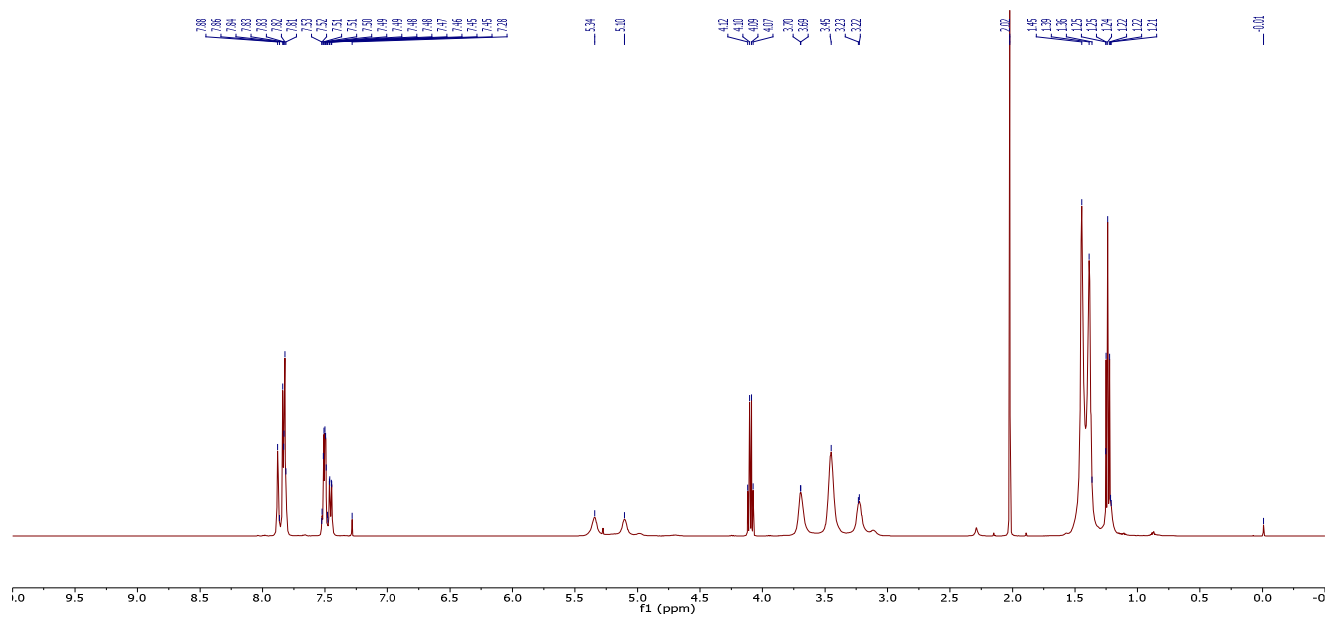
^1H NMR (CDCl_3) and ^{13}C NMR (CDCl_3) of **5.25**

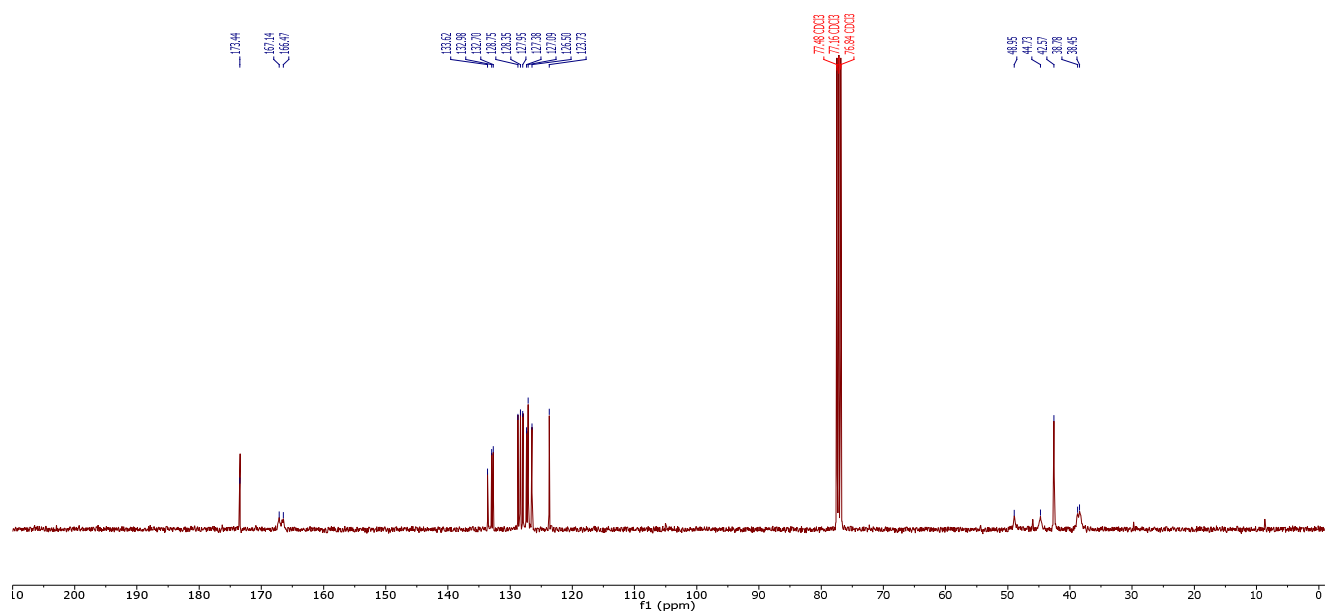
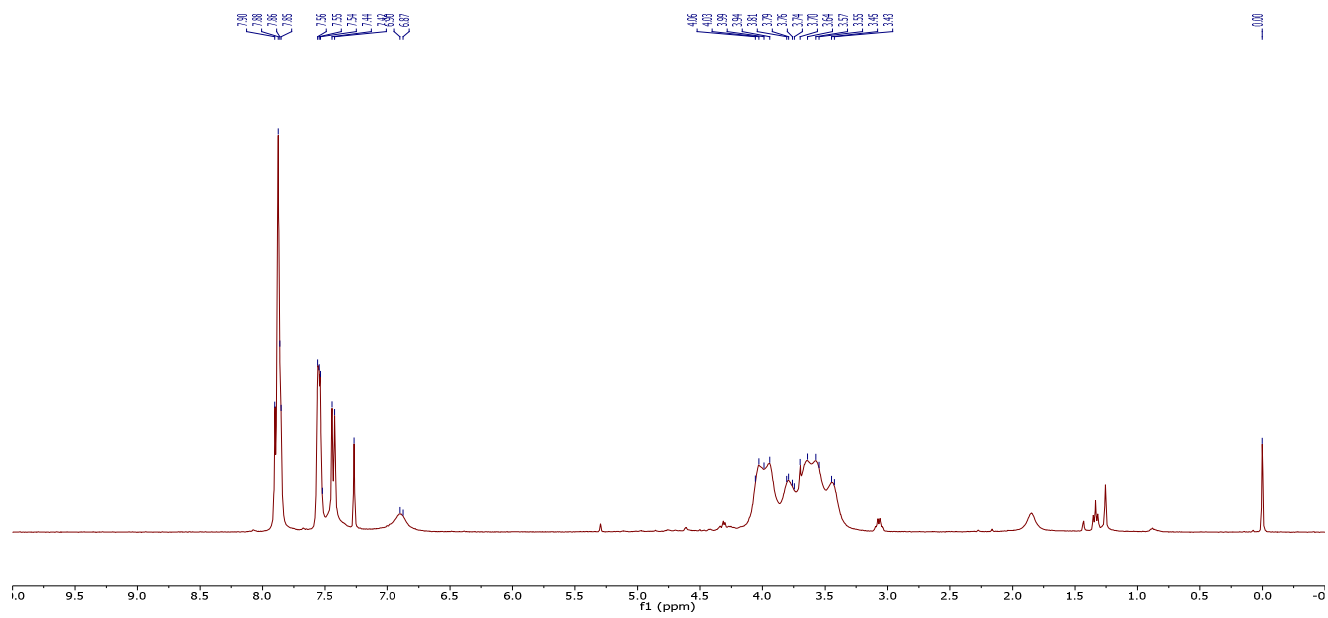
^1H NMR (CDCl_3) and ^{13}C NMR (CDCl_3) of **5.26**

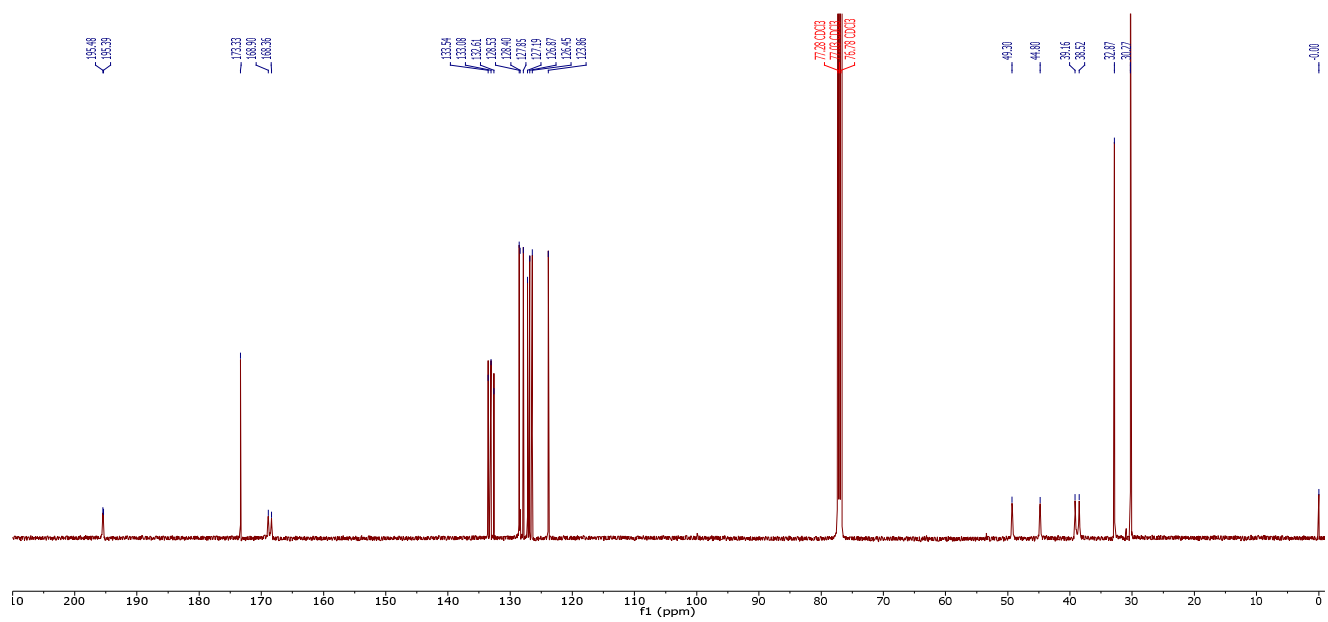
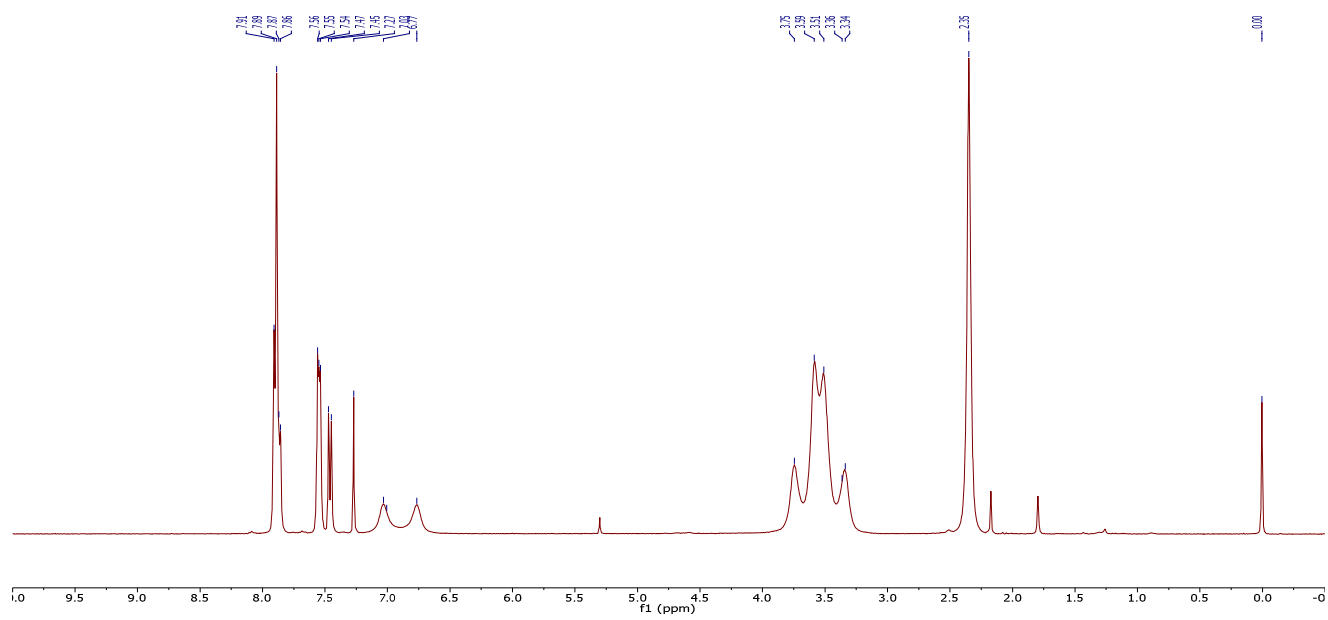
^1H NMR (CDCl_3) and ^{13}C NMR (CDCl_3) of **5.27**

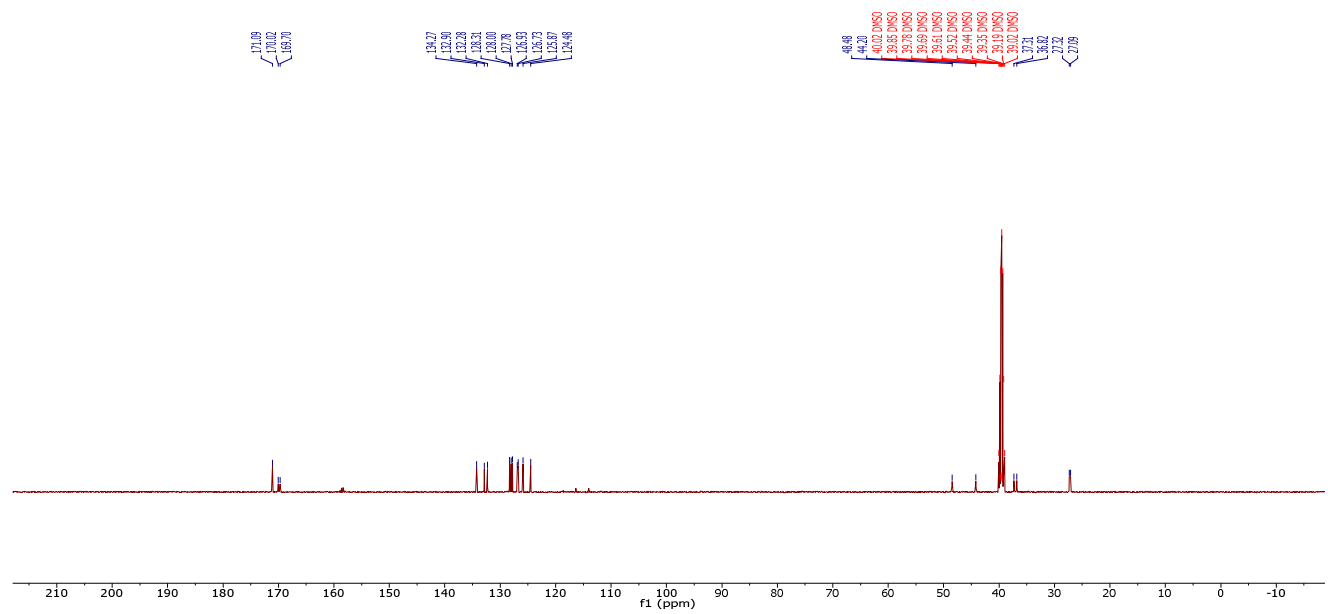
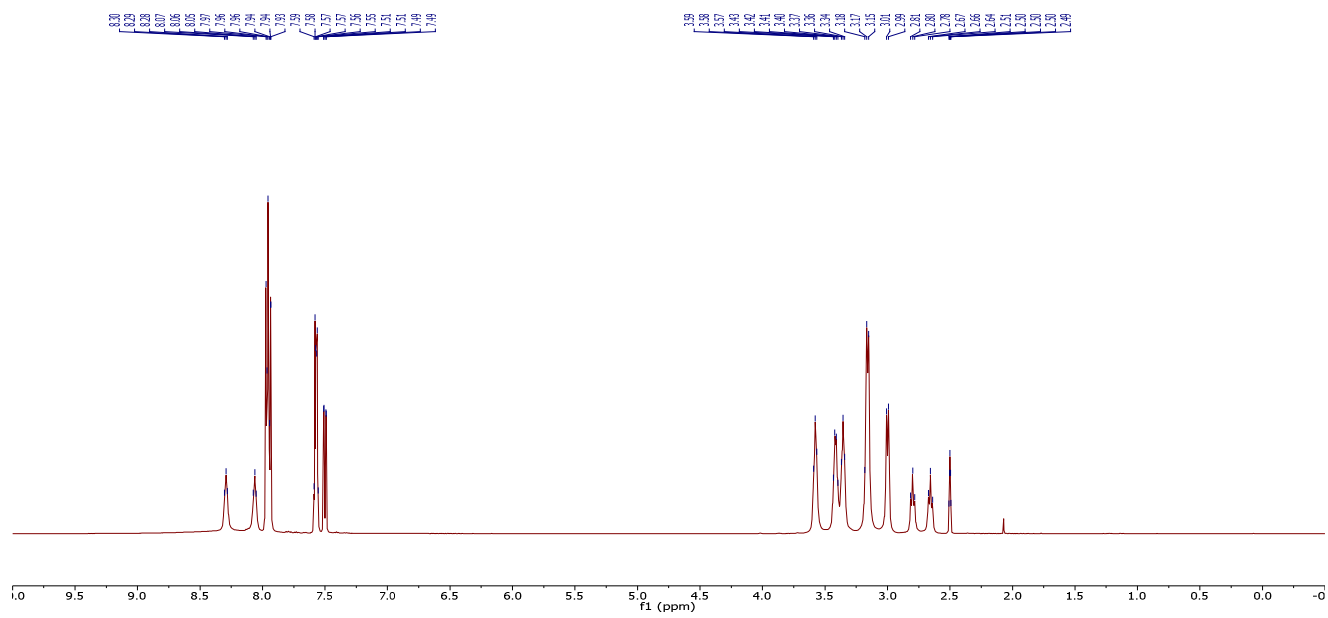
^1H NMR (DMSO- d_6) and ^{13}C NMR (DMSO- d_6) of **5.7**

^1H NMR (CDCl_3) and ^{13}C NMR (CDCl_3) of **5.28** in ethyl acetate



^1H NMR (CDCl_3) and ^{13}C NMR (CDCl_3) of **5.29**

^1H NMR (CDCl_3) and ^{13}C NMR (CDCl_3) of **5.30**

^1H NMR (DMSO- d_6) and ^{13}C NMR (DMSO- d_6) of **5.8**

Chapter 6: Future Directions

6.1 New Disulfide-Reducing Agents for Chemical Biology

The development of disulfide-reducing agents that can efficiently reduce disulfide bonds in proteins and other biomolecules is of paramount importance in biology and biochemistry.^{5,24} Over the years, several dithiol reagents with kinetic reactivity superior to that of DTT have been reported.^{27-29,42} Yet, none of these compounds possessed the thermodynamic strength of DTT. The development of disulfide-reducing agents that are both kinetically faster and thermodynamically superior to that of DTT is a difficult task. In general, disulfide bonds that are formed between more acidic thiols, which is necessary for enhanced reactivity in neutral water, are less stable and easier to reduce.¹⁰¹ Still, it could be possible to overcome this predicament by preorganizing the reducing agent for disulfide bond formation. As a general rule, six-membered cyclic disulfides are most stable. Nonetheless, one explanation for the enhanced reducing power of DTT relative to that of, say, 1,4-butanedithiol could stem from the *gauche* effect imparted by the two adjacent hydroxyl groups on DTT, which preorganizes its conformation in the reduced state and lowers the entropic cost of its oxidation. We attempted to accomplish analogous preorganization in Chapter 4 by using a highly electron-deficient pyrazine scaffold.⁴¹ Unfortunately, the stability of its oxidized form was diminished enthalpically as a result of two sp^2 -hybridized carbons in its six-membered ring. Figure 6.1 provides a short list of potential compounds that could fit this target description of being both kinetically and thermodynamically superior to that of DTT—possessing lower thiol pK_a values and a reduced number of degrees of rotational freedom in their acyclic form.

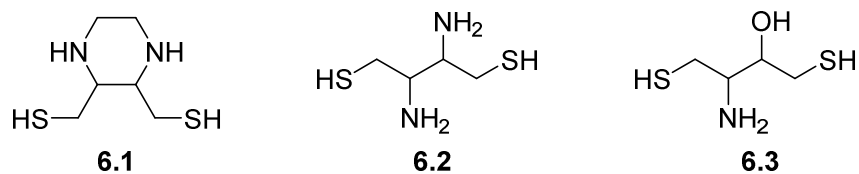


Figure 6.1 Proposed disulfide-reducing agents with enhanced reactivity that are pre-organized for disulfide bond formation.

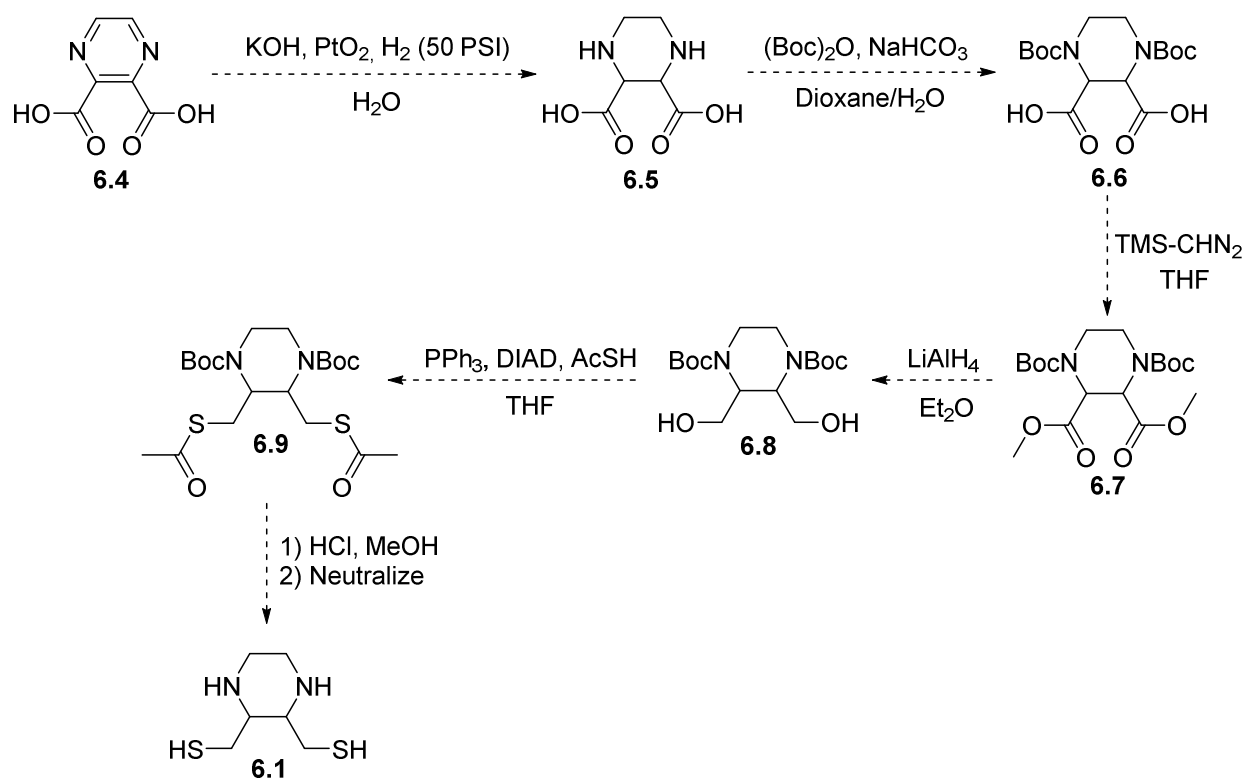


Figure 6.2 Proposed synthesis of **6.1**

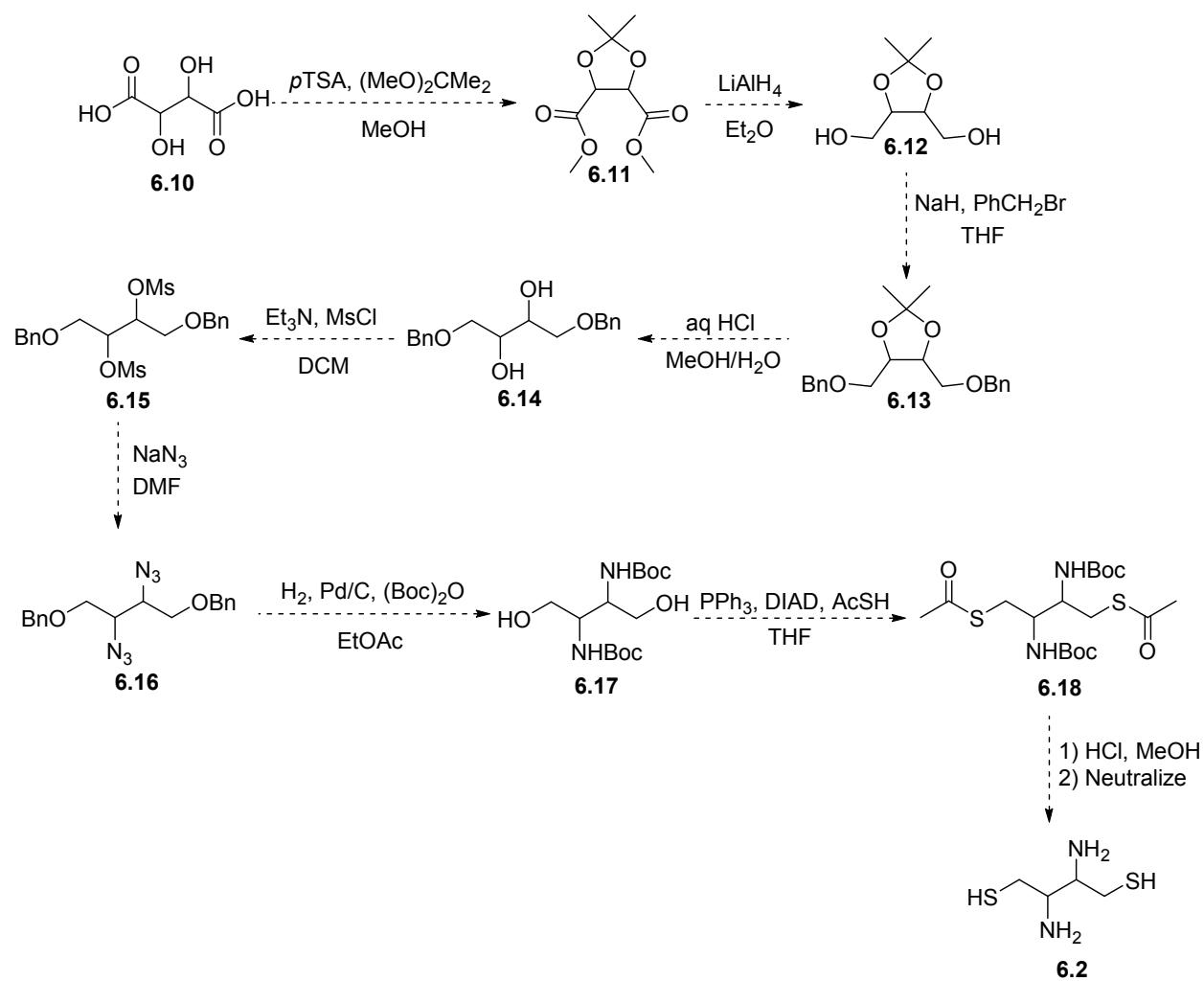


Figure 6.3 Proposed synthesis of **6.2**

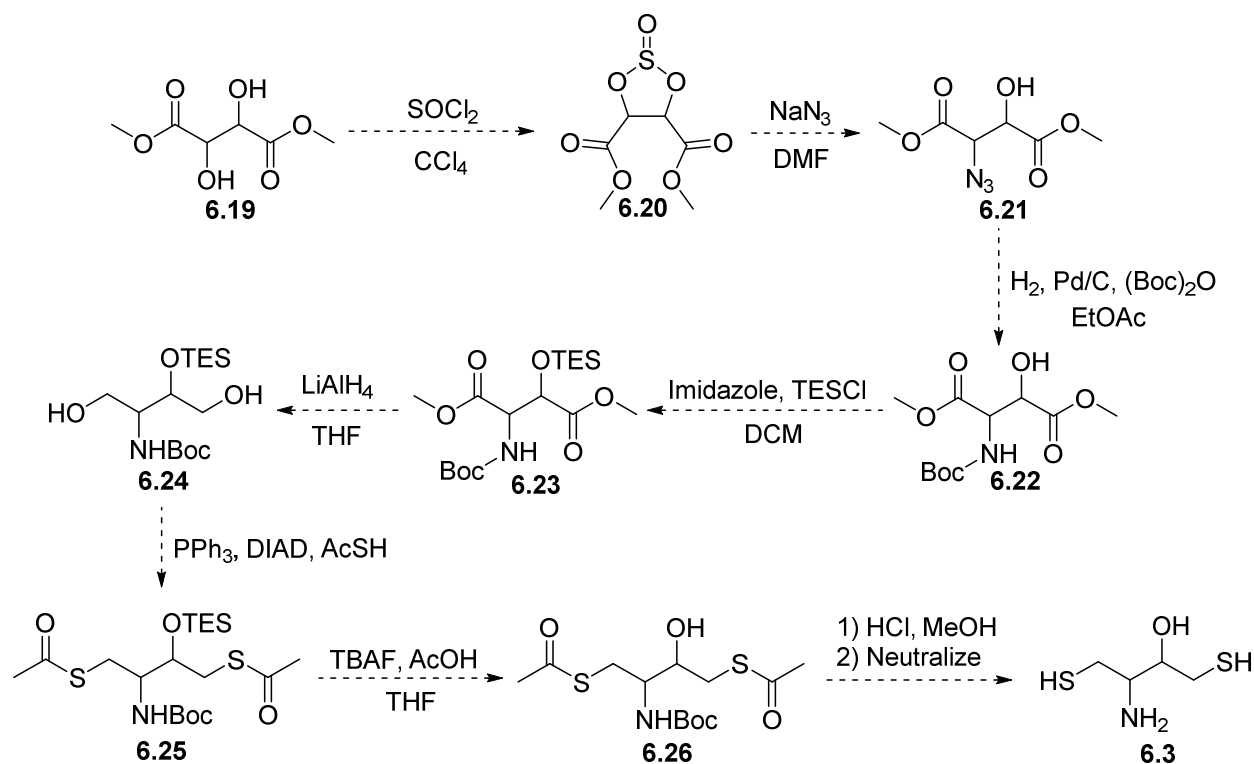


Figure 6. 4 Proposed synthesis of 6.3

6.2 Labeling of Proteins with Electron-Relay Catalysis System

The electron-relay catalysis system described in Chapter 3 could find significant use in common biochemical techniques, such as the reduction of native disulfide bonds in antibodies and other proteins to generate thiol groups that could then be labeled with a fluorophore or other soluble molecule.¹⁶⁰ The electrophilic partner for such processes is typically a thiol-specific reagent such as a maleimide or iodoacetamide. Still, the presence of large concentrations of disulfide-reducing agent (i.e., DTT) limits yield and efficiency of this method and requires its removal prior to labeling.^{160,188} The use of our electron-relay catalysis system, however, would allow for the rapid reduction of protein disulfides to take place in the presence of trace amounts

of soluble thiol or selenol, avoiding the need to remove excess reagent prior to labeling. Moreover, the use of sterically hindered selenols (or thiols) could be employed in our electron-relay system for the selective reduction of only the most sterically accessible disulfide bond in a protein or antibody—a challenging task that has had little success in the field of biotechnology.

6.3 Hydrophobic Diselenide Oxidants as Catalysts for Protein Folding

Diselenides have been shown to be outstanding catalysts for thiol–disulfide interchange chemistry and, as such, have been shown to quite useful in facilitating oxidative protein folding. An obvious extension to our work describing hydrophobic PDI mimics in Chapter 5 would be to employ a series of diselenides with similar hydrophobic moieties. The hydrophobic nature of the diselenide oxidants shown below (Figure 6.5) should enhance further the rate at which they promote disulfide-bond formation in unfolded proteins.

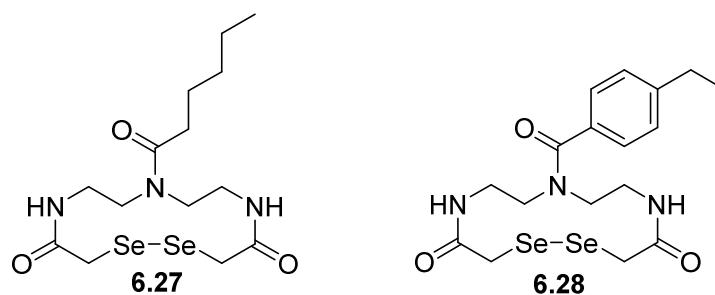


Figure 6.5 Hydrophobic cyclic diselenides for oxidative protein folding

As acyclic diselenides—such as selenoglutathione—are typically used as catalysts for protein folding, the use of cyclic diselenides could also confer additional benefits, such as

eliminating trapped selenysulfide intermediates and improving the overall yield of folded protein.

Appendix 1*: Acetylated DTBA for the Treatment of Cystinosis

*This work is being performed in collaboration with the laboratory of Dr. Donald J. Brown at the University of California–Irvine.

A1.1 Author Contributions

D.J.B. proposed the use of DTBA to treat cystinosis. R.T.R. proposed the use of acetylated DTBA to improve stability and cellular delivery. J.C.L. synthesized and characterized acetylated DTBA. D.J.B. and his laboratory performed all other experiments.

A1.2 Introduction

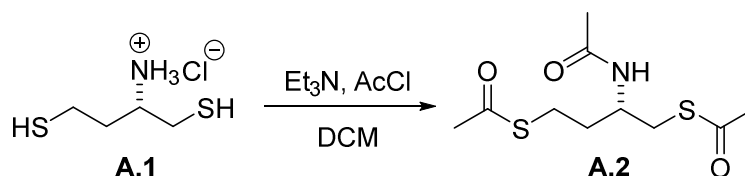
Cystinosis is a rare genetic disease which results in the accumulation of oxidized cysteine (cystine) in the lysosome of human cells as a result of defects in the cystinosin transport system.¹⁸⁹ Without treatment, the accumulation of cystine will continue, often resulting in tissue and/or organ damage. To date, the treatment of cystinosis has typically relied on the small-molecule reducing agent, cysteamine.¹⁹⁰ Cysteamine is a monothiol that reduces cystine down to cysteine, which can then be transported out of the lysosome. As a result, it was hypothesized that a stronger and more efficient disulfide-reducing agent—such as DTBA—would be beneficial in treating this disease. To improve stability and cellular delivery, acetylated DTBA (**A.2**) was synthesized and characterized.

A1.3 Materials and Methods

Commercial reagents were used without further purification. Dithiobutylamine (DTBA) was from Sigma-Aldrich (St. Louis, MO). All glassware was oven- or flame-dried, and reactions

were performed under $N_2(g)$ unless stated otherwise. Dichloromethane was dried over a column of alumina. Triethylamine was dried over a column of alumina and purified further by passage through an isocyanate scrubbing column. Flash chromatography was performed with columns of 40–63 Å silica, 230–400 mesh (Silicycle, Québec City, Canada). Thin-layer chromatography (TLC) was performed on plates of EMD 250- μm silica 60-F₂₅₄. The term “concentrated under reduced pressure” refers to the removal of solvents and other volatile materials using a rotary evaporator at water aspirator pressure (<20 torr) while maintaining the water-bath temperature below 40 °C. Residual solvent was removed from samples at high vacuum (<0.1 torr). NMR spectra were acquired at ambient temperature with a Bruker DMX-400 Avance spectrometer at the National Magnetic Resonance Facility at Madison (NMRFAM) and referenced to TMS or residual protic solvent. Electrospray ionization (ESI) mass spectrometry was performed with a Micromass LCT at the Mass Spectrometry Facility in the Department of Chemistry at the University of Wisconsin–Madison.

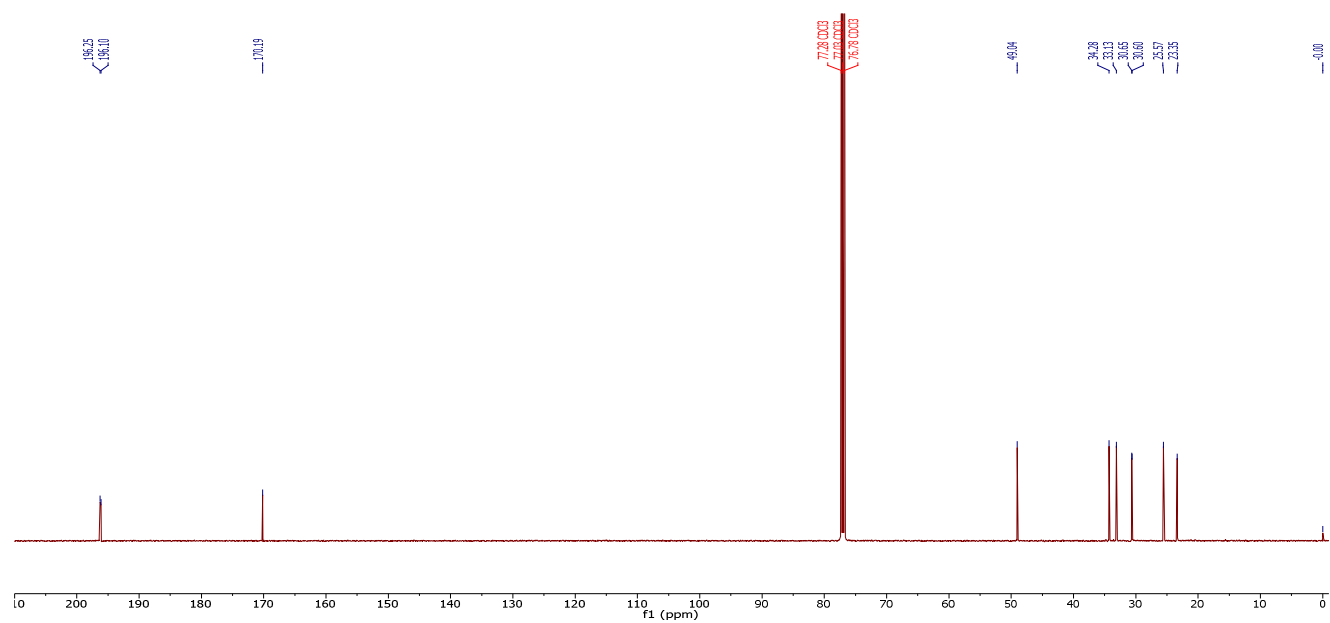
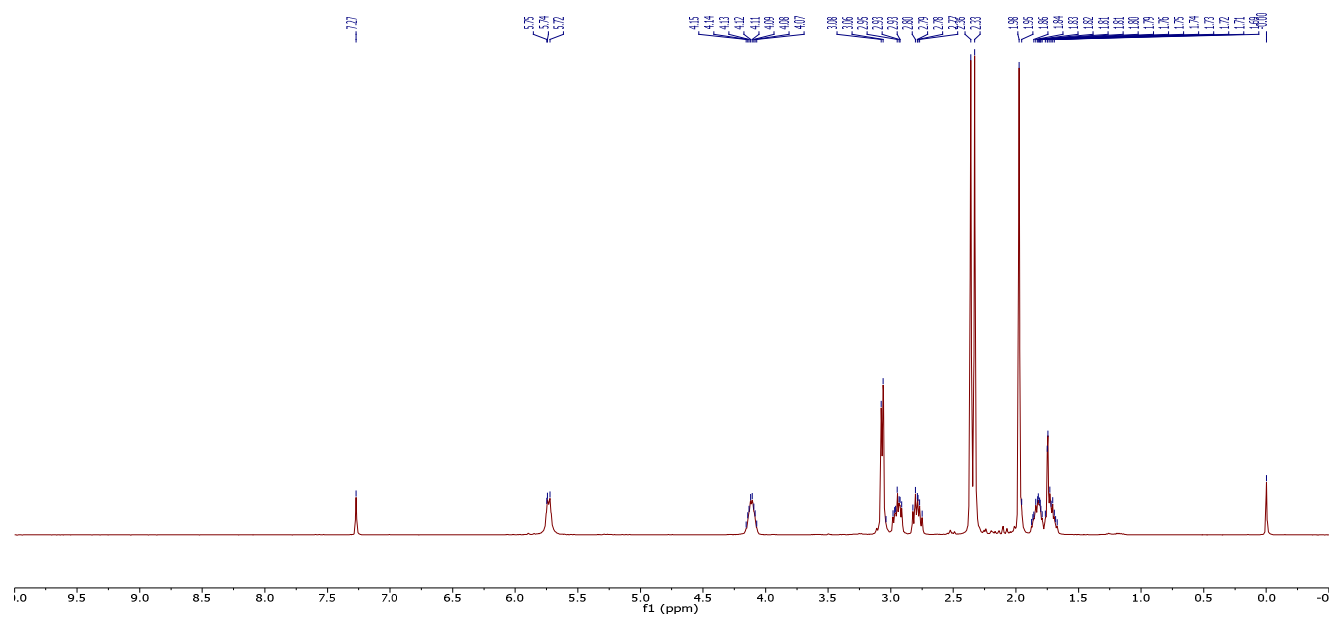
A1.4 Chemical Synthesis



To a round-bottom flask containing DTBA–HCl (**A.1**, 1.002 g, 5.768 mmol) was added 200 mL of dry dichloromethane. The mixture was then placed in an ice bath and cooled to 0 °C. Under an atmosphere of $N_2(g)$, triethylamine (8.0 mL, 57.7 mmol) and acetyl chloride (1.6 mL, 23.1 mmol) were added. After stirring for 4 h, the reaction mixture was concentrated under

reduced pressure, and the product was purified by column chromatography (silica, EtOAc), yielding **A.2** as a white solid (1.246 g, 82%).

¹H NMR (400 MHz, CDCl₃) δ = 5.73 (d, J = 7.9 Hz, 1H), 4.15–4.07 (m, 1H), 3.07 (d, J = 6.2 Hz, 2H), 2.98–2.91 (m, 1H), 2.82–2.75 (m, 1H), 2.36 (s, 3H), 2.33 (s, 3H), 1.98 (s, 3H), 1.88–1.79 (m, 1H), 1.76–1.67 (m, 1H); **¹³C NMR (100 MHz, CDCl₃)** δ = 196.3, 196.1, 170.2, 49.0, 34.3, 33.1, 30.7, 30.6, 25.6, 23.4; **HRMS (ESI)** calculated for [C₁₀H₁₈NO₃S₂]⁺ (M+H⁺) requires m/z = 264.0723, found 264.0730.

A1.5 NMR Spectra ^1H NMR (CDCl_3) and ^{13}C NMR (CDCl_3) of **A.2**

Appendix 2: Boronic Acid Inhibitors of HIV Protease

A2.1 Author Contributions

M.J.P. proposed the use of boronic acids as a way to increase HIV protease binding affinity. M.J.P. performed preliminary studies. J.C.L. synthesized and characterized HIV protease inhibitors. I.W.W. performed all other experiments and obtained an X-ray crystal structure of the HIV protease bound complex with inhibitors. K.T.F. assisted I.W.W. in structure determination. R.T.R., I.W.W. and M.J.P. planned experiments and analyzed data.

A2.2 Introduction

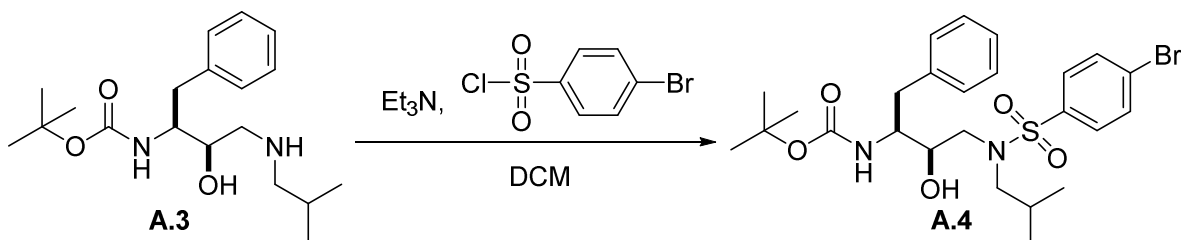
Boronic acids have shown utility in forming weak covalent bonds with organic oxyacids.¹⁹¹ Consequently, we hypothesized that the binding affinity of a small-molecule drug could be enhanced by using boronic acids to target the carboxylic acid residues of an active site.¹⁹² For our model protein • drug complex, we chose HIV protease and Amprenavir. Amprenavir has an aniline moiety that forms key hydrogen bonds with Asp29 and Asp30 of HIV protease.¹⁹³ In this study, we demonstrate that the binding affinity of Amprenavir can be enhanced by replacing the aniline amino group with a boronic acid.

A2.3 Materials and Methods

Commercial reagents were used without further purification. (2*S*,3*S*)-1,2-epoxy-3-(*boc*-amino)-4-phenylbutane was from Sigma-Aldrich (St. Louis, MO). All glassware was oven- or flame-dried, and reactions were performed under N₂(g) unless stated otherwise. Dichloromethane was dried over a column of alumina. Triethylamine was dried over a column of alumina and

purified further by passage through an isocyanate scrubbing column. Flash chromatography was performed with columns of 40–63 Å silica, 230–400 mesh (Silicycle, Québec City, Canada). Thin-layer chromatography (TLC) was performed on plates of EMD 250- μm silica 60-F₂₅₄. The term “concentrated under reduced pressure” refers to the removal of solvents and other volatile materials using a rotary evaporator at water aspirator pressure (<20 torr) while maintaining the water-bath temperature below 40 °C. Residual solvent was removed from samples at high vacuum (<0.1 torr). The term “high vacuum” refers to vacuum achieved by a mechanical belt-drive oil pump. NMR spectra were acquired at ambient temperature with a Bruker DMX-400 Avance spectrometer at the National Magnetic Resonance Facility at Madison (NMRFAM) and referenced to TMS or residual protic solvent. Electrospray ionization (ESI) mass spectrometry was performed with a Micromass LCT at the Mass Spectrometry Facility in the Department of Chemistry at the University of Wisconsin–Madison.

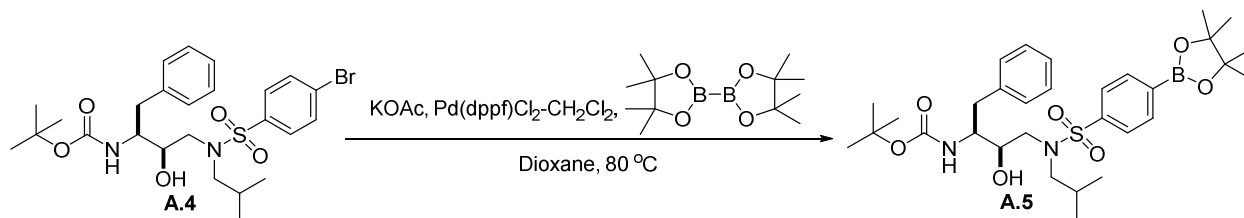
A2.4 Chemical Synthesis



A round-bottom flask containing **A.3**¹⁹⁴ (1.791 g, 5.323 mmol) was dissolved in 60 mL of dichloromethane, and the resulting solution was cooled to 0 °C. Triethylamine (1.2 mL, 8.6 mmol) and 4-bromobenzenesulfonyl chloride (1.362 g, 5.330 mmol) were then added, and the reaction mixture was left to stir overnight under an atmosphere of dry $\text{N}_2(\text{g})$. After 16 h, the reaction mixture was concentrated under reduced pressure, and the product was purified by

column chromatography (silica, 20% v/v EtOAc in hexanes), resulting in **A.4** as a white solid (2.543 g, 86%).

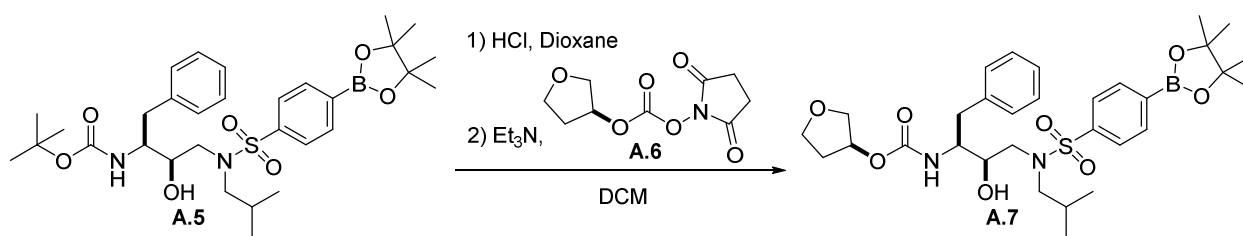
¹H NMR (400 MHz, CDCl₃) δ = 7.67–7.62 (m, 4H), 7.33–7.22 (m, 5H), 4.64 (d, J = 8.4 Hz, 1H), 3.87–3.76 (m, 3H), 3.11 (d, J = 6.1 Hz, 1H), 3.03–2.84 (m, 4H), 1.91–1.81 (m, 1H), 1.36 (s, 9H), 0.91 (d, J = 6.6 Hz, 3H), 0.88 (d, J = 6.6 Hz, 3H); **¹³C NMR (100 MHz, CDCl₃)** δ = 156.2, 137.8, 137.7, 132.5, 129.6, 128.9, 128.6, 127.9, 126.6, 79.9, 72.7, 58.4, 54.9, 53.4, 35.6, 28.4, 27.2, 20.2, 20.0; **HRMS (ESI)** calculated for [C₂₅H₃₅BrN₂O₅SNa]⁺ (M + Na⁺) requires m/z = 577.1343, found 577.1364.



A.4 (0.262 g, 0.472 mmol), KOAc (0.139 g, 1.416 mmol), bis(pinacolato)diboron (0.708 g, 0.180 mmol), and Pd(dppf)Cl₂-CH₂Cl₂ (34.54 mg, 0.0472 mmol) were placed in a dry Schlenk tube. The reaction flask was then evacuated and backfilled with N₂(g) five times. Freshly degassed 1,4-dioxane (5 mL) was then added, and the reaction mixture was heated to 80 °C and stirred for 24 h under a N₂(g) atmosphere. After 24 h, the reaction was vacuum filtered through a pad of Celite and concentrated under reduced pressure, and the product was purified by column chromatography (silica, 30% v/v EtOAc in hexanes), giving **A.5** as a white solid (0.253 g, 89%).

¹H NMR (400 MHz, CDCl₃) δ = 7.94 (d, J = 8.2 Hz, 2H), 7.75 (d, J = 8.2 Hz, 2H), 7.31–7.28 (m, 2H), 7.25–7.21 (m, 3H), 4.67 (d, J = 8.6 Hz, 1H), 3.93–3.91 (m, 1H), 3.84–3.81

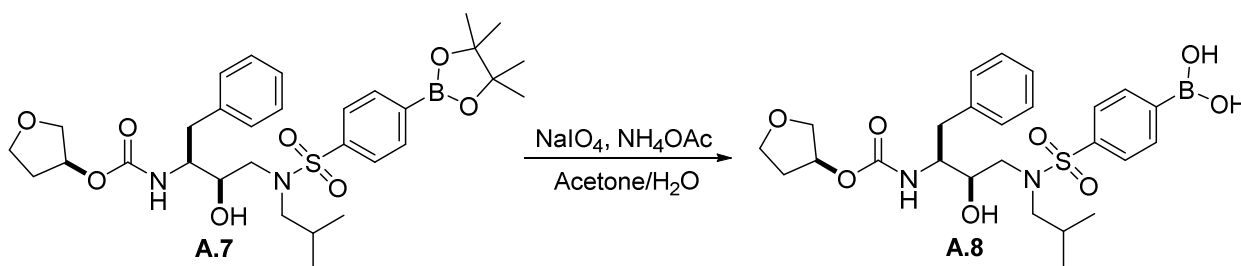
(m, 1H), 3.78–3.74 (m, 1H), 3.13–3.06 (m, 2H), 3.01–2.81 (m, 4H), 1.89–1.81 (m, 1H), 1.36 (s, 12H), 1.35 (s, 9H), 0.89 (d, $J = 6.6$ Hz, 3H), 0.86 (d, $J = 6.6$ Hz, 3H); ^{13}C NMR (100 MHz, CDCl_3) $\delta = 156.1, 140.6, 137.9, 135.5, 129.7, 128.6, 126.5, 126.4, 84.6, 79.8, 72.8, 58.6, 54.9, 53.7, 35.5, 29.8, 28.4, 27.2, 25.0, 20.2, 20.0$; HRMS (ESI) calculated for $[\text{C}_{31}\text{H}_{47}\text{BN}_2\text{O}_7\text{SNa}]^+$ ($\text{M} + \text{Na}^+$) requires $m/z = 624.3126$, found 624.3151.



To a round-bottom flask containing **A.5** (0.150 g, 0.249 mmol) was added 10 mL of 4.0 M HCl in dioxane. Precipitation occurred almost immediately as the Boc group was removed. After stirring for 4 h, the reaction mixture was purged with $\text{N}_2(\text{g})$ to remove excess $\text{HCl}(\text{g})$. Once the evolution of $\text{HCl}(\text{g})$ ceased, the reaction mixture was concentrated under reduced pressure and dried overnight under high vacuum. The residue was then dissolved in 6 mL of DCM and placed under an inert atmosphere. Triethylamine (0.17 mL, 1.2 mmol) and **A.6** (synthesized as described previously,¹⁹⁵ 0.086 g, 0.374 mmol) were then added, and the reaction mixture was stirred at room temperature overnight. After reacting for 16 h, the reaction was concentrated under reduced pressure, and the product was purified by column chromatography (silica, 50% v/v EtOAc in hexanes), yielding **A.7** as a white solid (0.121 g, 79%).

^1H NMR (400 MHz, CDCl_3) $\delta = 7.94$ (d, $J = 7.8$ Hz, 2H), 7.74 (d, $J = 7.8$ Hz, 2H), 7.32–7.28 (m, 2H), 7.25–7.21 (m, 3H), 5.12 (s, 1H), 4.85 (d, $J = 8.7$ Hz, 1H), 3.86–3.76 (m,

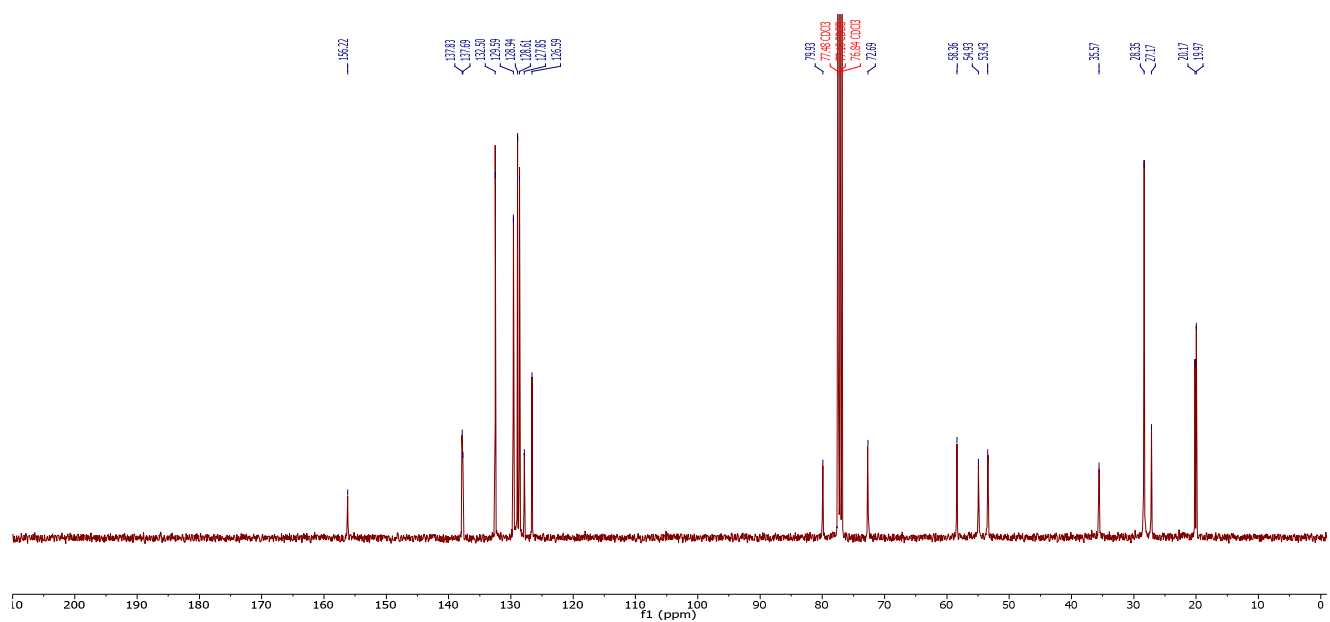
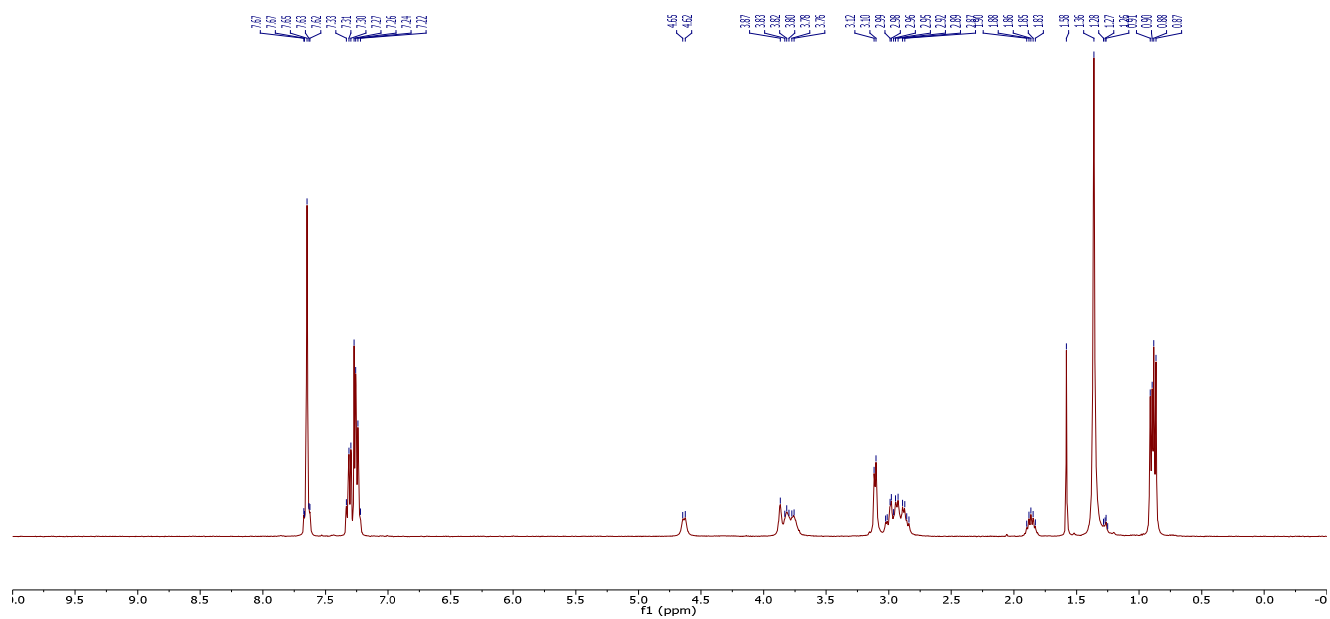
5H), 3.71–3.61 (m, 2H), 3.16–3.10 (m, 1H), 3.01–2.86 (m, 4H), 2.83–2.78 (m, 1H), 2.13–2.05 (m, 1H), 1.96–1.88 (m, 1H), 1.85–1.78 (m, 1H), 1.36 (s, 12H), 0.91 (d, $J = 6.6$ Hz, 3H), 0.86 (d, $J = 6.6$ Hz, 3H); ^{13}C NMR (100 MHz, CDCl_3) $\delta = 156.1, 140.4, 137.6, 135.5, 129.6, 128.7, 126.7, 126.4, 84.6, 75.5, 73.4, 72.6, 67.0, 58.8, 55.2, 53.8, 35.5, 32.9, 27.3, 25.0, 20.2, 20.0$; HRMS (ESI) calculated for $[\text{C}_{31}\text{H}_{49}\text{BN}_3\text{O}_8\text{SNa}]^+$ ($\text{M} + \text{NH}_4^+$) requires $m/z = 633.3365$, found 633.3386.

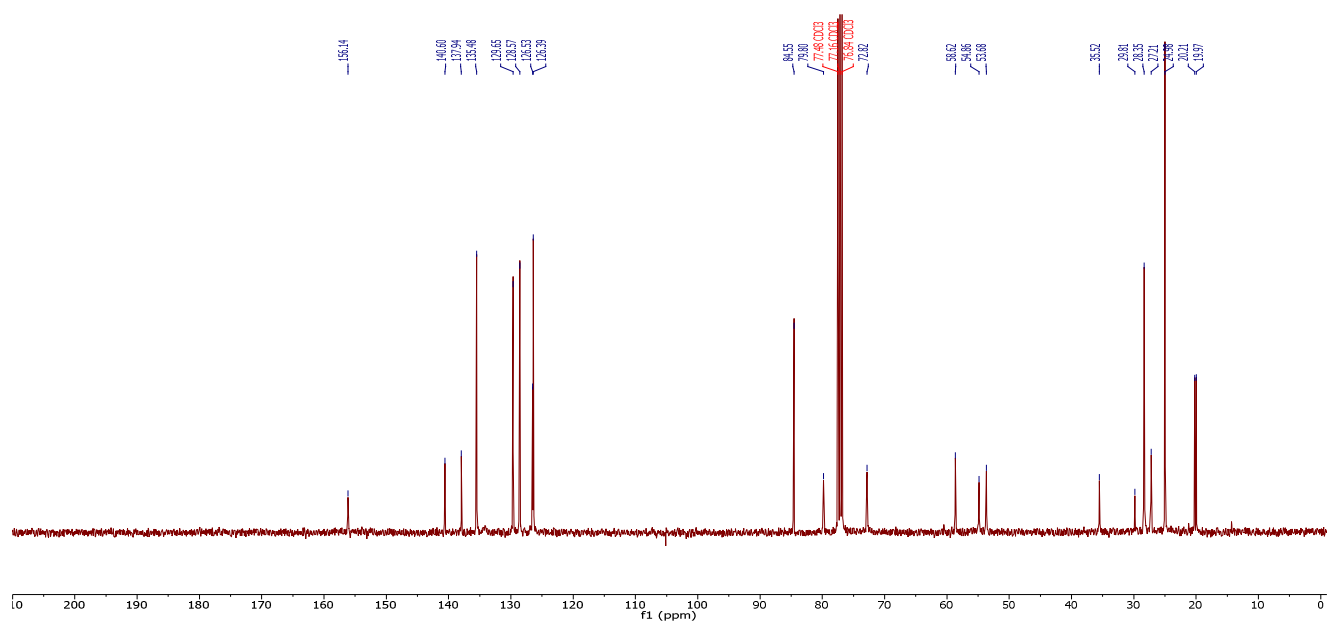
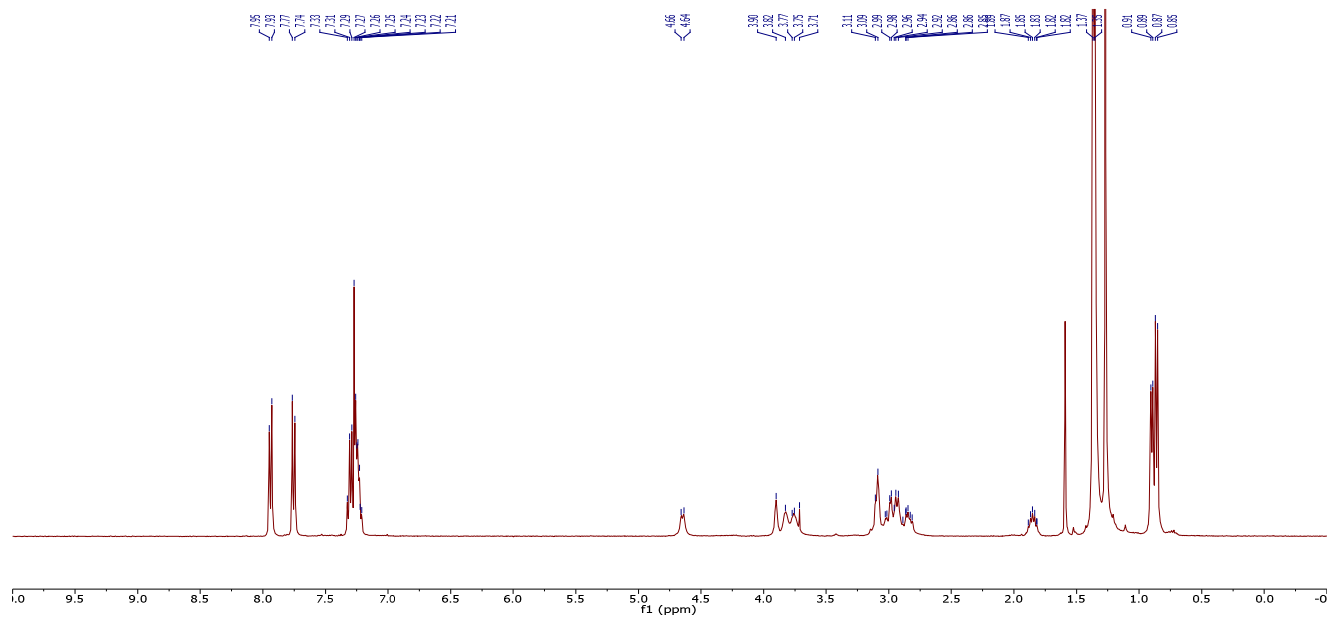


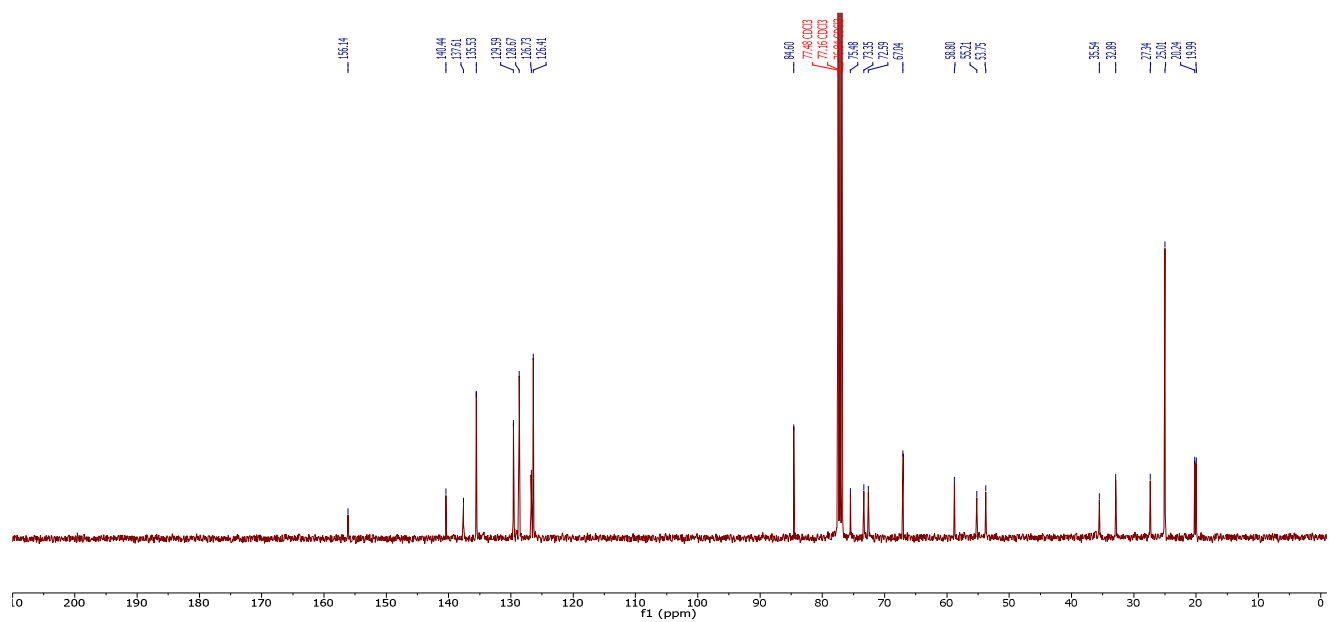
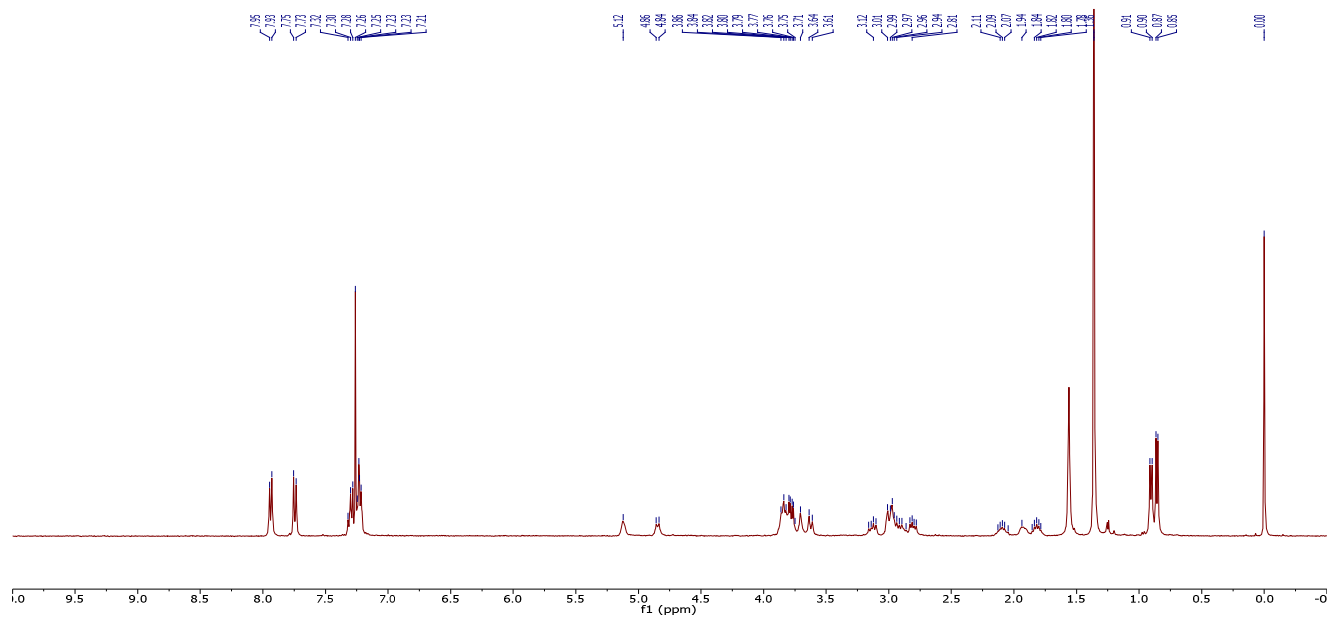
A round-bottom flask was charged with **A.7** (0.121 g, 0.196 mmol), which was dissolved in acetone (10 mL) and H_2O (10 mL). The resulting solution was placed under an atmosphere of dry $\text{N}_2(\text{g})$, and sodium periodate (0.168 g, 0.784 mmol) and ammonium acetate (60.43 mg, 0.784 mmol) were added. After stirring for 12 h, the reaction mixture was concentrated under reduced pressure, and the product was purified by column chromatography (silica, 20% v/v MeOH in DCM), giving rise to **A.8** as an off white solid (75.42 mg, 72%). An analytically pure sample of **A.8** was obtained by reverse-phase HPLC using a preparatory C18 column and a linear gradient of 10–80% v/v acetonitrile (0.1% v/v TFA) in water (0.1% v/v TFA) over 45 min. **A.8** eluted at 36 min and, after lyophilization, was isolated as a white powder.

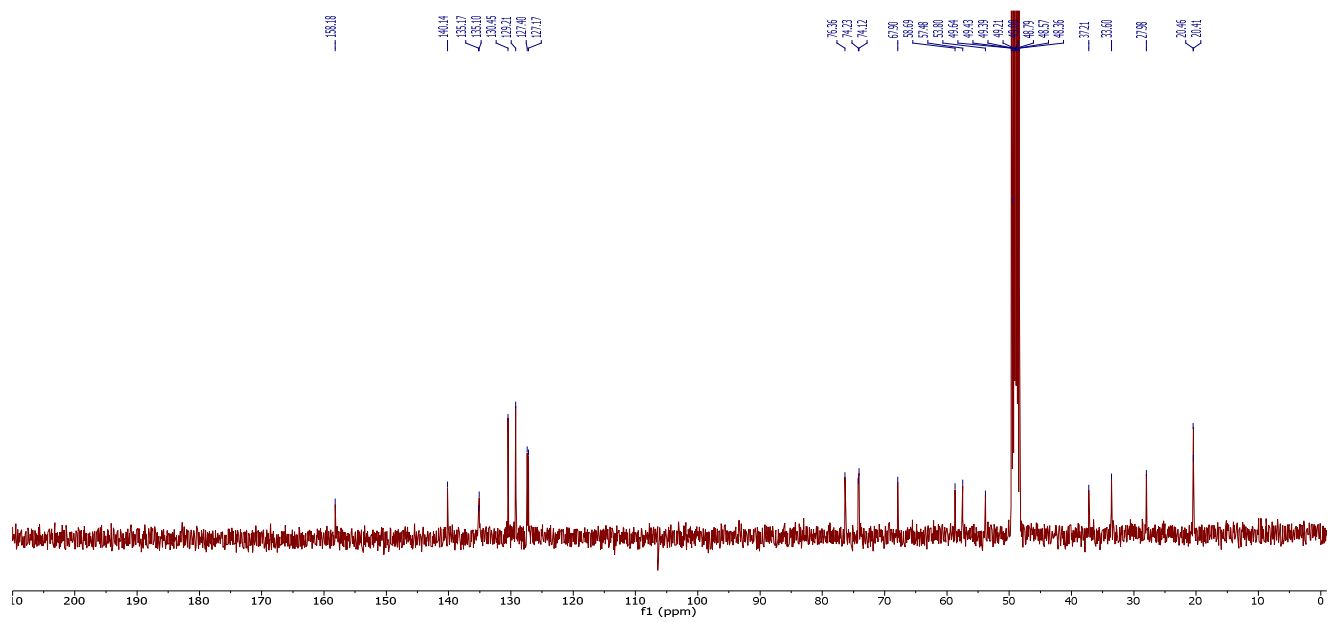
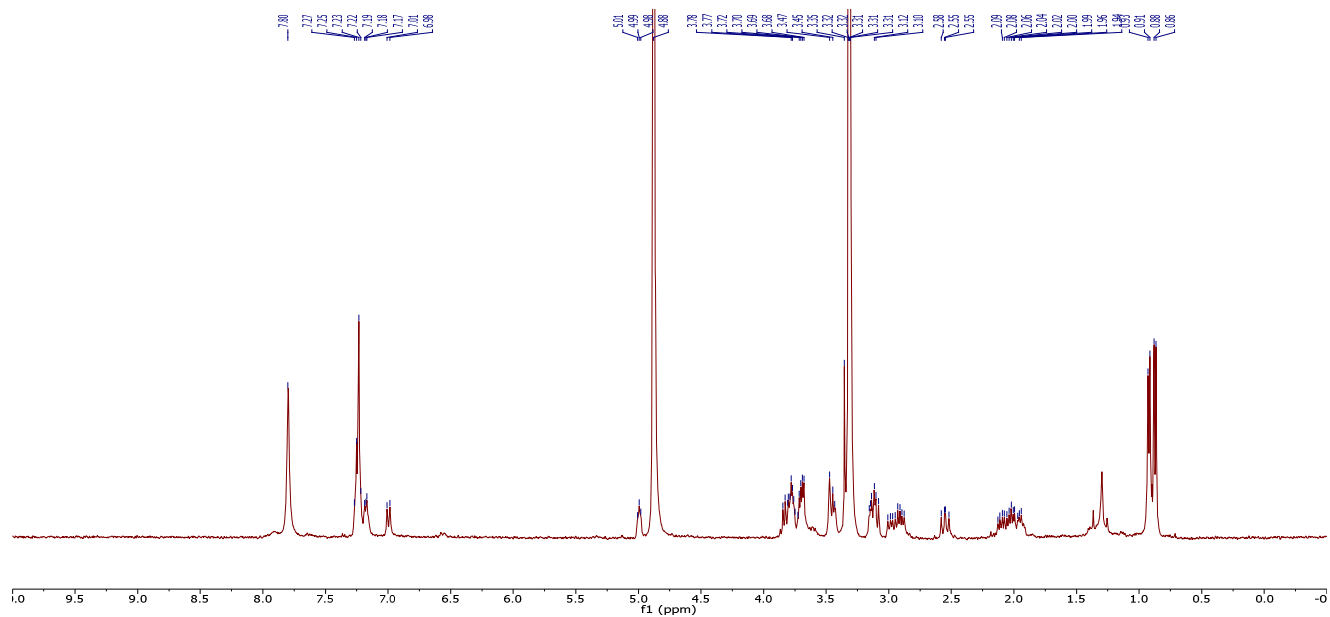
^1H NMR (400 MHz, Methanol- d_4) $\delta = 7.80$ (s, 4H), 7.27–7.22 (m, 3H), 7.19–7.15 (m, 1H), 7.00 (d, $J = 9.4$ Hz, 1H), 5.01–4.98 (m, 1H), 3.85–3.68 (m, 5H), 3.47–3.43 (m, 2H), 3.15–

3.08 (m, 2H), 2.98 (dd, $J = 15.1, 8.7$ Hz, 1H), 2.90 (dd, $J = 13.7, 6.7$ Hz, 1H), 2.55 (dd, $J = 13.8, 10.7$ Hz, 1H), 2.13–1.94 (m, 3H), 0.94 (d, $J = 6.6$ Hz, 3H), 0.86 (d, $J = 6.6$ Hz, 3H); ^{13}C NMR (100 MHz, Methanol- d_4) $\delta = 158.2, 140.1, 135.2, 135.1, 130.5, 129.2, 127.4, 127.2, 76.4, 74.2, 74.1, 67.9, 58.7, 57.5, 53.8, 37.2, 33.6, 28.0, 20.5, 20.4$; HRMS (ESI) calculated for $[\text{C}_{28}\text{H}_{42}\text{BN}_2\text{O}_9\text{S}]^-$ ($\text{M} + \text{OMe}^-$) requires $m/z = 592.2745$, found 592.2721.

A2.5 NMR Spectra ^1H NMR (CDCl_3) and ^{13}C NMR (CDCl_3) of **A.4**

^1H NMR (CDCl_3) and ^{13}C NMR (CDCl_3) of **A.5**

^1H NMR (CDCl_3) and ^{13}C NMR (CDCl_3) of **A.7**

^1H NMR (Methanol- d_4) and ^{13}C NMR (Methanol- d_4) of **A.8**

Appendix 3: Selective Disulfide-Reducing Agents for Phosphatase and Tensin Homolog (PTEN)

A3.1 Author Contributions

R.T.R. proposed the derivatization of DTBA to generate a selective disulfide-reducing agent for PTEN. K.K.W. assisted J.C.L. the synthesis and characterization of compounds. S.B.J. expressed and purified PTEN and performed all other relevant assays.

A3.2 Introduction

Phosphatase and tensin homolog (PTEN), is a cytosolic protein and a known tumor suppressor whose dysfunction is associated with many forms of cancer.¹⁹⁶⁻²⁰⁰ PTEN (Figure A3.1) contains an active-site cysteine residue (Cys124). Its thiol must remain in a reduced state for phosphatase activity. It has been shown that Cys124 is oxidized readily, forming a disulfide bond with nearby Cys71.^{201,202} This non-native disulfide inactivates the protein, resulting in the activation of downstream signaling cascades, which promote cell proliferation, survival, and tumor development.

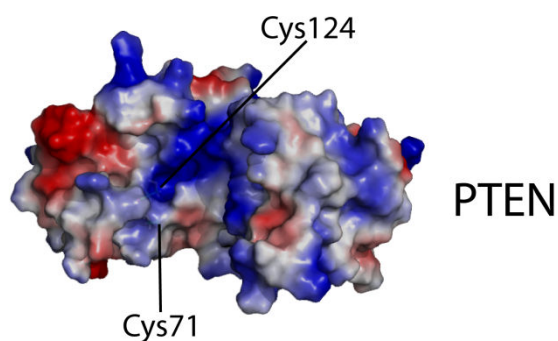


Figure A3.1 Electrostatic potential map of PTEN with red = anionic and blue = cationic, as generated by PyMOL (Schrödinger, Portland, OR). PDB: 1d5r²⁰⁰.

We recently reported on dithiobutylamine (DTBA), a novel disulfide-reducing agent with enhanced reactivity at physiological pH (See Chapter 2).⁴² The superior observed kinetics are attributable to low thiol pK_a s, likely resulting from the strong Coulombic and inductive effects of the protonated amino group of DTBA. The amino group, however, also confers the additional benefit of easy derivatization by attachment of another soluble molecule with simple reactions, such as reductive amination or *N*-acylation.⁵⁵

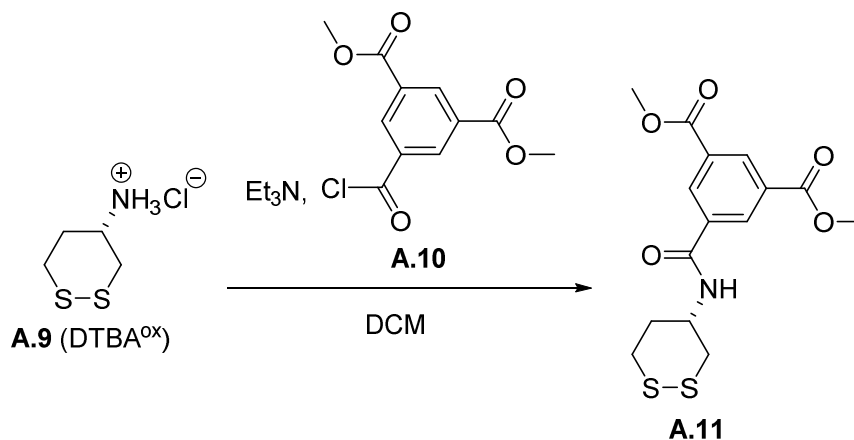
The physiological substrate of PTEN, phosphatidylinositol (3,4,5)-trisphosphate (PIP₃), is an inositol decorated with anionic phosphates that facilitate association with the cationic active-site of PTEN.^{196,202} With this in mind, we postulated that attaching a moiety to DTBA that mimics the substrate PIP₃ would result in a selective and efficient way to regenerate the activity of oxidized protein. We note that the development of additional "surgical disulfide-reducing agents" could have a profound impact on the treatment of other diseases associated with oxidative stress.

A2.3 Materials and Methods

Commercial reagents were used without further purification. Dithiobutylamine (DTBA) was from Sigma-Aldrich (St. Louis, MO). All glassware was oven- or flame-dried, and reactions were performed under N₂(g) unless stated otherwise. Dichloromethane was dried over a column of alumina. Triethylamine was dried over a column of alumina and purified further by passage through an isocyanate scrubbing column. Flash chromatography was performed with columns of 40–63 Å silica, 230–400 mesh (Silicycle, Québec City, Canada). Thin-layer chromatography (TLC) was performed on plates of EMD 250- μ m silica 60-F₂₅₄. The term "concentrated under

reduced pressure” refers to the removal of solvents and other volatile materials using a rotary evaporator at water aspirator pressure (<20 torr) while maintaining the water-bath temperature below 40 °C. Residual solvent was removed from samples at high vacuum (<0.1 torr). The term “high vacuum” refers to vacuum achieved by a mechanical belt-drive oil pump. NMR spectra were acquired at ambient temperature with a Bruker DMX-400 Avance spectrometer at the National Magnetic Resonance Facility at Madison (NMRFAM) and referenced to TMS or residual protic solvent. Electrospray ionization (ESI) mass spectrometry was performed with a Micromass LCT at the Mass Spectrometry Facility in the Department of Chemistry at the University of Wisconsin–Madison.

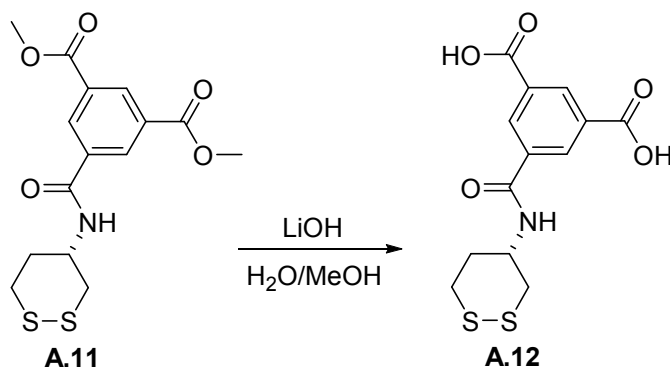
A3.4 Chemical Synthesis



A round bottom flask was charged with dichloromethane (150 mL), compound **A.9** (1.091 g, 6.354 mmol), and triethylamine (4.4 mL, 31.6 mmol), and placed under an atmosphere of dry $\text{N}_2(\text{g})$. The reaction mixture was then cooled to 0 °C, and 1.845 g (7.187 mmol) of **A.10** (which was synthesized as previously described) was added. After reacting at 0 °C for 2 h, the reaction mixture was warmed to room temperature and left to stir overnight. The reaction

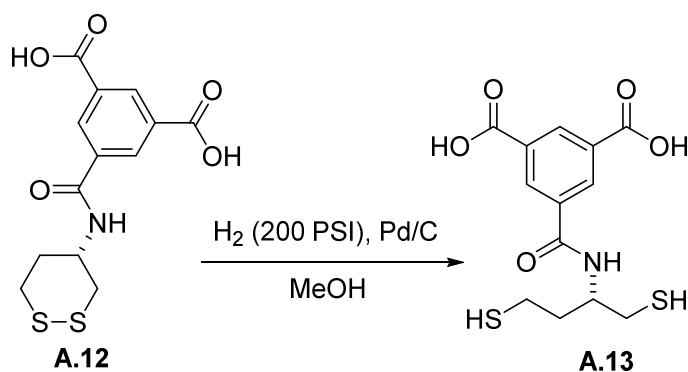
mixture was then concentrated under reduced pressure, and the product was purified by column chromatography (silica, 50% EtOAc in hexanes), resulting in **A.11** (1.716 g, 76%) as a white solid.

$^1\text{H NMR}$ (400 MHz, CDCl_3) δ = 8.82 (s, 1H), 8.62 (s, 2H), 6.66 (br, s, 1H), 4.53–4.45 (m, 1H), 3.99 (s, 6H), 3.29–3.25 (m, 1H), 3.14–3.09 (m, 1H), 3.00–2.93 (m, 1H), 2.84 (dd, J = 13.4, 7.9 Hz, 1H), 2.33–2.24 (m, 1H), 2.15–2.01 (m, 1H); $^{13}\text{C NMR}$ (100 MHz, CDCl_3) δ = 165.5, 164.4, 135.0, 133.4, 132.1, 131.3, 52.7, 46.5, 44.2, 40.9, 37.9; **HRMS** (ESI) calculated for $[\text{C}_{15}\text{H}_{18}\text{NO}_5\text{S}_2]^+$ ($\text{M} + \text{H}^+$) requires m/z = 355.05481, found 355.42918.



A round-bottom flask was charged with **A.11** (0.120 g, 0.338 mmol), which was dissolved in MeOH (15 mL) and H_2O (10 mL). Lithium hydroxide monohydrate (70.91 mg, 1.690 mmol) was then added, and the reaction mixture was stirred under $\text{N}_2(\text{g})$ overnight. After reacting for 16 h, the MeOH was removed under reduced pressure, and the resulting aqueous solution was extracted twice with 10 mL of dichloromethane. The aqueous layer was then acidified to pH 2, and the resulting white precipitate was isolated by vacuum filtration, washed with 1 M HCl and dried under high vacuum overnight, giving rise to **A.12** (78.56 mg, 71%).

¹H NMR (400 MHz, DMSO-*d*₆) δ = 13.50 (br, s, 2H), 8.93 (d, *J* = 8.0 Hz, 1H), 8.62 (s, 2H), 8.56 (s, 1H), 4.13–4.05 (m, 1H), 3.13–2.96 (m, 3H), 2.82 (t, *J* = 10.8 Hz, 1H), 2.20–2.16 (m, 1H), 1.92–1.82 (m, 1H); **¹³C NMR (100 MHz, DMSO-*d*₆)** δ = 166.2, 163.7, 135.2, 132.4, 132.1, 131.6, 48.2, 36.8, 34.5, 33.6; **HRMS (ESI)** calculated for [C₁₃H₁₄NO₅S₂]⁺ (M + H⁺) requires *m/z* = 328.0308, found 328.0311.



A.12 (78.56 mg, 0.240 mmol) and Pd/C (8.023 mg, 10 wt. % loading) were placed in a Parr reactor. 15 mL of MeOH was added, and the reaction mixture was placed under an atmosphere of H₂(g) (200 PSI) and left to stir until consumption of H₂(g) had ceased. The reaction mixture was then filtered through Celite, and concentrated under reduced pressure. The resulting residue was purified by reverse-phase HPLC using a preparatory C18 column and a linear gradient of 10–80% v/v acetonitrile (0.1% v/v TFA) in water (0.1% v/v TFA) over 45 min. **A.13** eluted at 29 min and, after lyophilization, was isolated as a white powder (67.98 mg, 86%).

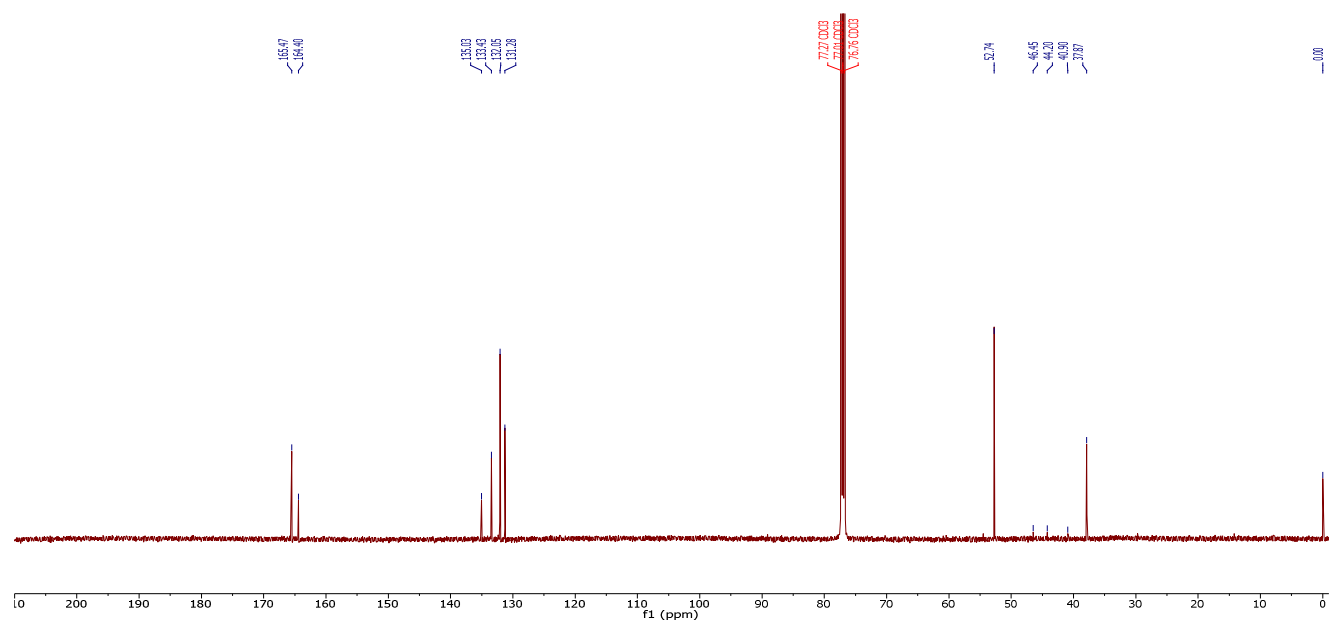
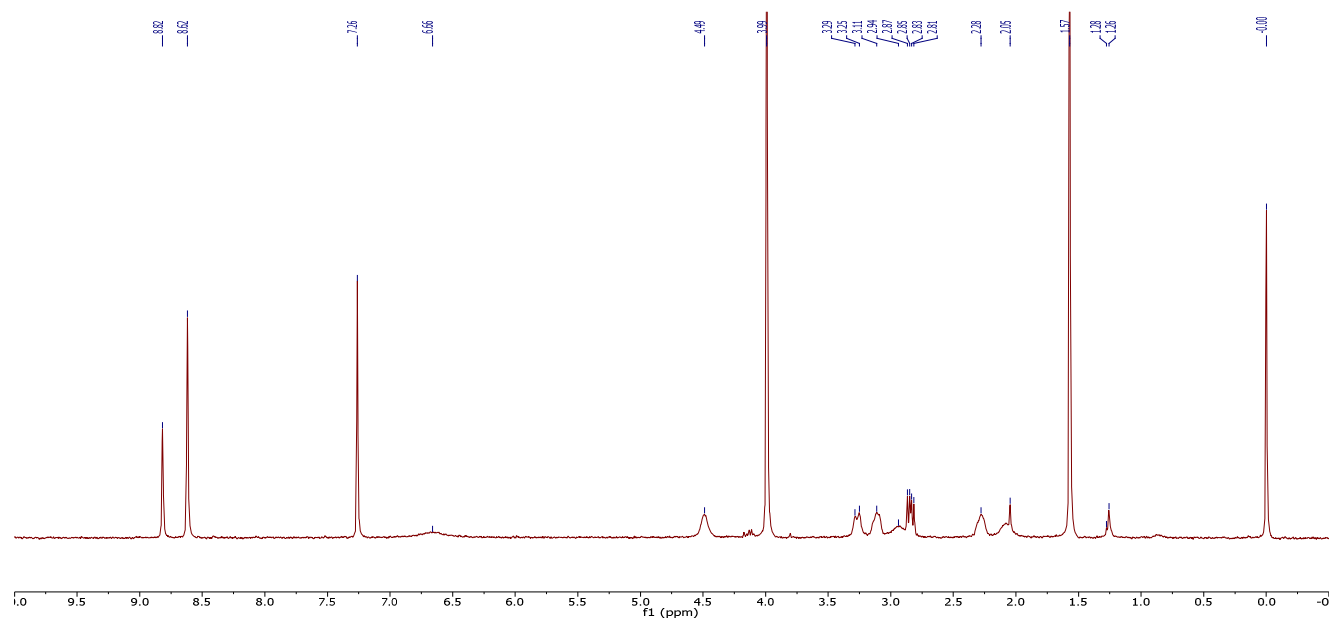
¹H NMR (400 MHz, DMSO-*d*₆) δ = 13.50 (s, 2H), 8.69–8.64 (m, 3H), 8.58 (s, 1H), 4.19–4.13 (m, 1H), 2.71 (t, *J* = 7.8 Hz, 2H), 2.40–2.34 (m, 2H), 1.93–1.85 (m, 2H); **¹³C NMR**

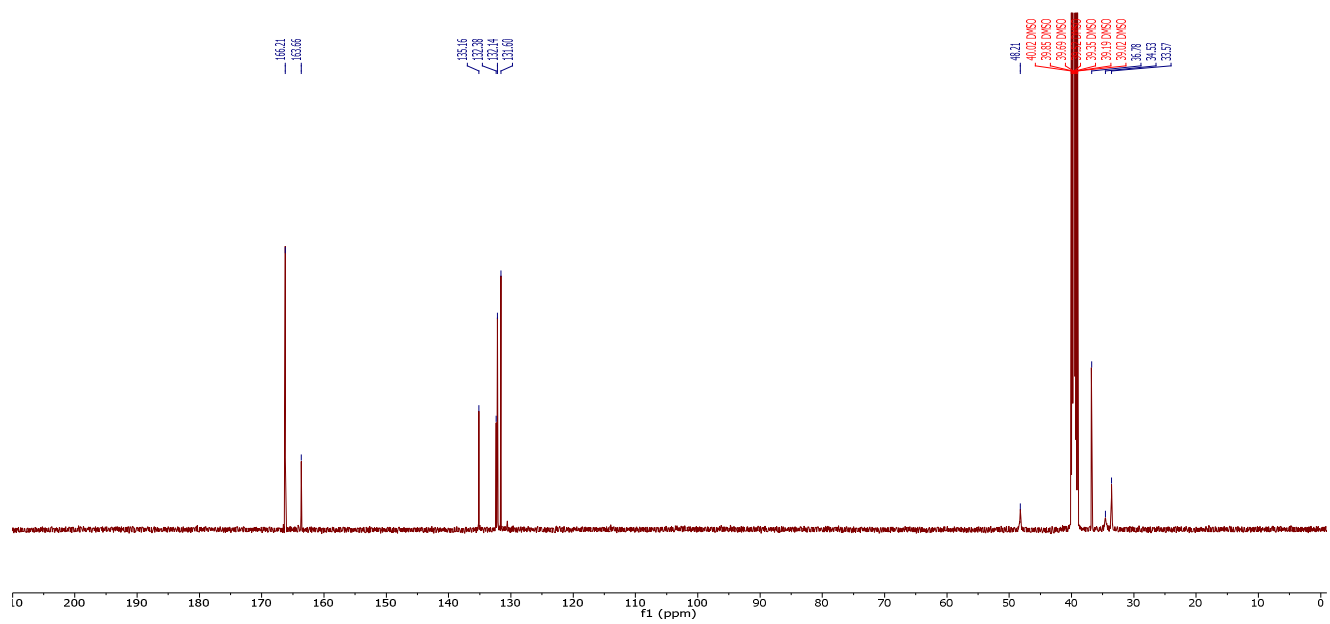
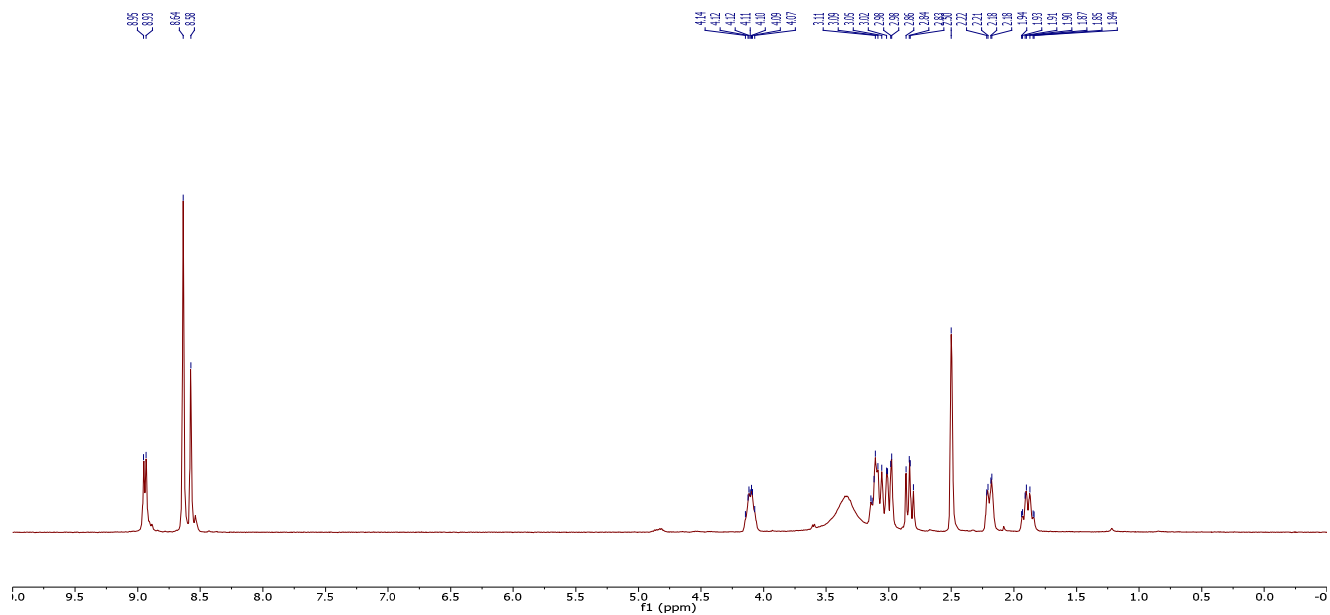
(100 MHz, DMSO-*d*₆) δ = 166.2, 164.8, 135.3, 132.2, 131.6, 131.5, 51.1, 37.1, 28.1, 20.8;

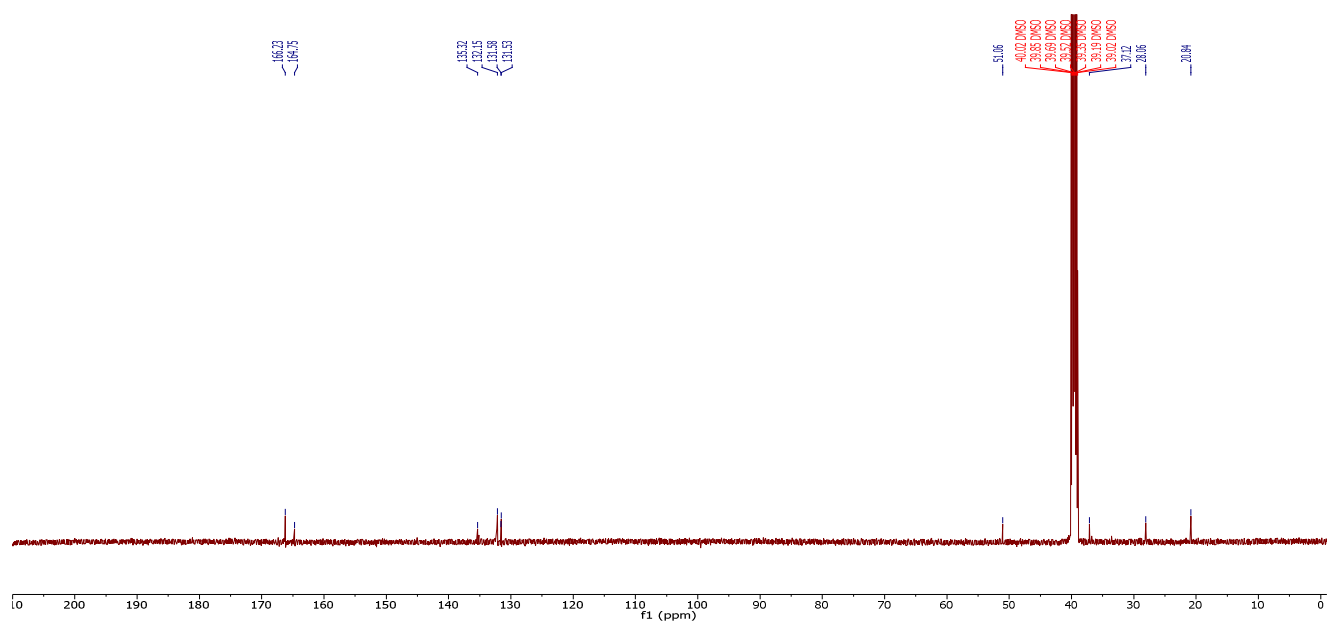
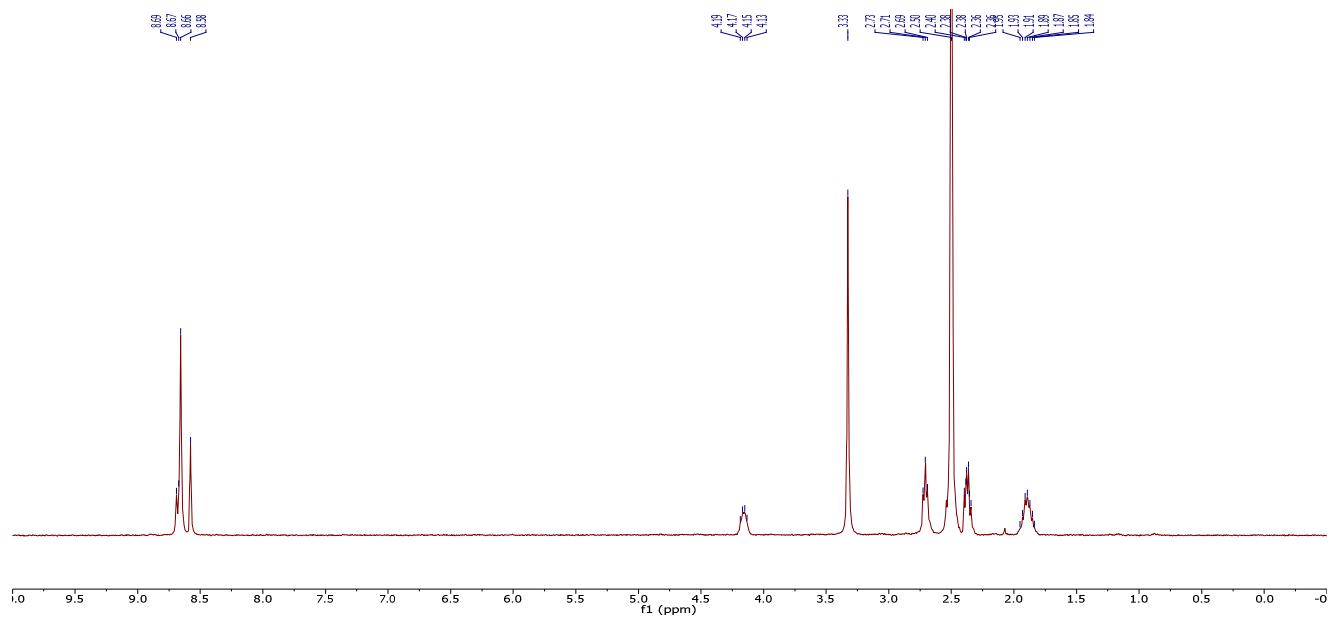
HRMS (ESI) calculated for [C₁₃H₁₆NO₅S₂]⁺ (M + H⁺) requires m/z = 330.0465, found 330.0465.

A3.5 NMR Spectra

^1H NMR (CDCl_3) and ^{13}C NMR (CDCl_3) of **A.11**



^1H NMR (DMSO- d_6) and ^{13}C NMR (DMSO- d_6) of **A.12**

^1H NMR (DMSO- d_6) and ^{13}C NMR (DMSO- d_6) of **A.13**

References

- (1) The disulfide proteome and other reactive cysteine proteomes: analysis and functional significance. Lindahl, M.; Mata-Cabana, A.; Kieselbach, T. *Antioxid. Redox Signal.* **2011**, *14*, 2581-2642.
- (2) Chemical 'omics' approaches for understanding protein cysteine oxidation in biology. Leonard, S. E.; Carroll, K. S. *Curr. Opin. Chem. Biol.* **2011**, *15*, 88-102.
- (3) Thiol–disulfide exchange in signaling: Disulfide bonds as a switch. Messens, J.; Collet, J. F. *Antioxid. Redox Signal.* **2013**, *18*, 1594-1596.
- (4) Molecular and cellular aspects of thiol–disulfide exchange. Gilbert, H. F. *Adv. Enzymol.* **1990**, *63*, 69-172.
- (5) *Biochemistry of the SH Group: The Occurrence, Chemical Properties, Metabolism and Biological Function of Thiols and Disulfides*; Jocelyn, P. C., Ed. London, U.K., 1972.
- (6) Oxidized redox state of glutathione in the endoplasmic reticulum. Hwang, C.; Sinskey, A. J.; Lodish, H. F. *Science* **1992**, *257*, 1496-1502.
- (7) Disulfide bonds: protein folding and subcellular protein trafficking. Narayan, M. *FEBS J.* **2012**, *279*, 2272-2282.
- (8) Catalysis of disulphide bond formation in the endoplasmic reticulum. Ellgaard, L. *Biochem. Soc. Trans.* **2004**, *32*, 663-667.
- (9) Forming disulfides in the endoplasmic reticulum. Oka, O. B.; Bulleid, N. J. *Biochim. Biophys. Acta* **2013**, *1833*, 2425-2429.
- (10) Contribution of disulfide bonds to the conformational stability and catalytic activity of ribonuclease A. Klink, T. A.; Woycechowsky, K. J.; Taylor, K. M.; Raines, R. T. *Eur. J. Biochem.* **2000**, *267*, 566-572.

- (11) Sulfur and selenium: the role of oxidation state in protein structure and function. Jacob, C.; Giles, G. I.; Giles, N. M.; Sies, H. *Angew. Chem. Int. Ed.* **2003**, *42*, 4742-4758.
- (12) Pathways for protein disulphide bond formation. Frand, A. R.; Cuozzo, J. W.; Kaiser, C. A. *Trends Cell Biol.* **2000**, *10*, 203-210.
- (13) Redox characteristics of the eukaryotic cytosol. Lopez-Mirabal, H. R.; Winther, J. R. *Biochim. Biophys. Acta* **2008**, *1783*, 629-640.
- (14) Simple alkanethiol groups for temporary blocking of sulfhydryl groups of enzymes. Smith, D. J.; Maggio, E. T.; Kenyon, G. L. *Biochemistry* **1975**, *14*, 766-771.
- (15) Low-molecular-weight thiols in thiol–disulfide exchange. Van Laer, K.; Hamilton, C. J.; Messens, J. *Antioxid. Redox Signal.* **2013**, *18*, 1642-1653.
- (16) Mechanism of thiolate-disulfide interchange reactions in biochemistry. Bach, R. D.; Dmitrenko, O.; Thorpe, C. *J. Org. Chem.* **2008**, *73*, 12-21.
- (17) Theoretical insights into the mechanism for thiol/disulfide exchange. Fernandes, P. A.; Ramos, M. J. *Chem. Eur. J.* **2004**, *10*, 257-266.
- (18) Chemical reduction of disulfides. Jocelyn, P. C. *Method. Enzymol.* **1987**, *143*, 246-256.
- (19) Effect of ring strain on the thiolate-disulfide exchange. A computational study. Bachrach, S. M.; Woody, J. T.; Mulhearn, D. C. *J. Org. Chem.* **2002**, *67*, 8983-8990.
- (20) Theoretical studies of the reactions of the sulfur–sulfur bond. 1. General heterolytic mechanism. Pappas, J. A. *J. Am. Chem. Soc.* **1977**, *99*, 2926-2930.
- (21) Structure reactivity relations for thiol disulfide interchange. Houk, J.; Whitesides, G. M. *J. Am. Chem. Soc.* **1987**, *109*, 6825-6836.
- (22) The scission of the sulfur–sulfur bond. Parker, A. J.; Kharasch, N. *Chem. Rev.* **1959**, *59*, 583-628.

- (23) Simple alkanethiol groups for temporary blocking of sulfhydryl groups of enzymes. Kenyon, G. L. *Biochemistry* **1975**, *14*, 766-771.
- (24) Dithiothreitol, a new protective reagent for SH groups. Cleland, W. W. *Biochemistry* **1964**, *3*, 480-482.
- (25) Highly efficient propane-1,3-dithiol mediated thiol disulfide interchange - a facile and clean methodology for S-S reduction in peptides. Ranganathan, S.; Jayaraman, N. *Chem. Commun.* **1991**, 934-936.
- (26) Selective reduction of disulfides by tris(2-Carboxyethyl)Phosphine. Burns, J. A.; Butler, J. C.; Moran, J.; Whitesides, G. M. *J. Org. Chem.* **1991**, *56*, 2648-2650.
- (27) meso-2,5-Dimercapto-*N,N,N',N'*-tetramethyladipamide: A readily available, kinetically rapid reagent for the reduction of disulfides in aqueous solution. Lees, W. J.; Singh, R.; Whitesides, G. M. *J. Org. Chem.* **1991**, *56*, 7328-7331.
- (28) A reagent for reduction of disulfide bonds in proteins that reduces disulfide bonds faster than does dithiothreitol. Singh, R.; Whitesides, G. M. *J. Org. Chem.* **1991**, *56*, 2332-2337.
- (29) Synthesis of dithiols as reducing agents for disulfides in neutral aqueous-solution and comparison of reduction potentials. Lamoureux, G. V.; Whitesides, G. M. *J. Org. Chem.* **1993**, *58*, 633-641.
- (30) Reagents for rapid reduction of native disulfide bonds in proteins. Singh, R.; Whitesides, G. M. *Bioorg. Chem.* **1994**, *22*, 109-115.
- (31) Thiol/disulfide exchange equilibria and disulfide bond stability. Gilbert, H. F. *Method. Enzymol.* **1995**, *251*, 8-28.
- (32) Reagents for rapid reduction of disulfide bonds. Singh, R.; Lamoureux, G. V.; Lees, W. J.; Whitesides, G. M. *Methods Enzymol.* **1995**, *251*, 167-173.
- (33) Nucleophilic substitution at sulfur: S_N2 or addition-elimination. Bachrach, S. M.; Mulhearn, D. C. *J. Phys. Chem.* **1996**, *100*, 3535-3540.

- (34) Rates of thiol-disulfide interchange reactions between mono - and dithiols and Ellman's reagent. Whitesides, G. M.; Lilburn, J. E.; Szajewski, R. P. *J. Org. Chem.* **1977**, *42*, 332-338.
- (35) Equilibrium and kinetic constants for the thiol disulfide interchange reaction between glutathione and dithiothreitol. Rothwarf, D. M.; Scheraga, H. A. *Proc. Natl. Acad. Sci. U.S.A.* **1992**, *89*, 7944-7948.
- (36) Rates of thiol-disulfide interchange reactions involving proteins and kinetic measurements of thiol pK_a values. Shaked, Z.; Szajewski, R. P.; Whitesides, G. M. *Biochemistry* **1980**, *19*, 4156-4166.
- (37) Rate constants and equilibrium-constants for thiol-disulfide interchange reactions involving oxidized glutathione. Szajewski, R. P.; Whitesides, G. M. *J. Am. Chem. Soc.* **1980**, *102*, 2011-2026.
- (38) Equilibrium constants for thiol-disulfide interchange reactions: A coherent, corrected set. Lees, W. J.; Whitesides, G. H. *J. Org. Chem.* **1993**, *58*, 642-647.
- (39) Predicting the stability of cyclic disulfides by molecular modeling - effective concentrations in thiol-disulfide interchange and the design of strongly reducing dithiols. Burns, J. A.; Whitesides, G. M. *J. Am. Chem. Soc.* **1990**, *112*, 6296-6303.
- (40) Degenerate intermolecular thiolate-disulfide interchange involving cyclic five-membered disulfides is faster by $\sim 10^3$ than that involving six- or seven-membered disulfides. Singh, R.; Whitesides, G. M. *J. Am. Chem. Soc.* **1990**, *112*, 6304-6309.
- (41) Pyrazine-derived disulfide-reducing agent for chemical biology. Lukesh, J. C.; Wallin, K. K.; Raines, R. T. *Chem. Commun.* **2014**, *50*, 9591-9594.
- (42) A potent, versatile disulfide-reducing agent from aspartic acid. Lukesh, J. C.; Palte, M. J.; Raines, R. T. *J. Am. Chem. Soc.* **2012**, *134*, 4057-4059.
- (43) Microwave-mediated reduction of disulfide bridges with supported (tris(2-carboxyethyl)phosphine) as resin-bound reducing agent. Miralles, G.; Verdie, P.; Puget, K.; Maurras, A.; Martinez, J.; Subra, G. *ACS Comb. Sci.* **2013**, *15*, 169-173.

- (44) On-line cleavage of disulfide bonds by soluble and immobilized tris-(2-carboxyethyl)phosphine using sequential injection analysis. Tzanavaras, P. D.; Mitani, C.; Anthemidis, A.; Themelis, D. G. *Talanta* **2012**, *96*, 21-25.
- (45) New water-soluble phosphines as reductants of peptide and protein disulfide bonds: reactivity and membrane permeability. Cline, D. J.; Redding, S. E.; Brohawn, S. G.; Psathas, J. N.; Schneider, J. P.; Thorpe, C. *Biochemistry* **2004**, *43*, 15195-15203.
- (46) A procedure for quantitative determination of tris(2-carboxyethyl)phosphine, an odorless reducing agent more stable and effective than dithiothreitol. Han, J. C.; Han, Y. H. *Anal. Biochem.* **1994**, *220*, 5-10.
- (47) A tris (2-carboxyethyl) phosphine (TCEP) related cleavage on cysteine-containing proteins. Liu, P.; O'Mara, B. W.; Warrack, B. M.; Wu, W.; Huang, Y.; Zhang, Y.; Zhao, R.; Lin, M.; Ackerman, M. S.; Hocknell, P. K.; Chen, G.; Tao, L.; Rieble, S.; Wang, J.; Wang-Iverson, D. B.; Tymiak, A. A.; Grace, M. J.; Russell, R. J. *J. Am. Soc. Mass Spectrom.* **2010**, *21*, 837-844.
- (48) Some new reactions of organic disulfides, and the oxidation of organic compounds in the presence of disulfides. Schonberg, A. *Chem. Ber.* **1935**, *68*, 163-164.
- (49) Convenient supported recyclable material based on dihydrolipoil-residue for the reduction of disulfide derivatives. Bienvenu, C.; Greiner, J.; Vierling, P.; Di Giorgio, C. *Tetrahedron Lett.* **2010**, *51*, 3309-3311.
- (50) *N*-propyldihydrolipoamide glass beads. An immobilized reducing agent. Scouten, W. H.; Firestone, G. L. *Biochim. Biophys. Acta* **1976**, *453*, 277-284.
- (51) Polymer-bound dihydrolipoic acid: A new insoluble reducing agent for disulfides. Gorecki, M.; Patchornik, A. *Biochim. Biophys. Acta* **1973**, *303*, 36-43.
- (52) Reductive cleavage of aromatic disulfides using a polymer-supported phosphine reagent. Amos, R. A.; Fawcett, S. M. *J. Org. Chem.* **1984**, *49*, 2637-2639.
- (53) Redox-active polymers: synthesis and exchange reaction of amino compounds containing cyclic disulfide. Casolaro, M.; Busi, E. *Polymer* **1994**, *35*, 360-366.

- (54) Catalysis of protein folding by an immobilized small-molecule dithiol. Woycechowsky, K. J.; Hook, B. A.; Raines, R. T. *Biotechnol. Progr.* **2003**, *19*, 1307-1314.
- (55) Thiols and selenols as electron-relay catalysts for disulfide-bond reduction. Lukesh, J. C., 3rd; Vanveller, B.; Raines, R. T. *Angew. Chem. Int. Ed.* **2013**, *52*, 12901-12904.
- (56) Comparisons of rate constants for thiolate-disulfide interchange in water and in polar aprotic solvents using dynamic ¹H NMR line shape analysis. Singh, R.; Whitesides, G. M. *J. Am. Chem. Soc.* **1990**, *112*, 1190-1197.
- (57) Selenols catalyze the interchange reactions of dithiols and disulfides in water. Singh, R.; Whitesides, G. M. *J. Org. Chem.* **1991**, *56*, 6931-6933.
- (58) Strategic use of non-native diselenide bridges to steer oxidative protein folding. Metanis, N.; Hilvert, D. *Angew. Chem. Int. Ed.* **2012**, *51*, 5585-5588.
- (59) Catalytic selenols couple the redox cycles of metallothionein and glutathione. Chen, Y.; Maret, W. *Eur. J. Biochem.* **2001**, *268*, 3346-3353.
- (60) Labeling of antibodies by in situ modification of thiol groups generated from selenol-catalyzed reduction of native disulfide bonds. Singh, R.; Maloney, E. K. *Anal. Biochem.* **2002**, *304*, 147-156.
- (61) Catalysis of oxidative protein folding by small-molecule diselenides. Beld, J.; Woycechowsky, K. J.; Hilvert, D. *Biochemistry* **2008**, *47*, 6985-6987.
- (62) Integrated oxidative folding of cysteine/selenocysteine containing peptides: improving chemical synthesis of conotoxins. Walewska, A.; Zhang, M. M.; Skalicky, J. J.; Yoshikami, D.; Olivera, B. M.; Bulaj, G. *Angew. Chem. Int. Ed.* **2009**, *48*, 2221-2224.
- (63) Selenogluthathione: efficient oxidative protein folding by a diselenide. Beld, J.; Woycechowsky, K. J.; Hilvert, D. *Biochemistry* **2007**, *46*, 5382-5390.
- (64) Diselenides as universal oxidative folding catalyts. Beld, J.; Woycechowsky, K. J.; Hilvert, D. *J. Biotechnol.* **2010**, *150*, 481-489.

- (65) Reagentless oxidative folding of disulfide-rich peptides catalyzed by an intramolecular diselenide. Steiner, A. M.; Woycechowsky, K. J.; Olivera, B. M.; Bulaj, G. *Angew. Chem. Int. Ed.* **2012**, *51*, 5580-5584.
- (66) Selenium and sulfur in exchange reactions: a comparative study. Steinmann, D.; Nauser, T.; Koppenol, W. H. *J. Org. Chem.* **2010**, *75*, 6696-6699.
- (67) Catalysis of reduction of disulfide by selenol. Singh, R.; Kats, L. *Anal. Biochem.* **1995**, *232*, 86-91.
- (68) Methods in selenium chemistry. 2. Bis(Methoxymagnesium) diselenide a novel reagent for introduction of selenium into organic molecules. Gunther, W. H. H. *J. Org. Chem.* **1967**, *32*, 3929-3939.
- (69) Methods in selenium chemistry. 4. Synthetic approaches to polydiselenides. Gunther, W. H. H.; Salzman, M. N. *Ann. N.Y. Acad. Sci.* **1972**, *192*, 25-43.
- (70) Chemistry of biologically important synthetic organoselenium compounds. Muges, G.; du Mont, W. W.; Sies, H. *Chem. Rev.* **2001**, *101*, 2125-2179.
- (71) Identification and characterization of a selenoprotein family containing a diselenide bond in a redox motif. Shchedrina, V. A.; Novoselov, S. V.; Malinouski, M. Y.; Gladyshev, V. N. *Proc. Natl. Acad. Sci. U.S.A.* **2007**, *104*, 13919-13924.
- (72) Selenoproteins-What unique properties can arise with selenocysteine in place of cysteine. Arner, E. S. J. *Exp. Cell. Res.* **2010**, *316*, 1296-1303.
- (73) Differing views of the role of selenium in thioredoxin reductase. Hondal, R. J.; Ruggles, E. L. *Amino Acids* **2011**, *41*, 73-89.
- (74) Why do proteins use selenocysteine instead of cysteine. Nauser, T.; Steinmann, D.; Koppenol, W. H. *Amino Acids* **2012**, *42*, 39-44.
- (75) Why selenocysteine replaces cysteine in thioredoxin reductase: A radical hypothesis. Nauser, T.; Steinmann, D.; Grassi, G.; Koppenol, W. H. *Biochemistry* **2014**, *In press*.

- (76) Selenocysteine in thiol/disulfide-like exchange reactions. Hondal, R. J.; Marino, S. M.; Gladyshev, V. N. *Antioxid. Redox Signal.* **2013**, *18*, 1675-1689.
- (77) Compensating for the absence of selenocysteine in high-molecular weight thioredoxin reductases: the electrophilic activation hypothesis. Lothrop, A. P.; Snider, G. W.; Flemer, S., Jr.; Ruggles, E. L.; Davidson, R. S.; Lamb, A. L.; Hondal, R. J. *Biochemistry* **2014**, *53*, 664-674.
- (78) Selenocysteine confers resistance to inactivation by oxidation in thioredoxin reductase: comparison of selenium and sulfur enzymes. Snider, G. W.; Ruggles, E.; Khan, N.; Hondal, R. J. *Biochemistry* **2013**, *52*, 5472-5481.
- (79) Selenium as an electron acceptor during the catalytic mechanism of thioredoxin reductase. Lothrop, A. P.; Snider, G. W.; Ruggles, E. L.; Patel, A. S.; Lees, W. J.; Hondal, R. J. *Biochemistry* **2014**, *53*, 654-663.
- (80) Resolution of oxidative stress by thioredoxin reductase: Cysteine versus selenocysteine. Cunniff, B.; Snider, G. W.; Fredette, N.; Stumpff, J.; Hondal, R. J.; Heintz, N. H. *Redox Biol.* **2014**, *2*, 475-484.
- (81) Multienzyme complexes. Reed, L. J. *Acc. Chem. Res.* **1974**, *7*, 40-46.
- (82) Disulfide bond formation in prokaryotes: History, diversity and design. Hatahet, F.; Boyd, D.; Beckwith, J. *Biochim. Biophys. Acta* **2014**, *1844*, 1402-1414.
- (83) Competition between glutathione and protein thiols for disulphide-bond formation. Cuozzo, J. W.; Kaiser, C. A. *Nat. Cell. Biol.* **1999**, *1*, 130-135.
- (84) Native disulfide bond formation in proteins. Woycechowsky, K. J.; Raines, R. T. *Curr. Opin. Chem. Biol.* **2000**, *4*, 533-539.
- (85) Catalysis of protein folding by protein disulfide isomerase and small-molecule mimics. Kersteen, E. A.; Raines, R. T. *Antioxid. Redox Signal.* **2003**, *5*, 413-424.

- (86) Protein disulfide isomerase: the structure of oxidative folding. Gruber, C. W.; Cemazar, M.; Heras, B.; Martin, J. L.; Craik, D. J. *Trends Biochem. Sci.* **2006**, *31*, 455-464.
- (87) The crystal structure of yeast protein disulfide isomerase suggests cooperativity between its active sites. Tian, G.; Xiang, S.; Noiva, R.; Lennarz, W. J.; Schindelin, H. *Cell* **2006**, *124*, 61-73.
- (88) Combinations of protein-disulfide isomerase domains show that there is little correlation between isomerase activity and wild-type growth. Xiao, R.; Solovyov, A.; Gilbert, H. F.; Holmgren, A.; Lundstrom-Ljung, J. *J. Biol. Chem.* **2001**, *276*, 27975-27980.
- (89) An introduction to thiol redox proteins in the endoplasmic reticulum and a review of current electrochemical methods of detection of thiols. Kruusma, J.; Benham, A. M.; Williams, J. A.; Katakly, R. *Analyst* **2006**, *131*, 459-473.
- (90) Structure and function of DsbA, a key bacterial oxidative folding catalyst. Shouldice, S. R.; Heras, B.; Walden, P. M.; Totsika, M.; Schembri, M. A.; Martin, J. L. *Antioxid. Redox Signal.* **2011**, *14*, 1729-1760.
- (91) Protein disulfide isomerases exploit synergy between catalytic and specific binding domains. Freedman, R. B.; Klappa, P.; Ruddock, L. W. *EMBO Rep.* **2002**, *3*, 136-140.
- (92) The crystal structure of the protein-disulfide isomerase family member ERp27 provides insights into its substrate binding capabilities. Kober, F. X.; Koelmel, W.; Kuper, J.; Drechsler, J.; Mais, C.; Hermanns, H. M.; Schindelin, H. *J. Biol. Chem.* **2013**, *288*, 2029-2039.
- (93) Structure of TcpG, the DsbA protein folding catalyst from *Vibrio cholerae*. Hu, S. H.; Peek, J. A.; Rattigan, E.; Taylor, R. K.; Martin, J. L. *J. Mol. Biol.* **1997**, *268*, 137-146.
- (94) Crystal structure of the DsbA protein required for disulphide bond formation *in vivo*. Martin, J. L.; Bardwell, J. C.; Kuriyan, J. *Nature* **1993**, *365*, 464-468.
- (95) Crystal structures of human Ero1alpha reveal the mechanisms of regulated and targeted oxidation of PDI. Inaba, K.; Masui, S.; Iida, H.; Vavassori, S.; Sitia, R.; Suzuki, M. *EMBO J.* **2010**, *29*, 3330-3343.

- (96) The essential function of protein-disulfide isomerase is to unscramble non-native disulfide bonds. Laboissiere, M. C.; Sturley, S. L.; Raines, R. T. *J. Biol. Chem.* **1995**, *270*, 28006-28009.
- (97) Sulfhydryl oxidation, not disulfide isomerization, is the principal function of protein disulfide isomerase in yeast *Saccharomyces cerevisiae*. Solovyov, A.; Xiao, R.; Gilbert, H. F. *J. Biol. Chem.* **2004**, *279*, 34095-34100.
- (98) The uncharged surface features surrounding the active site of *Escherichia coli* DsbA are conserved and are implicated in peptide binding. Guddat, L. W.; Bardwell, J. C.; Zander, T.; Martin, J. L. *Protein Sci.* **1997**, *6*, 1148-1156.
- (99) Protein disulfide isomerase overexpression increases secretion of foreign proteins in *Saccharomyces cerevisiae*. Robinson, A. S.; Hines, V.; Wittrup, K. D. *Biotechnology* **1994**, *12*, 381-384.
- (100) Solution structure of the bb' domains of human protein disulfide isomerase. Denisov, A. Y.; Maattanen, P.; Dabrowski, C.; Kozlov, G.; Thomas, D. Y.; Gehring, K. *FEBS J.* **2009**, *276*, 1440-1449.
- (101) The CXXC motif: a rheostat in the active site. Chivers, P. T.; Prehoda, K. E.; Raines, R. T. *Biochemistry* **1997**, *36*, 4061-4066.
- (102) The CXXC motif: imperatives for the formation of native disulfide bonds in the cell. Chivers, P. T.; Laboissiere, M. C. A.; Raines, R. T. *Embo. J.* **1996**, *15*, 2659-2667.
- (103) The CXXC motif: crystal structure of an active-site variant of *Escherichia coli* thioredoxin. Schultz, L. W.; Chivers, P. T.; Raines, R. T. *Acta Crystallogr. D Biol. Crystallogr.* **1999**, *55*, 1533-1538.
- (104) The reactivities and ionization properties of the active-site dithiol groups of mammalian protein disulphide-isomerase. Hawkins, H. C.; Freedman, R. B. *Biochem. J.* **1991**, *275*, 335-339.

- (105) Determination of the reduction-oxidation potential of the thioredoxin-like domains of protein disulfide-isomerase from the equilibrium with glutathione and thioredoxin. Lundstrom, J.; Holmgren, A. *Biochemistry* **1993**, *32*, 6649-6655.
- (106) Refolding of recombinant proteins. De Bernardez Clark, E. *Curr. Opin. Biotechnol.* **1998**, *9*, 157-163.
- (107) The purification of eukaryotic polypeptides synthesized in *Escherichia coli*. Marston, F. A. O. *Biochem. J.* **1986**, *240*, 1-12.
- (108) On the cysteine and cystine content of proteins. Differences between intracellular and extracellular proteins. Fahey, R. C.; Hunt, J. S.; Windham, G. C. *J. Mol. Evol.* **1977**, *10*, 155-160.
- (109) Disulfide bridges in globular proteins. Thorton, J. M. *J. Mol. Biol.* **1981**, *151*, 261-287.
- (110) Going non-native to improve oxidative protein folding. Lees, W. J. *ChemBioChem* **2012**, *13*, 1725-1727.
- (111) Effects of redox buffer properties on the folding of a disulfide-containing protein: Dependence upon pH, thiol pK_a, and thiol concentration. Gough, J. D.; Lees, W. J. *J. Biotechnol.* **2005**, *115*, 279-290.
- (112) Oxidative folding of lysozyme with aromatic dithiols, and aliphatic and aromatic monothiols. Patel, A. S.; Lees, W. J. *Bioorg. Med. Chem.* **2012**, *20*, 1020-1028.
- (113) Increased catalytic activity of protein disulfide isomerase using aromatic thiol based redox buffers. Gough, J. D.; Lees, W. J. *Bioorgan. Med. Chem.* **2005**, *15*, 777-781.
- (114) Aromatic thiol pK_a effects on the folding rate of a disulfide containing protein. Gough, J. D.; Gargano, J. M.; Donofrio, A. E.; Lees, W. J. *Biochemistry* **2003**, *42*, 11787-11797.
- (115) Ortho- and meta-substituted aromatic thiols are efficient redox buffers that increase the folding rate of a disulfide-containing protein. Gough, J. D.; Barrett, E. J.; Silva, Y.; Lees, W. J. *J. Biotechnol.* **2006**, *125*, 39-47.

- (116) A small-molecule catalyst of protein folding *in vitro* and *in vivo*. Woycechowsky, K. J.; Wittrup, K. D.; Raines, R. T. *Chem. Biol.* **1999**, *6*, 871-879.
- (117) The CXC motif: A functional mimic of protein disulfide isomerase. Woycechowsky, K. J.; Raines, R. T. *Biochemistry* **2003**, *42*, 5387-5394.
- (118) Peptide disulfides CGC and RKCGC facilitate oxidative protein refolding. Wang, G. Z.; Dong, X. Y.; Sun, Y. *Biochem. Eng. J.* **2011**, *55*, 169-175.
- (119) Peptide disulfide RKCGCFF facilitates oxidative protein refolding by mimicking protein disulfide isomerase. Liu, H.; Dong, X. Y.; Sun, Y. *Biochem. Eng. J.* **2013**, *79*, 29-32.
- (120) Prediction of disulfide-bonded cysteines in proteomes with a hidden neural network. Martelli, P. L.; Fariselli, P.; Casadio, R. *Proteomics* **2004**, *4*, 1665-1671.
- (121) A comparison between the sulfhydryl reductants tris(2-carboxyethyl)phosphine and dithiothreitol for use in protein biochemistry. Getz, E. B.; Xiao, M.; Chakrabarty, T.; Cooke, R.; Selvin, P. R. *Anal. Biochem.* **1999**, *273*, 73-80.
- (122) Organo-sulfur mechanisms. 5. Lone pair-lone pair interactions in unsymmetrical systems - RSSR Vs RSOR. Snyder, J. P.; Carlsen, L. *J. Am. Chem. Soc.* **1977**, *99*, 2931-2942.
- (123) Directional preferences of nonbonded atomic contacts with divalent sulfur. 1. electrophiles and nucleophiles. Rosenfield, R. E.; Parthasarathy, R.; Dunitz, J. D. *J. Am. Chem. Soc.* **1977**, *99*, 4860-4862.
- (124) Kinetics and equilibria of thiol disulfide interchange reactions of selected biological thiols and related molecules with oxidized glutathione. Keire, D. A.; Strauss, E.; Guo, W.; Noszal, B.; Rabenstein, D. L. *J. Org. Chem.* **1992**, *57*, 123-127.
- (125) Dithiols. Part III. Derivatives of polyhydric alcohols. Evans, R. M.; Fraser, J. B.; Owen, L. N. *J. Chem. Soc.* **1949**, 248-255.
- (126) Oligopeptide biases in protein sequences and their use in predicting protein coding regions in nucleotide sequences. McCaldon, P.; Argos, P. *Proteins* **1988**, *4*, 99-122.

- (127) Design and synthesis of a novel site-directing reducing agent for the disulfide bond involved in the acetylcholine binding site of the AChR. Kessler, P.; Servent, D.; Hirth, C. *Tetrahedron Lett.* **1994**, *35*, 7237-7240.
- (128) Preparation of carboxylic esters and phosphoric esters by the activation of alcohols. Mitsunobu, O.; Masahiko, E. *Bull. Chem. Soc. Jpn.* **1971**, *44*, 3427-3430.
- (129) The acid strength of the -SH group in cysteine and related compounds. Benesch, R. E.; Benesch, R. *J. Am. Chem. Soc.* **1955**, *77*, 5877-5881.
- (130) Reactivity of small thiolate anions and cysteine-25 in papain toward methyl methanethiosulfonate. Roberts, D. D.; Lewis, S. D.; Ballou, D. P.; Olson, S. T.; Shafer, J. A. *Biochemistry* **1986**, *25*, 5595-5601.
- (131) An amplified assay for thiols based on reactivation of papain. Singh, R.; Blattler, W. A.; Collinson, A. R. *Anal. Biochem.* **1993**, *213*, 49-56.
- (132) On the size of the active site in proteases. I. Papain. Schechter, I.; Berger, A. *Biochem. Biophys. Res. Commun.* **1967**, *27*, 157-162.
- (133) Structure of monoclinic papain at 1.60 Å resolution. Pickersgill, R. W.; Harris, G. W.; Garman, E. *Acta Crystallogr., Sect. B* **1992**, *48*, 59-67.
- (134) Crystal structure of rabbit muscle creatine kinase. Rao, J. K.; Bujacz, G.; Wlodawer, A. *FEBS Lett.* **1998**, *439*, 133-137.
- (135) Rabbit muscle creatine-phosphokinase - cDNA cloning, primary structure, and detection of human homologs. Putney, S.; Herlihy, W.; Royal, N.; Pang, H.; Aposhian, H. V.; Pickering, L.; Belagaje, R.; Biemann, K.; Page, D.; Kubly, S.; Schimmel, P. *J. Biol. Chem.* **1984**, *259*, 4317-4320.
- (136) Rabbit muscle creatine kinase: Consequences of the mutagenesis of conserved histidine residues. Chen, L. H.; Borders, C. L.; Vasquez, J. R.; Kenyon, G. L. *Biochemistry* **1996**, *35*, 7895-7902.

- (137) Inactivation of rabbit muscle creatine kinase by reversible formation of an internal disulfide bond induced by the fungal toxin gliotoxin. Hurne, A. M.; Chai, C. L. L.; Waring, P. *J. Biol. Chem.* **2000**, *275*, 25202-25206.
- (138) *The Protein Protocols Handbook*; 3rd ed.; Walker, J. M., Ed.; Humana Press: Totowa, NJ, 2009.
- (139) *Purifying Proteins for Proteomics: A Laboratory Manual*. Simpson, R. J.; Cold Spring Harbor Laboratory Press, 2004.
- (140) Kinetics of papain-catalyzed hydrolysis of alpha-N-benzoyl-L-arginine-p-nitroanilide. Mole, J. E.; Horton, H. R. *Biochemistry* **1973**, *12*, 816-822.
- (141) *Oxidative Folding of Peptides and Proteins*; Buchner, J.; Moroder, L., Eds.; The Royal Society of Chemistry: Cambridge, UK, 2009.
- (142) Protein disulfide bond formation in prokaryotes. Kadokura, H.; Katzen, F.; Beckwith, J. *Annu. Rev. Biochem.* **2003**, *72*, 111-135.
- (143) Oxidative protein folding in eukaryotes: mechanisms and consequences. Tu, B. P.; Weissman, J. S. *J. Cell Biol.* **2004**, *164*, 341-3466.
- (144) How proteins form disulfide bonds. Depuydt, M.; Messens, J.; Collet, J. F. *Antioxid. Redox Signal.* **2011**, *15*, 49-66.
- (145) Protein folding and modification in the mammalian endoplasmic reticulum. Braakman, I.; Bulleid, N. J. *Annu. Rev. Biochem.* **2011**, *80*, 71-99.
- (146) Small-molecule catalysts of oxidative protein folding. Lees, W. J. *Curr. Opin. Chem. Biol.* **2008**, *12*, 740-745.
- (147) Protein refolding using chemical refolding additives. Yamaguchi, S.; Yamamoto, E.; Mannen, T.; Nagamune, T. *Biotechnol. J.* **2013**, *8*, 17-31.

- (148) The use of insoluble polymer supports in general organic synthesis. Leznoff, C. C. *Acc. Chem. Res.* **1978**, *11*, 327-333.
- (149) *Continuous-Flow Peptide Synthesis on PSPOE-Graft-Copolymers*; Rapp, W.; Zhang, L.; Bayer, E., Eds. Oxford, 1989.
- (150) Structure and properties of TentaGel resin beads: Implications for combinatorial library chemistry. Quarrell, R.; Claridge, T. D. W.; Weaver, G. W.; Lowe, G. *Molec. Divers.* **1995**, *1*, 223-232.
- (151) The L-cysteine/L-cystine shuttle system provides reducing equivalents to the periplasm in *Escherichia coli*. Ohtsu, I.; Wiriyathanawudhiwong, N.; Morigasaki, S.; Nakatani, T.; Kadokura, H.; Takagi, H. *J. Biol. Chem.* **2010**, *285*, 17479-17487.
- (152) Electron transfer in peptides with cysteine and methionine as relay amino acids. Wang, M.; Gao, J.; Muller, P.; Giese, B. *Angew. Chem. Int. Ed.* **2009**, *48*, 4232-4234.
- (153) Effect of ring strain on nucleophilic substitution at selenium: A computational study of cyclic diselenides and selenyl sulfides. Bachrach, S. M.; Walker, C. J.; Lee, F.; Royce, S. *J. Org. Chem.* **2007**, *72*, 5174-5182.
- (154) Mechanical force can fine-tune redox potentials of disulfide bonds. Baldus, I. B.; Grater, F. *Biophys. J.* **2012**, *102*, 622-629.
- (155) The effect of ring size on the rate of solvolysis of the 1-chloro-methylcycloalkanes. Brown, H. C.; Borkowski, M. *J. Am. Chem. Soc.* **1952**, *74*, 1894-1902.
- (156) Kinetics of thiol-disulfide exchange. Fava, A.; Iliceto, A.; Camera, E. *J. Am. Chem. Soc.* **1957**, *79*, 833-838.
- (157) The chemistry of selenocysteine. Metanis, N.; Beld, J.; Hilvert, D.; John Wiley & Sons, L., Ed.; John Wiley & Sons, Ltd.: 2011.
- (158) Catalysts of reduction of disulfide by selenol. Singh, R.; Kats, L. *Anal. Biochem.* **1995**, *232*, 86-91.

- (159) Syntheses and structural characterization of water-soluble selenium reagents for the redox control of protein disulfide bonds. Iwaoka, M.; Takahashi, T.; Tomoda, S. *Heteroat. Chem.* **2001**, *12*, 293-299.
- (160) *Bioconjugate Techniques*; 3rd ed.; Hermanson, G. T., Ed.; Academic Press: New York, NY, 2013.
- (161) Tissue sulfhydryl groups. Ellman, G. L. *Arch. Biochem. Biophys.* **1958**, *82*, 70-77.
- (162) A convenient synthesis of alkali-metal selenides and diselenides in tetrahydrofuran and the reactivity differences exhibited by these salts toward organic bromides - Effect of ultrasound. Thompson, D. P.; Boudjouk, P. *J. Org. Chem.* **1988**, *53*, 2109-2112.
- (163) Intermediates in the folding reactions of small proteins. Kim, P. S.; Baldwin, R. L. *Annu. Rev. Biochem.* **1990**, *59*, 631-660.
- (164) Reactivity and pH dependence of thiol conjugation to *N*-ethylmaleimide: detection of a conformational change in chalcone isomerase. Bednar, R. A. *Biochemistry* **1990**, *29*, 3684-3690.
- (165) *Catalysis in Chemistry and Enzymology*; Jencks, W. P., Ed.; McGraw-Hill: New York, NY, 1969.
- (166) Gaussian 09, Revision A.1. Frisch, M. J. T., G. W.; Schlegel, H. B.; Scuseria, G. E.; Robb, M. A.; Cheeseman, J. R.; Scalmani, G.; Barone, V.; Mennucci, B.; Petersson, G. A.; Nakatsuji, H.; Caricato, M.; Li, X.; Hratchian, H. P.; Izmaylov, A. F.; Bloino, J.; Zheng, G.; Sonnenberg, J. L.; Hada, M.; Ehara, M.; Toyota, K.; Fukuda, R.; Hasegawa, J.; Ishida, M.; Nakajima, T.; Honda, Y.; Kitao, O.; Nakai, H.; Vreven, T.; Montgomery, Jr., J. A.; Peralta, J. E.; Ogliaro, F.; Bearpark, M.; Heyd, J. J.; Brothers, E.; Kudin, K. N.; Staroverov, V. N.; Kobayashi, R.; Normand, J.; Raghavachari, K.; Rendell, A.; Burant, J. C.; Iyengar, S. S.; Tomasi, J.; Cossi, M.; Rega, N.; Millam, J. M.; Klene, M.; Knox, J. E.; Cross, J. B.; Bakken, V.; Adamo, C.; Jaramillo, J.; Gomperts, R.; Stratmann, R. E.; Yazyev, O.; Austin, A. J.; Cammi, R.; Pomelli, C.; Ochterski, J. W.; Martin, R. L.; Morokuma, K.; Zakrzewski, V. G.; Voth, G. A.; Salvador, P.; Dannenberg, J. J.; Dapprich, S.; Daniels, A. D.; Farkas, Ö.; Foresman, J. B.; Ortiz, J. V.; Cioslowski, J.; Fox, D. J.; Gaussian, Inc.: Wallingford, CT, 2009.

- (167) Oxidation/reduction potential of glutathione Millis, K. K.; Weaver, K. H.; Rabenstein, D. L. *J. Org. Chem.* **1993**, *58*, 4144-4146.
- (168) Notes: Basicity and ionization constants of some pyrazine derivatives. Keyworth, D. A. *J. Org. Chem.* **1959**, *24*, 1355.
- (169) The syntheses of pyrazino-containing sultines and their application in Diels-Alder reactions with electron-poor olefins and. Liu, J. H.; Wu, A. T.; Huang, M. H.; Wu, C. W.; Chung, W. S. *J. Org. Chem.* **2000**, *65*, 3395-3403.
- (170) Principles that govern the folding of protein chains. Anfinsen, C. B. *Science* **1973**, *181*, 223-230.
- (171) Sequence of protein disulphide isomerase and implications of its relationship to thioredoxin. Edman, J. C.; Ellis, L.; Blacher, R. W.; Roth, R. A.; Rutter, W. J. *Nature* **1985**, *317*, 267-270.
- (172) Thioredoxin catalyzes the reduction of insulin disulfides by dithiothreitol and dihydrolipoamide. Holmgren, A. *J. Biol. Chem.* **1979**, *254*, 9627-9632.
- (173) Catalytic mechanism of Dsba and its comparison with that of protein disulfide-isomerase. Darby, N. J.; Creighton, T. E. *Biochemistry* **1995**, *34*, 3576-3587.
- (174) Catalysis of oxidative protein folding by mutants of protein disulfide isomerase with a single active-site cysteine. Walker, K. W.; Lyles, M. M.; Gilbert, H. F. *Biochemistry* **1996**, *35*, 1972-1980.
- (175) Scanning and escape during protein-disulfide isomerase-assisted protein folding. Walker, K. W.; Gilbert, H. F. *J. Biol. Chem.* **1997**, *272*, 8845-8848.
- (176) Disulfide bond structures of IgG molecules: structural variations, chemical modifications and possible impacts to stability and biological function. Liu, H.; May, K. *MAbs* **2012**, *4*, 17-23.

- (177) Catalysis of the oxidative folding of ribonuclease A by protein disulfide isomerase: pre-steady-state kinetics and the utilization of the oxidizing equivalents of the isomerase. Lyles, M. M.; Gilbert, H. F. *Biochemistry* **1991**, *30*, 619-625.
- (178) The hydrophobic effect in protein folding. Lins, L.; Brasseur, R. *FASEB J.* **1995**, *9*, 535-540.
- (179) Acyl cystamine: small-molecular foldase mimics accelerating oxidative refolding of disulfide-containing proteins. Wang, G. Z.; Dong, X. Y.; Sun, Y. *Biotechnol. Progr.* **2011**, *27*, 377-385.
- (180) Ribonuclease A. Raines, R. T. *Chem. Rev.* **1998**, *98*, 1045-1066.
- (181) Hypersensitive substrate for ribonucleases. Kelemen, B. R.; Klink, T. A.; Behlke, M. A.; Eubanks, S. R.; Leland, P. A.; Raines, R. T. *Nucleic Acids Res.* **1999**, *27*, 3696-3701.
- (182) Octanol-water partition coefficients of simple organic compounds. Sangster, J. *J. Phys. Chem. Ref. Data* **1989**, *18*, 1111-1227.
- (183) Binding-energy and enzymatic catalysis. Hansen, D. E.; Raines, R. T. *J. Chem. Ed.* **1990**, *67*, 483-489.
- (184) Protein disulfide isomerase and assisted protein folding. Gilbert, H. F. *J. Biol. Chem.* **1997**, *272*, 29399-29402.
- (185) Achiral oligoamines as versatile tool for the development of aspartic protease inhibitors. Blum, A.; Bottcher, J.; Sammet, B.; Luksch, T.; Heine, A.; Klebe, G.; Diederich, W. E. *Bioorg. Med. Chem.* **2008**, *16*, 8574-8586.
- (186) Triazine dendrimers with orthogonally protected amines on the periphery. Masking amines with Dde and BOC groups provides an alternative to carrying protected alcohols and disulfides through an iterative synthesis. Umali, A. P.; Crampton, H. L.; Simanek, E. E. *J. Org. Chem.* **2007**, *72*, 9866-9874.

- (187) A novel function of Escherichia coli chaperone DnaJ. Protein-disulfide isomerase. de Crouy-Chanel, A.; Kohiyama, M.; Richarme, G. *J. Biol. Chem.* **1995**, *270*, 22669-22672.
- (188) Reaction of tris(2-carboxyethyl)phosphine (TCEP) with maleimide and alpha-haloacyl groups: anomalous elution of TCEP by gel filtration. Shafer, D. E.; Inman, J. K.; Lees, A. *Anal. Biochem.* **2000**, *282*, 161-164.
- (189) Cystinosis. Fagg, G. *J. R. Soc. Med.* **1954**, *47*, 882-883.
- (190) Cysteamine therapy: a treatment for cystinosis, not a cure. Cherqui, S. *Kidney Int.* **2012**, *81*, 127-129.
- (191) Multistep synthesis of complex boronic acids from simple MIDA boronates. Gillis, E. P.; Burke, M. D. *J. Am. Chem. Soc.* **2008**, *130*, 14084-14085.
- (192) Therapeutic potential of boron-containing compounds. Baker, S. J.; Ding, C. Z.; Akama, T.; Zhang, Y. K.; Hernandez, V.; Xia, Y. *Future Med. Chem.* **2009**, *1*, 1275-1288.
- (193) Crystal-structure of Hiv-1 protease in complex with VX-478, a potent and orally bioavailable inhibitor of the enzyme. Kim, E. E.; Baker, C. T.; Dwyer, M. D.; Murcko, M. A.; Rao, B. G.; Tung, R. D.; Navia, M. A. *J. Am. Chem. Soc.* **1995**, *117*, 1181-1182.
- (194) Benzoxazole and benzothiazole amides as novel pharmacokinetic enhancers of HIV protease inhibitors. Jonckers, T. H. M.; Rouan, M. C.; Hache, G.; Schepens, W.; Hallenberger, S.; Baumeister, J.; Sasaki, J. C. *Bioorg. Med. Chem. Lett.* **2012**, *22*, 4998-5002.
- (195) Rapid discovery and structure-activity profiling of novel inhibitors of human immunodeficiency virus type 1 protease enabled by the copper(I)-catalyzed synthesis of 1,2,3-triazoles and their further functionalization. Whiting, M.; Tripp, J. C.; Lin, Y. C.; Lindstrom, W.; Olson, A. J.; Elder, J. H.; Sharpless, K. B.; Fokin, V. V. *J. Med. Chem.* **2006**, *49*, 7697-7710.
- (196) Redox regulation of PI 3-kinase signalling via inactivation of PTEN. Leslie, N. R.; Bennett, D.; Lindsay, Y. E.; Stewart, H.; Gray, A.; Downes, C. P. *EMBO J.* **2003**, *22*, 5501-5510.

- (197) Reversible oxidation and inactivation of the tumor suppressor PTEN in cells stimulated with peptide growth factors. Kwon, J.; Lee, S. R.; Yang, K. S.; Ahn, Y.; Kim, Y. J.; Stadtman, E. R.; Rhee, S. G. *Proc. Natl. Acad. Sci. U.S.A.* **2004**, *101*, 16419-16424.
- (198) Cys-oxidation of protein tyrosine phosphatases: Its role in regulation of signal transduction and its involvement in human cancers. Meng, T. C.; Lou, Y. W.; Chen, Y. Y.; Hsu, S. F.; Huang, Y. F. *J. Cancer Mol.* **2006**, *2*, 9-16.
- (199) Alkylation of the tumor suppressor PTEN activates Akt and beta-catenin signaling: a mechanism linking inflammation and oxidative stress with cancer. Covey, T. M.; Edes, K.; Coombs, G. S.; Virshup, D. M.; Fitzpatrick, F. A. *PLoS One* **2010**, *5*, 1-11.
- (200) Regulation of protein tyrosine phosphatases by reversible oxidation. Ostman, A.; Frijhoff, J.; Sandin, A.; Bohmer, F. D. *J. Biochem.* **2011**, *150*, 345-356.
- (201) Reversible inactivation of the tumor suppressor PTEN by H₂O₂. Lee, S. R.; Yang, K. S.; Kwon, J.; Lee, C.; Jeong, W.; Rhee, S. G. *J. Biol. Chem.* **2002**, *277*, 20336-20342.
- (202) Crystal structure of the PTEN tumor suppressor: Implications for its phosphoinositide phosphatase activity and membrane association. Lee, J. O.; Yang, H. J.; Georgescu, M. M.; Di Cristofano, A.; Maehama, T.; Shi, Y. G.; Dixon, J. E.; Pandolfi, P.; Pavletich, N. P. *Cell* **1999**, *99*, 323-334.